

**Internal architecture, geometry and reservoir characterisation of
depositional lobes in outcrop and subsurface:
examples from S-Turkey and the North Sea.**

**Dissertation
zur Erlangung des Grades eines Doktors der Naturwissenschaften**

**der Geowissenschaftlichen Fakultät
der Eberhard-Karls-Universität Tübingen**

**vorgelegt von
Renate Kostrewa
aus Bülach/Schweiz**

2004

Tag der mündlichen Prüfung: 13. 05. 2004

Dekan: Prof. Dr. Dr. h.c. M. Satir

1. Berichterstatter: Prof. Dr. HP Luterbacher

2. Berichterstatter: Prof. Dr. T. Aigner

Acknowledgements

This study was sponsored by a consortium of five oil companies (Amarada Hess, Amoco (now BP-Amoco), Conoco, Elf and Enterprise) as part of a larger research project studying deep-water clastic systems under supervision of Prof. Dr. A. Hurst and Dr. B. Cronin at the University of Aberdeen and Prof. Dr. G. Kelling (em.), Keele University.

The research was continued and completed under supervision of Prof. Dr. HP Luterbacher at Tübingen University who is kindly thanked for providing this opportunity and Prof. T. Aigner for serving as second referee. Prof. E. Mutti is especially thanked for offering his expert opinion on the final draft.

The well data for the Scapa Field was kindly provided by Elf Occidental Caledonia Ltd. Aberdeen (now Elf Enterprise Caledonia Ltd.) and Dr. B. Rovelli served not only as the contact person, but provided great assistance with the data acquisition and motivation and found time for inspiring discussions despite his numerous work commitments. He is especially thanked for initially obtaining Elf's permission for transferring the data to Tübingen University. Since May 2000 the Scapa Field data has been in the possession of Talisman Ltd. Aberdeen and Mr. Jerry Dennis, Production Manager Scapa and Claymore Area, is kindly thanked for obtaining Talisman's permission to allow the data to be published in this thesis.

During the extensive field work in Turkey, Ezher Gülbas and Hakan Günlay, both of Cukurova University, Adana, are thanked for their assistance in the field. Special thanks to Mrs. Judith Christie (Aberdeen) and others for sorting out all my computer problems and Mr. Walter Ritchie (Aberdeen) for always promptly preparing slides and photographs. Dr. Bernd Kaufmann (Tübingen) could be persuaded to turn his attention to clastics and is kindly thanked for proof-reading parts of this thesis in his customary critical approach.

Special thanks to Dr. M. Leishman (Amarada Hess), Mrs. R. Jones (formerly of Enterprise) and Dr. C. Stevens (formerly of Amoco) for their great encouragement when it was most needed.

Last but not least, to my family, friends and colleagues who supported, encouraged and suffered with me, I reserve my greatest appreciation and dedicate this thesis to them.

TABLE OF CONTENTS

ZUSAMMENFASSUNG	I
ABSTRACT	III
1 INTRODUCTION	1
1.1 DEEP-WATER CLASTIC SYSTEMS AS IMPORTANT EXPLORATION TARGETS	1
1.2 AIMS OF THESIS	1
1.3 STATE OF THE ART: DEEP-WATER CLASTIC SYSTEMS - PROCESSES AND FACIES MODELS	2
1.3.1 <i>Lobe deposits</i>	5
1.4 FIELD AREAS, DATABASE AND METHODS	9
2 CHARACTERISATION OF LOBE DEPOSITS IN OUTCROP: E-FAN, CINGÖZ FORMATION, S-TURKEY	12
2.1 GEOLOGICAL BACKGROUND	12
2.1.1 <i>Location and setting</i>	12
2.1.2 <i>Tectono-sedimentary evolution and stratigraphy of the Adana Basin</i>	13
2.2 THE CINGÖZ FORMATION	16
2.2.1 <i>The western and eastern fan</i>	17
2.2.2 <i>Eastern fan framework</i>	20
2.2.2.1 Feeder channel systems	21
2.2.2.2 Facies distribution and architecture of the non-channelized E-Fan sections	22
2.2.2.3 Lithologic and biostratigraphic correlations	26
2.3 GEOMETRY OF THE FAN - SLOPE CONTACT	27
2.3.1 <i>Contact relationships</i>	27
2.3.2 <i>Western versus eastern fan-slope contacts</i>	30
2.4 NON-CANNELIZED FAN ENVIRONMENTS	32
2.4.1 <i>Channel-lobe transition zone</i>	32
2.4.1.1 Component analysis: internal organisation and geometry	35
2.4.1.2 Channel-lobe transition zone: processes, facies and controls	39
2.4.1.3 Lobe A accumulation	41
2.4.1.4 Channel-lobe transition zones associated with feeder channels 3 and 4	41
2.4.2 <i>Proximal Lobe Zone</i>	43
2.4.2.1 Component analysis: internal organisation and geometry	44
2.4.2.2 Lobe B accumulation	49
2.4.3 <i>Distal lobe deposits</i>	51
2.4.3.1 Component analysis: internal organisation and geometry	52
2.4.3.2 Lobe C accumulation	57
2.4.4 <i>Downcurrent evolution in lobe accumulation</i>	60
2.5 CONTROLS	61
2.5.1 <i>Basin physiography, basinfloor and depositional topography</i>	62
2.5.2 <i>Tectonics</i>	65
2.5.3 <i>Sediment supply and climate</i>	66
2.5.4 <i>Sea-level changes</i>	68
2.5.5 <i>Water depth, contourites and other controls</i>	70
2.6 EVOLUTION OF THE E-FAN	71
2.7 DISCUSSION	75
2.7.1 <i>Biostratigraphic framework</i>	75
2.7.2 <i>E-Fan vs W-Fan</i>	75
2.7.3 <i>Dynamic depositional model</i>	76
2.7.4 <i>Lobe accumulation</i>	78
2.7.5 <i>Controls</i>	78
2.8 CONCLUSION	79
2.9 FURTHER WORK	80
2.10 SUMMARY	81

3	CHARACTERISATION OF SUBSURFACE LOBE DEPOSITS: S10 INTERVAL, SCAPA SANDSTONE MEMBER, SCAPA FIELD, BLOCK 14/19 NORTH SEA, UK.....	81
3.1	GEOLOGICAL BACKGROUND.....	81
3.1.1	<i>Location.....</i>	81
3.1.2	<i>Tectono-sedimentary evolution and stratigraphy of the Scapa Syncline.....</i>	82
3.1.3	<i>The Scapa Sandstone Member.....</i>	84
3.2	THE S10 INTERVAL.....	86
3.2.1	<i>S10 framework.....</i>	86
3.2.2	<i>Interwell correlation.....</i>	90
3.3	FAN ENVIRONMENTS.....	91
3.3.1	<i>Distributary channels.....</i>	91
3.3.2	<i>Non-channelized sand-dominated deposits.....</i>	94
3.3.3	<i>Shale-dominated deposits.....</i>	96
3.3.4	<i>Hemipelagic marls.....</i>	97
3.4	LOBE ACCUMULATION.....	98
3.4.1	<i>Temporal and spatial development of the S10 Interval.....</i>	98
3.4.2	<i>Controls.....</i>	100
3.4.2.1	<i>Basin physiography, geometry and seafloor topography.....</i>	100
3.4.2.2	<i>Tectonism.....</i>	101
3.4.2.3	<i>Rate, type and source of sedimentary supply.....</i>	102
3.4.2.4	<i>Sea level changes.....</i>	103
3.5	DISCUSSION.....	104
3.5.1	<i>Interwell correlation.....</i>	104
3.5.2	<i>Depositional model and controls.....</i>	104
3.5.3	<i>Lobe accumulation.....</i>	107
3.6	CONCLUSION.....	107
3.7	FURTHER WORK.....	108
3.8	SUMMARY.....	108
4	RESERVOIR CHARACTERISATION.....	109
4.1	LOBE DEPOSITS OF E-FAN, CINGÖZ FORMATION.....	110
4.1.1	<i>Lobe A.....</i>	110
4.1.2	<i>Lobes B.....</i>	112
4.1.3	<i>Lobe C.....</i>	113
4.2	LOBE DEPOSITS OF THE S10 INTERVAL, SCAPA SANDSTONE MEMBER.....	117
4.3	POSTDEPOSITIONAL CHANGES AND RESERVOIR DELINEATION.....	118
5	DISCUSSION OF LOBE DEPOSITS.....	118
5.1	DEPOSITIONAL LOBES IN ANCIENT SYSTEMS.....	119
5.1.1	<i>Turbidites versus sandy debris flow deposits.....</i>	119
5.1.2	<i>Vertical sequences – fact or fiction.....</i>	120
5.1.3	<i>Geometries – to be or not to be.....</i>	122
5.2	LOBES IN THE SUBSURFACE.....	123
5.3	OUTCROP VERSUS SUBSURFACE DATA: OPPORTUNITIES AND LIMITATIONS.....	124
5.4	LOBES - A FUNDAMENTAL ELEMENT IN MODELS.....	125
5.5	LOBES OR WHAT?.....	126
6	CONCLUSION AND FURTHER WORK.....	127
	REFERENCES.....	131
	PHOTOPLATES.....	145
	APPENDIX.....	163
	ENCLOSURE.....	175

ZUSAMMENFASSUNG

Nicht-kanalisierte, sandige Tiefwasserablagerungen, allgemein *lobe deposits* („Lobus-Sedimente“) nach Mutti & Normark (1987) benannt, sind ein grundlegendes Element vieler submariner Tiefseefächer und verwandter Turbiditsysteme. Ihr Kohlenwasserstoffpotential ist von ökonomischem Interesse und ein gutes Verständnis ihrer Faziesbeziehungen, Geometrie und Reservoirqualität sind unabdingbar für eine zielgerichtete Exploration und Produktion. Es hat sich jedoch gezeigt, dass die strikte Anwendung des ursprünglichen Begriffs *lobe deposits* zu restriktiv ist, um die Vielfalt der beobachteten lateral weit aushaltenden, nicht-kanalisierten sandigen *lobe deposits* zu umfassen. Eine weiter gefasste Definition dieser Ablagerungen hat in den letzten Jahren an Akzeptanz gewonnen.

Der E-Fan der Mittel-Miozänen Cingöz Formation (Südtürkei) ist ein bis dato wenig untersuchtes Beispiel eines regressiven, extrem sandreichen von mehreren Quellen gespeisten klastischen Tiefwassersystems, das in einem Trippepunkt *escape basin* liegt und von dem aufsteigenden Taurus Orogen gespeist wird. Zeit-stratigraphische Veränderungen des E-Fan führten von einem konglomeratdominiertem System im späten (?) Burdigalian zu einem sanddominierten System im späten Burdigalian – Langhian, wo Sande hauptsächlich in mächtigen, lateral weit aushaltenden *lobe deposits sensu lato* abgelagert wurden. Charakteristische Komponentenassoziationen des *channel-lobe* Übergangs (Lobe A), der proximalen (Lobe B) und distalen (Lobe C) Ablagerungszonen, zeigen einen ausgeprägten strömungsabwärtsgerichteten Trend im Ablagerungsmuster. Wechselnde räumliche und zeitliche Ablagerung deutet tektonische Aktivität als einen bestimmenden Mechanismus an, der das Muster der Sedimentzufuhr und die Beckentopographie kontrollieren, was zu einer begrenzten Geometrie und aggradierend-gestapelten *lobe deposits* führt, die das Ergebnis von niedrig- und hochkonzentrierten, sandreichen Trübe- und sandigen Schuttströmen im Sinne von Shanmugam (1996) sind. Auffallendes *fining upward* der Loben- und des Turbiditsystems, dokumentiert einen allmählich ansteigenden Meeresspiegel, wohingegen vereinzelte Progradations-Phasen und/oder der Eintrag grobklastischer Sedimente auf höherfrequente Meeresspiegelschwankungen oder tektonische Bewegungen des Hinterlandes schließen lassen.

Der S10 Interval des Scapa Sandstone Members (U-Kreide, Scapa Field, UK block 14/19, North Sea) ähnelt nach Reading & Richards (1994) einem von mehreren Quellen gespeisten tonig/sandreichen bis sandreichen submarinem Rampensystem, mit einigen *slope apron* Merkmalen, das sich während steigendem Meeresspiegel entwickelte. Sedimente wurden am von Konglomeraten umsäumte Halibut Schelf vorbei geleitet und durch ein verzweigtes Kanalsystem tiefer in das Scapa Becken verteilt. Die Masse der Sande wurde in gering bis unkanalisierten, sandigen *lobe* und *lobe fringe deposits* sedimentiert. Die *lobes* sind hauptsächlich aus sandigen, hochkonzentrierten und verdünnten Trübeströmungen und wahrscheinlich auch sandigen Schuttströmen (Shanmugam 1996) aufgebaut. Ihre Position und Geometrie deutet auf einen starken Einfluß des Liefergebietes hin. Grabentektonik führt zu lokaler, Lobenaggradation mit oftmals länglicher Geometrie, was auf einen begrenzten Ablagerungsraum hindeutet.

Die makro- und megaskopische Reservoircharakterisierung der Cingöz *lobe deposits* macht ihr Potential als Explorationsziel deutlich, besonders wegen ihrer großflächigen Ausdehnung, dem generellen hohen Nettosandgehalt und der extrem guten vertikalen und lateralen Konnektivität. Migrationsbarrieren, wie zum Beispiel Tonlagen, sind in den proximalen Bereichen (Lobe A/B) nicht vorhanden und treten nur in einer strömungsabwärtsgerichteten Richtung auf. Sie führen zu einer Kompartimentalisierung des distalen Reservoirs (Lobe C). Jedoch zeigt sich, dass Diagenese die Reservoirqualität entscheidend negativ verändern kann, wie zum Beispiel in den *lobe deposits* des Scapa Felds, wo stark variierende Zementation zur Reservoirkompartimentalisierung führt.

ABSTRACT

Non-channelized, sandy deep-water deposits, commonly termed lobe deposits *sensu* Mutti & Normark (1987), form an elemental building block of many submarine fans and related turbidite systems. They possess an important hydrocarbon reservoir potential and a clear understanding of their geometry, facies relationships and reservoir quality are imperative for effective exploration and exploitation. However, the *sensu stricto* definition proves to be too restrictive to embrace the great variety of the laterally extensive, non-channelized, sandy depositional bodies observed and in recent years a broader, in essence *sensu lato* definition has gained acceptance.

The E-Fan of the Mid-Miocene Cingöz Formation (southern Turkey) is a to date little studied example of a regressive, extremely sand-rich, multi-sourced deep-water clastic system deposited in a triple junction escape basin sourced from the emerging Tauride Orogen. Time-stratigraphic changes show that the E-Fan system evolve from a gravel-dominated system during late? Burdigalian to a sand-dominated one in late Burdigalian – Langhian times where the bulk of the sand accumulated in thick, laterally extensive, sandy lobes *sensu lato*. Unique component associations characterise the channel-lobe transition (Lobe A), proximal (Lobe B) and distal (Lobe C) depositional zones, recording a distinct downcurrent change in sedimentation pattern. Changing spatial and temporal deposition indicates tectonism as the fundamental mechanism controlling the sediment supply pattern and basinfloor topography which is reflected in the confined geometry and aggradational stacking of the lobes. They are the products of deposition by low- and high-density sand-rich turbidity currents and possibly sandy debris flows *sensu* Shanmugam (1996). Conspicuous fining upward at lobe- and system- scale document the gradually rising sea level while sporadic phases of progradation and/or coarse clastic sediment supply imply higher frequency sea-level fluctuations and tectonically-driven source area control.

The S10 interval of the Lower Cretaceous Scapa Sandstone Member (Scapa Field, UK block 14/19, North Sea) is akin to a multiple sourced mud/sand-rich to sand-rich submarine ramp system *sensu* Reading & Richards (1994) with some features of a slope apron system developing during times of gradual sea-level rise. Sediment bypassed the conglomerate-fringed Halibut Shelf and funnelled further into the Scapa sub-basin by a distributary channel system. The bulk of the sand-grade material was deposited in little to non-channelized, detached sandy lobe and lobe fringe deposits. Lobes are mainly composed of sandy high-density turbidity currents and diluted flows and possibly sandy debris flows *sensu* Shanmugam (1996). The location and geometry of the lobe deposits is strongly determined by source-area and basinal tectonism which led to localised, stacked, aggradational lobe accumulation of elongate geometry indicating that deposition was restricted.

The macro- and megascopic reservoir characterisation of the Cingöz lobe deposits clearly shows their attraction as exploration target due to their great areal extend, the overall high net sand content and the extremely good vertical and lateral connectivity. Flow barriers, such as shale layers, are absent in the most proximal areas (Lobe A/B) and only appear in a down-current direction, compartmentalising the distal reservoir (Lobe C). However, diagenesis may have an overriding effect on the reservoir quality as documented in the S10 lobe deposits where varying degrees of cementation are responsible for reservoir compartmentalisation.

1 INTRODUCTION

1.1 Deep-water clastic systems as important exploration targets

In the early 1990s, 25% of the known hydrocarbon reservoirs were located within deep-water clastic systems (Weimer & Link 1991). Turbidites as the volumetrically most significant deep-water deposits are the primary reservoir type within these plays. Since 1970 a three-fold increase in discovered turbidite reservoirs has been recorded. This trend is expected to rise considerably in the future (Pettingill 1998). Presently, turbidites are known to produce oil and/or gas in more than 80 basins world wide, totalling 1200 to 1300 oil and gas fields including discoveries and producing fields (Stow & Mayall 2000). It has been predicted that in the future 75% of the potential hydrocarbon reservoirs are to be found in deep-water clastic systems. Consequently, the global turbidite exploration is presently considered to be at an immature stage but will play a significant role in the future of hydrocarbon exploration and production (Pettingill 1998).

Deep-water clastic systems, comprising submarine fan systems and related turbidite systems (Reading 1996), host large volumes of oil-in-place, but the recovery factor is low due to their complex reservoir architecture. A clear understanding of their geometry, facies relationships and reservoir quality is therefore critical for exploring and exploiting these deposits effectively (Tyler *et al.* 1984).

Most studies have focused on channel-fill deposits which form well constrained, linear reservoir bodies with typically high porosities and permeabilities due to general better sorting, larger grain size, thicker beds and fewer interbedded shaley permeability barriers. An abundance of literature exists (e.g. Walker 1978, 1980; Bouma *et al.* 1985; Damuth *et al.* 1988; Clark & Pickering 1996; Pirmez *et al.* 1997). However, relatively little research has gone into the equally attractive exploration target of the non-channelized units which possess an important hydrocarbon reservoir potential because of their large areal extent (Schuppers 1995). These often comprise sheet-sands and are commonly termed lobe deposits. McLean (1981) demonstrated that particularly proximal lobe deposits with their high sand/shale ratios and likely higher porosities and permeabilities are of special interest. Turbidites in distal lobe position have also proven to be highly permeable (Hewlett & Jordan 1993). Studies focus especially on reservoir characterisation in terms of lithohydraulic units, where lithological and petrophysical entities form flow units.

Due to the economic importance and the scientific challenge deep-water clastic systems pose, key research areas have been outlined at the beginning of the 21st century in order to grasp their complexity (Stow & Mayall 2000). One focal point is to scrutinise these systems at the level of architectural building blocks including the quantification of their attributes. At a larger scale it is important to examine the fundamental controls which determine deep-water facies and architecture.

1.2 Aims of thesis

A consortium of 5 oil companies (Amarada Hess, Amoco – now BP-Amoco, Conoco, Elf and Enterprise) sponsored this detailed, primarily field-based study (Cingöz Formation, S-Turkey) to analyse the internal architecture of non-channelized, sandy turbiditic deposits and the factors governing their evolution in the context of their particular fan setting. The application of field-derived concepts to a subsurface data set (Scapa Field, North Sea) is evaluated. This study was carried out as part of a larger research project of the deep water clastic research group at Aberdeen University, UK.

The aims of the study were:

- to identify different subenvironments within the sandy, primarily non-channelized fan deposits and define their basic building blocks (architectural elements) *sensu* Mutti & Normark (1987) and subenvironments (components) *sensu* Mutti (1977).
- to unravel sandbody geometries and lithological continuity at different hierarchies of scale and quantify their physical attributes.
- to identify vertical / lateral trends in the differentiated subenvironments (lobe types) as well as analyse the observed down-current trends.

- to investigate heterogeneities at different scales for the identified elements (lobe types) and their implication in terms of hydrocarbon exploration.
- to re-evaluate the existing fan framework for the two study areas to place the observed deposits and field relationships into a more refined context.
- to analyse the stacking patterns and quantify the key controlling factors influencing lobe and fan development and discuss the constraints/limitations of models.
- to evaluate the application of field-derived concepts on a subsurface data set and address the problems which exist. The limitations and resulting implications are discussed.

Outcrop study: E-Fan, Cingöz Formation, Southern Turkey

The Mid-Miocene Cingöz Formation (Adana Basin, southern Turkey) is a to date little studied example of a multi-sourced slope apron - basin floor fan deposited in a triple junction escape basin exhibiting typical foreland basin character during a time of gradually rising sea level (Gökçen *et al.* 1988; Ünlügenç *et al.* 1992; Gürbüz 1993; Gürbüz & Kelling 1993). Exposures of thick units of primarily non-channelized sheet-sands are relatively good and of large lateral extent, partly at interwell scale (up to 1.5 km). They permit detailed studies in key proximal and distal locations within the fan system. Additionally, the complex relationship of the submarine fan with the slope can be studied. Earlier research and this study permit the establishment of a relatively well known fan framework and thus the controlling factors of the lobe development can be studied in detail.

Subsurface study: S10 interval, Scapa Field, North Sea.

The Lower Cretaceous Scapa Sandstone Member (Scapa Field, North Sea) is an example of a slope-apron fan deposited in a half-graben system during rising sea level (Harker & Chermak 1992; Hendry 1994). The deposits of the Scapa System have been described to be mainly composed of channel-fill and subordinate lobe deposits (McAfee 1993). With the exception of Riley *et al.* (1992) who introduced the chronostratigraphic environmental reconstruction at a relatively broad scale for the Scapa Field, all published and unpublished reports use fluid-flow units (reservoir/non-reservoir units), which essentially are diachronous, as the basis of their evaluation. The recognition and characterisation of lobe deposits, based on core and well log data in conjunction with outcrop-derived concepts is tested on the largest oil-bearing unit within the system, the chronostratigraphic S10 interval.

1.3 State of the art: deep-water clastic systems - processes and facies models

Until the beginning of this century, the sediments on the sea floor were thought to be solely composed of fine-grained biogenic oozes and pelagic muds (Friedman & Sanders 1997). When coarse clastic sediments were discovered in the deep sea, transport and depositional mechanisms became the object of investigation. It was shown that the deposits of gravity-controlled mass-transport processes (turbidites and debris flows) are the major components of deep-water clastic systems (e.g. Mutti 1992; Stow *et al.* 1996; Friedman & Sanders 1997). The first models classifying the processes, deposits and the anatomy of these observed systems emerged in the 1960's and early 70's (Reading 1996; *historic review in:* Shanmugam 2000). The establishment and evolution of depositional models has been very dynamic and occasionally confusing. At the end of the 20th century many of these models have been challenged, some, in fact, were abandoned. Common points of dispute are the validity of the turbidite paradigm, where turbidites are considered to make up the bulk of deep-water clastic systems. Shanmugam (2000), for example, has long disputed this suggesting that many turbidites are in fact sandy debris flow deposits. Distinct facies cyclicity, long considered to be diagnostic of fan environments and development, was shown to be questionable as Anderton (1995) demonstrated a predominance of random processes in fan deposition. Over the years, the looser usage of terms and definitions has clearly resulted in creating confusion (Miall 1999). Stow & Mayall (2000), Shanmugam (2000) and Miall (1999) present summaries and discussions of these topics.

Deep-water processes and classification of deposits

Gravity-driven processes are responsible for a range of deposits found in the deep sea. Slumps and debris flows tend to dominate more proximal and turbidites more distal settings. However, either type of deposit can occur at any location. It is generally accepted that turbidites are the most common deposits in deep-water clastic systems (Stow & Mayall 2000)

After 50 years, the turbidite paradigm is still dominant and everything from a 1 cm thick silt-laminated mudstone to a 50 cm thick boulder-pebble-sand graded megabed has been called a turbidite (Stow & Mayall 2000). Kuenen & Migliorini (1950) suggested density currents as agents for transporting coarse sediment into the deep sea, leaving graded deposits behind. Bouma (1962) was the first to propose a vertical facies model for turbidites which is commonly referred to as the Bouma Sequence or 'classic turbidite'. Turbidites are principally recognised by i) normal size grading, ii) sharp basal contacts, iii) gradational upper contacts, iv) Bouma divisions (Ta-Te; fig. 1.1; Bouma 1962; Middleton & Hampton 1973) and v) deep-water fossil assemblages. Because many of the deposits found in deep-water systems did not always fit that definition in terms of accommodating the variety of grain sizes and sedimentary features, the original definition of turbidites was expanded. Stow & Shanmugam (1980) added a more detailed division for the silt-mud facies to the original model (fig. 1.1) and Lowe (1982) expanded it for the coarse grained fraction (subdivisions R₁– S₃). He classified turbidity currents into two main types: low-density flows, producing the classic turbidites, and high-density flows, producing coarser grained turbidites. This division is based on grain-size populations, particle concentrations and sediment-support mechanisms. This concept is now widely accepted. Shanmugam (2000) disputes this and regards high-density turbidites as sandy debris flow deposits, a concept first introduced by Hampton (1975) and further developed by Shanmugam *et al.* (1995) and Shanmugam (1996, 1997, 2000). This interpretation has been met by scepticism (e.g. Hiscott *et al.* 1997; Bouma *et al.* 1997, Lowe 1997), however, there is no current consensus (Shanmugam *et al.* 1997; Shanmugam & Muiola 1997). The different genetic implication is of great importance to the petroleum industry in terms of predicting reservoir geometry (Slatt *et al.* 1997) since high-density turbidites are considered to show great lateral extent as opposed to sandy debris flows. Recently, Shanmugam (2000) has implied that sandy debris flows are also capable of depositing thick, sandy and areally extensive deposits.

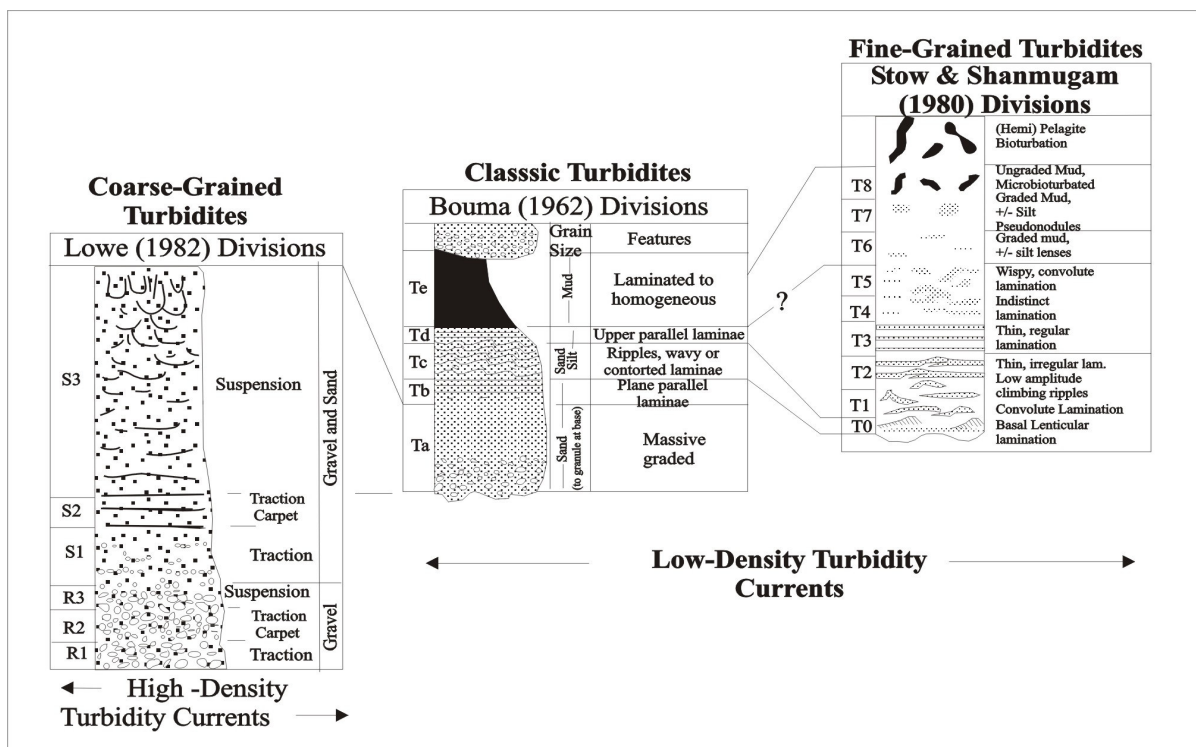


Fig. 1.1: Vertical facies model of (1) coarse-grained turbidites (Lowe 1982), (2) classic turbidites (also known as Bouma Sequence) and (3) fine-grained turbidites (Stow & Shanmugam 1980). Correlation of the S3 division with the turbidites with the Ta division of the Bouma Sequence is after Lowe (1982). Correlation of various divisions between classic turbidites is after Pickering *et al.* (1989) (from Shanmugam 2000).

Not many sediment beds in the deep-sea were found to exhibit simple normal grading as was originally defined for turbidites. Harms & Fahnstock (1965), for example, suggested massive sandstones to result from turbidity currents. Kneller's (1995) time-space matrix for turbidity currents led to the expansion of the model (fig. 1.2) recognising normal grading, massive (i.e. no grading) and inverse grading for turbidites depending on the flow conditions (waning, steady or waxing). Apart from the common Bouma (1962) and Lowe (1982) classification systems for turbidites (fig. 1.1), several other facies schemes exist. Mutti & Ricci Lucchi (1972), for example, introduced a scheme where deposits are divided according to grain size (gravel to mud) forming seven facies associations (A-G), which are produced by a limited range of processes. They are considered to be diagnostic of specific depositional environments, though, Shanmugam & Muiola (1988) and Bouma *et al.* (1985) showed that this approach is too simplistic.

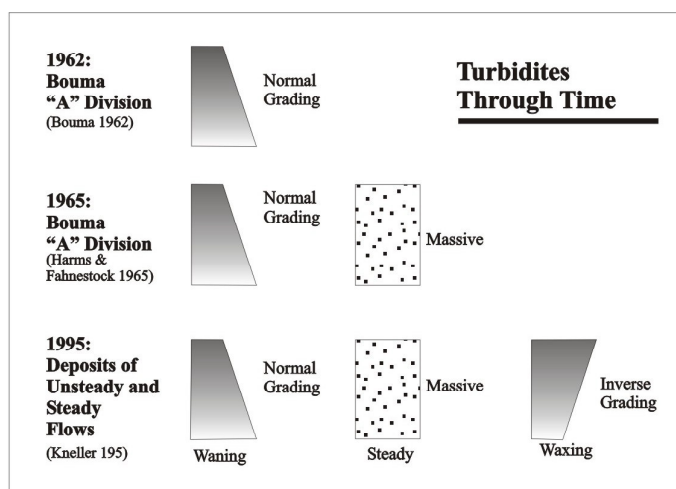


Fig. 1.2: Three publications showing how opinions on nature of grading in turbidites have changed through time. Top: Bouma (1962) suggested normal grading for turbidites. Middle: Harms & Fahnstock (1965) proposed normal grading and massive (i.e. no grading) for turbidites. Bottom: Kneller (1995) advocated normal grading, massive (i.e. no grading) and inverse grading for turbidites (from Shanmugam 2000).

and lower fan are characterised by distinct facies. This approach proved to be too simplistic and it was subsequently refined as more and more data from modern submarine fan systems became available (Miall 1999). Many parameters such as basin size and shape, source, duration of activity, sediments etc. which are unique to a system were now taken into account to accommodate the complexity and range of deep-water clastic systems (Reading & Richards 1994). The environmental classification of turbidite systems, including fans, ramps and slope aprons, is now relatively well established. Stow & Mayall (2000) present a summary of models (fig. 1.3) which are classified on the basis of (i) volume and grain size of available sediment, and (ii) the nature of the supply system (number of input points) based on work by Reading & Richards (1994) and Stow *et al.* (1996). Gradations between the individual models are common. However, the long-reigning single universal model encompassing all aspects of deep-water clastic systems has been abandoned (Normark 1991; Walker 1992; Miall 1999).

Architectural elements, hierarchies and geometries

Because many models of deep-water clastic systems proved to be too broad to place observed subenvironments into context, attempts were made to break systems down into their fundamental building blocks, or architectural elements (Miall 1999).

The concept of elements as the main building blocks which is equally applicable to modern and ancient submarine fan systems was put forward by Mutti & Normark (1987). They introduced five unique elements characterised by a suite of sedimentological features: (i) channel deposits, (ii) scours, ranging in size from large slope scours to macro-scale ones, (iii) lobes, which are defined as non-channelized sandstone deposits, (iv) channel-lobe transition zone, which contains features of both the channel and the lobe environment and (v) overbank deposits which are in lateral associations with the channel environment. Other approaches

Their scheme was further developed by Stow (1985a) and Pickering *et al.* (1986) who produced a scheme with classes, groups and facies with organised and disorganised groups and new classes (chaotic units and hemipelagites, oozes, chalks and cherts). Ghibaudo (1992) uses a descriptive scheme using 13 facies and 22 subfacies which are distinguished mainly on the basis of sediment type, i.e. grain size and composition, while subfacies further describe internal structures.

Deep-water clastic facies models

In the 70's, two approaches were developed i) ancient fan models based on outcrop studies (Mutti & Ricci Lucci 1972) and ii) models based on the study of modern submarine fan systems (Normark 1970). Both approaches were combined to a simple, all-purpose fan model by Walker (1978), the extended suprafan model where the feeder channel, upper fan, mid-fan/suprafan lobe

which are based on Miall's (1985) classification scheme were developed (Pickering *et al.* 1995). Here, an architectural element is defined as a lithosome characterised by its geometry, facies composition, and scale representing a particular process or suite of processes occurring within a depositional system. The architectural geometries are independent of scale and facies.

Stow & Mayall (2000) summarise the presently recognised architectural elements (fig. 1.4):

- hiatuses, erosional plains and other bounding surfaces
- erosional slide and slump scours.
- canyons, troughs, channels and gullies.
- channel levees and overbank deposits.
- depositional lobes (isolated, clustered, splay).
- irregular mounds (slide, slump and debrite masses).
- contourite drifts (elongate mounded, irregular patch, contourite-fan).
- sheets and drapes on slopes, basins, fans and drifts.
- megaturbidites and other megabeds
- tectonic features (growth faults, diapirs, compressional fault mounds).

Each element may occur at a range of scales and within a hierarchy of similar features. The sedimentary composition, including facies associations and vertical sequences, that make up any one element, can vary, typically within a limited range.

This "element" approach has initially caused confusion since the scale (from turbidite bed to turbidite complex (basin-fill scale), features (map-type or packets of beds) and stacking pattern have been used loosely by different systems. However, Stow & Mayall (2000) believe that for both outcrop studies and reservoir characterisation the "element" approach is an important one to follow, being ever mindful of the scale and stacking pattern of individual elements.

1.3.1 Lobe deposits

The term 'lobe' covers a wide spectrum of depositional facies associated with submarine fans. It originates from the lobate bulge first identified from *modern* submarine fan systems (Normark 1970). In *outcrop* this large-scale geometry is not readily recognised, often only inferred to be lobate, and Mutti & Ghibaudo (1972) and Mutti & Ricci Lucchi (1972) and Mutti & Normark (1987, 1991) presented field criteria to recognise them. These criteria are primarily based on vertical bed stacking patterns and facies associations. In the *subsurface*, lobe deposits have frequently been recognised (Mitchum 1985; Hewlett & Jordan 1993; Mitchum *et al.* 1993). Their planform geometry is readily distinguished on seismic data, but core information calibrated with interpretations of wireline logs are commonly used to interpret the depositional environment (Bryant & Flint 1993). Here, the recognition of bed boundaries plays an important role (e.g. Pickering *et al.* 1995; Reading 1996; Hurst *et al.* 1999).

Not only is it difficult to tackle the problem of identifying 'lobes' in ancient and modern systems as well as recognising them in the subsurface, but inadequacies with respect to the existing terminology and criteria for submarine fan lobes, their implications for different lobe models and the resulting reservoir geometry exist. Shanmugan & Moiola (1991) discuss the common 'lobe' terminology (fig. 1.5):

- a) The *braided suprafan lobe* is composed of stacked channel sand bodies with good lateral and vertical communication forming excellent reservoir facies.
- b) *Fanlobes*, which refer to meandering channels and associated levee facies of large mud-rich submarine fans (e.g. Mississippi Fan), are characterised by offset stacked sand bodies with poor lateral and vertical communication.
- c) *Ponded lobes* are representing mud-rich slump facies of slope environments, comprising generally poor reservoir facies because of their low sand content and poor sand-body connectivity.

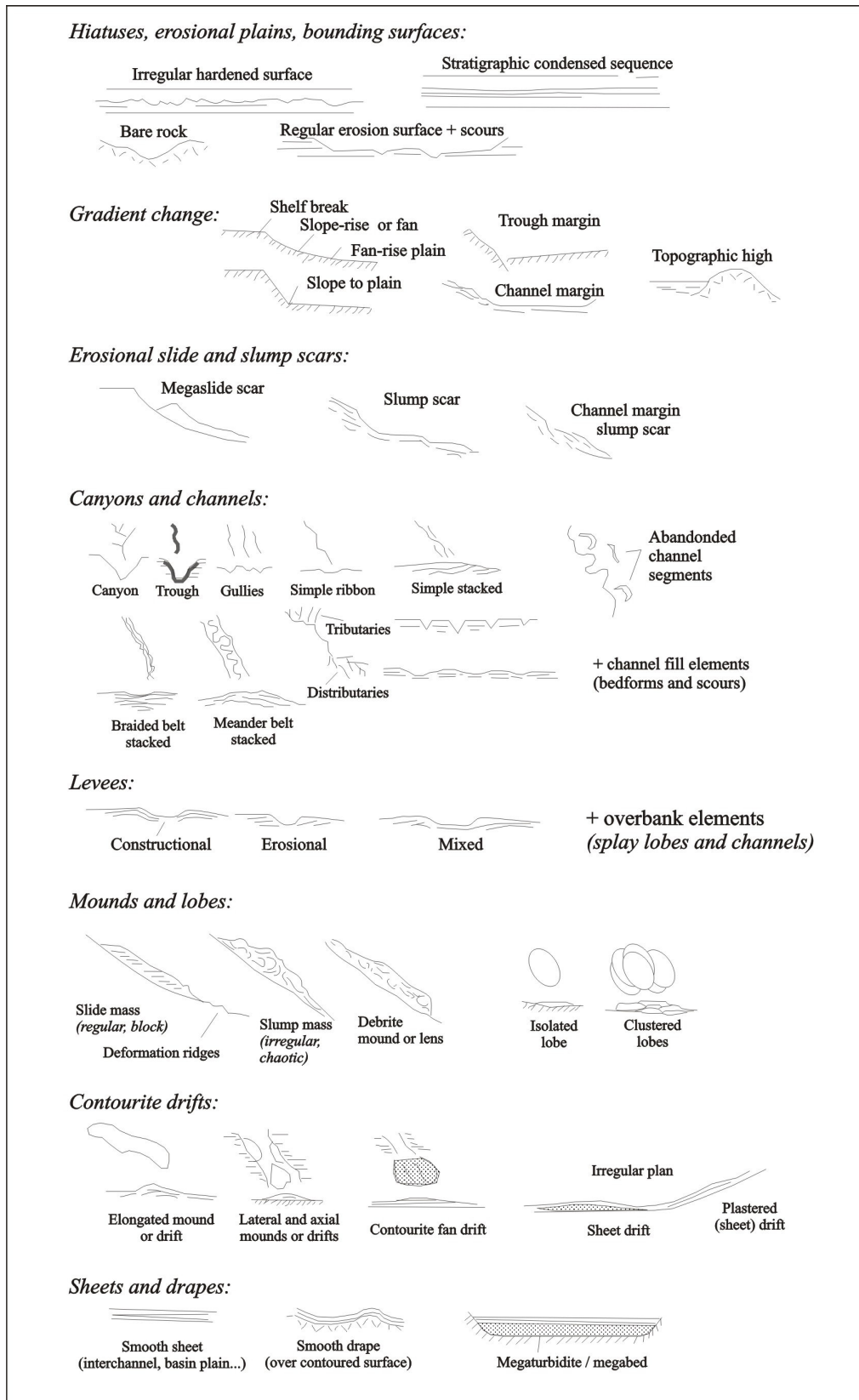


Fig. 1.4: The principle architectural elements in deep-water systems (from Stow & Mayall 2000).

- d. The term *depositional lobe sensu* Mutti & Normark (1987, 1991) is applied to the non-channelized, laterally extensive sheet-like sandbodies observed in the field with good lateral and moderate vertical communication. They were first described from the Miocene Bobbio Formation / Italy by Mutti & Ghibaudo (1972). They are typically located in the outer fan environment *sensu* Mutti & Ricci Lucchi (1972).

The main characteristics of ancient depositional sandstone lobes are:

- packages bounded by even, parallel surfaces of thick, relatively coarse-grained sandstones, commonly 3-15 m thick.
- isolated bodies within mudstone sequences of few kms to several 10s of kms basinward extend.
- basin-wide features exhibiting abrupt onlap terminations with the slope facies and forming convex-upward bodies wedging gradually into thinner-bedded lobe-fringe deposits.
- exhibit grading (Bouma sequence) and vertical development of internal structures.
- show superposed, small-scale thickening-upward sequence, composed of a limited number of beds (<10; = compensation cycles).
- commonly display planar scours, chaotic impact features and rip-up clasts.
- They represent the maximum reach of sand transported into basin.

Ultimately, the size and appearance of lobe deposits are recognised to be a function of the size of the system, the basin size and its configuration and the volume of individual turbidity currents. Lobe deposits can therefore have very different dimensions and shapes (Mutti & Normark 1987, 1991; Normark *et al.* 1993) with the underlying topography having a major effect on their development (Schuppers 1995).

Outcrop and subsurface studies illustrated the difficulties of applying the term 'lobe'. In practice there may be a tendency to infer the presence of lobes when one lacks evidence for channels.

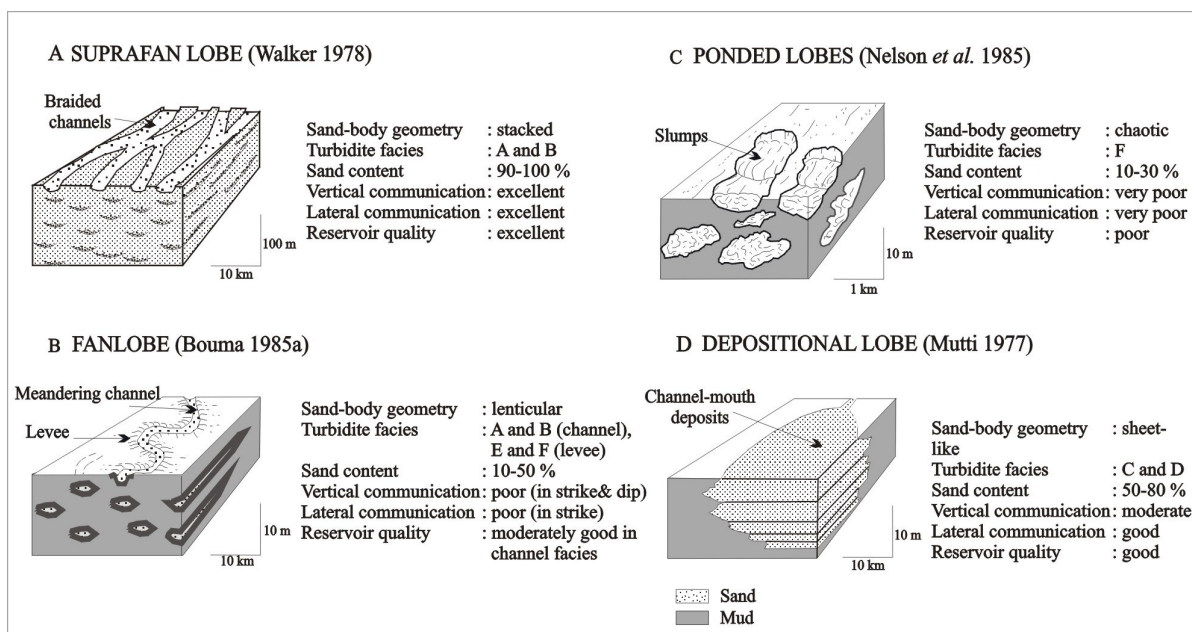


Figure 1.5: Conceptual models showing 3D sand-body geometry of (A) suprafan lobes (e.g. Upper Miocene Capistrano Formation, California), (B) fanlobes (e.g. modern Mississippi fan, Gulf of Mexico), (C) ponded lobes (e.g. modern Ebro fan, Mediterranean), and (D) depositional lobes (e.g. Eocene Hecho turbidite system, Spain) with their generalized reservoir properties. Turbidite facies nomenclature after Mutti & Ricci Lucchi (1972), sand content information from cited examples (from Shanmugam & Moiola 1991).

1.4 Field areas, database and methods

1) Outcrop study: E-Fan, Cingöz Formation

Field area and database

The field area, approximately 400 km², comprises the eastern fan (E-Fan) of the Cingöz Formation. It is located about 50 km north of Adana, S-Turkey (fig. 1.6). The area is relatively densely wooded with the best outcrops occurring mostly along road cuts, locally deforested areas and rivers. Rare long lateral sections of several kilometres in length are exposed along hill sides. The beds generally dip gently southwards (10-20°) and show hardly any tectonic deformation. The outcrop quality is strongly affected by deep weathering, differential cementation and pervasive coating by lichens.

The submarine fan systems of the Cingöz Formation have not been studied in detail in terms of modern sedimentological approaches. First attempts were made by Gürbüz (1993) and Gürbüz & Kelling (1993), who concentrated on the general fan development, facies associations and provenance studies. This study utilised their work as a broad basis for a detailed sedimentological analysis, however, major amendments to the previous interpretations proved to be necessary (Kostrewa *et al.* 1997; Satur 1999; Satur *et al.* 1997, 2000). Topographic maps at the scale of 1:25000 were used for facies mapping and orientation in the field (Adana – Sheets N34 – b1 & b2, {subordinately: ‘b3’ & ‘b4’}, Series K816, Edition 2THGK, 199).

a) Facies mapping

Facies mapping was carried out in order to establish fan/slope and channelized/non-channelized facies relationships. The mapped units are differentiated into channelized and non-channelized fan sediments, large-scale debris flow units, slope and carbonate platform deposits. Mapped units correspond to those differentiated by Gürbüz (1993) and Satur *et al.* (1997), the latter having carried out the bulk of the mapping in the NW area of the E-Fan, comprising the channelized unit.

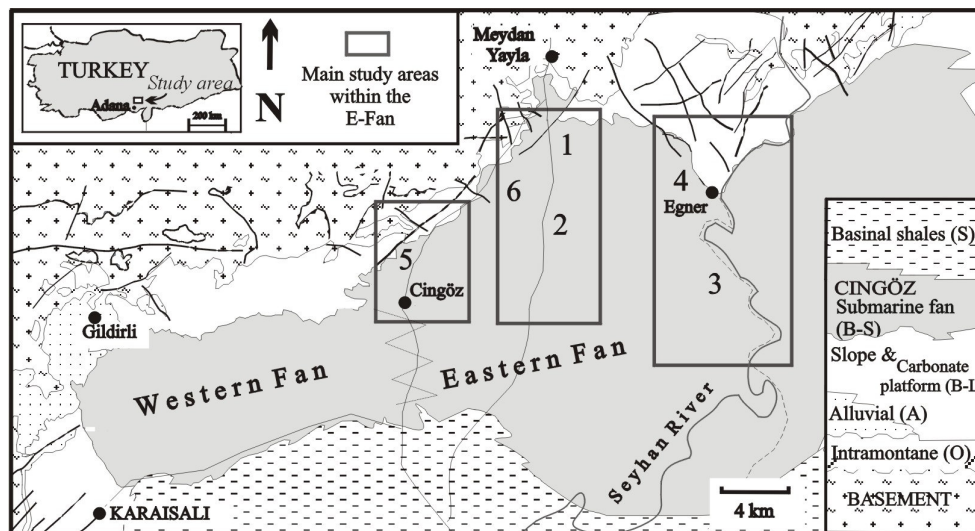


Figure 1.6: Main study areas within the E-Fan of the deep-water clastic Cingöz Formation, Northern Adana Basin, S-Turkey (modified after Gürbüz 1993). Numbers 1-3: non-channelised sandy sections; 4 & 5: fan-slope contact; 6: transition channelised / non-channelised deposits. Basement: , intramontane , alluvial, slope and carbonate platform, deep-water fan, basinal shales. O = Oligocene, A = Aquitanian, B = Burdigalian, L = Langhian, S = Serravallian.

b) Logging

Three N-S cross-sections were logged initially at a scale of 1:100, concentrating on the primarily non-channelized sandy deposits to provide an overview and refine the previous fan-framework in order to tie in the detailed key study areas. Information from the channelized units was used from Satur *et al.* (1997) and

for the more distal, less sandy and less well exposed sections of the fan system from Gürbüz (1993). The Bouma (1962) and Lowe (1982) classification systems were largely applied.

The key study sections were chosen based on a) exposure, b) accessibility and c) location within the fan system. Six main study areas were defined: three fairly well-exposed primarily non-channelized sandy sections of relatively large extent (fig. 1.6; no. 1-3), two sections studying the fan-slope contact (fig. 1.6; no. 4-5) and one analysing the transition between the channel-fill and non-channelized deposits (fig. 1.6; no. 6). Logs were initially recorded at scales 1:10 and 1:20 with even the smallest sedimentological structures observed included.

c) Lateral logging

The technique of lateral logging is tested to qualify and quantify small-scale sedimentological variations within individual sandstone beds and packages of sandstones in the distal lobe environment where the outcrop quality is relatively good (fig. 1.6; no. 3). Three sections were selected, their length varying between 10 to 45 m. The following procedure was carried out:

- A) selection of sandstone beds based on sufficient lateral extent and accessibility in already identified depositional sub-environments.
- B) superimposition of a horizontal grid (1m spacing) and data recording to a resolution of 0.5 cm.
- C) recorded data: bed thickness, grain size, internal structures (stratification), dish structures, shale clasts (type, amount), bioturbation (horizontal, vertical, infill), amalgamation planes (length, type, with / without clay drape), sole marks (type, amount) and scours (width, depth, infill).
- D) calculated data: net:gross ratio, % sand, % shale.
- E) quantification of data within grid spaces are represented by histograms and/or distribution curves in order to obtain information of lateral net:gross variability.

The analysis provides additional information about small-scale heterogeneities with respect to the continuity and connectivity within individual sandstone beds and/or packages.

d) Biostratigraphy

A well established biostratigraphic framework based on planktonic foraminifer exists for the western and central part of the E-Fan (Nazik & Gürbüz 1992; Gürbüz 1993) whereas the eastern section (fig. 1.6; no. 3) has neither been logged nor sampled before. Ten biostratigraphic samples were taken to broadly tie this section into the overall framework. The irregular spacing of the sample points was determined by accessibility and exposure of sediments.

2) Subsurface study: S10 interval, Scapa Sandstone Member, Scapa Field

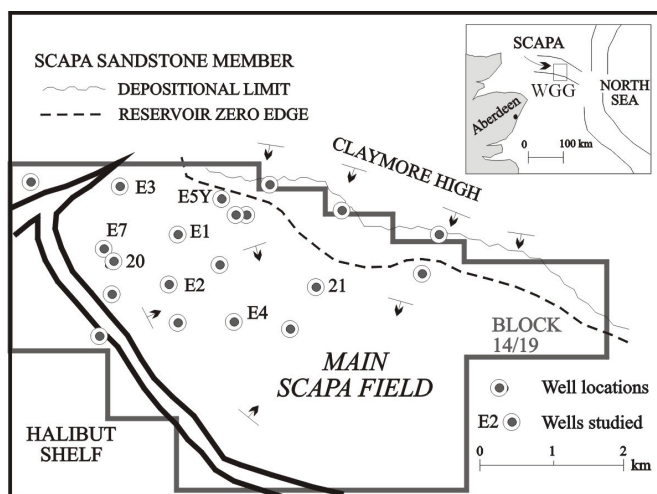


Fig. 1.7: Wells studied and their location in the Scapa Field, Block 14/19 Witch Ground Graben, North Sea (after McGann *et al.* 1991).

Study area and data base

The Scapa Field is located in UK block 14/19 in the Witch Ground Graben (WGG) of the Outer Moray Firth, approximately 175 km north east of Aberdeen (fig. 1.7), in a water depth of 385 feet (120m).

Cores, well data and unpublished internal reports (structural maps, stratigraphic cross sections, biostratigraphic charts, stratigraphic columns, reservoir unit correlations) were provided by Elf Occidental Caledonia Ltd., Aberdeen. They form the basis of this study in conjunction with published literature.

Eight wells of the Main Scapa Field were selected for studies, based on the recorded presence of the S10 interval (Appendix 1: wells and logged intervals). The

biostratigraphic subdivision of the Scapa Sandstone Member (SSM) is based on dinocyst taxa (well reports; Riley *et al.* 1992). Two wells (E3, E4) comprise undifferentiated S10 subzones, while wells E2 and E7 are known to contain the S10 interval but no biostratigraphic differentiation. For the overall analysis of the depositional model, the S10 interval with its subdivisions were utilised.

Core Logging

Cores were logged at an initial scale of 1:20 and a total of 785 feet (238 m) true stratigraphic thicknesses (TST) of the S10 interval were logged, as well as 250 feet (76 m) of undifferentiated Scapa Sandstone Member which are presumed to be part of the S10 interval. In none of the wells, the complete S10 interval was cored.

Small scale structures and very thin beds were retained in the smaller scale and may therefore appear exaggerated (enclosure 1).

All wells are deviated from the vertical by varying degrees. Core logging was carried out in drillers' depth (feet) and conformed to log depth (feet) for the overall representation of the wells. Thicknesses have been calculated according to conversion factors provided by Elf Enterprise Caledonia Ltc. and given in metric TST throughout the text.

a) Lithofacies and facies associations

It became necessary to establish a refined lithofacies scheme to incorporate all the observed lithologies and sedimentary structures. The scheme generated 6 different lithofacies groups with 20 subtypes. Elf Occidental's internal reports provided additional information on the petrography, diagenesis and poro-perm characteristics of the studied rocks. Lithofacies distribution patterns were established, analysed and facies associations determined.

b) Wireline data

Wireline data were provided by Elf Occidental at a scale of 1:40 and 1:200. Log readings of calliper (CL), gamma-ray (GR), sonic log (SL), resistivity log (RT), density (DL) and neutron log (NL), presented on logging depth and true vertical thickness (TVT) depth scale, were utilised (*see* Rider 1996) for detailed description of the application of wireline logs). In this study, the wireline log information was used for:

- a) characterisation of the differentiated lithofacies.
- b) obtaining approximate lithologies and trends from gaps in the lithology logs which are due to missing core sections (10 to 350 cm thick gaps) calibrated with information obtained from a) and to broadly identify lithologies from uncored parts of the S10 interval.
- c) electrosequential analysis *sensu* Rider (1996) for the identification of distinctive trends within the S10 interval in conjunction with identified lithofacies sequences for interwell comparison.

d) Statistical analysis

A variety of statistical methods were used to determine trends within the sandy successions. Since long strings of data are required for consequential analysis, only 4 wells were tested: E1, E2, E5Y and E7.

- Facies relationship diagrams (Selley 1969; Reading 1996), a visual appraisal of data to test sequential or non-sequential facies relationships in order to determine the most common facies transitions.

For the above methods, lithofacies groups (n = 6) rather than types (n = 20) were used to get meaningful, predicative trends.

- Bed thickness analysis by RUNS analysis (Davis 1986; Murray *et al.* 1996) where asymmetric bed thickness trends can be tested for:
 - a) RAM: 'runs about median' (record '1' for bed thicker than median, '0' for thinner than median) used for sequence grouping of thick or thin beds
 - b) RUD: 'runs up and runs down' (an observation exceeds or is smaller than the preceding observation)
 - i) compare bed with preceding one (1 = thicker; 0 = thinner)

- ii) compare averaged thickness of next two succeeding beds with preceding one (1 = thicker; 0 = thinner) [two bed moving average after Heller & Dickinson (1985)]
used for the identification of upward thickening and upward thinning bed cycles

Both RAM and RUD calculations were carried out.

Davis (1986), Reading (1996), Murray *et al.* (1996) and Chen & Hiscott (1999a) discuss the common pitfalls in the application of statistical analysis and this study is sensitive to their comments when interpreting the results

2 CHARACTERISATION OF LOBE DEPOSITS IN OUTCROP: E-FAN, CINGÖZ FORMATION, S-TURKEY

2.1 Geological background

2.1.1 Location and setting

The Miocene Cingöz Formation forms part of the thick Tertiary infill of the southern Turkish Adana Basin in a tectonically complex collisional setting. The basin is bound by the Ecemiş Fault Zone in the west, the Misis Structural High in the southeast and the overthrust Tauride Orogenic Belt in the north (Williams *et al.* 1995; fig. 2.1). The basin forms the northern part of the greater Çukurova Basin, separated from its southern part, the Iskenderum Basin, by the NE-SW trending Misis Structural High (Kelling *et al.* 1987). The Çukurova Basin extends submarine to Cyprus as the Cilicia-Adana Basin (Williams *et al.* 1995).

The Çukurova Basin is located entirely on the Anatolian Plate (Williams *et al.* 1995) above the zone of Cenozoic suturing between the Afro-Arabian and the Euro-Asian plates (Sengör & Yilmaz 1981; Dewey *et al.* 1986). The age of the plate collision is not established, various authors assigning different ages to it: Late Cenozoic (Kelling *et al.* 1987), Early Miocene (Jackson & McKenzie 1984), Middle Miocene (Sengör 1979) and has most recently suggested to be of Eocene to Miocene age (Hempton 1982; Yilmaz 1993).

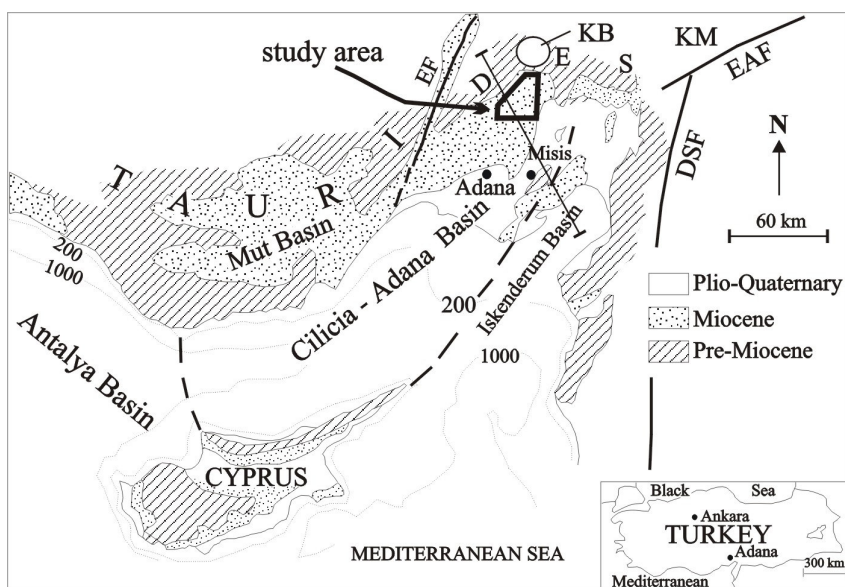


Figure 2.1: Map for the northeastern Mediterranean region showing the general geological setting and the main localities: DSF = Dead Sea Fault; EAF = East Anatolian Fault, EF = Ecemiş Fault zone; KB = Karsanti Basin; KM = Kharamanmaras (from Yetis *et al.* 1995). Box: location of study area. Line: NNW-SSE cross-section of figure 2.2.

The structural evolution of SE Turkey is controlled by the interaction of several major wrench faults in the Kahraman Maraş triple junction (fig. 2.1), the N-S trending Dead Sea fault zone (Africa-Arabia), the NE-SW trending Bitlis Suture (Arabia-Eurasia) and the eastern part of the Hellenic Trench (Africa subducted under Eurasia) (Williams *et al.* 1995). The Adana Basin is thought to have formed as a result of the incompatibility problems arising at this triple junction (Hempton 1982; Robertson 1998). Gökçen *et al.* (1988) suggest that the basin originated as a perisutural foreland basin which subsequently developed into a transpressional basin

complex related to the creation of the Kahraman Maraş continental triple junction (Sengör *et al.* 1985; Görür 1992; Ünlügenç 1993). A variety of other basin types have been suggested to fit the observed tectonic and sedimentary configuration of the Adana Basin, they include fore-arc basin (Aktaş & Robertson 1984; Aksu *et al.* 1992; Görür 1992), extensional fore-arc basin (Jackson & McKenzie 1984), back-arc basin (Floyd *et al.* 1992), foreland basin (Kelling *et al.* 1987; Williams *et al.* 1995) and a flake and plate triple junction compatibility basin (Dewey *et al.* 1986).

In the Adana Basin, the basement units, consisting of an ophiolite complex and Palaeozoic and Mesozoic rocks, are unconformably overlain by an approximately 6000 m thick Cenozoic succession (fig. 2.2; Yetiş & Demirkol 1986; Görür 1992). No *in situ* Palaeocene and Eocene rocks are known. The Cenozoic sedimentation appears to begin with a group of redbeds of Oligocene age best developed in the Karsanti Basin, immediately north of the Adana Basin (Ünlügenç *et al.* 1992). Today, Tertiary units outcrop mainly in the northern part of the basin, whereas Quaternary deposits are exposed on its southern side (fig. 2.1). Generally, the Tertiary deposits exhibit complex lateral and vertical facies relationships (Yetiş *et al.* 1995).

2.1.2 Tectono-sedimentary evolution and stratigraphy of the Adana Basin

The initiation of the Adana Basin probably took place after the late Eocene to Oligocene thrust emplacement of an ophiolitic complex in the Taurides to the north of the basin (Williams *et al.* 1995; fig. 2.3). The formation of the foredeep was probably caused by southward compression and thrusting (Williams *et al.*

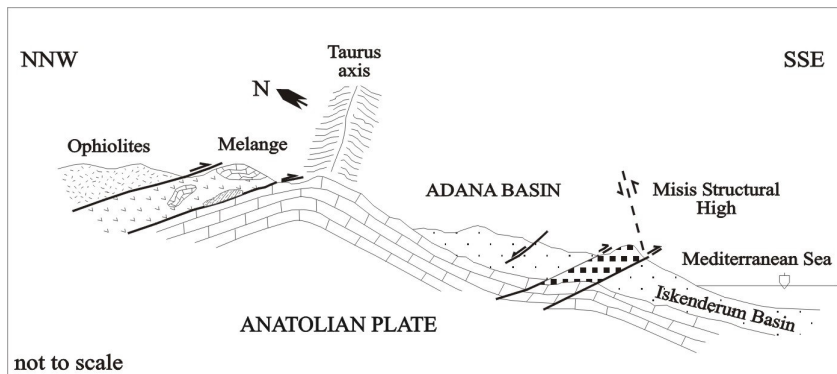


Figure 2.2: Generalised structural cross-section across the Adana Basin, Misis Complex and Iskenderum Basin (from Ünlügenç 1993). Location of cross-section marked in figure 2.1.

1995) or regional crustal extension and detachment faulting (Karig & Kozlu 1990). Robertson (1998) proposes a combination of these effects suggesting that regional convergence was partially adsorbed by crustal shortening to the north, and subduction 'roll-back' to the south, thus explaining why the Adana Basin shows some features akin to a foreland basin but without evidence of a preserved thrust load.

The Cenozoic development of the Adana Basin can be subdivided into an upward succession of pre-transgressive, transgressive and regressive character (Yetiş *et al.* 1995) which roughly corresponds to megasequences identified by Williams *et al.* (1995) (fig. 2.4). These megasequences are separated by distinct sequence boundaries visible in the subsurface data. In the Eocene, ophiolitic thrust sheets were obducted in a southerly direction, thereby overriding an ophiolitic melange (fig. 2.3). During the early Oligocene, erosion and planation of these thrust sheets took place. In the late Oligocene extensional faulting in the north of the region occurred creating major half-graben settings (Williams *et al.* 1995; Robertson 1998). This was controlled by deep-rooted basement faults that cut and displaced the thin-skinned ophiolitic thrust sheets. In these half-grabens continental sediments were deposited, the alluvial to lagoonal redbeds of the **Karsanti Formation** and the alluvial to coastal **Gildirli Formation**. They form the pre-transgressive deposits of Yetiş *et al.* (1995) (fig. 2.3; 2.4). The Karsanti Formation is dominantly exposed in the Karsanti Basin.

Following a regionally extensive phase of tectonic compression, a major marine transgression commenced in the late Oligocene in northern Cyprus and in the early Miocene in adjacent southern Turkey. During this time, continental deposition continued only in the area of the Ecemiş Fault Zone (Yetiş *et al.* 1995).

In the Miocene (Aquitainian and Burdigalian) minor extensional faulting occurred which William *et al.* (1995) believe to result from renewed thrust activity in the Taurides to the north. Robertson (1998), however, suggests regional extension originating to the south to be responsible. During this time reef growth began on the top of fault blocks (**Karaisali Formation**; fig. 2.3).

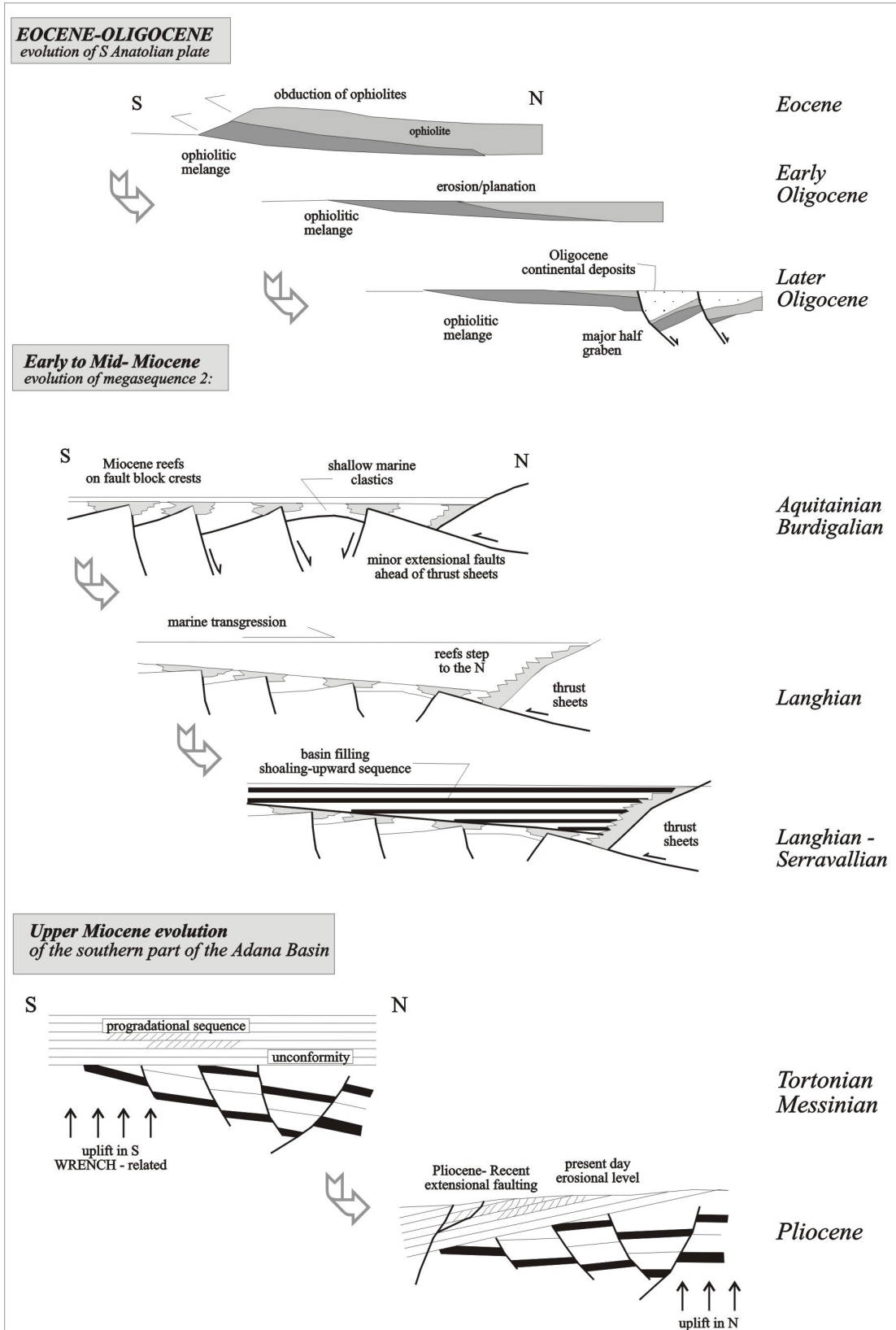


Figure 2.3: Eocene to mid-Miocene evolution of the northern Adana Basin and upper Miocene evolution of the southern Adana Basin (redrawn from Williams *et al.* 1995).

The continued deepening generated a deep underfilled basin. The relatively high sea level of this transgressive phase caused the northward migration of the carbonate reefs (**Karaisali Formation**) (Williams *et al.* 1995; Yetiş *et al.* 1995; Robertson 1998). The shallow marine, fossiliferous clastic deposits of the **Kaplankaya Formation** are associated with the reefal and slope environment (Görür 1979, 1992; Yetiş & Demirkol 1986; Nazik & Gürbüz 1992; Gürbüz 1993).

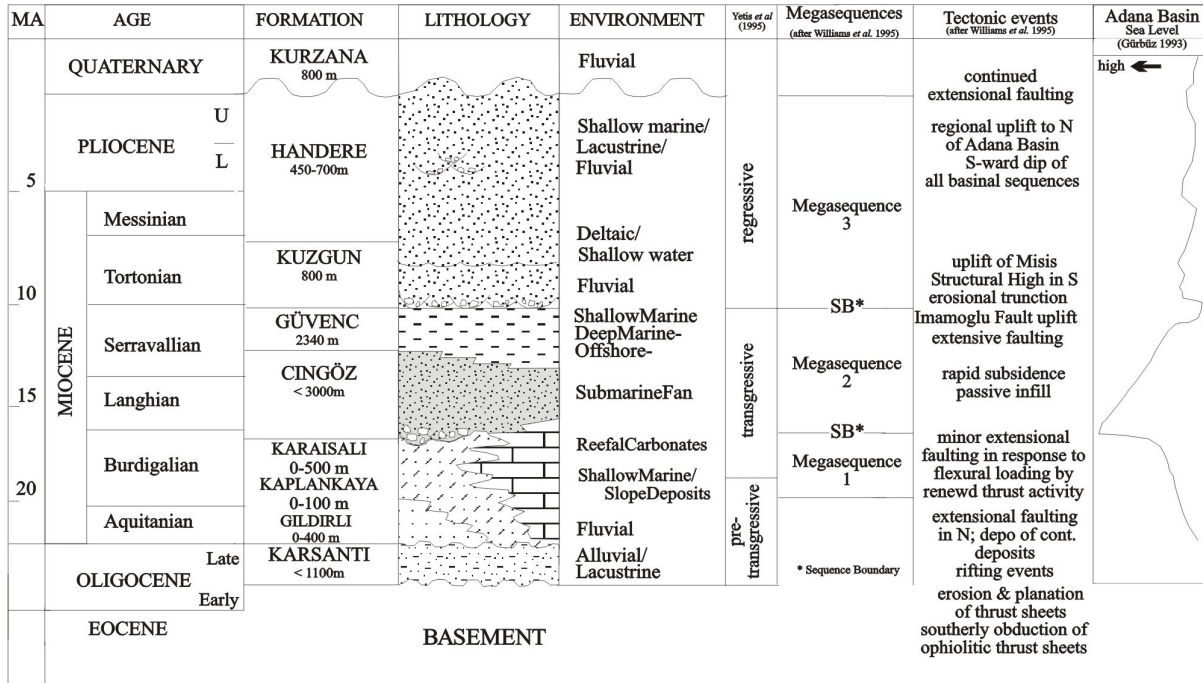


Figure 2.4: Generalised stratigraphic columns of the Adana and Karsanti Basin. Compiled from Nazik & Gürbüz (1992), Gürbüz (1993), Yetiş *et al.* (1995) and Williams *et al.* (1995). Gürbüz (1993) used time scale of Harland *et al.* (1990), other authors put the Langhian age from 16.5 to 15 MA (Robertson 1998) or 21.5 - 20 MA and a top Serravallian age of 15 MA (Haq *et al.* 1987a).

The basin is then filled with a shoaling upward sequence of turbidites (**Cingöz Formation**) and deep marine basinal shales (**Güvenç Formation**) during late Burdigalian, Langhian and Serravallian times (Ünlügenç *et al.* 1992; Gürbüz 1993). The deep-water clastic system shows no syntectonic sedimentation effects in seismic profile. Its seismic character reveals aggradation consistent with the passive infill of an underfilled foreland basin (Ünlügenç *et al.* 1992; Williams *et al.* 1995). The geometric and stratigraphic facies relationships are very complex. The **Cingöz Formation** is partly coeval with and partly superimposed on the **Kaplankaya**, **Karaisali** (both: Burdigalian-early Serravallian: Yetiş 1988) and **Güvenç Formations** (Burdigalian-Serravallian: Özelik 1993) (Yetiş *et al.* 1995) largely representing lateral facies variations of each other passing from the subaerial alluvial facies of the **Gildirli Formation** to alluvial fan, fan delta and shallow marine facies of the **Karaisali** and **Kaplankaya Formation** in to deep-marine facies of the **Cingöz** and **Güvenç Formation** (Satur 1999). The latter is younger in its upper units, transgressing over the **Cingöz**

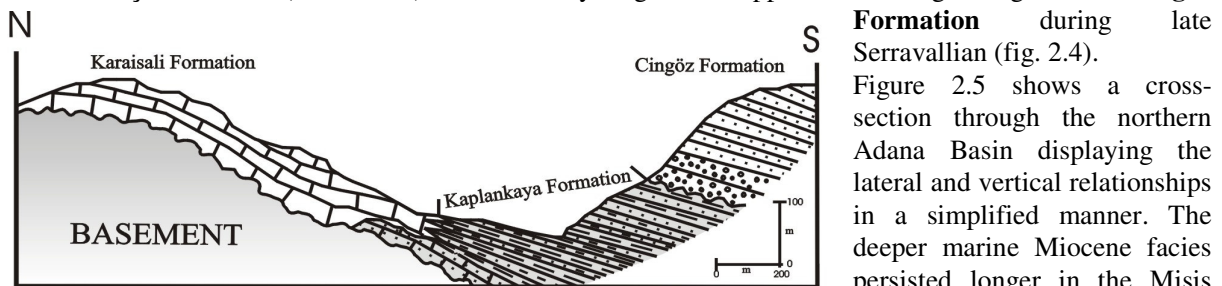


Figure 2.5: Schematised geometric and stratigraphic relationship between the basement rocks, the Karaisali, Kaplankaya and Cingöz Formation in the northern Adana Basin from Gürbüz (1993), modified after Yetiş & Demirkol (1986).

transgressive units after Yetiş *et al.* (1995), and based on their seismic character, the first two megasequences of Williams *et al.* (1995; fig. 2.4).

During the Late Miocene (Tortonian to Messinian) the uplift of the Misis Structural High in the south caused erosion of the basin fill prior to the deposition of continental deposits. The shallow marine and terrestrial clastics of the **Kuzgun Formation** and the predominantly fluvial **Handere Formation** reflect the shoaling of the basin (third megasequence of Williams *et al.* 1995). The Imamoglu Fault Zone to the east is reactivated as a positive flower structure during and after the deposition of continental deposits (Sengör & Yilmaz 1981; Kelling *et al.* 1987; Karig & Kozlu 1990).

Later, regional uplift to the north of the basin generates a 15 - 20° southern dip on all basinal sequences resulting in the present day geometry of the basin (fig. 2.3).

The relative sea-level curve (fig. 2.4), which Gürbüz (1993) constructed for the Tertiary of the Adana Basin closely mirrors the Cypres and global sea-level curves of Robertson *et al.* (1991) and Haq *et al.* (1987a,b) respectively suggesting that the Cingöz Formation was deposited during regression which continued into the late Serravallian. However, Yetiş *et al.* (1995) more detailed analysis of the Neogene infill of the Adana Basin suggests that the Cingöz Formation was in fact deposited during gradually rising sea level, spanning from the lowstand of the alluvial to coastal Gildirli Formation to the highstand of the deep-marine Güvenç Formation (Satur 1999).

2.2 The Cingöz Formation

Traditionally, the Cingöz Formation is subdivided into 3 members: the conglomeratic Ayva Member, the sandstone-shale Topalli Member and the shale-dominated Köpekli Member (Schmidt 1961). Görür (1977) interpreted the Ayva Member to represent proximal and the Topalli Member to be distal turbidites. Yetiş & Demirkol (1986) later assigned the Köpekli Member to the Güvenç Formation. This study does not employ these local stratigraphic subdivisions but uses generic deep-water clastic terminology for a more general approach. Yetiş & Demirkol (1986) and Yetiş (1988) recognised the Cingöz Formation to consist of two sandy lobes within the Güvenç Formation which Ünlügenç *et al.* (1992) interpreted to be submarine fan deposits (fig. 2.6). Gürbüz (1993) and Gürbüz & Kelling (1993) acknowledged them to be two small, laterally coalescing submarine fan systems, which were deposited in a rapidly subsiding basin during late Burdigalian to early Serravallian times (fig. 2.7; Nazik & Gürbüz 1992). The Cingöz System was active for approximately 2.7 myr during which approximately 3000 m of sediments were deposited (Gürbüz 1993). Foraminiferal dating reveals an latest early to middle Miocene age (*Praeorbulina glomerosa curva*, *Orbulina suturalis* and *Globorotalia mayeri* zones / foraminiferal biozones PN8 – PN11), while calcareous nanoplanktons disclose an early-middle Miocene age (*Sphenolithus leterorphus* Zone [NN5]) to middle Miocene age (*Discoaster exilis* Zone [NN6]) (Toker *et al.* 1998). The Cingöz system is interpreted to have been deposited under temperate conditions with water temperatures gradually becoming colder due to influx of cold-water currents (Demircan & Toker 1998).

The Cingöz Formation extends from the Karaisali-Gildirli Line in the west to Memişli in the east and southeast (fig. 2.6), where its development is restricted by a probable structural high, the Imamoglu Fault Zone (Kelling *et al.* 1987). The total exposed area amounts to ~ 900 km². Seismic and borehole data [Gilbaş 2 Well: N 37°13'15"; E 35°25'28"] reveal the subcrop presence of approximately 1640 m of Cingöz deposits, overlain by 1190 m of basin plain sediments approximately 20 km southeast of Çatalan village (Naz *et al.* 1991; *pers. comm.* Naz 1997). The total southern extent is unknown. Seismic profiles present an aggradational character (Williams *et al.* 1995). Extensional faulting in the north and northwest (NE-SW and ENE-WSW trending faults) and in the northeast (NW-SE to NNW-SSE trending faults) is commonly observed, particularly throughout the northern Cingöz Formation (Ünlügenç 1993). Based on seismic data, Ünlügenç (1993) demonstrates that extensional events of three different ages have affected the basin fill i) early to mid Miocene, ii) late Miocene and iii) late Pliocene (“neotectonic stage”). However, it is difficult to relate the faulting events recognised in the field to the faults interpreted on seismic sections.

Gürbüz (1993) interpreted the Cingöz Formation to represent an active margin fan complex *sensu* Shanmugam & Muiola (1988) due to its small size, the narrow contemporaneous shelf and coastal zone and the coarse sediment load.

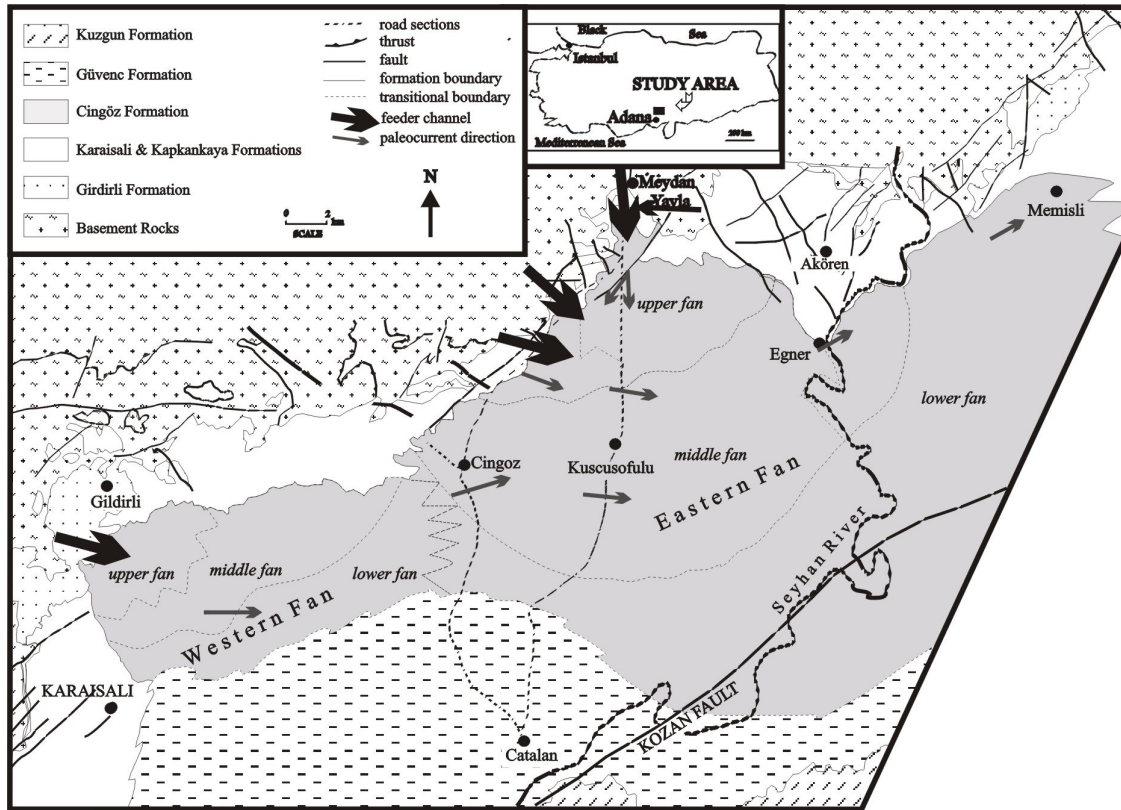


Figure 2.6: Geological map of the northern Adana Basin from Gürbüz (1993), modified after Satur et al. (1997).

2.2.1 The western and eastern fan

The two Cingöz fans, western and eastern fan after Gürbüz (1993), were fed by separate, incised feeder systems conveying gravel and sand from the adjacent, actively uplifted areas of the Tauride Orogenic belt, across a narrow (~ 3 km wide) carbonate platform (Karaisali Formation) into the basin. The western fan (W-Fan) was fed from the NW and the eastern fan (E-Fan) from the N and W (fig. 2.6; Gürbüz 1993; Satur 1999).

Both fans exhibit conglomeratic feeder-channel complexes, and into thick successions of turbidite sandstone and shale alternations in the basin (Görür 1977; Gürbüz 1993; Yetiş *et al.* 1995). But despite their contemporaneous deposition and some similarities, the development of the two adjacent fan systems differs (table 2.1).

The W-Fan is fed by one large feeder system which records a succession from alluvial fan and fan delta to deep marine sediments. The overall development is structurally and topographically controlled, showing a strong west-east confinement (Satur 1999). This conduit displays multiple phases of infilling indicating pulses of sediment supply. Apart from channel and lobe elements (Gürbüz 1993), non-erosional tongue-like sediment bodies were identified to be a major component of this fan system (Satur 1999).

The E-Fan is sourced by at least 4 feeder channels (fig 2.6: 3 main and 1 tributary feeders). These channels display multiple phases of infilling indicate initial deposition from fan deltas passing upward into non-channelized, sandy deeper water turbidites (Satur *et al.* 1997; Kostrewa *et al.* 1997; Satur 1999).

Gürbüz (1993) showed that at the early stage of the Cingöz system the western and eastern fan formed separate entities in late Burdigalian to early Langhian times. Western Fan progradation resulted in interfingering deposition during Langhian-Serravallian times (fig. 2.7) before retreating and their subsequent separation during the final stages of their development (late Serravallian). Satur (1999), however, believes W-Fan deposition to begin later and end earlier than the E-Fan one (table 2.1).

	WESTERN FAN	EASTERN FAN
Areal extent	~ 150 km ² exposed, eastern and subsurface extent unknown	~ 750 km ² exposed, southward subsurface extension at least 20 km
Stratigraphic thickness	maximum thickness around 1500m	maximum thickness around 3000 m
Feeder system	one sand-rich fairway	one main feeder and 3 tributary channels
Grain size	coarser at base	relatively less conglomeratic
Sequences	2 main megasequences	at least 8 (thinner) megasequences
Source and transport direction	sourced from NW ; transport towards SE	sourced from N, NW, W; transport towards SW in lower part, deflected to ENE in upper part
Development	lower stacked channel sequence and upper lobe dominated sequence, gradually passing upward into outer fan/basin plain but with some small channels and lobes	thick basal sequence of isolated channels, followed by lobes; during a second phase, small channel sequence followed by succession of lobe-dominated 'midfan' sequences
Time of activity (Nazik & Gürbüz 1992) *	late Burdigalian – Serravallian	late Burdigalian - Serravallian
Fan system after Mutti (1985a) through time (Toker <i>et al.</i> 1998; Satur 1999) *	1) absent (lower Langhian) 2) Type I: bulk sand depositon in channel-detached lobes 3) Type II: bulk sand deposition in channel- attached lobes and channel-fill sequences 4) absent (upper Serravallian)	1) Type I 2) Type II 3) Type II 4) Type III: channel-levee complex without lobes
Structural control	channel confinement; restriction to west basement structure to south	channel confinement; restriction to east by a probably structural barrier, shallowing to east
System tract after Posamentier <i>et al.</i> (1988)**	lowstand to transgressive / highstand system tract	lowstand to transgressive / highstand system tract
Ichnofossil assemblages	Cruziana	Mixed and Nereites
Environmental conditions	eutrophic (high organic productivity)	oligotrophic (low organic productivity)
Bathymetry	shallower (sublitoral zone; ~ 200m water depth)	relatively deeper (abyssal; (500) to > 2000 m water depth)

Table 2.1: Main features of the western and eastern submarine fans, compiled after Naz *et al.* (1991), Gürbüz (1993), Ünlügenç (1993), Toker *et al.* (1998), Demircan & Toker (1998) and **Satur (1999).

Petrographic studies of the conglomerates, the coarse- and medium-grained sandstones reveal subtle differences in the composition of the different fans reflecting their respective source areas (table 2.1 ; Naz *et al.* 1991; Gürbüz & Kelling 1993; Gürbüz 1993). This was confirmed by a recent geochemical pilot study (Satur 1999). The Early Cenozoic fold-thrust belt to the north of the basin with incorporated ophiolite bodies and magmatic arc rocks forms the major source (Gürbüz & Kelling 1993; Gürbüz 1993). Cronin *et al.* (2000) identified mixed siliclastic carbonaceous turbidites to be prominent close to the slope margin. W-Fan deposits accumulated to approximately 1500 m (table 2.1) while the E-Fan thickness amounts to 2500 m (Gürbüz 1993; fig. 2.8). It is thought that local basement topography, possibly created by local tectonics, played a major factor controlling the differences in dimension and thickness observed (fig. 2.9).

*Note the differing ages given for the inception of the Cingöz deep-water clastic system based on either foraminiferal (Nazik & Gürbüz 1992) or nanoplankton (Toker *et al.* 1998) dating. Satur (1999) utilises the nanoplankton biostratigraphy, while other workers in the Adana Basin prefer the foraminiferal-based biostratigraphy (e.g. Gürbüz & Kelling 1993; Gürbüz 1993; Yetiş *et al.* 1995; Cronin *et al.* 2000; this study).

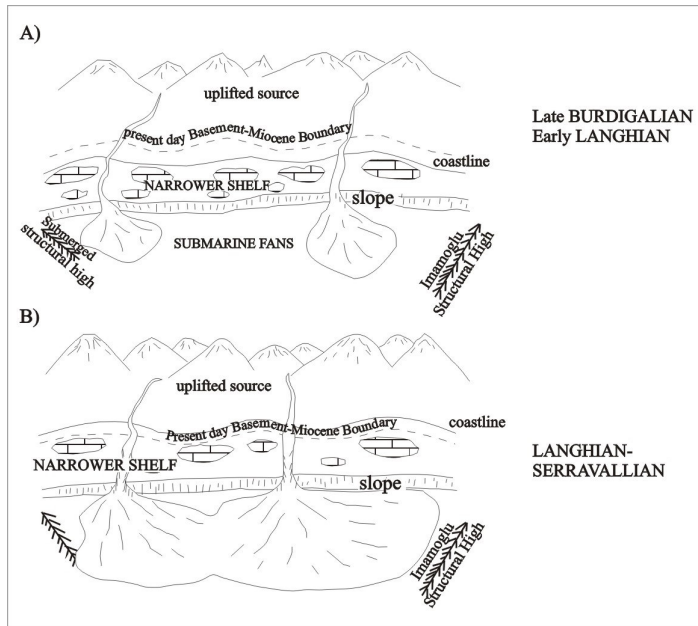


Figure 2.7: Schematic diagram showing the evolution of the Cingöz submarine fans in the northern part of the Adana Basin (from Gürbüz 1993).

Different rates of subsidence within the receiving basin sectors must have allowed these gross thickness changes and different accumulation rates in the same time interval (Gürbüz 1993; Ünlügenç 1993; Kostrewa *et al.* 1997).

Local topography further played a role in influencing the development of the individual systems. The prevalent transport direction of the W-Fan is towards the SE-E and remnants of Palaeozoic and Mesozoic rock to the W and SW (west of Karaisali) suggest a topographic high limiting growth towards this direction (Gürbüz 1993; fig. 2.6). Satur (1999) found a palaeotopographic high to the south to be responsible for the distinct, elongate W-E trend of the system. The extent of the E-Fan is restricted to the east and SE by a probable structural high, the Imamoglu Fault, with strike-slip character, which was active during the Miocene (Williams *et al.* 1995). Sedimentological evidence like facies variations and contrasting

palaeocurrents further support this (Gürbüz & Kelling 1993; Gürbüz 1993). On this structural high, shallow marine sediments accumulated with occasional slumping directed to the SW (fig. 2.1).

Trace fossil assemblages are diverse and abundant. The W-Fan is marked by the *Cruziana* ichnofacies which indicates eutrophic, well oxygenated and shallower water conditions. Seilacher (1967) and Frey & Pemberton (1984) assign this ichnofacies to the sublittoral zone, to 0-200 m water depth. The E-Fan contains mixed and *Nereites* ichnofacies assemblages indicating oligotrophic, less oxygenated, probably more restricted and relatively deeper water environments (table 2.1; Demircan & Toker 1998), which increased during deposition (Satur 1999).

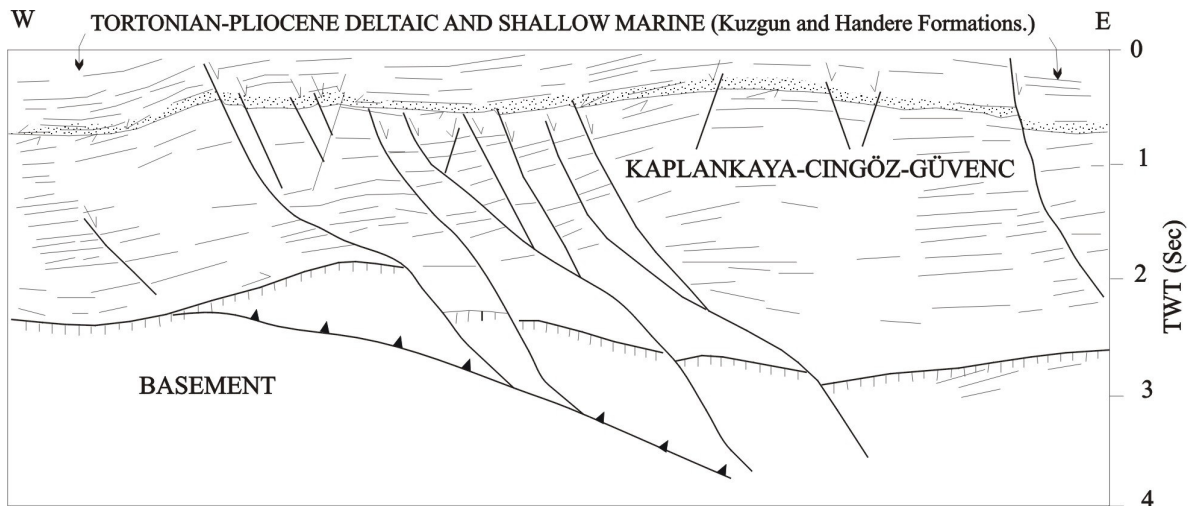


Figure 2.9: An interpreted seismic W-E line through the Kaplankaya, Cingöz and Güvenç Formations forming megasequence 2. It shows an aggradational nature of the reflectors and erosional truncations beneath megasequence 3 (top) in the west and central part of the line. Extensional faults with easterly component of downthrow are present (from Williams *et al.* 1995).

The Cingöz Formation is comprised of numerous vertically stacked, aggrading and prograding intervals formed during late Burdigalian - Serravallian age (Naz *et al.* 1991), which Satur's (1999) analysis of the channel-fill sequences of both the western and eastern fan confirmed. This study further supports these

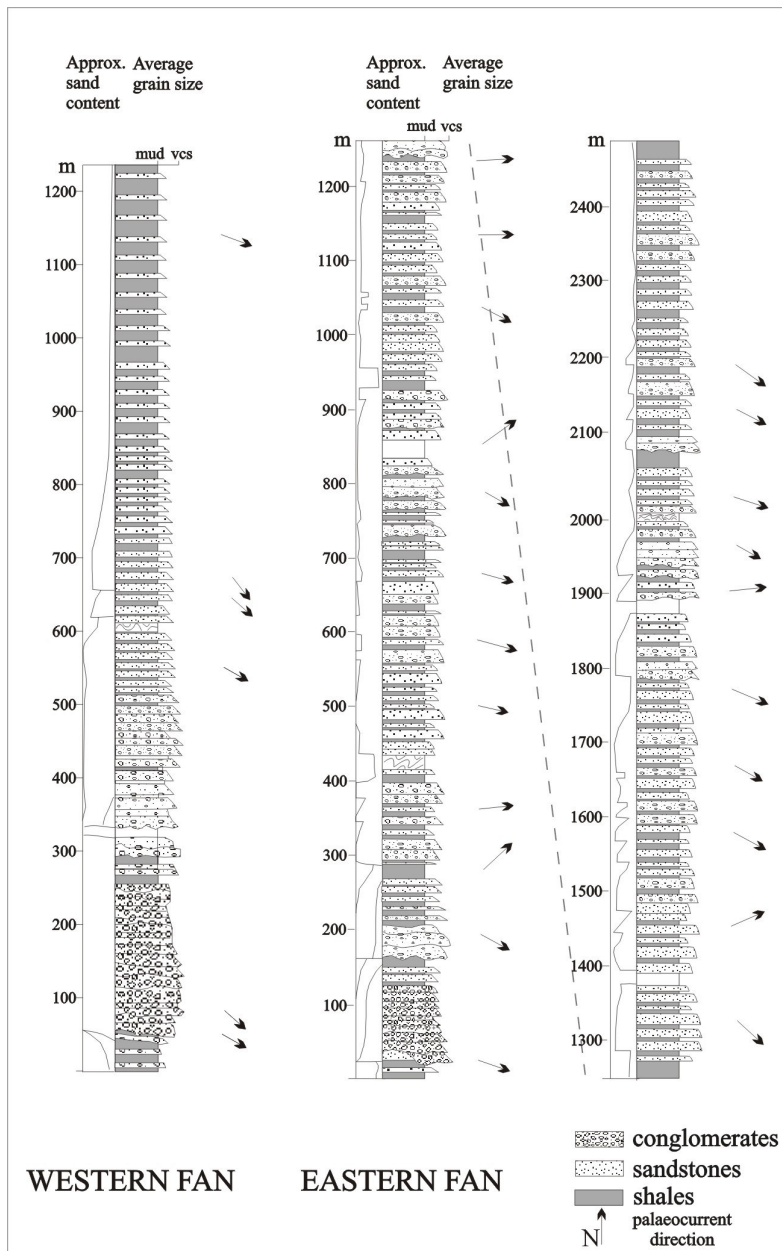


Figure 2.8: General logs through the western and eastern fan, Cingöz Formation (from Gürbüz 1993).

numerous investigations because of its well exposed and reasonably accessible channel-fill deposits. Recent studies include Gürbüz & Kelling (1993: provenance studies), Gürbüz (1993: palaeogeography, sedimentology, biostratigraphy), Ünlügenç (1993: regional and structural geology), Satur *et al.* (1997, 2000) and Satur (1999: proximal, channelized facies), Kostrewa *et al.* (1997: proximal and distal sandy, non-channelized facies) and Demircan & Toker (1998: trace fossil assemblages, palaeoenvironment) and Nazik & Gürbüz (1992) and Toker *et al.* (1998: biostratigraphy).

This study focuses on the primarily non-channelized sandy turbidites exposed in the northern and central fan area (fig. 2.10), their sedimentological character, their basic building blocks and subenvironments, and factors controlling their development. This necessitated a revision of the fan-framework to put the observed relationships into a new, improved context.

findings based on the analysis of the sandy non-channelized fan deposits of the E-Fan system (chapter 2.4). But while Naz *et al.* (1991) and Gürbüz (1993) suggest the Cingöz Formation to be an example of a typical lowstand fan system, Yetiş *et al.* (1995) and Satur (1999) believe the Cingöz Formation to be a good example of a fan system developing during a transgressive phase where local tectonics, the basin configuration and sediment supply are thought to have a fundamental influence on the development (Gürbüz 1993; Ünlügenç 1993).

Satur (1999) recently suggested to refer to the eastern and western fan of the Cingöz Formation as eastern and western area of a single Cingöz fan system, which are characterised by different depositional styles. However, this study retains the old names “eastern fan” and “western fan” which are compatible to the eastern and western area of Satur (1999).

2.2.2 Eastern fan framework

The eastern fan (E-Fan) is the larger of the two Cingöz fan systems. The total exposed area is approximately 750 km². It reaches from Cingöz in the west to Memişli in the east (fig. 2.6). The deposits in the far NE are believed to be of shallower origin (Ünlügenç 1993).

This fan has been the object of

2.2.2.1 Feeder channel systems

Previous studies suggested that the E-Fan was a single-sourced system with approximately 500 m of channel-fill deposits preserved (Gürbüz & Kelling 1993; Gürbüz 1993; *pers. comm.* Gürbüz 1996). Satur *et al.* 1997) and Satur (1999) investigated the spatial and temporal changes in facies and architecture of the proximal, channelized E-Fan. They found the fan to be sourced by at least 4 feeder channels (fig. 2.10). The north-south trending bypass channel 1 is the main feeder channel. Tributary channel 2 in the east believed to have been a shorter-lived subsidiary to the main channel (Satur 1999). Channels 3 and 4, which trend northwest-southeast and west-east respectively, are located at the northwestern margin (fig. 2.10).

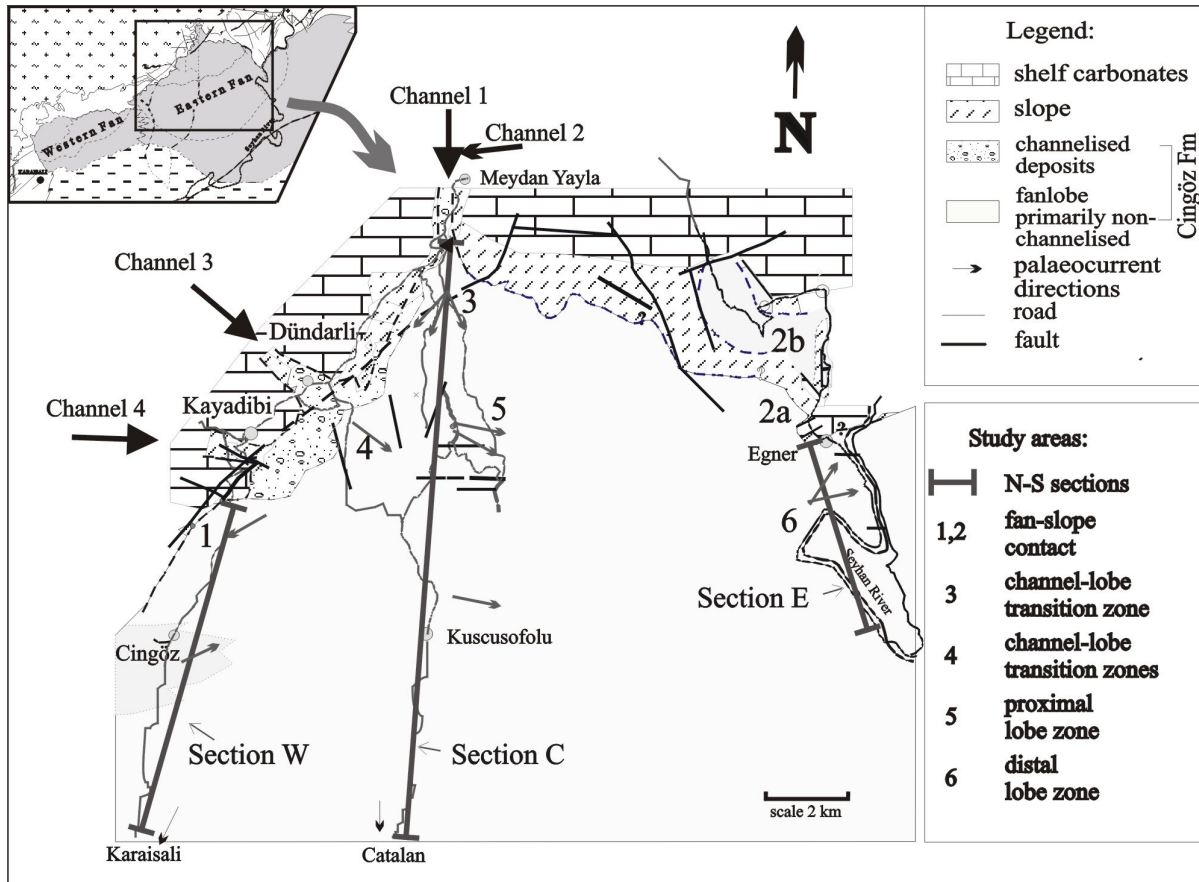


Figure 2.10: Geological map of the central and northern part of the exposed E-Fan and adjacent formations with location of key study areas (after Satur *et al.* 1997, Kostrewa *et al.* 1997, Gürbüz 1993 and Ünlügenç 1993).

Channels 1, 3 and 4 appear to be structurally controlled and the facies point to deposition from fan deltas that pass upward into deeper water turbidites. The channel 1 and 3 have similar clast lithologies, while channel 4 shows a discretely different lithology. A confluence area in the north-west suggests channels 1 - 3 to be partly coeval, while channel 4 became active at a later stage, partly eroding into and reworking channel 3 deposits (Satur 1999). The channel-fill of channel 1 records a mixed system where initial erosion is followed by a period of low sedimentation and deposition of clastic sheets. In a lateral, downcurrent direction, variations in the internal architecture and channel-floor gradient within a seven km depositional-dip section of channel 1 records changes in the hydraulic conditions with complex inter-relationship between the flow turbulence, erosion, gradient and confinement of the turbidity currents.

The channels range in size from 45 – 600 m in width and between 6 – 90 m in thickness of channel-fill deposits are preserved (Satur 1999). They pass upward into thick, sandy, predominantly non-channelized lobe deposits (Gürbüz 1993; Kostrewa *et al.* 1997; plate 2.1).

2.2.2.2 Facies distribution and architecture of the non-channelized E-Fan sections

Three overview logs were taken (table 2.2), recording the E-Fan deposits from the gravelly channel-fill and/or fan-slope contact in the north to the younger fan fringe sediments in a basinward direction to the south. They record the downcurrent as well as lateral development of the E-Fan sandy basin infill. Together with other study areas (fig 2.10; NW: transition channelized - non-channelized, WNW and NE: fan-slope relationship) and the detailed sedimentological study of various lobe depositional environments located in different fan positions (chapter 2.4), they provide the framework for understanding the development of the fan system. Additionally, data collected in other studies (Gürbüz 1993; Satur *et al.* 1997; Satur 1999) is utilised as indicated (fig. 2.11). The zone of interfingering between the eastern and western fan, which is exposed around Cingöz village (fig. 2.10), is included in this study.

Relogging of major parts of the E-Fan, with emphasis on the sand-dominated proximal to mid-section areas, has revealed that the total fan thickness is 3700 m in the central section of the E-Fan. This is considerably thicker than previously recorded (e.g. 2500 m of Gürbüz 1993). However, marked thickness variations (table 2.2; fig. 2.11) are present from west to east as well as distinctly changing lithofacies associations, suggesting a more complex development of the fan system than previously interpreted. The deposits show little to no deformation. Faulting is abundant, mostly of unknown vertical and/or lateral displacement (Ünlügenç 1993; this study).

SECTION	THICKNESS	N-S EXTEND	BEGINNING	END
Section W (west)	1700 m	fan - slope to fan – basin plain contact	N 37 24'20'' E 035 16'53''	N 37 16'29'' E 035 16'17''
Section C (central)	3700 m	channel-fill to fan - basin plain contact	N 37 28'48'' E 035 20'37''	N 37 18'20'' E 035 17'58''
Section E (east)	870 m	fan - slope to distal fan fringe; stratigraphic top of fan not exposed	N 37 25'20'' E 035 26'20''	N 37 23'00'' E 035 27'10''

Table 2.2: Location, thickness and extend of overview logs (fig. 2.10)

Central section (Section C of fig. 2.11):

An overall fining-upward succession from proximal to distal fan deposits comprising channel-fill deposits at its base, passing upward into 100s of metres of thick successions of coarse, thick-bedded sandstones subsequently thinning and fining upward to the fan fringe deposits located in a distal, southward direction. The central section can be grouped into 7 units of distinctive sedimentological character (fig. 2.11: marked as C1-C7 in section C):

- C1) An 80 m thick conglomeratic unit (incised channel 1 fill deposits (Satur *et al.* 1997)) of clast and matrix-supported conglomerates with very little finer-grained material (plate 1.2). The clast lithologies encountered are: basement ophiolites (~ 50%), Karaisali Limestone (~ 40%) and basement sandstone and limestone (~ 10%), with maximum clast sizes reaching 10 m (Karaisali Limestone). Feeder channel 1 is interpreted to have been approximately 600 - 750 m in width (aspect ratios: 7.5 - 9.7) transporting sediments in a SSE-SSW (200/160) direction. Few laterally persistent siltstone beds are present, which are thought to represent periods of quiescence during the channel development.
- C2) A 40 m thick debrite, consisting mostly of chaotic, fossiliferous Kaplankaya slope siltstones. Internal deformation and few floating clasts are conspicuous. This unit was previously interpreted to represent slope progradation over temporarily abandoned channel segments (Satur 1999) and valley top-levee shales (Naz *et al.* 1991).
90 m of thin- to medium-bedded, dominantly fine- to medium-grained sandstones forming 2 - 6 m thick, thickening-upward cycles in an overall thickening and coarsening-upward succession (basal deposits: S₃ of Lowe (1982) / T_{a-d} of Bouma (1962) coarsening upward to S₁₋₃/T_{a,b} to T_{b-d} at the top of the section) (plate 1.3). Amalgamation, lensing and pinch-out of beds and smaller sandstone packages over distances of 10 - 15 m are common. Palaeocurrents scatter widely from NE to W transport directions (60 – 270°). These sediments are interpreted to represent channel mouth deposits *sensu* Mutti & Normark (1987). 13 m of channel-related

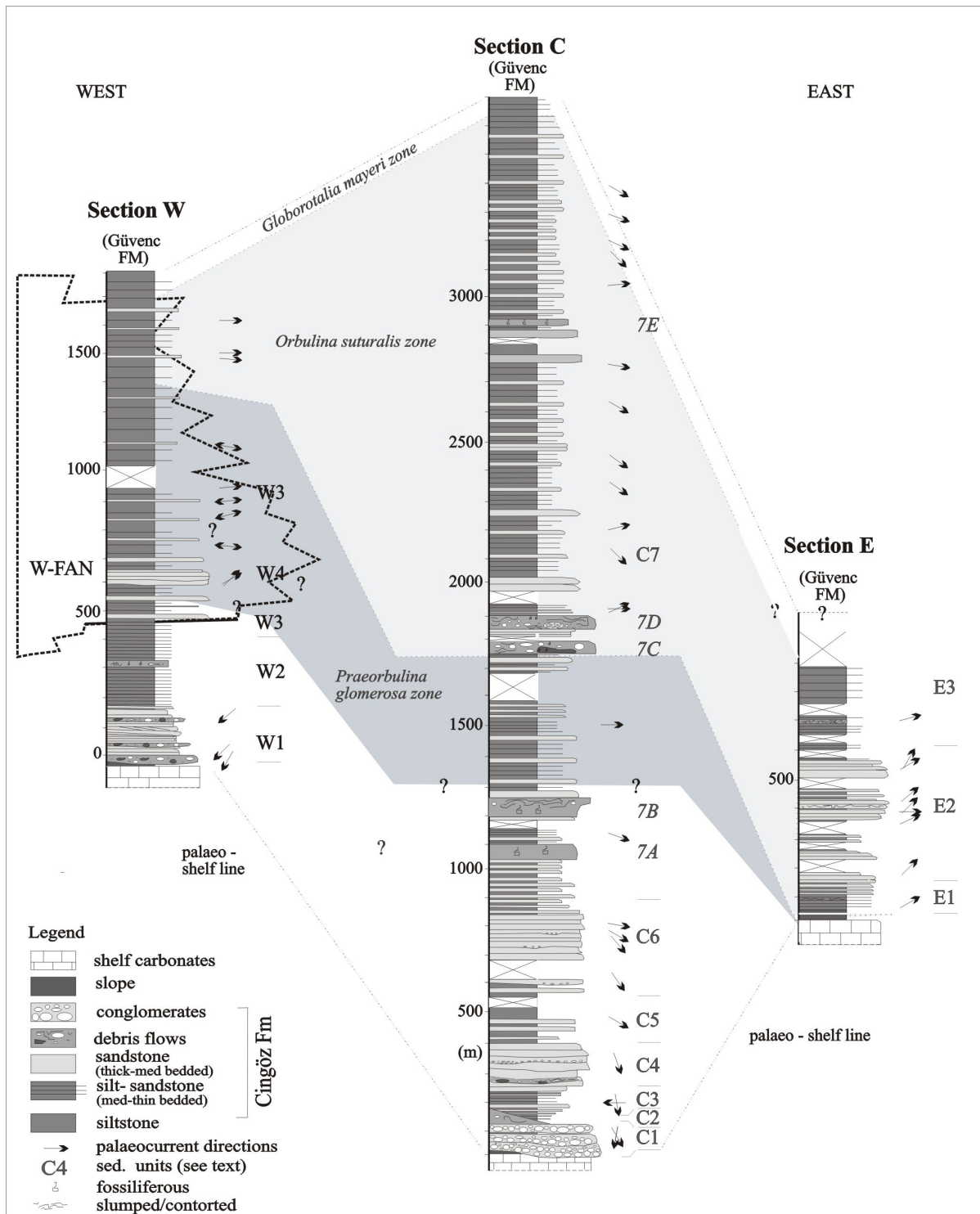


Figure 2.11: General logs through the E-Fan showing the vertical and lateral development within the western, central and eastern sectors. (Biostratigraphic data based on Gürbüz (1993) and Cronin *et al.* (2000); lithological data from Gürbüz (1993): Section W: 850 - 1800 m; Section C: 1900 - 3700 m and from Satur *et al.* (1997): Section C: 0 - 80 m. 7A-E of Section C represent debris flow deposits referred to in the text.

overbank deposits (Mutti & Normark 1987) consisting of alternating beds of shales and extensively current-laminated, fine-grained sandstones ($T_{b,c}$) are intercalated. They are probably located on the edge of a channel (corresponding channel-fill not exposed) with ripple directions pointing towards 210 - 250°, thus approximately 50 - 90° oblique to the main

- N-S transport direction. Trace fossils (e.g. Palaeodictyon) and escape burrows are common. This unit was previously interpreted to represent middle fan lobe sequences (Naz *et al.* 1991).
- C3) 150 m of laterally extensive, coarse- to very coarse-grained sandstones (S₁₋₃, rarely T_{a-c}), pebbly sandstones, matrix-supported conglomerates (R₁-S₁) and occasional, limestone-rich debris flows (plate 1.3) follow. Channel and lobe elements were identified, organised in subtle fining-upward sequences in an overall fining unit. Palaeocurrents point to a SW - W (210 - 260°) transport direction. This unit represents a channel-lobe transition zone *sensu* Mutti & Normark (1987, 1991; *detailed analysis: chapter 2.4.1*). Previous interpretations include channel-fill deposits (*pers. comm.* Gürbüz 1996) and non-sequential channelized sandstones of the middle fan (Naz *et al.* 1991).
- C4) 130 m of typically normally graded, 1 - 35 cm thick, fine- to medium grained sandstones and siltstones (T_{b-e}), interbedded with coarser-grained and thicker-bedded sandstones (T_{a-d,e}) and rare pebbly sandstones. The deposits are arranged in 10 - 15 m thick coarsening- and thickening-upward sequences. Overall, a gradual thickening and coarsening of deposits towards the overlying sediments (C6) is present. Palaeocurrents have swung around to a SE (120°) transport direction. These sediments are interpreted to be non-channelized lobe and lobe fringe deposits sourced from feeder channel 1.
- C5) 550 m of laterally extensive, predominantly coarse-grained sandstones interbedded with pebbly sandstones and few conglomerates and siltstones (plate 1.4). Deposits are arranged in up to 40 m thick lobe deposits and subordinately in distributary channels and lobe fringe deposits representative of a proximal lobe environment (*detailed analysis: chapter 2.4.2*) This area was sourced from the NW-W (channels 3 and 4) and downcurrent transport directions point to the SE-E. The deposits transitionally pass upward into increasingly thinner-bedded and finer-grained deposits.
- C6) The poorly exposed top 2760 m are characterised by fine-grained and thin-bedded sediments interbedded with units of coarser- and thicker-bedded sediments. The uppermost 1200 m are arranged in up to 80 m thick thinning- and fining-upward cycles (Gürbüz 1993).
Coarser units (plate 1.5): typically 4 - 20 m thick, composed of normally graded, parallel-bedded, medium- to coarse-grained sandstone of 0.6 - 1.2 m thickness (S₂₋₃, T_{a-c,d}). Solemarks such as plumose, flute and/or groove casts are common. Scouring, amalgamation and bioturbation were rarely observed.
Finer units (plate 1.6): composed of regularly bedded, 3 - 8 cm thick very fine to fine sandstone beds (T_{c-d}) interbedded with 3 - 10 cm thick, mostly planar laminated or low angle cross laminated siltstones (T_{d,e}). Bioturbation is common. Larger, 1 - 5 m thick fining/thinning- and coarsening/ thickening-upward trends are present, but random trends dominate. Occasionally the deposits are less regularly bedded, displaying greater thickness ranges (1 - 30 cm). The interbedded siltstones are commonly thinner bedded (1 - 3 cm).
The coarser deposits are interpreted to represent lobe deposits (*sensu* Mutti & Ricci Lucchi 1972), while the interbedded fines are associated lobe fringe and/or interlobe deposits (*sensu* Mutti 1977). The contacts between the coarser- and finer-grained units is mostly transitional, resulting in thickening/coarsening- or thinning/fining-upward trends resulting from lobe migration or switching (Bouma 2000). But sharp and/or faulted contacts also exist.
Overall deposits thin and fine towards the top where thin-bedded, shale-rich sediment of the outer fan environment are present (Gürbüz 1993). The palaeocurrent directions indicate a gradual change from SE (130°) in midsection to a predominantly E-ENE direction in the youngest, most distal part.
At least 5 individual debris flows are randomly interbedded (7A-E). They are characterised by a chaotic matrix of fossiliferous siltstones (Kaplankaya slope deposits) and varying proportions of a) well-rounded ophiolitic clasts (Cingöz channel-fill conglomerates), b) limestone clasts (Mesozoic and Tertiary [Karaisali] Formations) and c) shale* clasts. The thickness of these debris flows varies between 7 m (7E) to maximum 80 m (7D) and can be traced laterally for up to 500 m (7D; outcrop limit). Basal contacts are sharp, the often irregular tops are overlapped by overlying deposits (plate 1.6).

* Throughout this study, the term shale (or shales) denotes sediments of clay- to silt grade unless indicated otherwise.

Previous interpretations of the debris flows include "conglomeratic distributary channel-fill deposit in mid-fan position overlain by levee deposits" ('7D'; plate 1.7; Gürbüz 1993). However, the chaotic fabric, internal deformation, squeezed-up shales and deformed sandstone bodies as well as the carbonaceous, shallower-water fossil content of the top siltstone unit with occasional larger, well-rounded floating clasts (plate 2.1), suggest that these deposits represent an unroofing sequences of a) semi-lithified Cingöz channel-fill deposits and b) Kaplankaya slope deposits being subsequently entrained in a debris-flow event.

Debris flows are typically initiated by seismic shock or rapid sedimentation and subsequent slope-oversteepening. Initial sediment failure as slumps or sediment creep may undergo internal deformation and develop into debris flows which can travel far into a basin (Normark *et al.* 1993; Reading 1996). The highly siltstone-rich debris-flow deposits with the entrained well-rounded gravels and large limestone clasts most likely result from a combination of effects such as uplift of the source area, seismic activity and slope failure.

Western section (Section W of fig. 2.11):

Four discrete sedimentary units are present, forming a total of 1700 m of fan sediments (fig. 2.11) encompassing fan-slope contact in the north to basal shales in the south:

W_{slope} Karaisali shelfal limestone succeeded by 15 m thick, fault-bounded Kaplankaya slope deposits dominated by very thinly-bedded, fossiliferous siltstones. Occasional debrites, sliding packages and slump scars are present (*chapter 2.3*).

W1) 170 m of dominantly medium- to thick-bedded, coarse- to very coarse-grained sandstones (S₁₋₃, T_{a-c,d}) interbedded with little silt (T_{d,e}) and occasional 1-3 m thick, slope-derived debris flows. Basal fan slope contacts display onlap and infill relationships. (*detailed analysis: chapter 2.3.1*). Lensing, wedging and compensation features are common in the basal sequence.

The debris-flow deposits (plate 2.2) mainly contain (shelfal-) limestones, deformed clasts of Kaplankaya slope material and a few well-rounded, mostly ophiolitic cobbles in a chaotic, silt-dominated matrix with a high fossil content.

Towards the east, these deposits can be traced into the coarser-grained central fan deposits. The palaeocurrent pattern points to a W to WSW transport direction indicating a lateral/marginal position to the main depositional fan area.

W2) 330 m dominated by a monotonous unit of laterally extensive, typically 5 - 15 cm thick, fine-grained sandstones displaying high sand/shale ratios (4:1; plate 2.3). In its lower part interbedding with occasional thick, coarse sandstones (S_{2,3}; T_{a-c}) and up to 1 m thick, limestone clast-rich debris flows are present. These, however, become less common towards the top, where a thick (> 10 m) fossiliferous, silt-dominated debris flow is present (fig. 2.11; plate 2.4; previously interpreted to represent levee deposits: Gürbüz 1993). The palaeocurrent indicators continue to point to a W-SW transport direction. These sediments are interpreted to represent marginal fan deposits (lobe fringe/fan fringe) interbedded with occasional debris flows originating from the basin margin to the north.

W3) 1100 m characterised by thick, relatively monotone successions of thinner-bedded (5 - 10 cm) and finer-grained sand- and siltstones of distinctly lower sand:silt ratio (2:1). From log metre 450 to 850 thick-bedded, very coarse sediments (unit W4) are frequently interbedded, prior to the monotone succession resuming and finally overlain by basal shales of the Güvenç Formation. The east-pointing transport directions are in stark contrast to the lower palaeocurrent pattern observed (W2/W3).

Previous studies (Gürbüz 1993; *pers. comm.* Gürbüz & Kelling 1996) interpreted the deposits to be part of the E-Fan based on the identified deeper-water ichnofacies, the somewhat puzzling palaeocurrent patterns are resulting from deflection on a westerly lying submarine high. However, this study proposes the deposits to represent western fan fringe sedimentation within the deepening basin (*discussion: chapter 2.5*).

W4) Over a ca. 400 m thick interval, very coarse-grained sandstones to pebbly gravelstones (plate 2.5, 2.6) (R₃, S₁₋₃ of Lowe 1982) alternate with thick units of finely laminated shales (T_{d,e} of Bouma 1962; T₃ of Stow & Shanmugam 1980; plate 2.7). The onset is marked by single or

amalgamated pebbly gravelstone beds (0.6 – 4 m thick) culminating in a 50 m thick package of very coarse, amalgamated deposits ($R_{2-3}; S_{1-3}$) outcropping at Cingöz Village (log metre: 600 – 650). The eastward-pointing palaeocurrent pattern and the markedly strong resemblance to W-Fan deposits located approximately 2 km to the west (this study, Gürbüz 1993) underline its western source. These coarse sediments appear to represent phases of progradation of the W-Fan in form of non-erosive sand tongues *sensu* Satur (1999) into an area otherwise receiving fan fringe sedimentation.

Eastern section (Section E of fig. 2.11)

870 m of fan sediments are exposed, encompassing the fan-slope contact in the north to distal turbidites in a basinal setting in the south. The stratigraphic top is not exposed. Abundant faulting and locally deep erosion by Quaternary fluvial gravels obscure parts of the section.

Three distinct sedimentary fan units are present (fig. 2.11):

- E_{slope} A basal thick succession of monotonously thin-bedded, fossiliferous siltstones of Kaplankaya slope deposits. Low angle unconformities within suggest synsedimentary sliding of slope material. A red marker horizon within the Kaplankaya slope deposits, 8 m below the onlap surface of turbiditic fan sediments, dates as the late Burdigalian - Langhian boundary (Cronin *et al.* 2000).
- E1) 40 m dominated by thin-bedded (1-6 cm) siltstones alternating with 1 - 3 cm thick very fine to fine-grained sandstones ($T_{c-d,e}$). Trace fossils and plant debris are abundant and up to 1 m thick slumped units are common. The basal 26 m are relatively monotone, then a noticeable upward increase in the sand/shale ratio is recorded by the presence of increasingly thicker-bedded and coarser-grained sandstones ($T_{c-d,e}$), forming isolated, up to 3 m thick sandstone packages. Laterally, the individual sandstone beds display a distinct thinning towards the slope, onlapping it with a low angle contact (*detailed analysis: chapter 2.2.1*), while thickening towards the basinal direction. These deposits are interpreted to represent marginal fan and lobe deposits.
- E2) The bulk of the section is formed by a 720 m thick sand-dominated unit characterised by up to 40 m thick discrete sandstone packages displaying very high sand/shale ratios (10:1). They are dominantly composed of laterally extensive, parallel-bedded, medium-grained sandstones ($S_3; T_{a-d,e}$), representing lobe deposits *sensu* Mutti & Normark (1987, 1991) (plate 2.8; *detailed analysis: chapter 2.4.3*). They are interbedded with finer-grained, thinner-bedded units of much lower sand/shale ratio of lobe fringe / interlobe origin *sensu* Mutti (1977) respectively. Contacts between the lobes and associated facies are mostly transitional resulting from lobe migration. Towards the top, lobe fringe deposits become increasingly more common. Palaeocurrents point to a general NE transport direction.
- E3) The top 110 m are dominated by noticeably finer-grained and thinner-bedded deposits characterised by a progressive upward decrease in the sand/shale ratio (ave. 3 - 1). Typically, 3-8 (max. 35) cm thick, fine-grained sandstones ($T_{b,c-d,e}$) are interbedded with 1-4 cm thick siltstones forming a thick, relatively monotonous unit especially towards the top. The sediments represent fan fringe deposits. The stratigraphic top of the Cingöz Formation is partly eroded into by Quaternary gravels partly not exposed, thus not permitting to determine the exact thickness of this unit. However, the recorded presence of Güvenç shales further upsection, suggests a possible maximum thickness of approximately 280 m of unit E3.

2.2.2.3 Lithologic and biostratigraphic correlations

Correlation between the individual sections proves difficult. This results from i) abundant faulting, ii) vast, heavily vegetated areas between the sections resulting in an “information gap” and iii) incomplete biostratigraphic data sets.

Deposits of the lowermost western section (W1) can be physically traced into the main fan area (study area 3; fig. 2.10, 2.11) which is interpreted to laterally correspond to the lowermost proximal lobe zone (C6) of the central fan section. The palaeocurrent pattern confirms the W1 sediments to be derived from this central fan area. Apart from this relationship, no direct lithologically-based correlations can be carried out.

The biostratigraphic data permits to tie most of the sections of the E-Fan into a temporal framework. During the incomplete (?) foraminiferal *Praeorbulina glomerosa curva* zone (late Burdigalian; Gürbüz 1993; Cronin *et al.* 2000) *, 730 m of sediments were deposited in the western section and 420 m in the central section. The lower boundary of this zone, however, is most likely to be incorrect, i.e. is expected to be lower, especially in the central section. Sedimentation was absent in the eastern section. During the foraminiferal *Orbulina suturalis* zone (Langhian; Gürbüz 1993; Cronin *et al.* 2000) major changes in depositional style occur (fig. 2.11). A 7.8-fold sediment increase from 250 m of dominantly shales in the west to 2000 m of dominantly lobe sandstones and associated deposits in the central area are present. Palaeocurrent indicators generally point to the S-SE.

Cronin *et al.* (2000) found that during the *Praeorbulina glomerosa curva* and the lower part of the *Orbulina suturalis* zones, Kaplankaya slope sediments were deposited in the eastern part of the E-Fan. Here, the deposition of the turbiditic Cingöz Formation sets in during the *Orbulina suturalis* zone. Thus making the whole eastern section (section E) younger than most of the central and western section.

The foraminiferal *Globorotalia mayeri* zone marks the top of the E-Fan succession, with 110 (section W) and 100 m (section C) respectively. The biostratigraphic data for the eastern section (section E) are missing, however, equally little sedimentation is likely to have occurred.

Further implications of the differing biostratigraphic dating on the fan model are discussed in chapters 2.5 – 2.7.

2.3 Geometry of the fan - slope contact

Excellent exposures of the Karaisali reefal complex, Kaplankaya slope and the Cingöz clastic deep-water system reveal the complex stratigraphic and geometric relationships between the three systems. The reefal complex and slope system laterally interfinger; they are initially older, however, towards their upper parts coeval with the encroaching clastic turbidite system (Yetiş & Demirkol 1986; Nazik & Gürbüz 1992; Gürbüz 1993; Yetiş *et al.* 1995). Active slope progradation during times of Cingöz fan deposition leading to interfingering slope and fan deposition were recorded by Satur (1999), Cronin *et al.* (2000) and in this study (*chapter 2.2*). Cronin's *et al.* (2000) recent study indicates that slope thickness and gradient vary considerably along its ~ 60 km Cingöz-lateral extent due to slumping and mass wasting within the slope formation resulting from instability.

Fan-slope contacts are exposed at a number of locations along the north-western and north-eastern E-Fan margin (fig. 2.10: study areas 1 & 2). The observed contacts were differentiated into three discrete types, two of which represent pinch-out of fan sediments against the slope while the third emphasises an active fan-slope relationship.

2.3.1 Contact relationships

i) pinch out: onlap termination (unconformable, non-erosive contact) (fig. 2.12a):

This type of fan-slope contact can be readily observed along both margins. It is characterised by i) gradual thinning of individual beds and larger sediment packages against the slope, ii) progressive fining and iii) relatively thin slumped units (dm to m scale) with the slump folds pointing away from the slope (fig. 2.13; 2.14).

The pinch-out of fan deposits involves different hierarchies of scale. Figures 2.14 and 2.15 show that individual beds (cm to m-scale) as well as thicker sandstone packages (m to 10s of m scale) pinch-out. Slope gradients may vary considerably. While in the east (fig. 2.15) the slope exhibits a low, approximately 2° angle, in the west turbidites onlap an 8° steep slope (plate 3.1).

Sediments at the eastern fan-slope contact (fig. 2.14) exhibit a high amount of synsedimentary dewatering structures (dish structures), destroying much of the primary sedimentary structures. Rapid deposition and

* Toker *et al.* (1998) put the depositional age of the Cingöz Formation from early-middle Miocene (Langhian) to middle Miocene (Serravallian) based on calcareous nanoplankton, this age Satur (1999) appears to have used in his recent study, while Nazik & Gürbüz (1992), Gürbüz (1993) and Cronin, Gürbüz, Hurst & Satur (2000) utilise the foraminiferal biozones which give a late Burdigalian to Serravallian depositional age for the Cingöz Formation.

sediment overload typically result in dewatering (Nichols *et al.* 1994). However, Cronin *et al.* (2000) suggest creep or slurring of sandstone beds responsible for dewatering in such a setting.

The few palaeocurrent data indicate a broad scatter of current directions, diverging up to 60° (fig. 2.14). Transport directions in the distal lobe setting are largely axial, i.e. slope parallel. However, here transport appears to be directed obliquely to the laterally confining palaeoslope. It has been shown that subsequent deflection of turbidity currents is likely to occur (Pickering & Hiscott 1985; Kneller *et al.* 1991; Sinclair 1994), but the sparse data set does not conclusively support this assumption. This type of relationship is well known from other deep-water clastic systems such as the late Eocene Annot Sandstone of S-France (Ravenne 1992; Hurst *et al.* 1999) and the Tertiary Cengio Turbidite System (Cazzola *et al.* 1985). Hurst *et al.* (1999) assign onlap termination to down-system pinchout and attribute it to a lack of confinement of flow, however, oblique lateral confinement by the slope is present here (fig. 2.12a). Cronin *et al.* (2000) found this down-system onlap termination to exist further to the NE of the eastern study area, where turbidites onlap a low-gradient west-facing slope indicating restriction in basin accommodation.

ii) pinch out: infill (unconformable, non-erosive contact) (fig. 2.12b):

Infill *sensu* Hurst *et al.* (1999) involves a more abrupt termination of fan deposits against the slope which is characterised by a more sudden thickness decline and relatively little change in grain size. Along the NW but particularly the NE margin (2b of fig. 2.10), this type of contact features steep-angled and/or stepped geometries (fig. 2.12b; plate 2.2; 2.3) These geometries are probably generated by an irregular slope topography which allows fan sediments to accumulate in “slope pockets”.

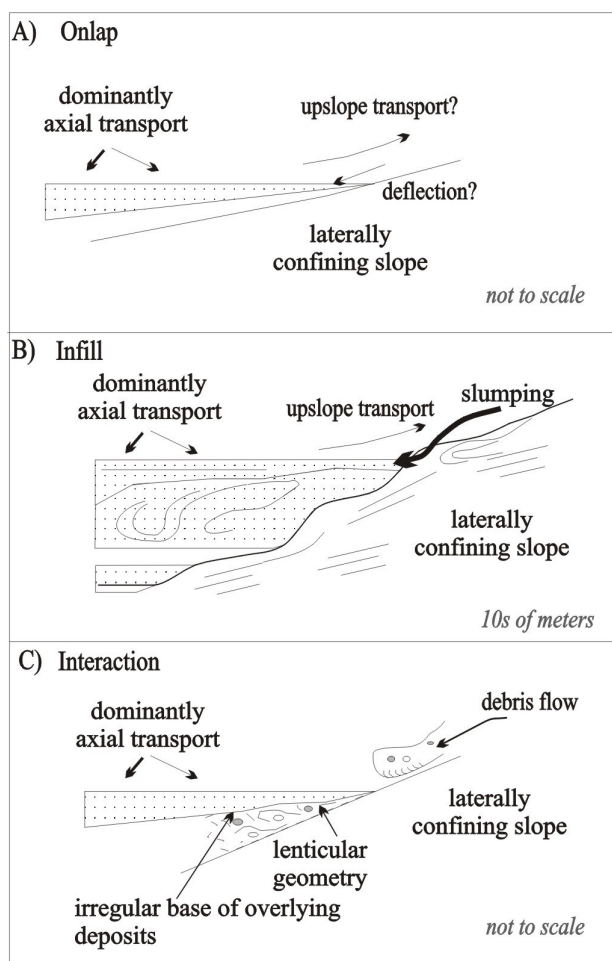


Figure 2.12: Schematic diagram showing the range of contact relationships encountered in the E-Fan. A and B represent different types of pinch out terminations.

The underlying slope sediments (plate 3.4) show abundant low angle unconformities believed to result from synsedimentary sliding of the slope deposits triggered by either high sedimentation rates, oversteepening of the slope and/or seismic activity thus producing the complex slope morphologies observed (Normark *et al.* 1993; Mulder & Cochonat 1996; Reading 1996; Cronin *et al.* 2000). These pockets may be anything from a few metres to 10s of metres in length and height (plate 3.2; 3.4), which are subsequently infilled by fan turbidites. Along the NE margin, abundant calcite harnishes were observed. They probably line synsedimentary glide planes which may be responsible for generating steep slope gradients. These gradients may be up to 24° (plate 3.4) and such steep slopes may promote sediment failure (Normark & Piper 1991).

Slumping and sliding involving individual beds or thicker fan-sediment packages commonly exist, but are particularly conspicuous in the NE, where metre-thick slumped packages are present (plate 3.4), infilling slope-pockets and/or occurring close to these. Muck & Underwood (1990) demonstrated that a considerable amount of upslope transport and deposition of turbidites can be expected when flows hit barriers, in this case the laterally confining slope. This may account for the deposition of fan sediments above the “active” depositional fan surface within the basin, their subsequent down-slope slumping and overlying by aggrading fan sediments.

The vertical and lateral changes within turbidites associated with infill geometries appear to be a

direct result of the underlying complex slope morphology where flow confinement results in steep pinch out relationships. Slumping and sliding of the underlying slope and of turbiditic fan sediments indicate an active fan margin environment.

iii interaction slope/shelf and fan sediments (fig. 2.12C)

Along the NW margin of the E-Fan (base of section W; chapter 2.2.2), another type of “active” fan-slope relationship is present (fig. 2.12C).

Log A (fig. 2.13) shows that fan turbidites are preceded by thick, lenticular debrites rich in lime- and siltstones as well as well-rounded, ophiolitic pebbles, passing upward into a thin succession of lenticular mixed pebbly – granule clastic and calcareous turbidites (plate 3.5, 3.6). These deposits appear to be confined to small channel-like fairways or slope gullies *sensu* Surlyk (1987) where erosion and filling are likely to be closely related processes. The slope gully fill is overlain by laterally more extensive sandstone beds rapidly terminating against a steep-angled (~ 15°) slope (infill-type; “marker bed”; fig. 2.13: Log B). Palaeocurrents indicate the clastic turbidites to derive from the NE-E, from the main fan area, while the underlying debrite and mixed turbidites were shed from the N of the shelf/slope. Stratigraphically upward lenticular, shelf/slope-derived debrites appear localised. Succeeding fan turbidites onlap their irregular topography (*chapter 2.2: Section W1/2*).

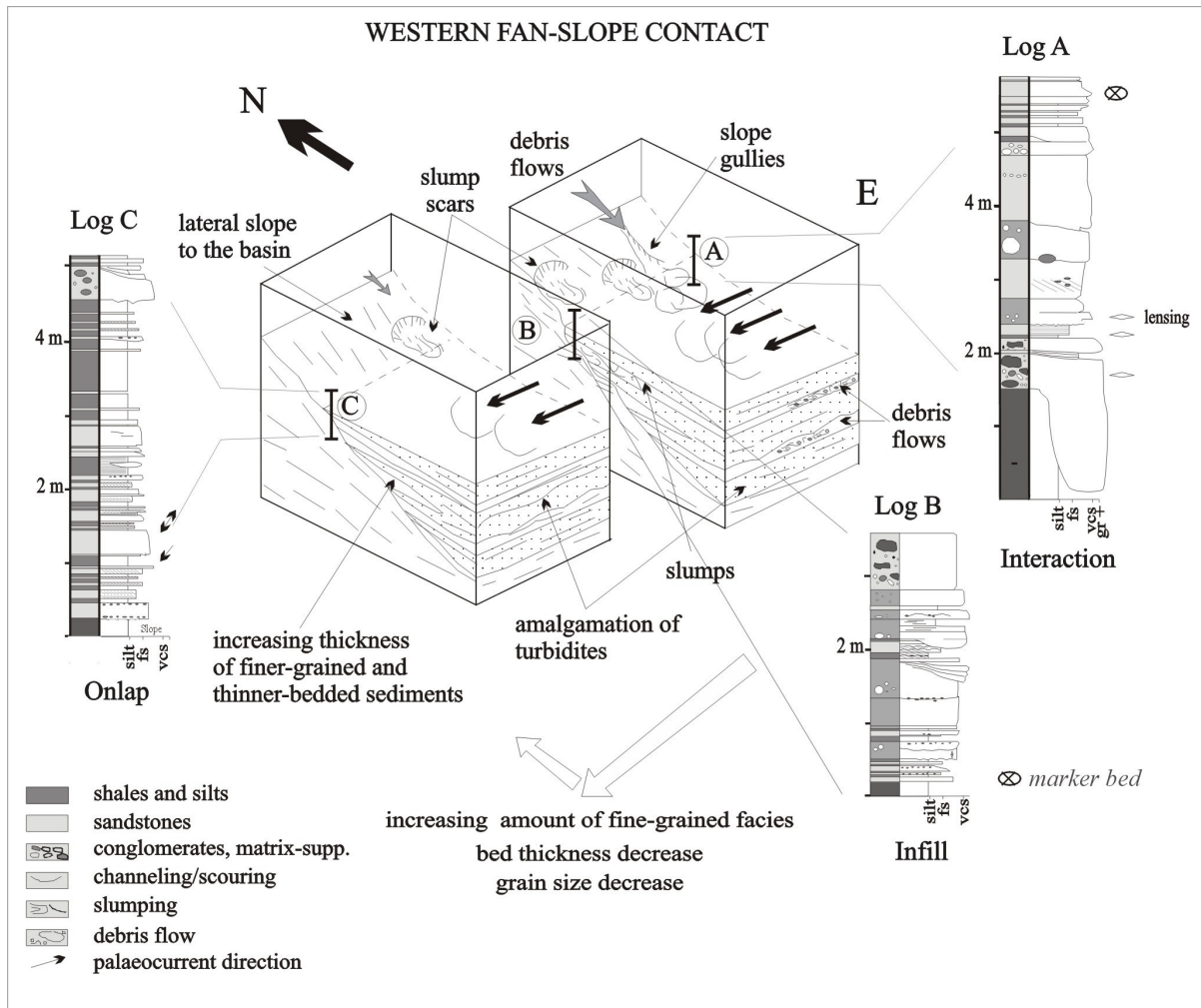


Figure 2.13: Schematic diagram showing the fan - slope contact along the north-western margin of the E-Fan. The type of contact varies from active fan-slope relationship with shelf/slope-derived debrites and calcareous turbidites to infill and onlap pinch out of fan deposits against the slope (location 1 of fig. 2.10.). Distance between logs: A - 50 m - B - 400 m - C.

Downcurrent, onlap termination of progressively finer-grained fan turbidites with only occasional slope-derived debrites higher up in the section was observed (fig. 2.13: log C). Up-current, towards the main fan

area and channel 4, slope-derived sediments are increasing in their frequency especially before or during onset of the fan encroachment. Small conglomeratic and/or debrite infilled bypass channels, showing accretion-like features, lensing, wedging and compensation features are occasionally present. The debrite clast content shows great similarity with the conglomeratic channel 4 deposits (*pers. comm.* Satur 1997) but with a much higher marly shale and shelfal limestone content.

Instability due to overloading/oversteepening and/or tectonic activity resulted in mass wasting of slope and shelf material just before and during the encroachment of the clastic turbidite system. On the one hand, it leads to the complex slope morphology prior to fan deposition with slump scars, varying gradients and slope gullies resulting in the observed contact geometries. On the other hand, slope instability, which appears to be greatest close to the fault-bounded channel 4, resulted in frequent debris flows and mixed turbidites coming from the shelf/slope interfingering with fan deposition. The debrite content suggests i) overspilling currents from the closeby, choked (?) channel 4 entraining shelf- or slope sediment or ii) other possibly fan delta-derived debrites deposited (?) at the upper shelf-break prior to its remobilisation due to oversteepening / seismicity and entrainment of shelf and slope sediments.

2.3.2 Western versus eastern fan-slope contacts

Slope stability and morphology profoundly influence the geometry of the fan-slope contact.

The western margin exhibits an active fan-slope relationship with abundant shelf/slope derived debrites and mixed turbidites closest to channel 4 changing to infill and onlap pinch-out (plate 3.1-2, 5-6) in a downcurrent, westward direction (fig. 2.13; table 2.3). The Cingöz turbidites display a progressive change by i) decrease in the sand/shale ratio, ii) dramatic decrease in grain size, iii) overall bed thickness decrease, iv) increase in amount of interbedded finer-grained facies and v) transition from proximal partly channelized to fan fringe deposition (fig. 2.13; table 2.3).

Logs	Debris flow : Sand : shale	Grain size	Bed thickness	Erosional contacts	Geometries	Depositional environment
Log A	0.9:1:0.1	cs-gr	ave. 80 cm	abundant	lensing, pinch-out (infill)	Channel influenced?, lobe fringe deposits
Log B	0.4:1:0.2	cs-vcs	ave. 60 cm	common	pinch-out (infill)	lateral lobe fringe?, fan fringe
Log C	0.2:0.6:1	vfs-fs	ave. 25 cm	rare	pinch-out (onlap)	lateral fan fringe

Abbreviations: gr=granule, vcs= very coarse sand, cs=coarse sand, fs=fine sand, vfs=very fine sand, ave=average

Table 2.3: Variations along the western fan-slope contact (fig. 2.13). Distances between logs: A – 50 m – B – 400 m – C.

The mean grain size of the sandstones along the NW margin is considerably coarser than that of the NE margin (*see below*), although the studied section is generally dominated by thick successions of finer-grained facies, where siltstones are commonly interbedded with relatively thin-bedded, coarse to pebbly units and occasional debris flows (*chapter 2.2*). Contemporaneous slope instability resulting in frequent mass wasting events is characteristic. Slumping of semilithified Cingöz deposits was not observed.

The deposits at the eastern margin are interpreted to be lobe and lobe-fringe deposits (*chapter 2.2*; table 2.4). The fan sediments onlap an approximately 2° angled slope (fig. 2.14, 2.15), however, locally steeper gradients (up to 24°) were recognised due to irregular slope topography resulting from sliding and slumping of underlying slope segments.

The palaeocurrent indicators point to a NE-ESE transport direction, which is nearly parallel to the confining slope. Oblique upslope transport and subsequent rebound of turbidity currents is likely to have occurred. Sand-rich sandstone packages (Log A) laterally thin, exhibiting a more distinct asymmetric, coarsening-upward signature and containing a higher mudstone content (Log B). These developments have also been observed elsewhere (e.g. Annot Sandstone: Sinclair 1994).

Logs	Sand : shale	Grain size	Bed thickness	slumping	Geometries	Depositional environment
Log A	1 : 0.5	ms	ave. 40 cm	common-axis away	pinch-out (onlap)	lobe- and interlobe deposits
Log B	1 : 0.9	fs	ave. 15 cm	common-axis away	pinch-out (onlap)	lobe - and interlobe deposits

Abbreviations: ms=medium sand, fs=fine sand, ave=average

Table 2.4: Variations along the eastern fan-slope contact (fig. 2.14, 2.15). Distances between logs: 200m.

Some of the studied sections along the NE-margin are within a large fault-displaced slab of Cingöz Formation and it is not possible to tie them into the E-Fan framework (Ünlügenç 1993; *pers. comm.* Ünlügenç 1996). These are the sections which exhibit the marked infill relationships, the thick slumped units of lobe and associated deposits infilling the underlying irregular slope topography.

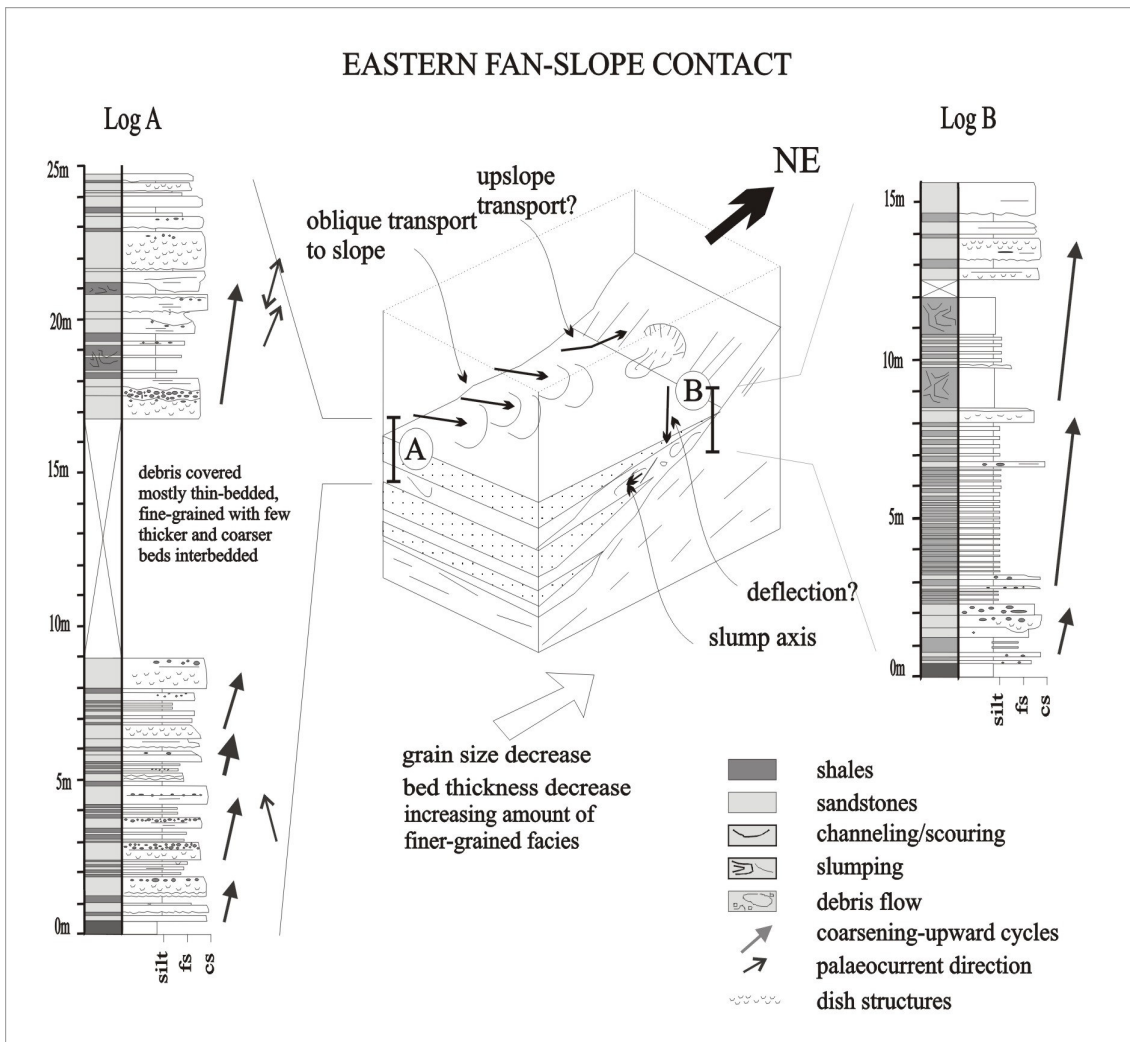


Figure. 2.14: Schematic diagram showing fan deposits onlapping the slope exposed in a cutbank north of Egner, E-Fan (Location 2a of fig. 2.10). The vertical fan development in both locations shows thickening and coarsening upward from the fan-slope contact. Laterally, marked grain size and bed thickness decrease towards the slope (A to B) takes place while the amount of finer-grained facies increases. The slope has an approximate gradient of 2°. Distance between logs: ~ 200 m.

2.4 Non-channelized fan environments

Three primarily non-channelized, sand-dominated depositional zones within the fan were selected for detailed studies (fig. 2.10). The selection was based on their location within the fan system as well as on the degree of exposure and accessibility. These zones were classified according to their facies characteristics, the recognition of their elemental building blocks (components) at different hierarchies of scale and their position within the fan system. A channel-lobe transition zone, a proximal lobe zone and a relatively distal (intermediate) lobe zone were identified as distinctive fan depositional environments within the sandy basin-fill of the E-Fan (fig. 2.10: localities 4 to 6).

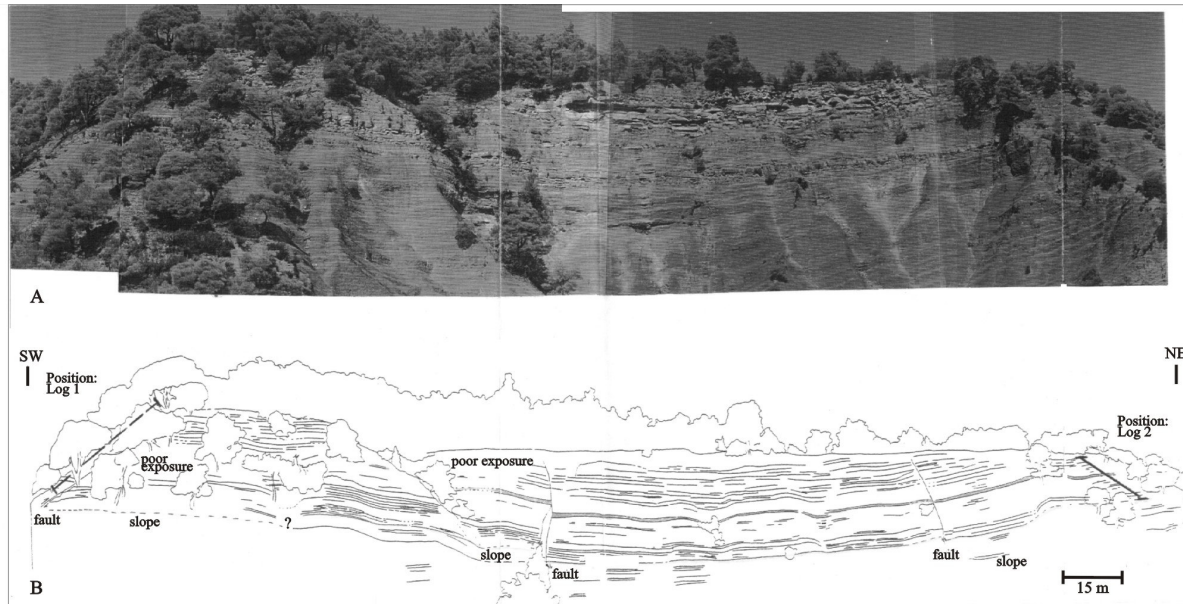


Figure 2.15: A) Photomosaic showing lobe and lobe fringe deposits onlapping a low-angled slope sediments in a SW-NE trending cutbank north of Egner, northeastern margin of E-Fan. The deposits dip to the NWN (340°) and the palaeocurrent directions point obliquely towards the slope. The underlying slope sediments form largely undeformed, monotonous successions.

B) Line drawing depicting the position of logs (fig. 2.14).

2.4.1 Channel-lobe transition zone

Thick successions of primarily non-channelized, coarse-grained sediments are exposed in the very north of the field area (fig. 2.10 [#4]). They stratigraphically succeed the feeder channel 1 complex and the associated overbank deposits. Sourced by feeder channel 1 in the north, palaeocurrent indicators point to a S-SW-ward transport direction (fig. 2.10). Neither the upstream, contemporaneous channel-fill deposits nor the corresponding downstream deposits are preserved and/or exposed. This unit is overlain by distinctly finer-grained and thinner-bedded lobe-like deposits (*chapter 2.2*; fig. 2.11).

Three overview logs were taken covering 150 m vertical extent (fig. 2.16), the stratigraphic top (80 m) is not exposed. Only limited lateral control can be exerted with a maximum of 300 m of continued tracing of selected beds. The geographic eastern margin is not exposed and/or inaccessible. No 3-D sections are present, therefore it is not possible to record downcurrent changes within this zone. Within the lower, better exposed part more detailed studies were carried out to obtain information about facies to mesoscale geometric variations.

Ancient channel-lobe transitions *sensu* Mutti & Normark (1987, 1991) are characterised by i) extensively scoured and amalgamated sandstone and pebbly sandstone facies ii) coarse-grained and lenticular, cross-stratified sandstone beds, iii) abundant out-sized rip-up mudstone clasts and iv) a variety of scours and cut-and-fill-structures. This channel-lobe transition zone (CLTZ; plate 4.1) is sand-dominated and contains the coarsest material of the sandy basin-fill of the E-Fan. Laterally extensive, coarse-grained to pebbly

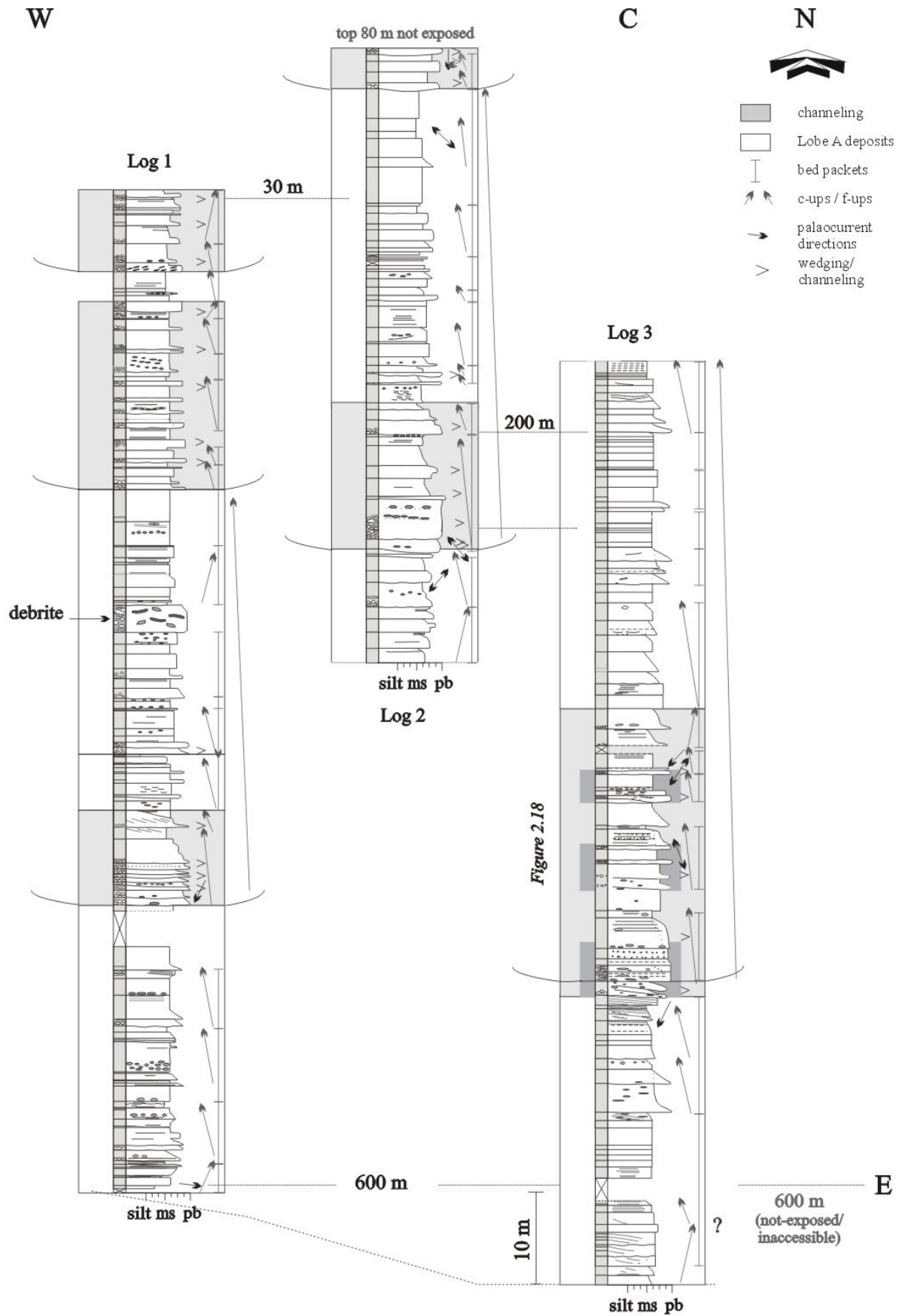


Fig. 2.16: Main logs through the western and central channel-lobe transition zone (CLTZ), showing the lateral and vertical distribution of Lobe A and channeling components. The CLTZ is sourced from the N, transport is towards the SSW-SSE. Log 1: Lobe A deposits aggrade onto mass-flow deposits made up of slope facies. Log 3: Lobe A deposits transitionally overlie channel mouth and overbank facies.

COMPONENTS	IDEALISED SECTION	SEDIMENTARY FEATURES	GEOMETRY	STACKING PATTERN	vertical COMPONENT ASSOCIATION
LOBE A	<p>mostly random arrangement</p> <p>poorly defined bed packets</p> <p>1m</p> <p>sandstone</p> <p>pebbly sandstone</p>	<p>0.8 m</p> <p>0.1 m max</p> <p>internally erosive, amalgamation of sandstones, shale rip-up clasts,</p>	<p>> 0.3 km</p>	<p>offset-stacked</p> <p>Progradational & retrogradational compensation shingling</p>	<p>A) poorly defined, transitional?</p> <p>B) erosive</p>
CHANNELLING	<p>subtle fining and thinning upward</p> <p>1m</p>	<p>0.6 m</p> <p>residual conglomerates, scouring, rapid lateral changes in microfacies, bedload transport</p>	<p>A 10 - > 40 m</p> <p>B channelling → Lobe A</p>	<p>isolated</p> <p>offset-stacked</p>	<p>base: erosive, top: gradational</p>
SCOURS	<p>0.5 m</p>	<p>ave. 0.25 m</p>	<p>0.7 - > 9.50 m</p> <p>plan view</p>	<p>isolated</p> <p>multiple scouring</p>	<p>A) in channelling</p> <p>B) in Lobe A</p>

Fig. 2.17: Facies, geometry and association of differentiated components of the channel-lobe transition zone, E-Fan.

sandstones (84 %) dominate, while pebbly to cobbly conglomerates (15 %) and shale beds (1 %) are subordinately present. An abundance of erosional bedding surfaces exist (32 %). The reworking of sediments is characteristic while fine sediment is bypassed and deposited further down-system. The deposits are arranged in distinctive packages which are attributed to discrete components.

2.4.1.1 Component analysis: internal organisation and geometry

Channeling

Up to 20 m thick, discrete conglomerate-dominated successions (fig. 2.16) are forming 30 % of the section (table 2.5). These successions are mainly composed of highly erosive pebbly to cobbly, matrix-supported conglomerates mostly interbedded with pebbly sandstones. The average ratio is 1.3:1 (conglomerates : pebbly sandstones). These units erosively cut into moderately-defined sand-rich packets^{*} and transitionally pass upward into these (fig. 2.16). The conglomerate-dominated units are laterally persistent and can be traced for up to 40 m (exposure limit).

The conglomerates can be classed as R1-3 deposits (Lowe 1982), exhibiting massive bases and crudely stratified tops (plate 4.3; fig 2. 17). Normal grading and non-grading are common, inverse grading rare. The conglomerates display rapid lateral and vertical changes in thickness (thickness: 0.1 - 1.6 m) and facies (conglomerate to pebbly sandstone; fig. 2.18). Some mud-supported conglomerates with outsized, floating clasts are randomly interbedded. The interbedded pebbly sandstones (R3 to S1-2 of Lowe 1982) show abundant traction features. The sediments result from deposition by coarse sandy to gravelly high-density turbidity currents and debris flows (Lowe 1982; Mutti & Normark 1987; Shanmugam 2000).

The amalgamation of sediments is persistent, shale partings were not observed. Fine-grained and shaly deposits are absent within the channeling component. However, reworked shale clasts are common throughout. Poorly rounded mudstone clasts are mostly concentrated within the lower parts of beds suggesting rapid erosion of underlying hydroplastic muds and short transport distances (Kano & Takeuchi 1989; Johansson & Stow 1995).

No actual channel geometries were observed. Channel margins with i.e. multiple onlapping infill geometries which form clear identification criteria for channels (Mutti & Normark 1987) are absent at outcrop scale. The channeling geometry is inferred by means of depositional characteristics. Smaller-scale lensing (up to 10 m in length), wedging beds and abundant cut- and fill structures are present (plate 4.2, 4.3). The at times rapid lateral facies change of individual beds (fig. 2.18) may indicate the progressive change towards marginal areas of the channelized area (Mutti & Normark 1987). The lack of steep-sided erosional channel margins suggests that the channels may have been fairly shallow features which could not necessarily contain the whole flow volume (Weimer 1989) and sheet-sand deposition outside the channelized area was probable, partly forming Lobe A deposits.

In the lower CLTZ, the channeling component is composed of three distinctive sub-packets (figs 2.16, 2.18), their individual bases marked by erosion (1st order bounding surfaces after Pickering *et al.* 1995) and conglomeratic lags. These up to 2.6 m thick sub-packets typically consist of 5 - 8 beds, defined by subtle 2 - 4 bed asymmetric sequences (58 %), while 42 % of the measured beds display random organisation. 3 - 4 bed thinning-upward sequences dominate (54 % of sequences; fig. 2.19) suggesting gradual channel abandonment or backfilling (e.g. Mutti & Normark 1987; Chen & Hiscott 1999a). The grain size trends largely reflect the bed thickness trends, however, fining upward was even observed in conjunction with distinct thickening upward (fig. 2.16, e.g. log 2: 20 - 28 m). The randomness and asymmetric sequences may result from variations in flow volume, concentration and/or flow path (Chen & Hiscott 1999a).

The stacking of 2 or more erosive bed packets within a channeling component (fig. 2.18) implies repeated episodes of increased activity resulting in erosion and deposition of coarse facies within this fairway suggesting it to be a more persistent feature.

* bed packets *sensu* Chen & Hiscott (1999a) are defined as groups of beds sharing similar facies characteristics and an overall grain size distinct from strata immediately above and below corresponding to, for example, channel-fill and lobe deposits. 'Bed packets' correspond to 'bed packages' of Normark *et al.* (1993). Sub-packets is used here to describe subtle but recognisable differences in grain size and bedding pattern within the individual component / bed packet / package.

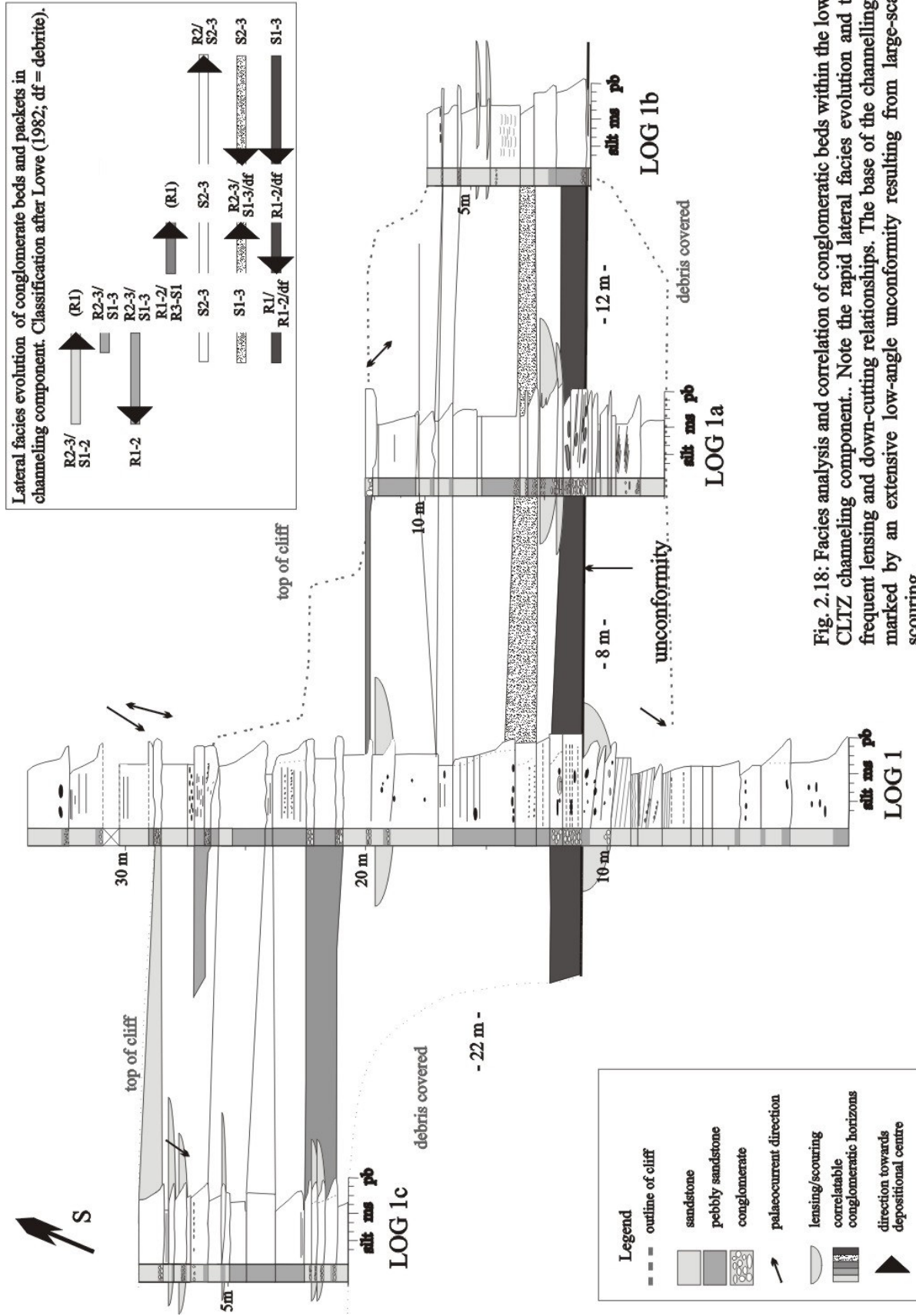


Fig. 2.18: Facies analysis and correlation of conglomeratic beds within the lower CLTZ channeling component.. Note the rapid lateral facies evolution and the frequent lensing and down-cutting relationships. The base of the channeling is marked by an extensive low-angle unconformity resulting from large-scale scouring.

The base of one of the lowermost channeling components is marked by a subtle, low angle unconformity which can be traced for a minimum of 40 m (fig. 2.18; plate 4.1 & 4.3). It is believed to result from mega-scale scouring (Mutti & Normark 1991; *see below: scours*).

Within the channeling components of the CLTZ an upward decrease in pebble size was observed perhaps related to an overall decrease in flow competence (Chen & Hiscott 1999a) and/or denudation of the hinterland in connection with increased transport distance through rising sea level.

Component	Total %	Magnitude components (v:lat in m)	Magnitude sediment beds (v:lat in m)	Constituents ratio (ave) (C/S/SH)	Sedimentology	Cycles
Channeling	30 %	< 20 : > 40	C: 0.4 – 2.5: < 10 - > 40 ave. 0.40 S: 0.5 : > 25	1.3/1/0	R1-3; R3S1-3 debrites	subtle asymmetric cycles and randomness
Lobe A	70%	5 - 33 : > 300	C(ave): 0.2 : > 1 S(ave): 0.6: >300 SH: 0.05: > 10	1/17/0.2	S1-3, rare R1-3, rare Td,e sandy debrites	random, some subtle f-up
Scours	5 % of channeling	? : > 40 : ? (d/w/l)	0.5 : 2.5 : 8 (d/w/l)	1/0/0	R1	non

(Abbreviations: v=vertical, lat=lateral, d=depth, w=width, l=length, C=conglomerate, S=sandstones, SH=shales)

Table 2.5: Hierarchy of scales of components in channel-lobe transition zone. Note that lateral extent is limited by degree of exposure.

Lobe A deposits

70 % of the unit are made up of between 5 - 33 m thick successions of coarse- to very coarse-grained sandstones, pebbly sandstones and occasional conglomerates, characterised by a high net sand content (> 90 %) (fig. 2.16, 2.17; table 2.5). The sandstones are thick-bedded (0.6 to 3.0 m), laterally extensive (traceability up to 300 m) and highly amalgamated (plate 4.4) resulting in some composite beds of up to 14 m thickness with poorly distinguishable amalgamation surfaces. Basal scouring is common but beds appear mostly parallel bedded. Sorting is generally poor to moderate. Individual beds either display normal grading with unstratified basal parts and crudely stratified tops (45 % of beds), or are structureless and ungraded (55 %). The deposits can be classified as Lowe's (1982) S1-3 division (~Bouma Ta, Tab) and deep-water massive sands (DWMS of Johansson *et al.* 1998; Stow & Johansson 2000) suggesting deposition from gravelly to sandy high-density turbidity currents and sandy debris flows. Inclined traction structures indicate bedload transport (Mutti & Normark 1987; plate 4.5). Rippled tops are rarely observed, they exhibit abundant plant debris and coalified material (plate 4.6). Parting lineation, indicating high flow velocities (Tucker 1996), is occasionally present. Trace fossils were not observed.

Internally, the lobe deposits are composed of poorly defined, up to 6 m thick bed sub-packets. They occasionally feature coarser sediments and sometimes erosive bases (10 %), showing subtle fining upward at sub-packet and lobe scale. Coarsening upward is rarely observed (fig. 2.16). Beds are arranged in crude 2-5 bed asymmetric bed thickness sequences (40 % of measured beds) with 2-bed thinning- and thickening-upward sequences the most striking ones (total: 70 % of ordered beds; fig. 2.19). However, random vertical organisation prevails. Random, disordered vertical bedding organisation and smaller asymmetric trends reflect irregularities in the volume of flow, concentration, grain size and the pathways of turbidites, compensating pre-depositional relief such as subtle topographic depressions

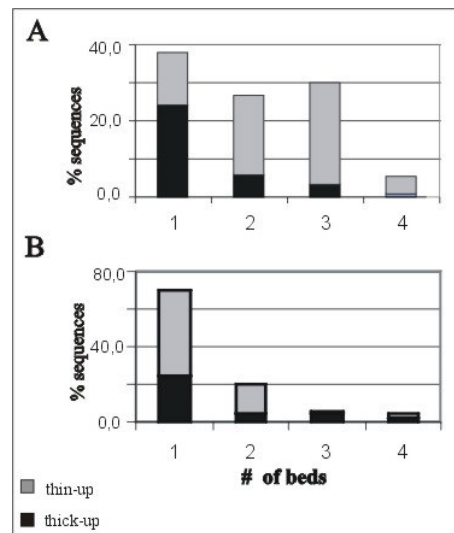


Fig. 2.19: Bedding sequences within A) channeling and B) Lobe A deposits of the channel-lobe transition zone, Cingöz Formation (2-bed moving-average smoothing technique after Heller & Dickinson 1985). Vertical ordering in A) comprised 58% and in B) 40% of the total beds; remainder are randomly organised.

(“compensation cycles”^{*} of Mutti & Sonnino 1981; Millington 1995; Chen & Hiscott 1999a).

Within the Lobe A deposits fine-grained sediments and shales are rare (1 %). They are thin bedded and laterally inextensive (10s of metres), often erosionally cut-off by succeeding flows. Despite the paucity of preserved shale beds, pebble- to small cobble-sized shale clasts are common. They are often associated with coarse-grained to pebbly sandstones with erosive bases.

Scours

Concave-upward scours (*sensu* Mutti & Normark 1987; Pickering *et al.* 1995) produced by intense turbulence are common within the channeling- and lobe deposits, however, they are present at different scales. The smaller scours, micro-scale (cm-dm), are primarily associated with the Lobe A deposits while

scour	length (cm)	width (cm)	l/w	minimum depth (cm)	infill	shape	strike
1	350	240	1.45 : 1	20	CLC	elongate	160 - 340
2	70	60	1.16 : 1	60	CLC	sub-rounded	
3	800	250	3.2 : 1	18	CLC	elongate	35 - 215
3a	250	120	2.08 : 1	?	CLC	elongate	
3b	130	70	1.85 : 1	?	CLC	elongate	
6	950	250	3.8 : 1	30	CLC	elongate	0 - 180

Table 2.6: Scours in the channeling component of the channel-lobe transition zone. Data obtained from scours exposed in plan view. CSC = clast-supported conglomerate.

meso-scale scours (dm-m) are typically found with channeling (fig. 2.16). In the latter, they amount to approximately 5 % of the total component. Here they form isolated, shallow cut-and fill features indicating erosion and subsequent depositional fill. They are typically infilled by pebbly to cobbly, clast-supported conglomerates and pebbly sandstones (plate 4.7). While the lobe and channeling components are 10s of metres thick and 100s of m in lateral extent, these scours appear an order of magnitude smaller (fig. 2.17; table 2.5). Their elongate, flute-like geometries (high length/width ratios, table 2.6) are interpreted to embody the early development of a scour (Allen 1971), which Millington (1995) ascribed to immaturity, assigning them to an unstable depositional environment. Mature scours approach ratio values of 1:1

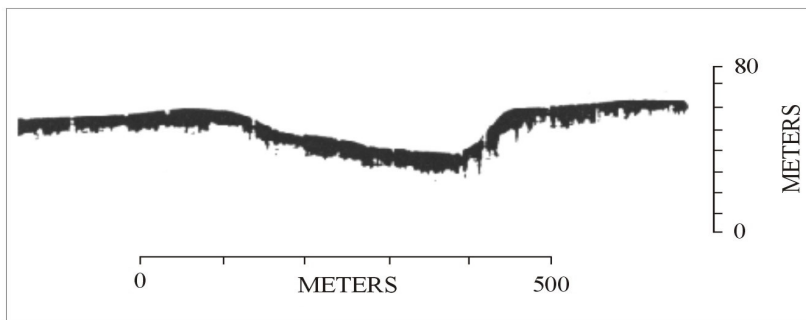


Figure 2.20a : Large-scale scours on Navy fan as observed with deep-tow side-looking sonar. Profile is a dip section showing the steep headwall scarp and that the relief is cut below an otherwise fairly uniform fan surface slope (from Mutti & Normark 1991; adapted from Normark *et al.* 1979).

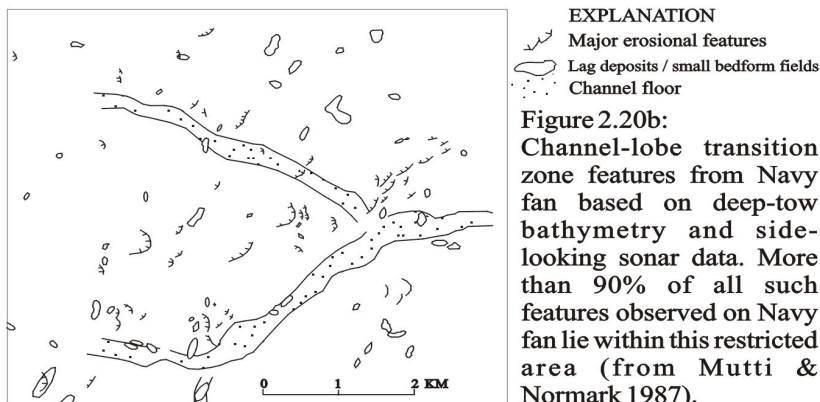


Figure 2.20b: Channel-lobe transition zone features from Navy fan based on deep-tow bathymetry and side-looking sonar data. More than 90% of all such features observed on Navy fan lie within this restricted area (from Mutti & Normark 1987).

* compensation cycles: a set of turbidite beds that collectively fill in low areas created by earlier turbidite deposition that had resulted in local aggradation of the surfaces (Normark *et al.* 1993).

(Allen 1971). The conspicuous absence of mud-drapes suggests that the scour and its infill may be produced by the same flow or that a mud-drape was eroded by a later flow (Mutti & Normark 1991). Macro-scale scours in the order of 100s of metres could not be observed, however, a subtle, low angle unconformity is present in the lower CLTZ (fig. 2.18; plate 4.3). Although no direct reference is made to low angle unconformities being a feature of transition zones, the large shallow scours seen in modern fans must produce some localised discordances at outcrop scale. Scours observed in transition zones of modern fans (fig. 2.20a,b) may reach depth of up to 100 m and 1 km across (Laurentian Fan: Shor *et al.* 1990) and may occur as groups of scours (5 – 30 m across / 1 – 2 m deep: Navy Submarine Fan: Normark *et al.* 1979). Cazzola *et al.* (1981) suggest that by increasing depth, the infill of large scours may grade into channel-fill deposits.

2.4.1.2 Channel-lobe transition zone: processes, facies and controls

The study area displays characteristics of both the channelized and lobe depositional environments. This is typical of channel-lobe transition zones (CLTZ) which are defined as regions within any turbidite system which separate well-defined channel-fill deposits from well-defined lobe facies (*sensu* Mutti & Normark 1987). CLTZs are regarded as poorly understood sectors of subaqueous fan systems and only few outcrop studies exist (e.g. Marnoso Arenacea: Ricci Lucchi 1981; Rocchetta Formation: Cazzola *et al.* 1981; Hecho Group: Mutti *et al.* 1985; Hecho Group/Morillo system: Millington 1995; Charo-Arro System: Millington & Clark 1995; Peary Land Group/Merqujoq Formation: Surlyk 1995; Macigno costiero: Cornamusini & Sandrelli 2002). Wynn *et al.* (2002) suggest that channel-lobe transition zones should be a common feature worldwide and studies of modern fans include, for example, the Crati Fan (Ricci Lucchi *et al.* 1985), Navy Fan (Normark 1970; Normark *et al.* 1979), Laurentian Fan (Shor *et al.* 1990) and Petite Rhone Fan (Millington 1995). CLTZs have also been recognised in "subseismic"-scale as areas with great relief dissected by numerous low-relief channels, e.g. the Paola Basin systems (Trincardi *et al.* 1995).

The classification of the study area as a channel-lobe transition zone is supported by its position within the fan framework, deposition resulting from turbidity currents undergoing hydraulic jump conditions, the presence of both channeling and lobe deposits and reworked sediments.

The CLTZ is located at the termination of the northernmost feeder canyon (channel 1). The adjacent shelf carbonates and slope (fig. 2.21a) indicate partial areal confinement and thus a more gradual opening up of the basin towards the south. Therefore, the initially confined and channelized flows undergo non-radial flow expansion before becoming completely unconfined (Mutti & Normark 1987, 1991; Millington 1995).

The study of modern fans shows that transition zones are commonly underlain by breaks in slope, creating

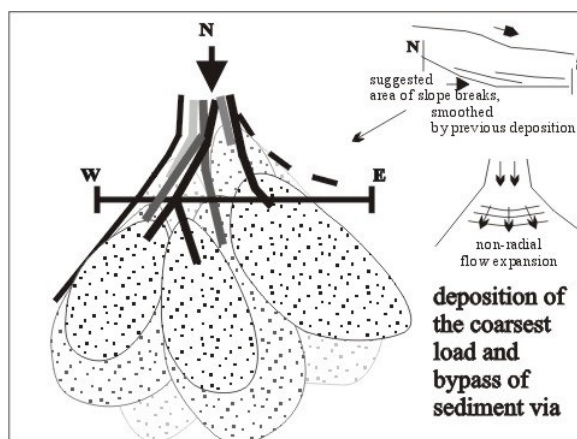


Fig. 2.21a: Conceptual sketch showing channeling and lobe development in the CLTZ. The confining margin allows for a gradual opening up into the basin. Channelised flows are poorly confined and develop laterally into Lobe A deposits. Darker colours indicate youngest deposits.

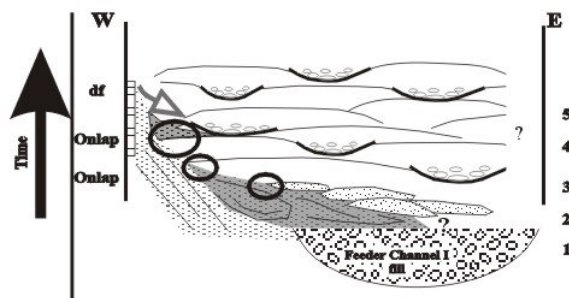


Fig. 2.21b: Cross-section of the CLTZ illustrating the development of the northernmost fan area. Abandoned (?) segments of feeder channel 1 (1) are overlain by collapsed slope deposits (2). Channel mouth and overbank deposits (3) onlap in more central location, indicating renewed channel activity. The channel system is backfilled by the mixed shingled-compensational stacked Lobe A (4) and channeling deposits (5) forming the sand-rich CLTZ. Poorly confined channelized flows may laterally develop into Lobe A deposits. Towards western margin, CLTZ deposits aggrade against collapsed slope debris.

rough morphological expressions (Navy Fan: Normark *et al.* 1979). However, the apparent backfilling of the feeder channel 1 system by the CLTZ deposits (fig. 2.21b) indicates that previous deposition has probably smoothed slope breaks, giving rise to reduced slope angles (Millington 1995). Nevertheless, as a result of the change in gradient and/or flow expansion (Millington 1995) and/or the flow volume with regard to distance travelled along the longitudinal profile (Mutti & Normark 1987) turbidity currents may undergo hydraulic jump causing increased internal turbulence, enlargement and dilution of flow and a marked increase in erosion (Normark & Piper 1991). As a result of these major changes in flow condition, a highly dynamic erosional-depositional environment with sediment bypass marks the CLTZ. Scouring and amalgamation, rapid deposition of the coarsest sediment fraction, reworking of sediments as well as winnowing and bypassing of the finer sediment load are the result.

Millington's (1995) study of the Hecho Supergroup shows that flow bypassing should either erode sediment or rework surface deposits with little to no new net deposition. Scours are located where flow stripping most commonly occurs and the recorded elongate, flute-shaped scours point to immaturity and unstable depositional conditions (Allen 1971; Millington 1995). In this dynamic environment even the creation of large scours can be a matter of minutes rather than hours (Shor *et al.* 1990). Mud-draped scours as typical bypass features (Mutti & Normark 1991) are lacking which may be due to subsequent erosion.

The CLTZ contains the coarsest facies of the sandy basin-fill of the E-Fan (*chapter 2.2*), the deposits often showing inclined traction (bedload) structures indicative of bedload transport (Mutti & Normark 1987) or are thick structureless sediment bodies. Winnowing and bypass of the finer-grained fraction is typical of transition zone (Mutti & Normark 1987, 1991; Millington 1995). The overall paucity of fines is in stark contrast to the relatively high abundance of shale rip-up clasts within the channeling and Lobe A deposits. The large size and angularity of the shale clasts point to short transport distances (Johansson & Stow 1995), suggesting that shales were either deposited within the CLTZ possibly as interchannel or interlobe deposits or slightly further upstream and were subsequently eroded by successive flows. Along the western margin, shale beds and reworked clasts are especially common (fig. 2.16), suggesting that more tranquil conditions favoured shale deposition and preservation in the marginal area. Millington (1995) demonstrated that deceleration in flows exiting a confined environment is not uniform but that the flanks of an expanding flow decelerate much more rapidly than the centre, giving rise to a zonation in facies associations; the centre being erosive in nature resulting in scour- and fill structures, while the flanks are more likely to deposit, for example, thick structureless sandstones (e.g. fig. 2.16, log 1: m 50-60).

Although well-defined channels *sensu* Mutti & Normark (1987) are conspicuously absent, the sedimentary nature of the deposits and the geometric features observed suggest that the conglomerate-dominated areas are associated with channeling. Cazzola *et al.* (1981) studied the channel-lobe transition zone of the Tertiary Rocchetta Formation (Piedmont Basin, NW Italy) and found that "channeling" is the product of scouring rather than true channeling. Their differentiation is based on i) the relatively shallow erosional depressions infilled by the same flow that was responsible for the erosion and ii) by the one-bed infill of erosional structures instead of the progressive multiple bed infill clearly onlapping onto channel walls which is characteristic of "proper" channel-fill deposits. However, with increasing depth of a scour, the number of beds infilling a scour will also increase and may eventually grade into channel-fill deposits (Cazzola *et al.* 1981), while through progressive flattening of a scour, gradation into parallel-sided sandstones may take place. Surlyk (1995) and Millington & Clark (1995) found abundant cut-and fill features and small channels filled with relatively few medium- to thick-bedded turbidites to represent the respective channel-lobe-transition zone. Their interpretations are supported by the position of the CLTZ with respect to the mid-fan channels and lobe deposits.

Stratigraphically, the CLTZ is located between well-defined channel-fill deposits up-system and lobe deposits in a down-system position. According to Ricci Lucchi (1985), this suggests an attachment between channel and lobe deposits, typical of sand-rich, low efficiency turbidite systems (*sensu* Mutti 1979). The resulting downcurrent geometry would typically be wedge-like (Millington 1995).

The overall lateral geometry of the channel-lobe transition zone (fig. 2.21a,b) is strongly controlled by the presence of the confining margins (*see above*) at least during the early stages of the CLTZ development. In its geographic centre, the CLTZ is at its thickest, thinning towards the western margin (fig. 2.18, 2.21b). Underlying chaotic slope deposits, thought to have collapsed into the basin margin forming a depositional wedge, are most likely aggraded on to by the CLTZ. Contacts are not exposed, however, onlapping and/or infilling the topography with localised erosion is most likely. Shelf/slope-derived debris flows presumably triggered by seismic activity and/or slope oversteepening or overloading have been recognised elsewhere in

the E-Fan (*chapter 2.3*) and are occasionally found interbedded within the Lobe A and channeling deposits (fig. 2.21a) forming localised topographic obstacles.

The crude fining-upward sequences of 60 to 80 m thickness throughout the CLTZ are created (fig. 2.16) by the highly erosive channeling components at the bases which transitionally fine upward into Lobe A deposits driven by channel abandonment and relocation. In conjunction with the overall fining observed within the channeling component throughout the CLTZ a continued gradual landward shift in the depositional focus is suggested as already indicted by the backfilling of feeder channel 1. This may be driven by the general rise in sea level in conjunction with denudation of the hinterland (Ericella *et al.* 1998). As demonstrated, the unique development of the CLTZ is controlled by a variety of parameters. These systems may mature through time with continued deposition smoothing out the initial irregular profile and thus display less typical transition zone features (Millington 1995).

2.4.1.3 Lobe A accumulation

The identified Lobe A deposits are unlike the classical lobe deposits *sensu strictu* Mutti & Ricci Lucchi (1972) and Mutti & Normark (1987, 1991). The Lobe A deposits of the channel-lobe transition zone are characterised by an abundance of erosional surfaces, high sediment amalgamation and a conspicuous lack of fine-grained material in an environment marked by its erosional-deposition style and sediment bypass. Associated channeling components appear to pass laterally and vertically into Lobe A deposits.

The clear lack of vertical organisation at sub-packet and lobe scale in conjunction with dominantly crude fining upward suggests an overall aggradational mode in lobe accumulation (e.g. Ricci Lucchi 1985; Shanmugam & Muiola 1988; Chen & Hiscott 1999a), while locally distinctive thickening upward indicates lobe migration into these particular areas (i.e. basal sequences at western margin and central section; fig. 2.16). The presence of channeling indicates sediment-bypass and thus some degree of fan progradation.

Internal cross-current variations in Lobe A facies, i.e. the presence of preserved interbedded fines and abundant shale clasts at the marginal CLTZ position versus the central CLTZ, is probably related to different rates of flow deceleration of the expanding flows with the resulting lateral variation from an erosional-depositional to a more depositional nature (*see above*).

Individual lobe geometries cannot be observed in outcrop and can only be inferred by circumstantial evidence. Field observations indicate that the high concentration turbidity currents were locally erosive, but amalgamated to form tabular, laterally extensive packages. However, the Lobe A bodies are not believed to form “basin-wide” features, i.e. across the total W-E extent (fig. 2.21a,b), as channeling is i) present at more or less all stratigraphic levels and ii) believed to be relatively shallow and not deeply erosive features. Therefore the Lobe A geometry is rather believed to be driven by the upstream switching of the distributary channels, shifting lobe accumulation into depositional depressions resulting in relatively narrow (maximal width: 600 – 1200 m), elongate, sheet-like bodies (fig. 2.21a).

The component distribution also suggests that channeling is a mostly isolated, relatively short-lived features marked by the frequent lateral and vertical relocation throughout the CLTZ. This observed channel migration may result from i) fairway plugging, ii) topographic lobe build-up and/or channel avulsion due to bifurcation not far upstream (Normark *et al.* 1979; Kneller 1995). Only the observed multistory stacking pattern in the lower CLTZ suggests repeated episodes of increased activity within a more persistent fairway. The distribution of Lobe A and channeling components and their downcurrent and cross-current relationships suggests an offset-stacked pattern akin to a mixed shingled-compensational stacking of Bouma (2000) rather than a simple vertical stacking of the lobes (fig. 2.17). Mixed retrogressive shingling due to a progressive landward shift mixed with occasional progradation is likely (fig. 2.17)

2.4.1.4 Channel-lobe transition zones associated with feeder channels 3 and 4

Channel-lobe transition zones were identified in the NW of the E-Fan but of much poorer exposure (study area 3; fig. 2.10). Transsection and offsetting by multiple faulting prohibits a detailed analysis. They appear to be associated with feeder channels 3 and 4 respectively, passing into lobe deposits located to the south and east. Here, the transition from channelized, conglomeratic deposits to sandstone-dominated, non-channelized deposits can be observed (fig. 2.22).

Just like the CLTZ associated with feeder channel 1, laterally extensive, very coarse- to coarse-grained, amalgamated sandstones dominate, while occasional conglomerates and pebbly sandstones are confined to

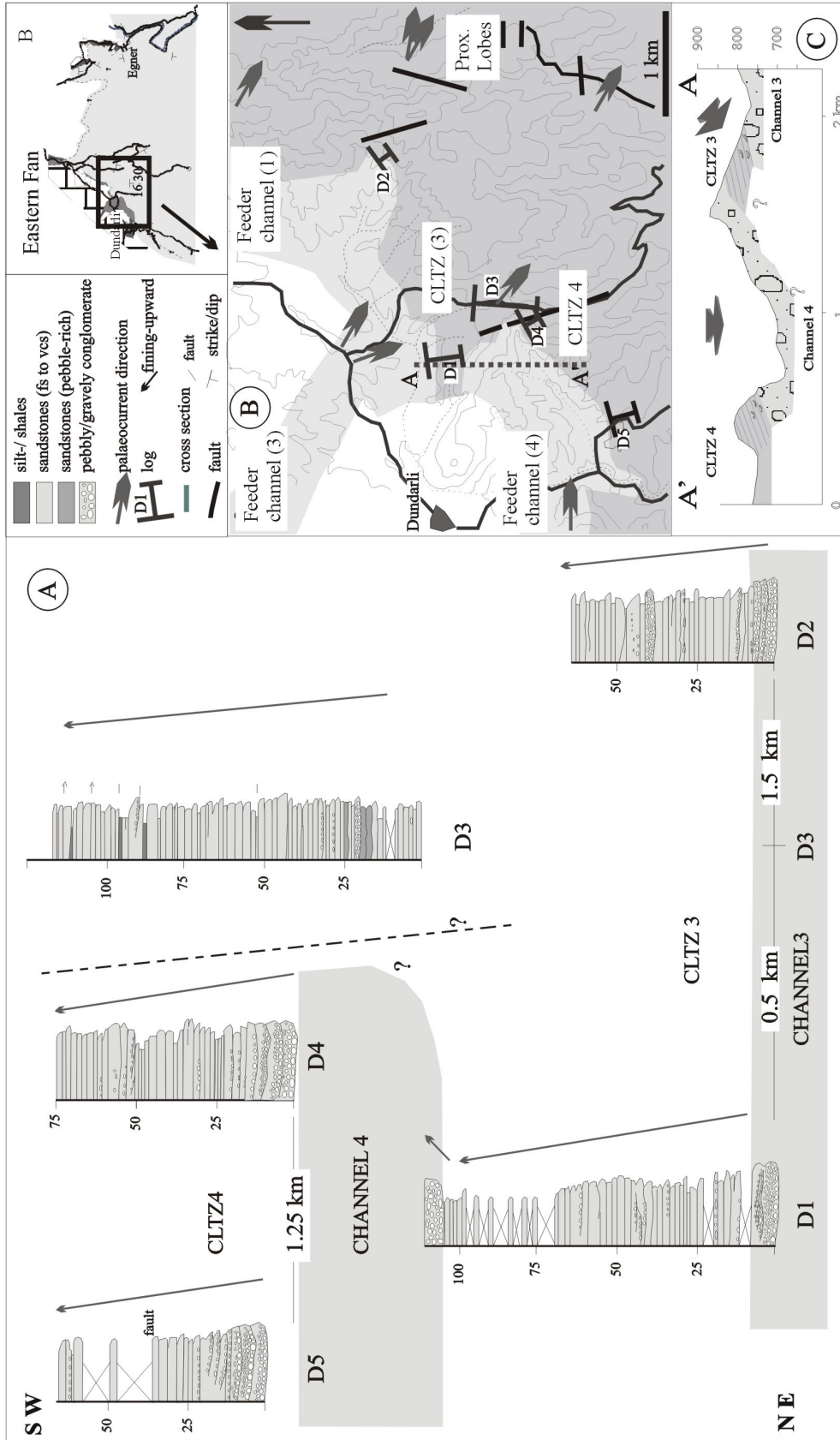


Fig. 2.22: A) Facies of transition zones associated with feeder channels 3 and 4 are located in the NW of the E-Fan. B) Location map indicating position of logs and cross-section as well as the relationship with proximal lobe section to the east. C) Cross-section through CLTZ and channel fill deposits showing the position of the respective fan environments (channel-fill mapped by N. Satur).

small-scale cut- and fill structures (fig. 2.22). Scouring and traction structures are common. The large overall fining-upward sequences are believed to have been generated by upward-passing into Lobe A deposits, upstream channel switching or forced migration due to topographic build-up of Lobe A deposits. In contrast to the northern CLTZ, no areal confinement of the zone appears to be present thus flow expansion must have been more rapid than at the CLTZ associated with feeder channel 1 resulting in more pronounced "typical" transition zone features described in literature (e.g. Mutti *et al.* 1985; Millington 1995). It is believed that the lower proximal lobe zone is the downcurrent equivalent of CLTZ associated with channel 4 and/or of the possible (?) confluence of channel 3 and 4, if channel 3 was still active at this time. However, the exact relationship cannot be conclusively established.

2.4.2 Proximal Lobe Zone

In the north-western fan area an approximately 300 m thick coarse-grained, sandy complex stratigraphically succeeds the channel-lobe transition zone to the west (*chapter 2.2*). Overlying sediments gradually thin and fine upward into distinct lobe packages interbedded with increasingly thicker interlobe and/or lobe fringe and fan fringe deposits in a distal, basinward direction.

The top 230 m are well exposed in a N-S, near dip-parallel section along a deforested hillside, roughly perpendicular to the palaeocurrent direction (fig. 2.23). The palaeocurrent indicators point to SE-E transport directions suggesting that this area was sourced from the west, from feeder channels 3 (?) and/or 4 (fig. 2.10). The up-stream, contemporaneous channel-fill deposits are not preserved, deposits of the top CLTZ associated with feeder channel 4? may correspond to the lowermost proximal lobe zone, however, relationships are obscured by abundant faulting. The down-stream deposits are not exposed.

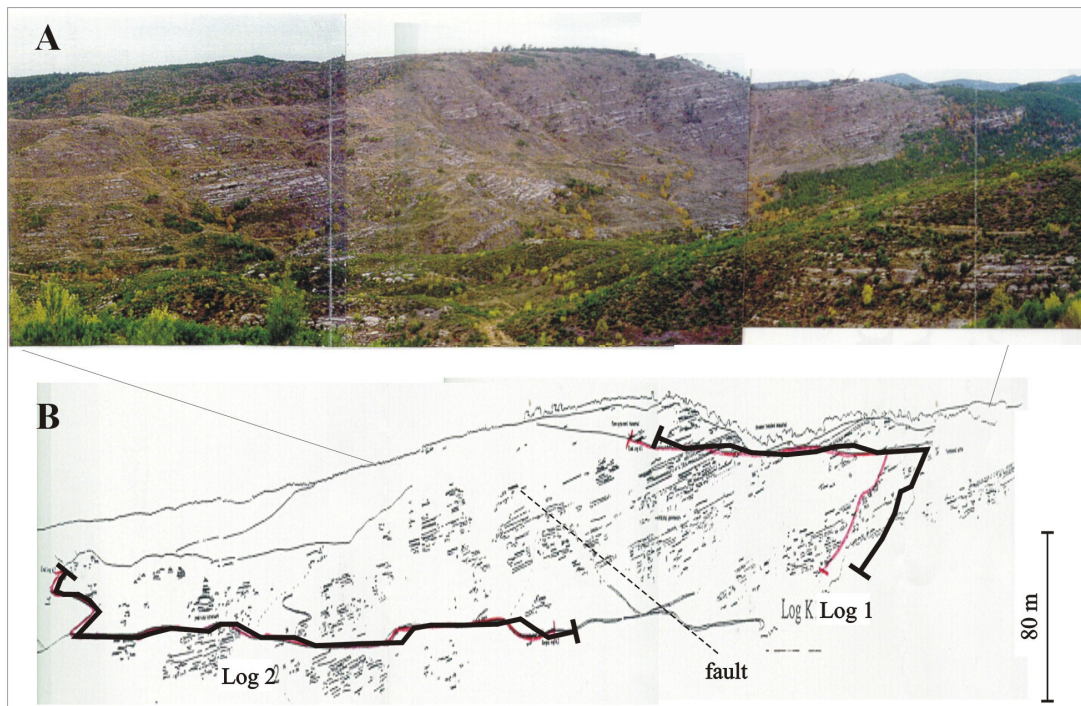


Figure 2.23: A) Aerial photograph showing the northern part of the proximal lobe zone. The hillside faces east, feeder channels 3 and 4 are located approximately 3 km to the west, behind the hill. Palaeocurrents point to SE-E transport direction. Beds dip 15° to south (left).

B) Line drawing of the northern and central proximal lobe zone with 2x height exaggeration. Position of Logs 1 and 2 are indicated.

Three logs were recorded, essentially covering the lateral development within these deposits (fig. 2.24). Generally, the outcrop quality is limited by i) at times poor exposure and ii) the sediments having undergone deep weathering and pervasive coating by lichens. Individual sandstone bodies can be traced for a maximum distance of 1.2 km before being displaced by faulting. Faulting is abundant (fig. 2.24), offsetting deposits of

mostly unknown vertical and lateral extent. The geometry of the lobe sequence was distinguished by means of photomosaics and linedrawings.

This complex is characterised by a very high sand/shale ratio (32:1). Thick-bedded, laterally extensive, coarse-grained sandstones and pebbly sandstones are arranged in discrete units (fig. 2.24) which are occasionally cut into by shallow channelized components or overlain by fine-grained fringe components. Conglomeratic beds and shale beds are rare, predominantly confined to the channel and fringe deposits respectively. Overall, distinctly pebble-rich and finer-grained sections are present, depicting 4 subtle fining-upward trends (log 1; fig. 2.24) in an overall fining-upward sequence.

2.4.2.1 Component analysis: internal organisation and geometry

Lobe B deposits

90 % of the proximal lobe zone are made up of 8 - 50 m thick lobe deposits characterised by a high net sand content (> 95 %), very coarse bases and an overall fining upward (fig. 2.24; table 2.7). Individual lobe bodies commonly succeed each other, their basal boundaries marked by sharp grain-size increases (fig. 2.25) while the tops are occasionally erosively cut into by distributary channels or transitionally or abruptly pass upward into finer-grained lobe fringe deposits.

Component	Total %	Magnitude components (v:lat in m)	Magnitude sediment beds (v:lat in m)	Constituents ratio (C/S/SH)	Sedimentology	Cycles
Lobe B	90 %	8 - 50: > 1200; downcurrent extend: ~ 2400 - 4800	S: 0.6-2.5: > 1200	0/20/1	pebbly S & S1-3, rare SH, sandy debrites	crude f-ups, rare c-ups asymmetric & random bedding organisation
Distributary channels	8 %	1 - 5 d : 20 w	S: 0.1 - 1.3 : 20 C: 0.1 - 0.5: 1.5	1/10/1	R3,S1-3, pebbly S, rare C (R1)and SH, sandy debrites	subtle f-up, thin-ups
Lobe fringe	2 %	2-8 : >700	S: 0.05 - 0.2: > 700	-/3/1	Tc-e	thin-ups

(Abbreviations: v=vertical, lat=lateral, d=depth, w=width, l=length, C=conglomerate, S=sandstones, SH=shales, f-up=fining upward, c-up=coarsening upward)

Table 2.7: Hierarchy of scales of components of the proximal lobe zone.

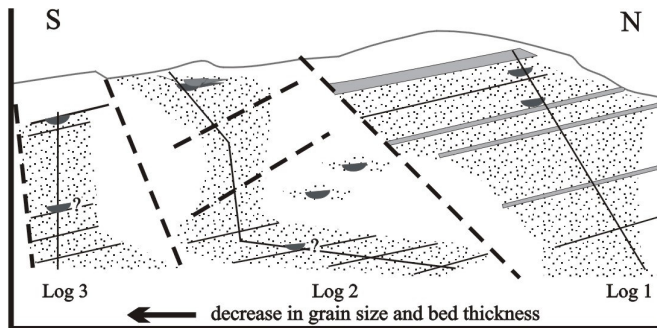


Figure 2.25: Diagram showing component arrangement in the proximal lobe zone. Pod-like structures identified from photomosaics revealed coarser, strongly erosive, and partly wedging sandstone bodies which are interpreted to represent distributary channels. Components: Lobe B deposits (*sandstone signature*), interlobe deposits (*grey*), distributary channels (*dark grey*). Blank areas denote dominantly very poor or no exposure, only major faults are shown. Distances from base Log 1 to base Log 3 approximately 1.8 km. 5 x vertical exaggeration.

The Lobe B deposits are composed of coarse-grained sandstones and pebbly sandstones (fig. 2.24, plate 5.1) which typically exhibit massive bases and some crude stratification, poor to moderate sorting and normal grading (59 % of beds). Occasional parallel lamination and trough-cross bedding are present as well as zones of syndimentary water escape structures (plate 5.2). Bioturbation (burrowing) is rare (plate 5.3). Beds are highly amalgamated, and they appear to be between 0.4 to 1.2 m thick. Composite beds with indistinguishable amalgamation surfaces may reach thicknesses of up to 3-4 m, (plate 5.4), in some cases forming up to 35 m thick amalgamated complexes. These composite beds are often structureless, non-graded and may contain abundant shale clasts resembling deep-water massive sands (DWMS) of Stow

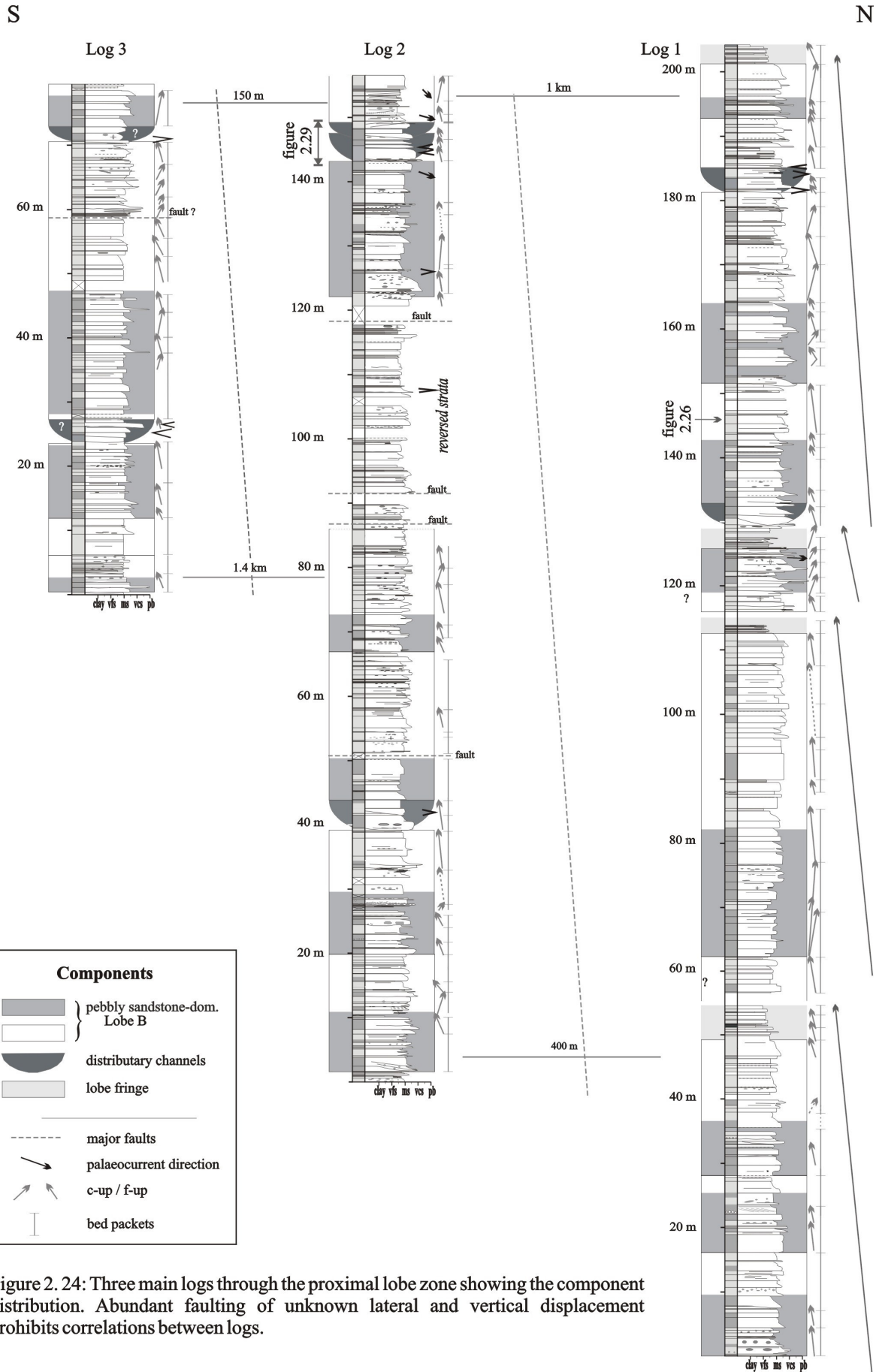


Figure 2. 24: Three main logs through the proximal lobe zone showing the component distribution. Abundant faulting of unknown lateral and vertical displacement prohibits correlations between logs.

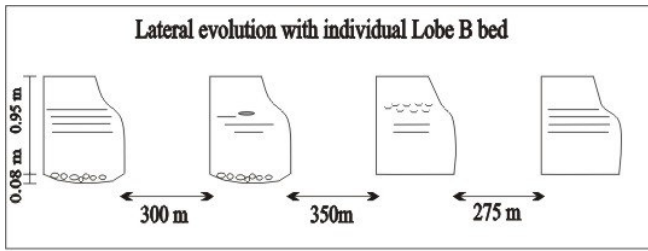


Figure 2.26: Over 925 m lateral extent no significant changes in grain size and thickness are present. Thickness variations are a function of the depth of scours.

beds can be observed (plate 5.5). The deposits can be classified as R3,S1-3 deposits of Lowe (1982) and DWMS (Stow & Johansson 2000), resulting from deposition of gravelly to sandy high density turbidity currents and sandy debris flows (*sensu* Shanmugam 1996). Little shale and fine-grained facies are preserved, however, shale-rip up clasts are common suggesting initial shale deposition and subsequent erosion and short transport distances by succeeding flows (Johansson & Stow 1995).

Internally, the lobes are composed of poor to moderately defined bed sub-packets (fig. 2.24). These are typically 2-6 m thick (max. 11 m), involving an average 6-8 beds and are characterised by either asymmetric or random organisation or distinctive grain sizes and often display erosional bases. Asymmetric bed thickness trends (52 %) slightly dominate over random arrangements (44 %), with 3 - 4 bed thinning-upward sequences the most common (fig. 2.27). Symmetric sandstone compensation cycles or microsequences suggested to be characteristic in proximal lobe environments (Stow & Johansson 2000) are rare (4 %). Similar to Lobe A deposits, the small asymmetric and random bedding organisation are believed to reflect different process such as irregular variations in flow volume and concentration and topographic compensation (e.g. Mutti *et al.* 1978; Chen & Hiscott 1999a). The differentiated fining-/coarsening-upward trends at bed sub-packet scale (fig. 2.24) do not always correlate well to the observed bed thickness trends. Individual lobes show crude fining upward, however, some basal coarsening upward (centre log 1, fig. 2.24) and overall coarsening upward (top log 1) has been observed. Generally, though, the observed overall lack of well-defined vertical order at bed package and lobe scale is striking and typifies an aggradational mode in lobe accumulation (Ricci Lucchi 1985; Chen & Hiscott 1999a).

In absence of the complete lateral and 3-D exposure, the general Lobe B geometry can only be inferred. Lensing was not observed at outcrop scale, at 1.2 km lateral extent, the beds, bed packages and lobe bodies appear to possess a more tabular geometry which is believed to reflect the whole-body geometry (fig. 2.28; Stow & Johansson 2000). Deposits in the south of the study area (log 3; fig. 2.25) are slightly thinner-bedded and finer-grained, essentially suggesting that these inhabit a more lateral (cross current) position within the proximal lobe depositional environment (*see Lobe B accumulation*).

Distributary channels

The lobe deposits are occasionally cut into by prominent, shallow channels (8 % of total section; fig. 2.24; table 2.7). These channels display width/depth ratios of 20:1 to 4:1 (1 - 5 m deep / up to 20 m across).

Their infill is characterised by moderately defined bed sub-packets of 3- 5 beds of very coarse-grained sandstones, pebbly sandstones and pebbly conglomerates (R1 and R3, S1-2 of Lowe 1982), arranged in thinning- and fining- upward sequences (67 % of sequences; fig. 2.27). Irregular interbedding with thinly-bedded fine sand and shales (Tc,d of Bouma 1962) is present. The conglomerate/sand/shale ratio is 1:10:1.

& Johansson (2000). Sandstone beds and DWMS are laterally extensive and can be traced for up to 1.2 km maximum without displaying any significant thickness changes apart from irregular, but abundant basal scouring (11 % of beds) resulting in subtle thickness variations. No significant lateral facies changes were observed (fig. 2.26). Pebbly sandstones and matrix-supported pebbly conglomerates are mostly confined to scour-infills. Occasionally, distinct wedging of

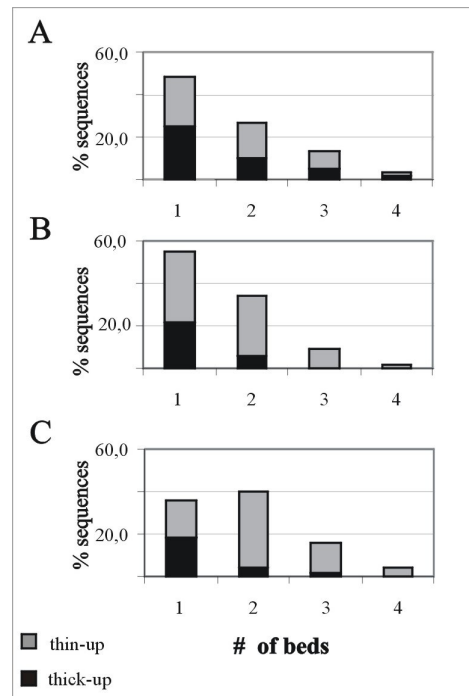


Figure 2.27: Asymmetric bedding sequences within A) Lobe B, B) distributary channels and C) lobe fringe deposits of the proximal lobe zone (2-bed moving-average smoothing technique after Heller & Dickinson 1985). Note that 44% of beds in Lobe B deposits show random vertical organisation.

Multiple-stage infill is occasionally present (fig. 2.29). The infills display a series of erosional features such as scours, cut-downs and the deposition of residual facies representing the erosional-depositional channel type *sensu* Normark (1970) and Mutti & Normark (1987). 0th to 2nd order bounding surfaces, based on Pickering *et al.* (1995), are present (table 2.28).

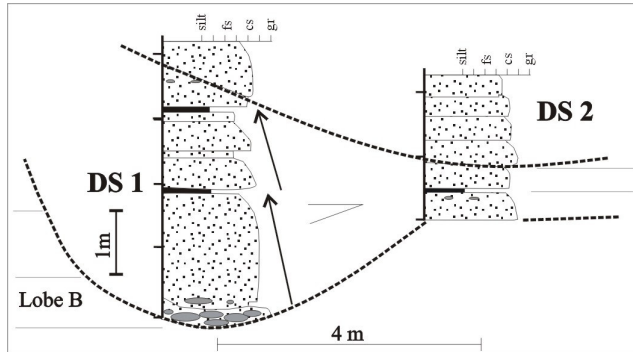


Figure 2.29: Channel amalgamation and multistage infill of distributary channel component. Note erosion into Lobe B to left and “wing”-development to right of DS1.

The channels represent isolated features within the proximal lobe deposits (fig. 2.25). However, plate 5.1 shows an example of a multilateral offset-stacked channel growth pattern (*sensu* Pickering *et al.* 1995). The distinct wedging of beds towards the channel margin (65 % thickness decrease) and bed continuation beyond the actual channel geometry (plate 5.6; fig. 2.29) suggest that the shallow depth of the channel could probably not retain the head of the density current (Weimer 1989). It thus resulted in deposition outside the channel geometry, leading to a wing-like geometry (fig. 2.28).

Wüllner & James (1989) imply that the observed pod-like geometries and thinning-upward sequences are characteristic of meandering channel systems. Einsele *et al.* (1994) found fining-upward sequences to result from lateral channel migration. The flow conditions that could lead to the development of meandering or branching submarine turbidite channels are poorly known at present (Mutti & Normark 1987; Shanmugam 2000). The erosional-depositional style and the occasional channel amalgamation further suggest prolonged channel activity in places. The observed channel abandonment and/or shift may be caused by up-stream channel avulsion, the progressive plugging of a channel fairway or lobe build-up (Normark *et al.* 1979; Normark & Piper 1985; Surlyk 1995).

Bounding surfaces in distributary channels	Hierarchy after Pickering <i>et al.</i> (1995)	Architectural elements after Pickering <i>et al.</i> (1995)
Bed planes of laminae	0th order	Pebble and sandstone laminae (> 0.01 m thick)
Individual bedding planes	1st order	Individual bed (0.01 - 0.6 m thick)
Bed sub-packet planes	2nd order	Bed package (1.6 – 5 m thick)

Table 2.8: Bounding surfaces distinguished in distributary channels of proximal lobe zone.

Small distributary channels have been noted in the normally unchanneled lobe environment (Normark *et al.* 1979; Ericella *et al.* 1998) where they are commonly associated with the coarsest facies present (Cazzola *et al.* 1985), showing little to no associated levee development (Ricci Lucchi 1975a; Damuth & Flood 1985; Wilde *et al.* 1985). The lack of levee deposits in conjunction with the channel geometries may result from the rapid migration and deposition within this distributary system (Normark 1978; Normark & Piper 1985; Garrison *et al.* 1982).

The distributary channels associated with Lobe B deposits are probably located along their edges and/or in marginal depressions as suggested by the asymmetric erosional pattern where confinement by lobe deposits is present on one side and a partial wing development on the other. Fairways in that position may result from slightly accelerated turbidity current flow as the current moves off the lobe onto the adjacent lower surface of the fan (Normark *et al.* 1979; Normark & Piper 1985). Ricci Lucchi (1975a) found channeling in proximal lobe environment to result from fan progradation and their association with the pebbly sandstone-rich intervals is striking (fig. 2.24).

In other areas, well-defined channel geometries are absent but prominently wedging sediments, individual beds and groups of beds, are present. These are present throughout the whole section (fig. 2.24). Strongly wedging beds were observed in connection with channel geometries (this study), however, proximal lobes were found to have prominent topography (Normark *et al.* 1979) and wedging resulting from topographic compensation cannot be discounted (Kneller 1995).

COMPONENTS	IDEALISED SECTION	SEDIMENTARY FEATURES	GEOMETRY	STACKING PATTERN	vertical COMPONENT ASSOCIATION
LOBE "B"					<p>A) sharp, dominantly non-erosive</p> <p>B) erosive</p> <p>C) gradational</p>
DISTRIBUTARY CHANNEL			<p>A) 5-20 m</p> <p>B) "Channel wing" > 30 m</p> <p>C) wedging up to 60 m</p>	<p>isolated</p> <p>offset-stacked</p>	<p>base: erosive, top: gradational</p>
LOBE FRINGE				<p>isolated</p>	<p>Base: gradational top: sharp, dom. non-erosional</p>

Figure 2.28: Characteristics of differentiated components in proximal lobe zone, their sedimentology, geometries and stacking pattern.

Lobe fringe deposits

The lobe deposits may transitionally grade into distinctly finer-grained and thinner-bedded units which are characterised by a considerably lower net sand content (sand/shale ratio = 3:1). These deposits are interpreted to represent the fringe environment (*sensu* Mutti & Ricci Lucchi 1975; Ricci Lucchi 1981) of the proximal Lobe B deposits. The lobe fringes are always sharply overlain by lobe deposits (fig. 2.24).

The fringe facies is characterised by thin-bedded (2 - 20 cm), fine to very fine sand-sized sandstones, often displaying well developed lamination (Tc-e; Bouma 1962), which are typically interbedded with thinly-bedded shales (plate 5.7). The sediments indicate relatively more tranquil depositional conditions (Mutti & Normark 1987). Bioturbation was not observed. Beds are arranged in crude, up to 60 cm thick, thinning-upward sequences typically involving 2 - 4 beds (fig. 2.27). These sequences are likely to result from waning flow volume or concentration (Chen & Hiscott 1999a).

The overall thickness of the fringe deposits varies. In mid section (fig. 2.25), they are up to 2 m thick, becoming increasingly more common and thicker (> 6 m) towards the top. They are a laterally continuous feature which can be traced for approx. 1200m (midsection; top: 750 m; Log 1: fig. 2.24), before being obscured by vegetation and faulting. Throughout this lateral distance, no significant lateral changes in facies and thickness were observed. The absence of their lateral development into lobe deposits is striking.

Overall, the lobe fringe deposits appear as isolated features, representing approximately 2 % of the section (table 2.7). Their geometry is inferred to be smooth wedge-like representing the cross-current as well as downcurrent pinch-out of lobe deposits.

2.4.2.2 Lobe B accumulation

The depositional pattern of the Lobe B deposits does not fit the classical lobe definition *sensu strictu* Mutti & Normark (1987) where well-defined, coarsening-upward lobe deposits are encountered in the non-channelized outer-fan environment (*sensu* Mutti & Ricci Lucchi 1972), separated by variable amounts of fine-grained material. The Lobe B deposits are characterised by a very high net sand content, poor vertical organisation at bed sub-packet scale and often crude fining upward at lobe scale separated by minor intervals of thin-bedded turbidites in an overall fining-upward complex.

Irregular lobe topography and erosive flow power appear to characterise the proximal lobe depositional environment. For example, sandy to fine gravelly macrodunes with mean wavelength of several 100 m and > 5 m relief have been recognised in the proximal sandy lobes of the Laurentian Fan (Hughes Clarke *et al.* 1990; Normark & Piper 1991), while at the same time small-scale compensation cycles, expressed as asymmetric sequences, suggest progressive smoothing of topographic relief (Hecho Group: Mutti & Sonnino 1981; Mutti & Normark 1987). Similar small asymmetric compensation cycles are common throughout the Lobe B deposits, however, strongly wedging beds probably due to relief compensation (Kneller 1995) are most conspicuous. Subtle wedging beds (1 m over 100 m) of the proximal lobe environment of the Kongsfjord Formation (Pickering 1981) result from laterally subtle but extensive erosion. Similar lobe down-cutting was observed in the Laga Formation, Italy (Mutti *et al.* 1978). However, this cannot be confirmed for the E-Fan proximal lobes. Erosional flow power is confined to sediment reworking and relatively frequent basal scouring of individual beds, which Savoye & Piper (1990) relate to the initial erosive power of sandy flows before deposition takes place. Frequent scouring is a common feature in ancient proximal lobe depositional systems (e.g. Hecho Group/Fiscal Lobes: Mutti & Normark 1987; Laga Formation/Italy: Mutti *et al.* 1978).

The component arrangement reveals stacked Lobe B deposits forming a large, approximately 300 m thick sand-rich complex. The lobes are occasionally interbedded with shallow, isolated and/or offset-stacked distributary channels and isolated lobe fringe deposits (fig. 2.25). While the distributary channels form small entities within the large complex, both the Lobe B and lobe fringe deposits are laterally persistent features in excess of 1200 m. No lateral gradation to and from lobe to lobe fringe deposits was observed at outcrop scale.

The thinning- and fining upward of most of the lobes and the lobe complex contradicts the typical view of thickening-upward lobe successions, interpreted to result from lobe progradation (e.g. Mutti & Ricci Lucchi 1972). The internal organisation of the lobes reveals a slight dominance of asymmetric, mostly thinning-upward sequences, however, random arrangements are frequent. It has been recognised that lobes can form by aggradation resulting in the lack of thickening-upward successions (e.g. Ricci Lucchi & Valmori 1980; Hiscott 1981; Shanmugam & Moiola 1988; 1991; Chen & Hiscott 1999a). Rarely, the lobes display some

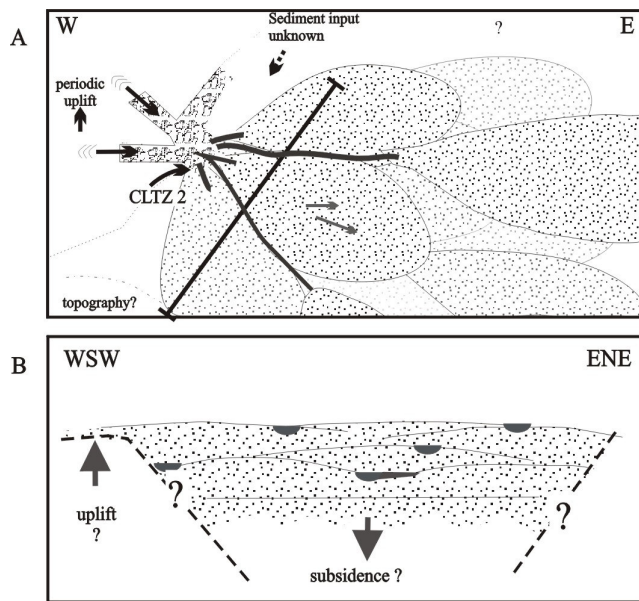


Figure 2.30: A) Conceptual drawing of Lobe B development in proximal lobe zone. The area is fed from the W and NW, the input from the N is believed to be diminished at this stage. The channel-lobe transition zones 3 / 4 are located between the feeder channels and the proximal lobe zone.

B) The pre-Cingöz basin topography was controlled by pre-existing structures (Williams *et al.* 1995) leading to locally enhanced sediment accumulation. A probably fault-controlled intrabasinal depression underlying the NW E-Fan area created a semi-restricted accommodation space which acted as sediment trap and fairway to more distal fan areas. Tectonic and/or bulk sediment weight controlled subsidence. Sporadic overspilling at topographic margins led to reduced sediment deposition in especially the WNW fan area.

sheet sandstones.

Chen & Hiscott (1999a) favour autocyclic mechanisms to drive lobe accumulation at 10s of metre scale discounting progressive basinward-landward advance or retreat of one sub-environment over another.

Simple lateral lobe switching resulting from lobe build-up, upstream channel switching and avulsion (e.g. Walker 1978; Chen & Hiscott 1999a) is likely to result in the observed vertical organisation and stacking pattern, producing a latero-vertical growth pattern akin to "compensation cycles" (Normark *et al.* 1979; Ricci Lucchi 1981; Surlyk 1995). As some progradation exists, a mixed shingled-compensational pattern *sensu* Bouma (2000) may be present, amalgamating lateral and progradational offset-stacking (fig. 2.30a).

However, a mechanism to explain the top lobe location of some of the channels suggests that other mechanisms such as tectonics, sediment supply and eustasy may play a role in the development of the proximal lobe zone (Normark & Piper 1991; Pickering *et al.* 1995).

basal or overall coarsening upward suggesting lobe progradation or migration into this particular depositional area. The presence of distributary channels throughout the lobe complex, however, suggests that some progradation is taking place (Ricci Lucchi 1981; Shanmugam & Muiola 1991).

Observations from the modern Navy Fan (Normark 1979; Normark *et al.* 1979) suggest that "true" distributary channels other than the depressions along the edges of lobes are not present in the proximal lobe environment. The lobe topography diverts distributary channels, following a path between the lobe depocentres leading to a sinuous channel pattern. While this appears to explain the isolated nature of the observed distributary channels underlining their status as short-term conduits and their abrupt channel relocation probably along the marginal lobe edge depressions (e.g. top log 2, fig. 2.24), it, however, does not explain channel positions not located at lobe edges (e.g. top log 1, fig. 2.24). They rather indicate channel formation on top of older lobes. Thus some channel locations appear to be controlled by allocyclic rather than autocyclic mechanisms. Lobe formation at the respective distributary channel mouth will either be located between or overlap with distal parts of previously deposited sandstone bodies. The development of channel wings, where poorly-contained flows laterally develop into sheet-sandstones blurs the difference between "true" channel and "true" lobe deposits (top log 2), leading to interlobe depressions filled with relatively coarse-grained

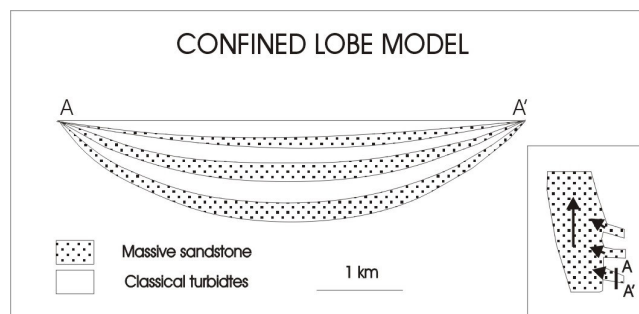


Figure 2.31: Diagrammatic representation of the confined lobe model, showing the vertical alternate stacking of broadly lenticular units composed of massive sandstone and classical turbidites. Deposition occurred in pre-existing topographic depressions that very likely acted as sediment fairways to the open basin. Inset shows the alleged position of the fairways with respect to the open Pindus Basin (from Schuppers 1995).

For one, tectonic activity causing localised uplift, exposing the hinterland and proximal (channelized) fan areas to erosion, proved to be frequent throughout the fan development (*chapter 2.2*). This may account for the observed increased supply of coarse material to the basin, periodically bringing on coarser sedimentation, resulting in the sharp, coarse onset of the Lobe B deposits. A gradual recession of an individual lobe following retrogressive slumping and headward migration of the source area may also account for the observed smaller-scale fining-upward cycles (Surlyk 1995) as well as higher frequency changes in relative sea level and/or changes in sediment supply, flow volume, shelfal accommodation space and denudation of the hinterland (Einsele & Ricken 1991; Normark *et al.* 1993; Mutti *et al.* 1994; Pickering *et al.* 1995; Chen & Hiscott 1999a). The observed sharp onset of lobe fringe deposits following a coarsening-upward Lobe B body (top log 1) suggests abrupt lobe abandonment in places. However, the overall facies organisation reflects the effect of a generally rising sea level and/or grain size reduction following denudation of the hinterland resulting in a landward shift of the depositional locus producing the observed overall fining-upward sequence.

The observed aggradational lobe-fill and mixed vertical, off-set stacking pattern reflect a semi-restricted spacial development where deposition is not free to migrate. Sedimentary input from the N (feeder channel 1) is unknown and no evidence of flow mixing is present. However, the rapid thickness reduction and eventually pinch-out towards the S-SW is striking (*chapter 2.2*, lateral-marginal fan facies). The complex seafloor topography prior to fan deposition (Williams *et al.* 1995) may lead to enhanced sediment deposition in some areas (Kneller 1995), while differential subsidence recognised within the basin allowed for vast thickness accumulations in the central basin sector during later stage fan development (*chapter 2.2*). Lobes B are believed to have developed in a similarly restricted environment, where tectonically driven and/or load induced differential subsidence of a basin segment created laterally restricted accommodation space akin to the confined lobe model of Schuppens (1995). But while the lobes of the Arakinthos Sandstone (Schuppens 1995; fig. 2.31) formed "depression-wide" features, the component distribution of the proximal lobe zone suggests at least some lateral migration of lobe deposition (fig. 2.30b), although intraformational onlapping was not observed. Ricci Lucchi & Valmori (1980) demonstrate that syndepositional subsidence maintained a topographic depression into which the Post-Contessa subinteral of the Marnosa Arenacea Formation was deposited resulting in the highest rate of deposition within the system, something similar which is suggested for the Lobe B accumulation. This probably fault-controlled topographic depression acted as a sediment trap but also as a fairway for sediment to more distal areas, damming lateral sediment dispersal (Ricci Lucchi 1975a, 1981; Normark & Piper 1991; Stow & Johansson 2000).

The lateral and vertical association of Lobe B with distributary channels and their proposed deposition in intervening lows suggests a more elongate, sheet-like geometry. Their areal extent, i.e. downcurrent extent, is suggested to range in excess of between 2400 to 4800 m based on length:width ratios of 2:1 to 4:1 for ancient lobes (Stow & Johansson 2000). The actual downcurrent extent is believed to be much greater, since only partial width measurements are available.

2.4.3 Distal lobe deposits

In the east sediments of the relatively distal fan environment are well exposed along the Seyhan River road cut (plate 6.1). 860 m of laterally extensive, sand-rich packages and associated finer-grained deposits span from the slope/fan contact in the north to the basinal shales in the south (fig. 2.32; *chapter 2.2*). The outcrop quality is generally good, only limited by occasional poor exposure and deep erosion by Quaternary fluvial gravels. The section essentially forms a linear exposure with maximal 200 m lateral control. The best exposed sections of primarily sand-dominated deposits were selected for detailed studies. Vertical and lateral logging was carried out to analyse the sedimentology and dynamics of the system, the elemental components, their geometry and small- to large-scale vertical and lateral variability. The detailed analysis of the lateral logging is discussed in chapter 4 (reservoir characterisation). The palaeocurrent pattern points to an ENE-NE transport direction which is near parallel to the confining northern basin margin. The sections are mostly dip-parallel and either perpendicular or slightly oblique (max. 15°) to the general palaeocurrent direction.

The deposits are of Langhian age and thus younger than the channel-lobe transition zones and proximal lobe zone. They are sourced from the same feeders (geochemical pilot study: Satur 1999).

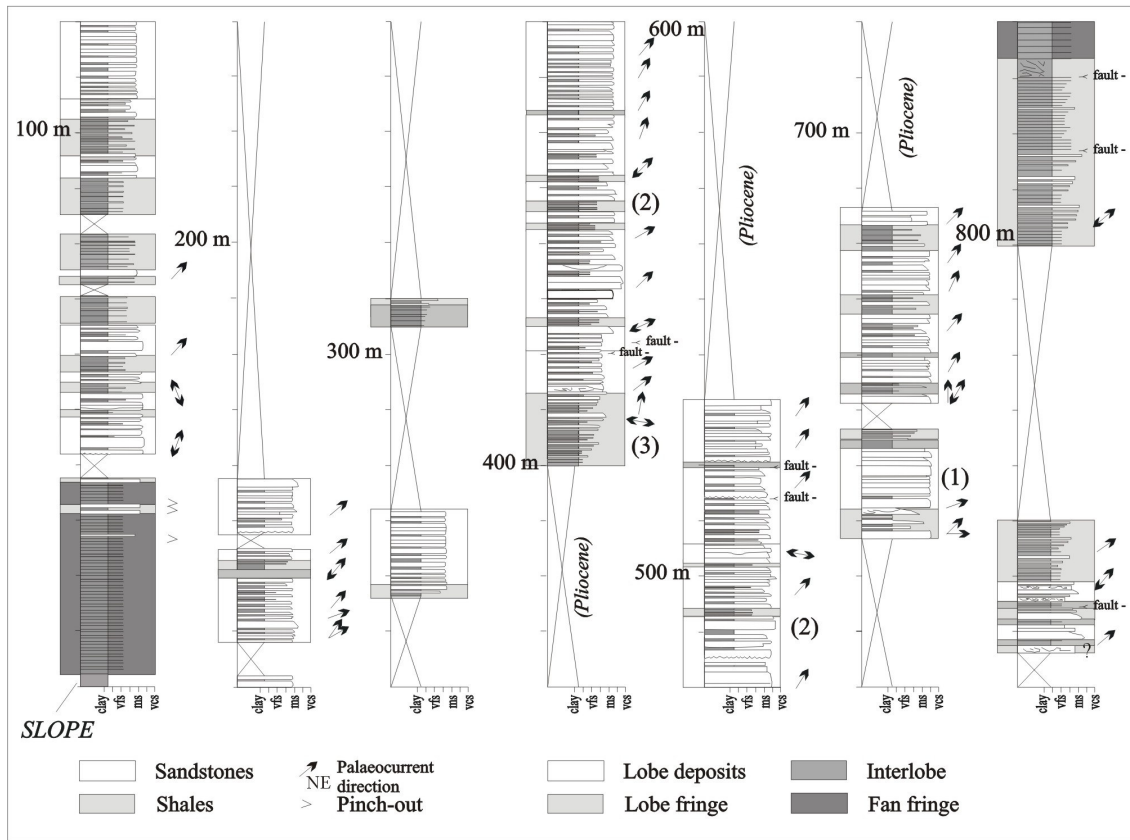


Figure 2.32: Summary log of the distal lobe zone exposed along the Seyhan River showing fan sediment from fan-slope contact in north (bottom left) to fan fringe deposits in south (top right). The palaeocurrent indicators point to a general NE transport direction. Detailed logs presented in chapter: (1) lobe fringe-lobe deposits, (2) bed thickness plot lobe deposits, (3) stacked lobe fringe. The component interpretation is based on detailed logs of the section.

2.4.3.1 Component analysis: internal organisation and geometry

Lobe C deposits

Discrete packages of high sand: shale ratio (6:1) dominate the eastern section. They form 65 % of the total section. Individual packages are between 4 - 35 m thick, dominated by non-erosive, laterally extensive sandstones. They are interbedded with distinctly finer-grained and thinner-bedded deposits exhibiting largely transitional contacts. They can be defined as “depositional lobes” *sensu* Mutti & Normark (1987).

Components	Total %	Magnitude components (v:lat in m)	Magnitude sediment beds (v:lat in m)	Constituents ave. ratio (S/SH)	Sedimentology	Vertical arrangement
Lobe C	65 %	4 – 35 : >200	S: 0.15-2.5 : >200; ave v: 0.45 SH: 0.01-0.1 : >200	6/1	S2-3, Ta-d(e), rare pebbly S & SH, sandy debris	random, some asymmetric c-up & f-ups
Lobe fringe	22 %	3 – 15 : > 150	S(ave): 0.2 : >150 SH: 0.01-0.12 : >150	2/1	S3, mostly Tc,d (e)	asymmetric, c-up & f-ups
Interlobe	4 %	5 – 15 : > 150	S(ave): 0.1 : >150 SH: 0.01-0.1 : >150	1/1	Tc-e	random; some symmetric
Fan fringe	9 %	> 10 : > 100	S: 0.05-0.1 : >100 SH: 0.5-0.2 : >100	1/1.5	Tc-e, hemipelagites	random

(Abbreviations: v=vertical, lat=lateral, S=sandstone, SH=shale, ave=average, f-up=fining up, c-up=coarsening up)

Table 2.9: Hierarchies of scales of components in the distal lobe zone.

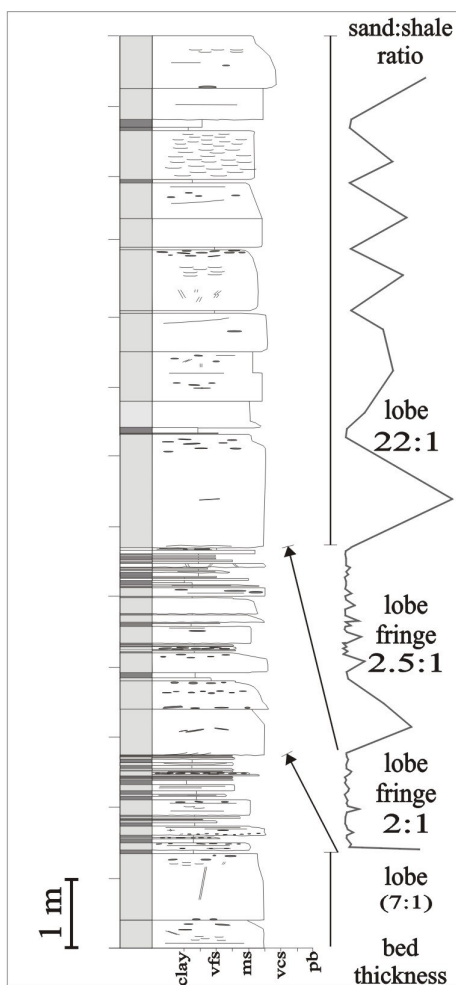


Figure 2.33: Stacked, fining-upward lobe fringe deposits, overlain by sand-rich Lobe C deposit (mid-section Seyhan River Section: (1) of figure 2.32)

Other common features include shale rip-up clasts, which suggest reworking of underlying beds (Stow & Johansson 2000). The net:gross ratio is high (see chapter 4), individual sandstone beds contain 90 – 100% and bed packages and lobes 75 - 90% net sand (fig.2.33). Syndepositional water-escape structures, i.e dish structures, are locally present. Bioturbation is abundant as burrows and top-bed features indicating relatively tranquil phases between sandstone deposition. The trace fossil assemblage is characterised by a mixed and *Nereites* fauna (Demircan & Toker 1998; plate 6.3). Slumping and shaley debris flows are a relatively common feature close to the slope margin area, less common in the main depositional area (plate 6.4), suggesting topographic relief and collapse of slope/fan fringe and lobe fringe deposits respectively.

Internally, the lobes are composed of moderately well defined bed sub-packets (fig. 2.33). These are 3 - 8 m thick and characterised by distinct bed thickness or grain size trends. The bed thickness analysis reveals that approximately 70 % of the beds are arranged in asymmetric bed thickness sequences, the remainder showing random organisation. Thinning-upward trends dominate, 3 and 4-bed sequences are the most common ones (fig. 2.34). Like in Lobe A and B deposits, the high number of 2-bed sequences (52 %) is striking.

The sand content varies widely reflecting the more central or marginal position of the lobe deposits respectively. The lobe deposits have sand/shale ratios ranging from 22:1 (central section; plate 6.1) to 4:1 (marginal areas). They are composed of medium- to coarse-grained sandstone beds averaging 0.45 m in thickness (fig. 2.33; table 2.9). Amalgamation of beds can lead to composite thicknesses of up to 2.50 m in places. The bed thickness can vary considerably at metre scale, which is largely a function of the size and depth of present scours. However, over 200 m lateral exposure, no significant overall thickness variations are present. Towards the marginal areas beds become thinner-bedded and finer-grained and eventually pinch out against the slope (chapter 2.3.1) and into fan-margin/basin plain facies respectively (fig. 2.32).

The moderately to well sorted sandstone beds show normal grading (75 % beds), often with rapid fining towards the top of beds (plate 6.2). Massive bases and stratified tops (S1-3 (Lowe 1982) and Ta-c(d,e) (Bouma 1962)) are most common, suggesting deposition from sandy, high-density turbidity currents and diluted flows (Lowe 1982) or occasionally from sandy debris flows (*sensu* Shanmugam 1996; discussion chapter 5.1). Deposits of high density currents are typically non-graded, however, the observed normal grading may result from syndepositional fluidisation (Nichols *et al.* 1994). In the marginal positions, beds show more often Tc-e (Bouma 1962) divisions.

The sandstone beds are often separated by thin shale to fine sands (T(c)d,e), equally, amalgamation of up to 2-3 beds, especially in the central section, is common. Here, clay-draped amalgamation surfaces prevail. Shallow scours, typically infilled with very coarse to granule sands, are rare. Their shallow tabular shape results primarily from impact of dense flows on soft substratum (Mutti & Normark 1987).

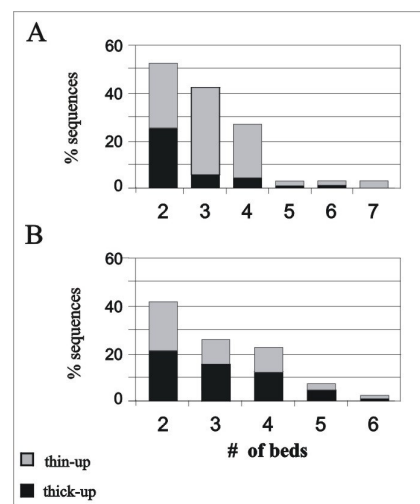


Fig. 2.34: Bedding sequences within A) Lobe C and B) lobe fringe deposits of the more distal lobe section determined by 2-bed moving-average technique (Heller & Dickinson 1985). 70% of the Lobe C and 72% of the fringe deposits show an ordered vertical arrangement.

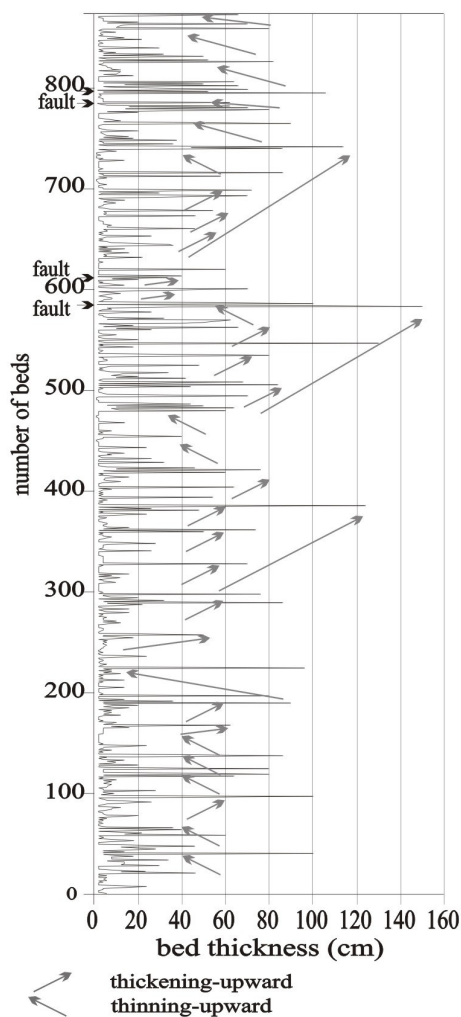


Figure 2.35: Bed thickness versus bed number plot for lobe and lobe fringe deposits of the Seyhan River Section, Cingöz Formation ((2) of fig. 2.32). Thickening- and thinning-upward trends at bed packet, stacked bed-packet and lobe scale are present throughout. Random arrangements are subordinately present.

and packages of beds appear to be sheet-like and laterally extensive, however, the observed gradual pinch-out of lobe bodies towards the margin with low angles of inclination (*chapter 2.3.2*) together with some degree of “fanning-out” transport directions presents limited evidence of a general (convex upward?) lobate geometry (fig. 2.37).

Lobe fringe deposits

Associated with the lobes are lobe fringe deposits (*sensu* Mutti & Ricci Lucchi 1975; Ricci Lucchi 1981), characterised by a lower average sand: shale ratio (2:1) and distinctly asymmetric bed thickness sequences (plate 6.6). Vertically, they transitionally grade to and from lobe and interlobe deposits respectively. Since lobe and lobe fringe deposits transitionally pass into each other, this study uses the arbitrarily chosen maximum sand/shale ratio of 3:1 to distinguish between them. Individual lobe fringe packages are between 3 - 15 m thick (fig. 2.38), forming approximately 22 % of the total section (table 2.9).

The sandstones are composed of 5 - 30 cm thick, fine- to medium-grained sandstones (S3 of Lowe 1982 and Tb-d(e) divisions of Bouma 1962) separated by 1 - 15 cm thick, thin-bedded silt-/mudstone alternations (Td,e) (fig. 2.38). Amalgamation is uncommon. Beds are laterally extensive and display very little facies and thickness changes at outcrop scale (~ 150 m).

Minor asymmetric sequences are interpreted to result from topographic compensation or variation in flow volume and concentration (e.g. Mutti & Sonnino 1981; Chen & Hiscott 1999a).

The above method, however, does not pick up the large-scale trends observed when plotting bed thickness against bed number. Figure 2.35 shows that some thickening-upward trends involving up to 130 beds are present, composed of a variable number of smaller-scale thickening- and/or thinning-upward trends involving approximately 20 - 35 beds. The thickening- in conjunction with coarsening-upward sequences suggest abrupt lobe abandonment (Pickering 1981). Thinning-upward and symmetrical sequences are subordinately present as well as some distinctly random vertical arrangements (bottom fig. 2.35).

Solemarks such as erosive groove and flute casts are common (plate 6.5), indicating a general ENE-NE transport direction (216 data points). On single bedding surfaces, flute casts are recording up to 60° divergence (mean 15°) in palaeoflow direction (fig. 2.36), the divergence probably resulting from a transversely divided current head (“lobes and clefts”) moving at slightly different rates in slightly different directions (Allen 1971). However, the general transport direction in i) individual beds, ii) individual Lobe C packages and iii) the individual lobes section is strikingly persistent throughout (fig. 2.32), suggesting that only the northern to north-eastern flank of much larger lobe deposits are exposed.

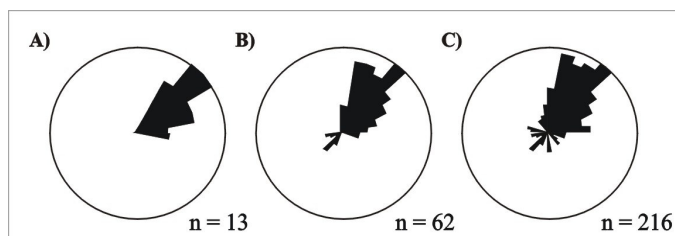


Figure 2. 36: Palaeoflow directions in a) individual bed, b) Lobe C and c) total eastern distal lobe zone.

The limited exposure of the Lobe C bodies prohibits direct observation of the complete lobe geometry. Individual beds

COMPONENTS	IDEALISED SECTION	SEDIMENTARY FEATURES	GEOMETRY	STACKING PATTERN	vertical COMPONENT ASSOCIATION
LOBE C	<p>random arrangement</p> <p>mostly c-upps, some f-ups</p>	<p>0.6 m</p> <p>0.2m max</p> <p>great divergence at bed scale</p>	<p>> 300 m</p> <p>sheet-like, some lobate</p>	<p>mixed shingled - compensational stacking?</p>	<p>A) sharp</p> <p>C) gradational</p>
LOBE FRINGE	<p>mostly thickening- / coarsening-upward</p>	<p>0.2 m</p> <p>some slumping</p>	<p>> 150 m</p> <p>sheet-like, smooth wedging</p>	<p>isolated</p> <p>stacked</p>	<p>mostly gradational, rarely sharp</p> <p>sharp</p>
INTERLOBE	<p>symmetric sequences or uniform</p>	<p>0.1 m</p>	<p>> 150 m</p> <p>broad, shallow infill</p>	<p>isolated</p>	<p>sharp</p> <p>transitional</p>
FAN FRINGE	<p>gradual fining-upward</p>	<p>ave. 0.05 m</p>	<p>> 100 m</p> <p>sheet-like, smooth wedging</p>	<p>probably stacked</p>	<p>towards basin</p> <p>transitional</p> <p>towards slope</p>

Fig. 2.37: Component characteristics and relationships within the distal lobe environment.

Bioturbation is abundant, showing the same trace fossil assemblage as the lobe deposits. Slumping is occasionally present (fig. 2.38), suggesting fringe collapse into adjacent interlobe depressions. Palaeocurrent indicators point to the ENE - NE direction (mean 032° / 24 data points), thus being consistent with the transport directions measured in the lobe deposits.

The deposits are arranged in up to 8 m thick well-defined asymmetric bed thickness cycles. These findings appear to be consistent with lobe fringe deposits as defined by Mutti & Ricci Lucchi (1975) belonging to the group of TBTs (thin-bedded turbidites) of Mutti (1977). Pickering (1981) and Surlyk (1995) recognised fining- and thinning-upward cycles also to be common in the lobe fringe. Both types of asymmetric bed thickness patterns were recorded in the lobe fringe deposits of the Seyhan River section with thickening-coarsening-upward sequences slightly more common (fig. 2.34). Figure 2.38 shows a distinct coarsening and thickening upward of the sandstones into lobe deposits associated with a marked upward increase in the sand/shale ratio from 1:1 (base) to 3:1 (top). The observed bed thickness cycles are both interpreted to result from lobe switching. While coarsening-/thickening-upward sequences are produced by lobe migration (progradation or lateral switching) into a particular area, the “shifting away” or retrogradation of a lobe leaves progressively thinning and fining deposits behind.

The lateral evolution of lobe fringe into lobe and interlobe deposits respectively could not be observed at outcrop scale. Studies by Mutti & Ricci Lucchi (1975), Mutti (1977), Ricci Lucchi & Valmori (1980) and Pickering (1981) show that lobe fringe deposits laterally grade into the coarse, thick-bedded sediments of depositional lobes. Lobe fringes can thus be classified as the peripheral fringes of lobe deposits, being their distal equivalents in a downcurrent and crosscurrent direction (fig. 2.39; Mutti 1977). At the stratigraphic top of the section, the lobe fringe deposits laterally grade into less sand-rich fan fringe sediments.

The lobe fringes are believed to have a very smooth wedging geometry since they represent the eventual lateral and distal pinch-out of the depositional lobes (fig. 2.37). The observed lobe/lobe fringe pinch-out against the slope underlines the presence of low angles of inclination at the lobe margins (*chapter 2.3.2*).

Interlobe deposits

Occasionally, the lobe and lobe fringe deposits are interbedded with distinctly finer-grained and thinner-bedded deposits which display an overall low sand/shale ratio of 1:1 (< 50 % sand). They classify as interlobe deposits (e.g. Kongsfjord Formation: Pickering 1981; Matilija Sandstone: Link & Welton 1982). Their deposition occurred in the intervening lows between individual depositional lobes (fig. 2.39), an area reached only by dilute currents. They therefore represent a fairly passive depositional environment within the fan lobe.

The interlobe deposits may reach between 5 - 15 m in thickness, forming approximately 4 % of the total section (table 2.9). Their basal and top contacts are mostly transitional, however, sharp contacts with overlying lobes may occur (plate 2.8).

Internally, the interlobe deposits are composed of well-sorted 1 - 15 cm thick sandstones of fine sand-size, commonly showing T(c)de subdivisions (Bouma 1962). They are separated by 1 - 10 cm thick shale beds (Td,e), forming relatively thick monotonous successions (plate 6.7). These sediments are the product of dilute turbidity currents depositing their fine-grained suspension load (Bouma 1962). Occasionally, isolated thicker-bedded and coarser-grained sandstone beds are present indicating sporadic spill-over of larger turbidity currents into the depression of the interlobe area, probably triggered by tectonic activity (Ricci Lucchi 1981). Symmetric bed thickness patterns are most common, marking the transition to and from lobe fringe deposits (fig. 3.37).

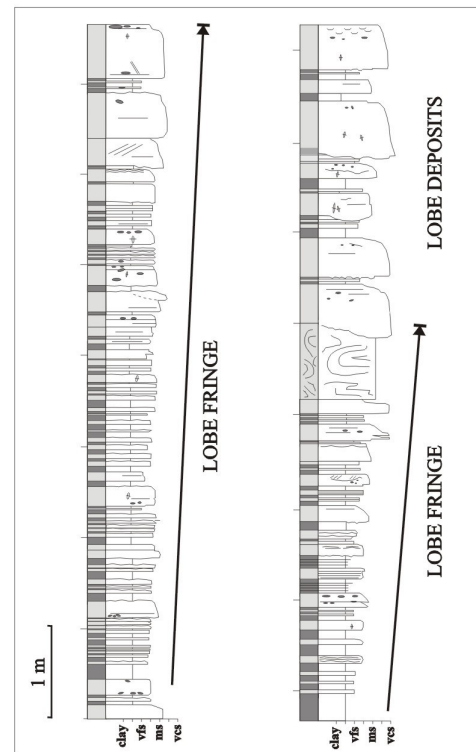


Figure 2.38: Stacked lobe fringe deposits showing distinct thickening- and coarsening-upward sequences ((3) of fig. 2.32). A distinct increase in the sand:shale ratio from 1:1 (base) to 3:1 (top) is present. Slumped features suggest occasional fringe collapse.

Plate 2.8 shows that the interlobe deposits have great lateral extent in excess of 150 m. The interlobes are inferred to possess a shallow, lenticular infill-geometry (fig. 2.37), reflecting the gradual infill of depressions between lobe mounds.

In their appearance the interlobe deposits (plate 2.8/6.7) are similar to fan fringe deposits (*see below*). The interlobe deposits are identified by their association with lobe and lobe fringe deposits, while fan fringe deposits are associated with lobe fringe and basin plain deposits (plate 6.8). Furthermore, the interlobe deposits of this study are characterised by a slightly higher sand content than the fan fringe deposits.

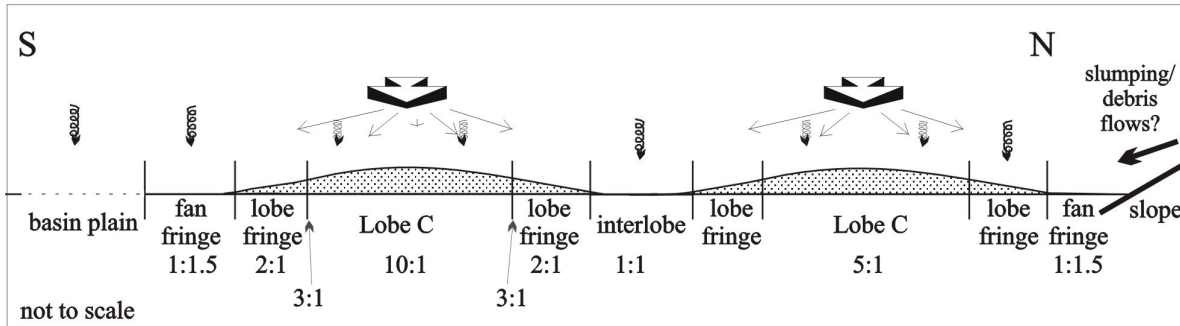


Figure 2.39: Schematic component association in the distally located eastern area of the E-Fan. Their differentiation is largely based on sand:shale ratios, their geometries inferred by vertical facies associations, diverging palaeocurrent patterns and field observations.

Fan fringe deposits

The top 15 m of the Seyhan River section are dominated by a monotonous sequence of alternating thin beds of sandstone, shales and hemipelagic marls, characterised by a low sand content (sand/shale ratio = 1:1.5; table 6.8). The contact with the underlying lobe fringe deposits is transitional. The contact with the overlying basin plain deposits (Güvenç Formation) is not exposed, however, it is believed to be transitional as recorded in the central and western section of the E-Fan (*chapter 2.2*). The fan fringe deposits form about 9 % of the eastern section.

The deposits are made up of 5 - 10 cm thick, fine- to very fine-grained sandstones (Tc-e; Bouma 1962), which are interbedded with 20 - 50 cm thick siltstone-shale intercalations (Td,e) and hemipelagic mud. The sediments are intensely bioturbated. Few thicker sandstone beds are randomly interbedded (plate 6.8). The sediments are the product of diluted turbidity currents (Ghibaudo 1980), while the interbedded thicker sandstones result from coarser flows occasionally reaching this area. The bedding arrangement appears impressively regular, however, a very subtle thinning and fining upward is present (fig. 2.32).

Their association with and position between basin plain and lobe fringe deposits (fig. 2.32; fig. 2.39) suggests them to be TBT fan fringe deposits *sensu* Mutti (1977). Fan fringe deposits are defined as representing the most distal submarine fan deposits both in a distal and lateral direction (Mutti 1977; Mutti & Johns 1978; Ghibaudo 1980; Pickering 1981). Thus, their geometry is believed to be smooth, sheet-like, eventually pinching out towards the basin plain (fig. 2.37; fig. 2.39, e.g. Macigno Formation: Ghibaudo 1980).

2.4.3.2 Lobe C accumulation

The distal lobe deposits, Lobe C, present the more classical lobe deposits often described in literature (e.g. Mutti & Ricci Lucchi 1972; 1975; Mutti *et al.* 1978; Walker 1978; Ghibaudo 1980; Pickering 1981; Mutti & Normark 1987, 1991; Surlyk 1995). They are non-channelized, sand-dominated deposits associated with lobe fringe, interlobe and towards the top of the section with fan fringe sedimentation. The Lobe C deposits are characterised by a high sand/shale ratio.

The internal organisation of the Lobe C shows smaller-scale asymmetric and random bedding organisation at bed sub-packet and stacked bed sub-packet-scale within overall coarsening-upward sequences, suggesting that aggradation is the dominant process at bed sub-packet-scale, while the entire lobe results from progradation and/or lateral migration, especially in mid-section (fig. 2.32; e.g. Mutti & Ricci Lucchi 1972; Mutti 1985b; Mutti & Normark 1987, 1991; Shanmugam & Moiola 1991). The observed thinning-upward

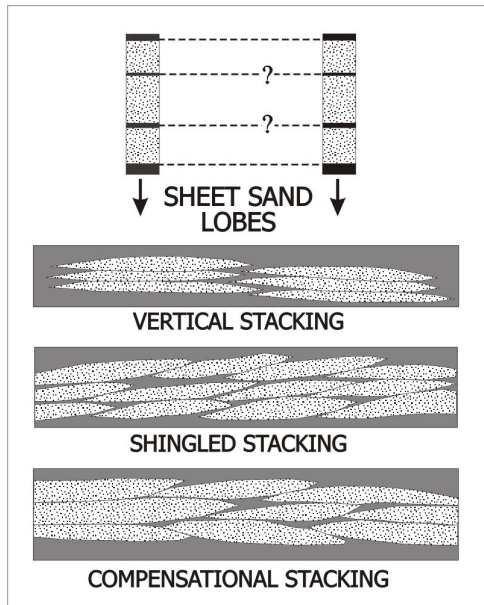


Figure 2.40: Schematic drawing of three possible stacking patterns resulting from lateral switching within sheet sand lobes. Presently it is not known which ones are the most common. It is likely that those patterns mix according to downdip gradients and the most favourable accommodation space (from Bouma 2000).

fringe.

The component arrangement reveals an irregular spacing of the lobes. The clustered appearance in mid-section points to the main depositional area. Here, the lobes occur either stacked or as isolated components separated by isolated and/or stacked lobe fringe and isolated interlobe deposits of varying thickness. Towards the fan margin (slope and basinal direction) the individual lobes are associated with increasingly thicker fine-grade material of lobe fringe and lobe- and fan fringe origin respectively. The observed vertical organisation may result from lobe switching due to lobe build-up, upstream channel switching and avulsion in mid-section (Mutti & Ricci Lucchi 1975; Walker 1978; Ghibaudo 1981; Ricci Lucchi 1985; Shanmugam & Moiola 1988; Surlyk 1995; Chen & Hiscott 1999a), producing an offset-stacked pattern within a relatively distal outer fan environment, leading to a mixed shingled-compensational stacking pattern (Bouma 2000), amalgamating progradation and lateral migration (fig. 2.40).

Towards the top of the section, increasing abandonment of the outer fan lobe is reflected by the (offset?-) stacked lobe fringe deposits. This resulted in lobe fringe and eventually fan fringe sedimentation in an area in which otherwise sandlobes would have been deposited, probably driven by the overall rising sea level (Yetiş *et al.* 1995; Kostrewa *et al.* 1997). Seismic and borehole data indicate that E-Fan deposition extends much farther to the south during its earlier development (*chapter 2.2.2*).

True lobe geometries are rarely observed in outcrop where down- and cross-current wedging of convex-upward bodies into lobe fringe deposits (Ricci Lucchi & Valmori 1980) with the resulting low angle inclinations at the margin of the lobe can be observed (Surlyk 1995). Cazzola *et al.* (1985) suggest that if slope-onlap can be observed, the lobes are likely to form basin-wide features. This, however, is not supported by the component distribution pattern (fig. 2.41) where mid-section interlobe deposits are believed to be flanked by lobe bodies on either side, although no lateral gradation to and from interlobe to lobe fringe/lobe has been observed. Lateral facies changes were only observed along the margins (lobe/lobe fringe pinchout and lobe fringe to fan fringe transition). It is not believed that the interlobe deposits are in fact fan fringe deposits, representing basin-wide features, thus indicating temporary, high frequency regression of the active fan lobe. That this landward-basinward shift resulting in cycles of progradation is driving lobe accumulation at 10s of metres of scale is unlikely (Chen & Hiscott 1999a) and rather the lateral shifting of depositional locus is favoured for the observed facies distribution.

sequences suggest gradual lobe abandonment (Mutti & Ricci Lucchi 1975; Pickering 1981) and/or in combination with the observed random vertical organisation reflect aggradation (e.g. Ricci Lucchi & Valmori 1980; Ricci Lucchi 1981, 1985; Hiscott 1981; Ghibaudo 1981; Shanmugam & Moiola 1991; Chen & Hiscott 1999a). Thus, Lobe C accumulation in the more distal fan area reflects some degree of fan progradation combined with latero-vertical growth (fig. 2.40).

The well developed, small-scale or high frequency cycles of bed sub-packets (roughly comparable to the elementary facies tract (EFT) of Mutti 1992) may result from a variety of autocyclic and allocyclic controls such as, for example, topographic compensation, flow path, flow volume and concentration, changing sediment supply, high frequency climatic changes in the source area, tectonic activity and high frequency sea-level fluctuations (*see* Normark *et al.* 1993; Mutti *et al.* 1994; Chen & Hiscott 1999a) for discussion). It is however acknowledged, that the reasons for high frequency cyclicity are largely unknown (Mutti *et al.* 1994).

The symmetrical coarsening/thickening upward to thinning/fining upward of the section (fig. 2.32) reflects the transition from fan margin to main depositional area to fan fringe and eventually basin plain deposits in the relatively distal outer fan environment (*sensu* Mutti & Ricci Lucchi 1972). The marginal and relatively distal fan areas received little sand deposition. This is reflected by the progressive increase in net sand content from 1:1 - 5:1 at the margin (slope) to 22:1 (mid-section), decreasing to 1:1.5 at the fan

The palaeocurrent pattern persistently points to a NE-ENE transport direction all throughout the section. Kneller & McCaffrey (1999) suggest that flow deflection may also have contributed to the phenomena of persistent slope-parallel palaeocurrent directions. This could be envisaged for the more marginal parts of the succession, however, it appears more likely that the exposed lobe deposits represent the north-eastern margin of much larger lobes while the top section lobe fringe / fan fringe palaeocurrent patterns indicate a general west-ward shift in the depocentre (fig. 2.41c).

Tectonic activity resulting in thick debris-flow deposits or the periodic onset of very coarse sedimentation as recorded in the proximal and central fan areas is not evident in the distal lobes of the Seyhan River section. Occasional slumping and thin-bedded debris-flow deposit associated with fringe collapse and proximity to the slope are believed to have been brought on by seismic activity and/or sediment instability due to overloading (Reading 1996). However, the thick slumped packages of fan sediments observed along the north-eastern margin (*chapter 2.3.2*) indicate that tectonic activity and/or oversteepening played a role during sediment accumulation. Underlying slope sediments are of late (?) Langhian age (Cronin *et al.* 2000), thus these thick slumps correlate time-wise with the Seyhan River section deposits and record fan aggradation against the slope at some stage during its development.

Lobe C accumulation within the distal lobe zone is controlled by a complex interplay of auto- and allocyclic mechanisms. Most apparent are lobe switching driven by topographic build-up and/or upstream channel avulsion, some degree of flow deflection along the confining margin as well as the overall rising sea level resulting in the observed retrogradation of the whole fan system. Basin topography apart from the confining margin, sporadic tectonic activity resulting in thick debris-flow deposits or significant changes in sediment availability and size as recorded elsewhere in the system appear to have less direct impact in the Lobe C accumulation.

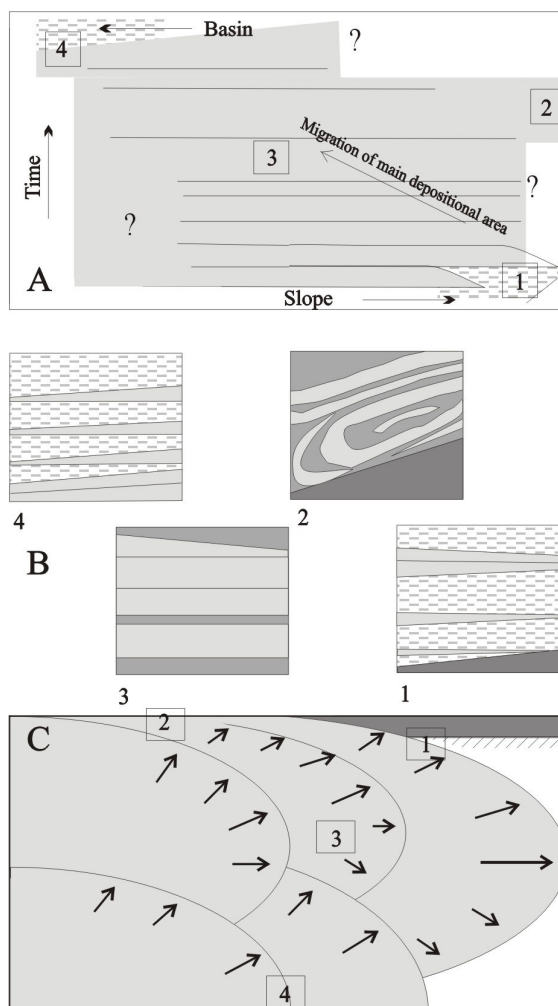


Figure 2.41: A) Diagramme showing the spatial and temporal component distribution in the more distal E-Fan area (Seyhan River road cut).

B) Schematic drawings of relationships between components located in marginal, main depositional centre and basinal position: 1) isolated lobes/lobe fringe onlap low-angle slope in area with mostly fan fringe sedimentation (lower Langhian); 2) massive slumping of aggraded, sandy fan sediments against steep slope (upper Langhian ?); 3) thick stacked lobes and associated lobe fringe and interlobe deposits in main depositional area; 4) lobe and fan fringe sedimentation towards the basin (upper Langhian?).

C) Conceptual drawing showing how lateral lobe switching generated observed component distribution.

Note that no absolute time and distances are implied.

2.4.4 Downcurrent evolution in lobe accumulation

The recognition of lobe deposits in proximal and distal locations is based on differing sedimentological character, internal organisation, vertical facies relationships, component associations and position within the fan framework. The studied lobe depositional environments do not represent true downcurrent representatives of each other (fig. 2.42a), their respective up- and/or downcurrent deposits are not exposed and/or not preserved. However, general proximal-distal changes in the lobe depositional environment can be observed. The distal lobes (Lobe C) are located in a more intermediate rather than true distal fan location (fig. 2.42b) as suggested by their high bulk net sand content and relative coarseness of sediments.

The different identified lobe types are characterised by a high net sand content throughout. In a downsystem direction the net sand content gradually decreases (Lobe A/B/C = 93/95/86 %), accompanied by a gradual decrease in grain size (very coarse to medium sand-sized) and bed thickness (ave. 0.6/0.8 - 0.50 m) and a substantial increase in shale content (fig. 2.42b).

Sediment emplacement within the different lobe environments took place by high and low density currents and, at times, sandy debris flows. Shanmugam *et al.* (1995) suggest to regard only normal grading as reliable indicator of deposition by turbidity currents. Thus the amount of "true" turbidite deposits is 45 % in Lobe A, 59 % in Lobe B and 75 % in Lobe C. A clear downcurrent increase in deposition by turbidity currents is present, paired with deposition from increasingly dilute currents, i.e. a decrease in competence, higher relative abundance of Bouma Tc-d structures. The observed non-graded, massive, crudely stratified beds are typically interpreted to represent deposition from high density turbidity currents (e.g. Lowe 1982; Hiscott *et al.* 1997), which some authors assign to sandy debris-flow deposits based on the apparent "non-turbulent turbidity current" flow rheology (e.g. Shanmugam *et al.* 1995; Shanmugam 1996, 2000). The crucial implication of this debate centres on the resultant sand body geometry; sandy debris flows are believed to form less extensive, discontinuous, disconnected sand bodies which are more sensitive to sea-floor topography (Shanmugam *et al.* 1995; McCaffrey in Purvis *et al.* 2002) than high density turbidity flows. Regardless of this, sandy debris flows and/or high density turbidity currents may evolve into low density turbidity currents (e.g. Stow & Johansson 2000; Shanmugam 2000; Purvis *et al.* 2002) thus explaining the downcurrent net increase in turbidites (for further discussion see chapter 5.1).

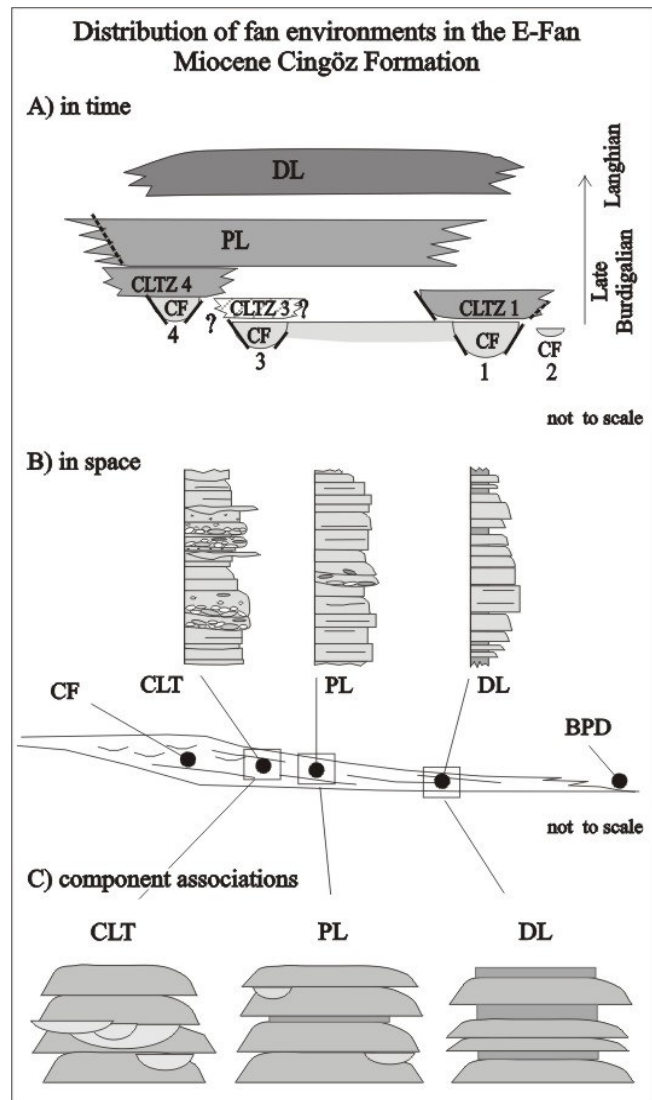


Figure 2.42: A) Schematic diagram showing the distribution of the channel-lobe transition zone (CLT), proximal lobe (PL) and distal lobe zone (DL) in a time-space matrix.

B) Showing the spatial position of the channel-fill (CF), (CLT), (PL), (DL) and basin plain deposits (BPD) within the E-Fan, Cingöz Formation (modified after Ricci Lucchi *et al.* 1987).

C) Stacking pattern and component association of CLTZ, PL and DL reflecting downcurrent decrease in channelling association, increase in lobe fringe/interlobe deposits and increase in vertical lobe spacing.

The proximal Lobe A and B deposits are highly amalgamated, composite beds of 10s of metres in thickness are common. Within the Lobe C deposits, shales commonly separate individual sandstone beds and amalgamation is relatively rare (fig. 2.42b). The internal organisation improves from near random and few well-defined asymmetric sequences at bed sub-packet-scale in Lobe A/B deposits to better organised Lobe C deposits. Generally, the significance of vertical arrangements as environmental indicators are questioned (e.g. Hiscott 1981; Millington 1995; Anderton 1995; Chen & Hiscott 1999a; Shanmugam 2000) and are rather believed to represent sensitive indicators of short term fluctuations in both allocyclic and autocyclic controls (Foster 1995). Chen & Hiscott (1999a) doubt the presence of any "organised" lobe development arguing that seismically- or flood-induced turbidites are sporadic events rather than following some sort of organisation. The recorded metre-scale sequences in the various lobe deposits are believed to reflect irregularities of flow volume, sediment supply, topographic compensation etc. (e.g. Mutti *et al.* 1994; Chen & Hiscott 1999a). These smaller-scale sequences are overprinted by the lobe-scale asymmetric sequences believed to be related either to progressive lobe progradation, retrogradation and/or lateral migration or as fining upward and/or random organisation implying aggradation. Anderton (1995) suggests that a more ordered vertical arrangement indicates relative depositional stability. This implies a downcurrent increase in depositional stability from Lobes A/B to C.

Unique component associations characterise the proximal-distal trend. The Lobe A and B deposits are associated with erosive components, i.e. channeling, scouring and/or small distributary channels, reflecting a highly dynamic erosive-depositional bypass environment. The per section lobe representation decreases from 70 % (CLTZ) and 90 % (proximal lobe zone) to 65 % in the distal lobe zone. The associated coarse channelized elements in the former two decrease from the CLTZ (30 %) to proximal lobe zone (8 %). In contrast, Lobe C deposits accumulated in a relatively tranquil depositional environment, underlined by the abundance of preserved bioturbation. Lobes in the CLTZ and partially the proximal lobe zone are poorly defined while in the distal lobe zone, lobes are often clearly separated by associated deposits (fig. 2.42c).

Lobe progradation, switching and overall aggradation result in the observed mixed shingled-compensational stacked Lobe A/B and partially C complexes, representing stable depositional environments (Pickering 1981). The isolated Lobe C deposits within areas of normally fan fringe sedimentation suggest episodic lobe migration into this area, indicative of unstable depositional processes, possibly reflecting source control (Pickering 1981) or lobe switching (this study). The recorded overall grain size decrease in all three lobe depositional environments appears to be related to reduction in grain size in the feeder system or an increase in distance from the input point perhaps due to rising sea level (*see chapter 2.5*). Retrogradation in response to decreased sediment supply and grain size is apparent in the unique Lobe B sequences, i.e. the distinct grain size and textural changes at lobe-scale.

While Lobes A and B developed within a semi-confined space inhibiting much lateral dispersal, the Lobe C deposits appear to be only peripherally restricted by the slope. The proposed elongated sheet-like geometries reflect the restricted environment while some lobate Lobe C geometries were identified.

Distinct downcurrent trends as observed in the lobe deposits of the E-Fan have also been recorded in other ancient deep-water clastic systems (e.g. Macigno Formation: Ghibaudo 1980; Kongsfjord Formation: Pickering 1981; Rocchetta Formation: Cazzola *et al.* 1981) where the decrease in grain size, bed thickness and net sand content are conspicuous. The emplacement mechanism and changing flow competence and capacity play a crucial role in the recorded evolution. Autocyclic controls, such as lobe switching due to lobe build-up, channel migration and avulsion, and allocyclic controls, such as the gradually rising sea level, tectonic activity in the source area and within the basin, govern the development and geometries of the various lobe depositional environments of the E-Fan.

2.5 Controls

Studies of modern and ancient submarine fan systems have shown that a range of auto- and allocyclic mechanisms play an important role in the spatial and temporal development of turbidite systems (e.g. Mutti & Normark 1991; Shanmugam & Moila 1991; Normark & Piper 1991; Reading & Richards 1994; Stow *et al.* 1996; Richards *et al.* 1998; Stow & Mayall 2000; Shanmugam 2000). Some controls including tectonics, climate and eustasy represent "causal" allocyclic factors (Einsele & Ricken 1991; Richards *et al.* 1998) while deposition is subject to modifying local environmental processes, for example, local differences in subsidence, supply and composition of sediments, various hydrographic regimes and autocyclic processes (fig. 2.43). The study of the different lobe depositional environments within the revised fan framework

suggests a much more complex development of the E-Fan, Cingöz Formation, than previously anticipated (e.g. Gürbüz & Kelling 1992; Gürbüz 1993).

2.5.1 Basin physiography, basin floor and depositional topography

During the deposition of the Cingöz turbidite system, the northern margin of the basin was formed by the actively uplifted Tauride orogenic belt, an adjacent narrow (~ 3 km), shallow marine carbonate shelf and a tectonically unstable, steep (~ 35°) foreslope, trending in a general W-E direction (Gürbüz 1993, Cronin *et al.* 2000).

The fans were fed by multiple, incised feeders, which were active at approximately the same time, funnelling sediment into the basin at different localities (Gürbüz 1993; Satur 1999). From west to east the basin deepened (Demircan & Toker 1998), allowing for vast sediment accumulation, particularly in the eastern fan area (Gürbüz 1993; this study), before distinct shallowing towards the extreme east took place (Ünlügenç 1993). Basin extension towards the south is documented by subsurface Cingöz deposits (Naz *et al.* 1991; Williams *et al.* 1995), however, the total southern extent is unknown. Initially, rapid deepening of the basin took place which was then passively infilled by the Cingöz turbidites (Gürbüz 1993; Williams *et al.* 1995).

While the unique basin physiography is one aspect in controlling the development of the E-Fan, topography, either resulting from basin-floor or depositional topography, additionally influenced the sediment distribution pattern and the geometry of sandstone deposits (e.g. Kneller 1995; Sinclair 2000; Burgess *et al.* 2000). Topographic expression may range from cm to km-scale.

Previous studies suggest that major structural highs influence the overall development of the Cingöz Formation (Gürbüz & Kelling 1992; Gürbüz 1993), restricting fan growth in a western and south-eastern to eastern direction respectively (*chapter 2.1*). Satur (1999) and Satur *et al.* 2000) found the elongated W-E trend of the W-Fan to result from the presence of various submarine highs.

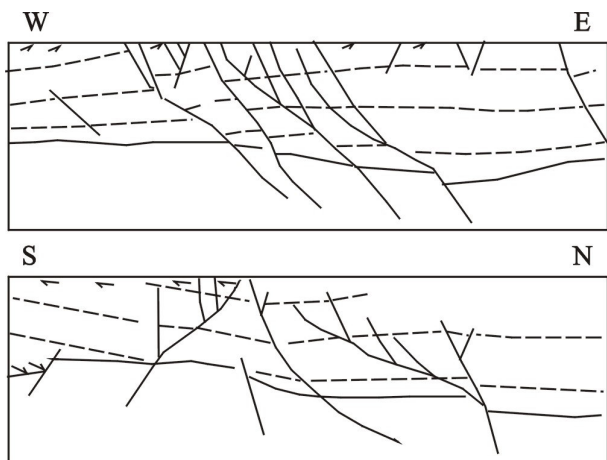


Figure 2.44: Line drawing interpretations of seismic lines flattened on base megasequence 3. Flattened sections show the control on thickness of megasequence 2 by NE-downthrowing extensional faults. No seismic-scale evidence of expansion or growth of sequences in hanging walls (from Williams *et al.* 1995).

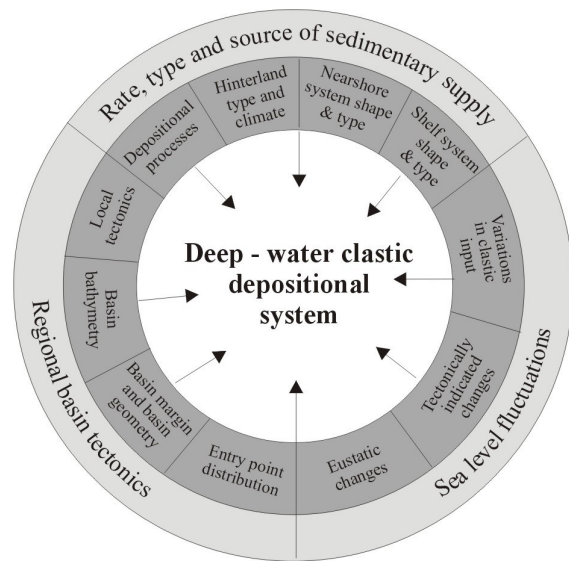


Figure 2.43: Schematic diagram illustrating the range of controls influencing deep-water sedimentation (Richards *et al.* 1998).

The analysis of the sandy basin infill of the E-Fan indicates the presence of basin floor relief during E-Fan deposition, strongly influencing the sediment accumulation pattern. In the early sandy stage of the E-Fan, Lobe B accumulation of the proximal lobe zone took probably place in an at least partially fault-bounded, intrabasinal depression, resulting in its aggradational, latero-vertical growth pattern akin to Schupperts (1995) confined lobe model of the Arakynthos Sandstone, Greece (*chapter 2.4.2.2*).

During the *Orbulina suturalis* biozone a 7.8-fold sediment increase over a distance of 6 km from the western to the central E-Fan area was observed. Palaeocurrents in the west and central area point to a general eastern direction, however, the contrasting lithologies, dominantly shales in the west and coarse sandstones in the central area strongly suggest that the deposits in the west record the distal stages of the W-Fan, while the central area was sourced by the E-Fan. Williams *et al.* (1995) seismic analysis shows that numerous

NE-downthrowing extensional faults cut the underlying strata and were active during the deposition of the Kaplankaya, Cingöz and the overlying Güvenç formations (fig. 2.44; note that seismic lines do not cover the actual study area). This synsedimentary extensional fault activity (Ünlügenç 1993) is believed to have led to basin compartmentalisation of relatively closely spaced basin sectors, resulting in a series of fault-controlled, stepped, interbasinal depressions, the lowest area underlying the central E-Fan area.

The resulting fault-scarp topography would have restricted the E-Fan's lateral development to the west while favouring enhanced sediment accumulation in the generated accommodation space in the central basin sector (fig. 2.45b). Differential subsidence driven and/or enhanced by bulk sediment weight may also have led to locally thicker sediment accumulation (Ricci Lucchi & Valmori 1980).

Documented fault trends in the Cingöz Formation range from NW-SE to NWN-SES ($45^{\circ}/30^{\circ}/15^{\circ}$) (Ünlügenç 1993; Satur 1999; this study), N-S (Satur 1999), E-W (Satur 1999; this study) to NE-SW (Unlügenç, 1993). High degrees of flow deflection have been recognised even on subtle confining topography (Hodgson *et al.* 2002). NW-SE to NWN-SES trending fault-scarps could result in $> 90^{\circ}$ flow deflection and account for the apparent south-eastern to eastern axial deflection recognised within the central and southern areas of the E-Fan (fig. 2.45a).

Complex, fault-scarp basinfloor topography resulting in basin compartmentalisation has been recognised in a number of deep-water systems (e.g. Claymore Sandstone/North Sea: Kane *et al.* 2002; Neuquen Basin/Jurassic turbidites: Burgess *et al.* 2000; Annot Sandstone/France: Kneller & McCaffrey 1999; Sinclair 2000) resulting in flow deflection subsequently controlling the sandstone distribution patterns (e.g. Marnoso-Arenacea/Italy: Ricci Lucchi 1981, 1985; Miocene Turbidite Systems/San Joaquin Basin: Nilsen *et al.* 2002a; Jaca-Fiscal lobe complex/Hecho Group: Millington 1995). Depositional thickening at faults and lateral restricted dispersal are common features of fault-controlled, restricted basins of tectonically active settings (e.g. Marnoso-Arenacea/Italy: Ricci Lucchi 1981; Gryphon Field/North Sea: Purvis *et al.* 2002; Stow & Johansson 2000). High seafloor topography generated by seamounts and ridges can result in dramatic lateral thickness variations of up to nearly 1000 m (e.g. Monterey and Delgada Fans/offshore California: Wilde *et al.* 1985).

Depositional topography resulting from the build-up of sediments affects later sediment accumulation. In general, the relative size, shape and orientation of an obstacle determines the degree of interaction between the flow and the topographic feature (e.g. Normark & Piper 1991; Kneller 1995). Succeeding flows need to find a path around the obstacle, seeking even subtle depressions, resulting in enhanced sedimentation rates in the latter relative to the adjacent depositional fan areas (Pickering 1981). All three lobe depositional environments were affected by the depositional relief, partially compounded by the existing structural topography resulting in 10s of metres thick "lobe-to-lobe" compensation cycles (lateral offset stacking) of the Lobe A, B and C deposits (*chapter 2.4*) akin to "compensation cycles" of Normark *et al.* (1993), Chapin *et al.* (1996) and Bouma (2000). This process appears to be common in turbidite systems (examples: table 2.10), modifying the local stacking pattern of individual sandstone beds, bed sub-packets and lobes (Mutti *et al.* 1994).

Proximal deposits of the channel-lobe transition and proximal lobe zone are known to possess distinct, often irregular topographic expression (Normark *et al.* 1979; Mutti & Normark 1991). At m-scale, the irregular topography of particularly the proximal Lobe B deposits (*chapter 2.4.2.1*) has led to bed-to-bed compensation resulting in lenticular or wedging sandstone geometries by infilling small depressions, thus compensating the pre-depositional relief (examples: table 2.10). Even, the position of distributary channels may be determined by relief (Normark *et al.* 1979; *chapter 2.4.2.1*) where distributary channels may have

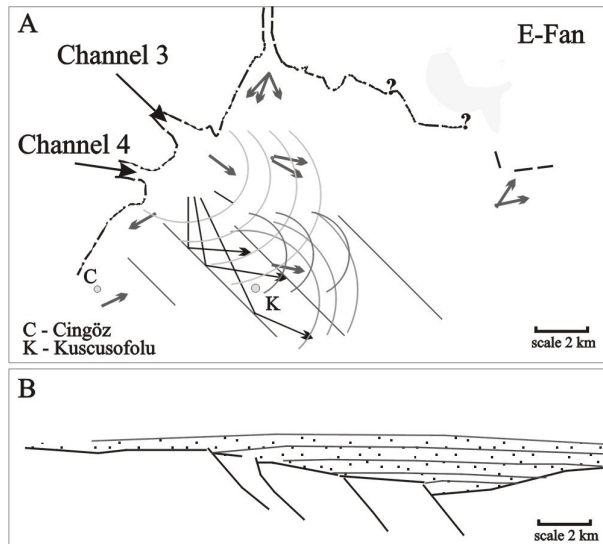


Figure 2.45: A) Schematic diagram illustrating how NE-downthrowing faults could result in eastern deflection of the E-Fan system. Dark grey arrows show measured palaeocurrent pattern in field.

B) Flattened W-E seismic line of Williams *et al.* (1995; fig. 2.45) showing suggested depositional thickening at faults, probably at subseismic scale. Shown seismic line lies approximately 30 km south of feeder channels 3/4.

inhibited marginal depressions along the lobe edges. Other, smaller-scale bed-to-bed compensation cycles were observed in the mouth bar facies associated with feeder channel 1 (*chapter 2.2.2.2: Section C: m 170 - 200*).

Topographic control	Result / Dimension	E-Fan	References
Fault scarps and/or local topographic highs	basin compartmentalisation, locally enhanced deposition (km-scale); system/flow deflection	7,8-fold thickness increase over 6 km lateral distance (central E-Fan: <i>chapter 2.2.2.2</i>) apparent eastern deflection of E-Fan system	e.g. Montereos Fan & Delgarda Fan/offshore Calif. (Wilde <i>et al.</i> 1985), Marnoso-Areneacea (Ricci Lucchi 1981, 1985), Claymore Sandstone (Kane <i>et al.</i> 2002), Miocene Turbidite Systems/San Joaquin Basin (Nilsen <i>et al.</i> 2002a)
Intrabasin depression / restricted development	restricted lateral development, vertical stacking, aggradation (100s m-scale)	proximal lobe zone (<i>chapter 2.4.2</i>)	e.g. Arakinthos Sandstone/Greece (Schuppers 1995), Marnoso-Areneacea (Ricci Lucchi 1981, 1985), Post-Contessa Subinterval/Italy (Ricci Lucchi & Valmori 1980)
Fault scarp/local highs	local obstacles (10s m-scale); forced lobe migration "lobe-to-lobe"	mouth of feeder channel 1 (north-central E-Fan: <i>chapter 2.2.2</i>); proximal and central fan area;	e.g. Nicolas Fan/offshore Calif. (Reynolds & Gorskine 1987), Kongsfjord Formation/Norway (Pickering 1981), Peary Land Group/Greenland (Surlyk 1987), Jaca-Fiscal Lobe Complex/Spain (Millington 1995), Pas-de-la-Cuse Lobe/France (Savary <i>et al.</i> 2002), Tanqua Karoo/RSA (Sixsmith <i>et al.</i> 2002)
Depositional topography: Debris flow, lobe topography	compensation cycles; local flow deflection, onlap onto obstacle	Lobe B deposits	
Fault scarp/local highs Depositional topography: Debris flow, lobe and irregular top lobe topography	relief compensation (m-scale & smaller) wedging, onlapping Onlapping/infilling of irregular top debris flow topography; bed-to-bed compensation	proximal lobe deposits (<i>chapter 2.4.2</i>), feeder 1 mouth bar facies (<i>chapter 2.2.2</i>) Proximal and distal lobe bodies; debris flow #5 (<i>chapter 2.4.2/3 & 2.2.2</i>)	e.g. Hecho Group/Spain (Mutti & Sonnino 1981, Millington 1995), Laga Formation (Mutti <i>et al.</i> 1987, 1994)

Table 2.10: Different scales of topography controlling the sandstone distribution pattern, with examples from literature.

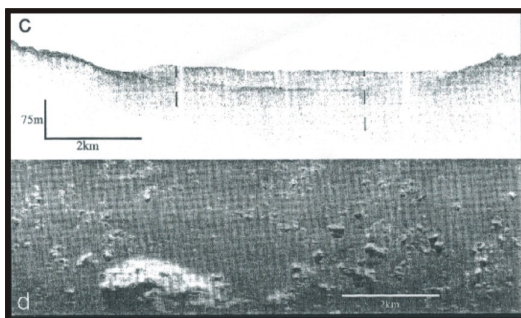


Figure 2.46: (c) 3.5 kHz-profile through a section of the Saharan Debris Flow. The debris flow deposit is the thick acoustically transparent layer lying within the topographic low. (D) TOBI image of a section of the Oratava-Icod-Tino debris avalanche complex north of Tenerife. Note the variation in size of avalanche blocks lying on the surface. Light shades indicate high backscatter, dark shades indicate low backscatter (from Wynn *et al.* 2000).

The thick debris-flow deposits encountered in the western and central E-Fan form 5-80 m thick localised depositional bulges, presenting obstacles to succeeding turbiditic and sandy debris flows *sensu* Shanmugam (1996). Flow interaction through multiple current directions, cannibalisation and incorporation of debris-flow material into succeeding flows may take place (e.g. Kneller 1995). The wedge-shaped debris-flow deposit just overlying the conglomeratic feeder channel 1 fill is onlapped by sandy mouthbar and associated deposits (*chapter 2.2.2.2: Section C: m 130 - 170*). Its emplacement may have temporarily interrupted and/or deflected the flow of channel 1. Reynolds & Gorskine (1987) demonstrate that temporary blockage of one of the main feeder channels of the modern Niclas Fan by debris-flow deposits resulted in a change in flow direction. At the top of the debris flow #5 (Section C: 1900 - 1980 m), overlying thinly-bedded, medium-grained turbidites onlap and infill its depositional topography (table 2.10). Mass flow deposits forming distinct topographic features with great extent (up to 2.5 km width

/ 20 km length) and irregular top relief (10s of metres) are known from other modern fan environments, for example, the Madgalena Turbidite System, Caribbean Sea (Ericella *et al.* 2002) and the Saharan Debris Flow and Oratava-Icod-Tino debris avalanche off Tenerife (fig. 2.46; Wynn *et al.* 2000).

The sand-rich proximal and central E-Fan area possess very little, mostly localised shale deposits. A downcurrent increase in shale content, thickness and areal distribution was recorded. Compaction of these shales through overlying sediment weight will have left localised depressions or irregularities leading to bed-to-bed compensation at meso- to mega-scale (e.g. Laga Formation/Italy: Mutti *et al.* 1978, 1994) or may even modify topography to a great extent influencing the location of later sand bodies (e.g. Frigg Field/North Sea: Heritier *et al.* 1979) or result in oversteepened mould-like geometries (Stow & Johansson 2000). However, potential effects of differential compaction were not observed in the E-Fan at outcrop-scale.

The effects of basinfloor and depositional topography on the reservoir geometry and quality are discussed in chapter 4.

2.5.2 Tectonics

Deep-water clastic systems located on active margins are greatly influenced by tectonics. Tectonic activity of the hinterland controls the number and location of sediment sources, the sediment supply and pathways, the shelf width as well as the duration of fan activity (e.g. Shanmugam & Moiola 1988; Posamentier *et al.* 1991; Trincardi *et al.* 1995; Bouma 2000). Tectonism also controls the size, shape and topography of the host basin (e.g. Mutti & Normark 1987) which has the most profound effect on increasing or decreasing accommodation space (Vail *et al.* 1991). Basinfloor topography can substantially modify sediment dispersal patterns and produce a variable degree of synsedimentary deformation (e.g. Ricci Lucchi 1975a; Trincardi *et al.* 1995; Burgess *et al.* 2000; *see chapter 2.5.1*). When coupled with climate, tectonism controls the type and amount of sediment filling the available accommodation space (Vail *et al.* 1991).

The northern Adana Basin is located in a tectonically active setting. Gürbüz & Kelling (1993) suggested the Adana Basin to fit a Type C turbidite basin (*sensu* Mutti & Normark 1987) representing a structurally controlled, elongate foreland basin underlain by continental crust with a large and long-lived sediment source comparable to, for example, the Pyreneen Basin (Hecho Group: Mutti 1985b, Mutti *et al.* 1985) or the northern Apennine foredeep (Miocene Italian Fans: Ricci Lucchi 1975a; 1981, 1985). However, the Adana Basin exhibits characteristics similar to a Type D basin (Satur 1999) where ongoing tectonic activity resulted in rapid changes in basin shape, short lived sediment sources and the development of a volumetrically much smaller, coarse-grained and short-lived fan. Ünlügenç (1993) and Williams *et al.* (1995) studied the pre- to post tectonism with respect to the Cingöz Formation identifying various structural highs limiting lateral evolution at formation-scale (*see* Gürbüz 1993) and significantly affecting the sediment distribution pattern and geometry of sand-bodies at meso to mega-scale (Satur 1999; Satur *et al.* 2000; *chapter 2.3-2.4*). The existing fault pattern most likely determined the sediment pathways.

In the E-Fan depositional area, the pre- and synsedimentary, extensional fault activity led to basin compartmentalisation resulting in laterally restricted fan development, partially enhanced sediment accumulation in intrabasinal depressions and axial, margin-parallel eastern deflection of the system (*chapter 2.5.1*).

Satur (1999) recognised a shift in the time and activity of the three, structurally controlled main feeder systems (channels 1, 3 and 4). These feeders represent fixed pathways with channel migration only possible within their respective confinements. An apparent westward shift in sediment supply to the basin is documented by the later initiation of feeder channels 3 and 4, while the activity of main feeder channel 1 appears to diminish dramatically (*chapter 2.4.2*). This migration of provenance areas and timing of active feeders has been recognised to result from tectonic activity in the source area (e.g. Paola Basin/Tyrrhenian Sea: Trincardi *et al.* 1995) such as episodic uplift associated with fault systems (Middle Tertiary submarine fan system/San Joaquin Basin: Nilsen *et al.* 2002b) which may control the volume of supplied sediment (e.g. Campos Basin: Bruhn & Walker 1995). Generally, tectonic uplift of the source area is held responsible for an increased sediment supply to a basin (e.g. Vail *et al.* 1991; Stow & Johansson 2000).

Tectonic control on the sandy-basin fill signature in the E-Fan is evident. During Burdigalian and Langhian times, thick debrites were deposited along the western margin and central E-Fan area. Their absence in the east may either be due to a more stable eastern margin or preferential erosion of Kaplankaya-rich debrites by Quaternary conglomerates (*chapter 2.4.3*). Cronin *et al.* (2000) found evidence of considerable tectonic

activity along the eastern margin during pre-Langhian times, however, no pre-Langhian Cingöz sediments are present, either due to non-deposition or burial. Some debrites contain lithified Cingöz channel-fill sediments (e.g. debris flow # 5), suggesting uplift of the basin margin area leading to exposure (?) and subsequent resedimentation of lithified Cingöz sediments. This scenario would involve debris flows being funnelled down the canyons and uplift and erosion of the later potential sandy channel-fill sediments, rather than being generated by mere slope collapse.

A progressive fining in grain size is conspicuous from sand body- to formation-scale. Other trends are rare and likely to be produced by lobe migration and/or progradation. The repeated onset of the distinctly coarse-grained basal Lobe B deposits indicates an episodic supply of coarse sediment to the basin believed to be brought on by uplift in the source area exposing rocks to erosion and/or reworking and the subsequent denudation of this area (*chapter 2.4.2*).

If uplift also resulted in tectonic tilting of the basin is speculative. Potential tilting should have left subtle discordances behind (at seismic or sub-seismic-scale) more pronounced in the proximal, smoothed out in the distal reaches. It might have encouraged the apparent easterly deflection of the E-Fan, however, thick sediment accumulation in the central fan area during the *Orbulina suturalis* zone as opposed to much lesser thickness in the east, underlines rather a fault-controlled deflection as suggested above (*chapter 2.5.2*). Abundant faulting along the margin is conspicuous (Ünlügenç 1993) and uplift may have effected only the basin margin and hinterland while differential subsidence either tectonically and/or sediment weight-induced acted in the basin (*chapter 2.4.2 / 2.5.1*). That basinfloor gradient can noticeably influence the overall fan geometry is shown by the canyon-mouth lobes off the Corsican and Sardinian shelf, which deviate to the south, following the overall gradient that extends towards the Blearri Abyssal Plain in the south (Kenyon *et al.* 2002). Tectonic uplift has even been shown to be responsible of preventing a fan-like morphology (e.g. Eel Fan: Reynolds & Gorsline 1987).

In combination with other controls, uplift of the source area and the increased sediment supply has been linked to the initiation of submarine fan systems, for example, the Cingöz Formation (Satur 1999) and the Indus Fan (Clift *et al.* 2001).

The effects of post-depositional tectonism on the reservoir geometry and quality are discussed in chapter 4: reservoir characterisation.

2.5.3 Sediment supply and climate

The E-Fan was initiated during late Burdigalian (Nazik & Gürbüz 1992), when significant tectonic activity led to uplift of the Taurus Mountains (Ünlügenç 1993; Williams *et al.* 1995), resulting in an increased sediment flux driving canyon initiation (Gürbüz & Kelling 1993; Gürbüz 1993; Satur 1999). Satur (1999) found the submarine feeder channels to be directly fed from fan deltas and alluvial fans. During its approximately 2.7 million years of activity (Nazik & Gürbüz 1992; Gürbüz 1993), about 3700 m (this study) of E-Fan sediment were accumulated, averaging sediment accumulation rates of 134 cm / 1000 yrs for the sandy basin fill.

The rate of terrigenous sediment input to the deep sea is controlled by mechanisms including sea level, climate and tectonic activity (e.g. Reading & Richards 1994; Bouma 2001; Stow & Mayall 2000). Sedimentation rates between 100 - 1000 m / myr are common in modern submarine fans, higher values may occur nearer the sediment source and in over-supplied basins (e.g. Einsele 1991). Weber *et al.* (1997) found extremely high sedimentation rates in the head of the Bengal Fan canyon with 1 m / yr. Very active ancient systems include the Merquijioq Formation/Greenland (Surlyk 1995) with depositional rates of 60 cm / 1000 yrs and the Fiscal lobes with 1 bed / 500 years (Millington 1995; though no average bed thickness provided). The extremely high sedimentation rates of the E-Fan indicate the availability of large volumes of sediment, with probably higher average sedimentation rates in the proximal than the distal depositional areas. The effect of locally enhanced sedimentation due to restricted sediment dispersal, e.g. in the proximal lobe zone and central fan area, compounds this effect. During the Langhian, sedimentation rates varied from ~ 16 cm / 1000 year in the western to ~ 130 cm / 1000 years in the central area.

The E-Fan is sourced from the Tauride orogen (e.g. Bolkar Mountain area, Inner Taurus belt) representing a tectonically modified combination of arc and recycled orogen provenances and its Palaeozoic and Mesozoic platform carbonate cover with minor contributions of the contemporaneous shelf carbonates (Gürbüz & Kelling 1993). The scattered coalified clasts and wooden fragments found in the channel-lobe transition and distal lobe deposits underline a terrigenous source area.

The size of the drainage basin as a proxy for sediment input appears to be the most important factor in governing the sediment distribution and the overall architecture of the margin (Kenyon *et al.* 2002), while the amount of available sediment controls the size of a river-fed deep-sea fan (Wetzel 1993). Fan length and depositional rate, i.e. fan volume/age, appear to be highly correlative (0.2 - 0.5 in downcurrent direction) for both river- and shelf-fed fans, regardless of tectonic setting, type of sediment source, time span and epoch of formation (Wetzel 1993).

Small to medium-sized mountainous rivers of tectonic, active settings have shown to play a major role in triggering submarine gravity flows and therefore in turbidite sedimentation (Mutti *et al.* 1996). The connection of the subaerial river system to the submarine feeder systems suggests (semi-) permanent flow discharge. Modern rivers in flood are known to form hyperpycnal flows which may directly transform into submarine turbidites (Mutti 1996; Bouma 2001). Heezen & Hollister (1971) found submarine cable breaks off rivers, for example the Madgalena, Congo and the fan deltas of the Gulf of Corinth, to correlate with times of peak fluvial discharge suggesting that turbidity currents occur at these times. However, the relationship between submarine fan sedimentation and type, volume and density of fluvial flow has been little studied so far (Bouma 2001). Other potential sediment sources for the E-Fan may include river mouth and the subaqueous delta front deposits, the litoral-drift system, sand remobilisation at the canyon heads induced by rip currents during exceptionally strong storms (e.g. Normark & Piper 1991), resuspension of marine sediment at the top of the continental slope and slope failure. The sedimentary discharge of the rivers and other sources would be captured by the three canyons. The gravity flows running through these canyons, together with the slumps and gullies formed on their walls developing into mass flows and/or turbidity flows, deposited their load in the compartmentalised basin. The complex palaeocurrent pattern results from the different feeders and the complex basinfloor topography (easterly flow deflection). Only the largest flows reach the distal fan depositional environment (Normark & Piper 1991), the available grain size range dictating the transport distance (Bouma 2000).

Two distinct sediment types are differentiated: i) the river/fan delta-fed sand-rich sediments forming the lobes and associated fan deposits, conveyed to the deep-sea via the incised canyons and ii) the debris-flow deposits scattered throughout the fan succession mostly resulting from shelf/slope collapse, feeding into the basin from the basin margin.

It appears that uplift of the source and basin margin area freed large volumes of dominantly coarse sediment. Varying sediment supply as, for example, recorded in the sequences of the proximal lobe zone (Lobe B) suggests periodic tectonism, i.e. uplift, bringing on coarser sedimentation, compounded by the presence of repeated mass wasting events throughout the Burdigalian and Langhian. Shanmugam *et al.* (1985) caution that uplift does not necessarily provide the sand- to clay-sized material needed for submarine fan growth since unconsolidated material is not readily available through initial uplift. They suggest that the break-down of coarse debris into finer size by fluvial and shallow-marine processes is required before transport to the deep-water fan by turbidity currents. If a humid climate is present, it favours the rapid break-down of uplifted landmasses whilst water serves as the required transport agent (Shanmugam *et al.* 1985; Ericella *et al.* 1998; Bouma 2000). The Agadir system off the coast of Morocco, for example, experiences progressively diminished sediment input related to increasing aridity and denudation of the hinterland compounded by subsiding continental tectonics thus promoting a landward migration of turbidite sedimentation (Ericella *et al.* 1998). Increasing aridity was also responsible for a decrease in turbidite sedimentation in parts of the Arabian Sea (Indus Fan: Prins & Postma. 2000). Wetzel (1993), however, suggests that uplift and average elevation of the drainage basin to be of greater importance than climate, i.e. mean annual precipitation (Pinet & Souriau 1988). No climatic information for the Adana Basin is available. Waters were described to be warm initially (Toker *et al.* 1998), their gradual cooling related to water influx from the south due to opening up of the Cyprus basin rather than a change in environmental conditions. General subtropical conditions affecting basin sedimentation are suggested.

Initially, the E-Fan appears to be a gravelly system (Satur 1999) with thick conglomeratic sequences present in the distal regions of the basin (Naz *et al.* 1991) before switching to a sand-dominated system during the later (?) Burdigalian (Gürbüz 1993; this study). Satur's (1999) study indicates that the exposed feeder system is older than the exposed sandy basin fill, its coeval deposits presenting an earlier stage of the fan development. The few published borehole and seismic data (Naz *et al.* 1991; Williams *et al.* 1995) infer lobe-shaped bodies in subcrop, but abundant faulting prohibits their direct association with the exposed feeder system. The gravelly phase of the E-Fan might be related to the initial uplift producing very coarse sediments before weathering, erosion, fluvial and shallow marine processes led to a gradual break-down in sediment size initiating the sandy basin-fill phase. The younger feeder channel 4 appears to reach the sandy

stage slightly later than the other feeder channels (Satur 1999), suggesting that its source area may have been uplifted and exposed to erosion later than the source areas of channels 1 / 2 and 3. The shifting source of sediment supply to the basin is directly related to tectonic activity, i.e. uplift in the hinterland and basin margin area (*see above*). This westward shift may correlate with the proposed later initiation of the W-Fan (Satur 1999) and its progradation during late Burdigalian times. However, during Langhian times, the W-Fan retreated (i.e. deposition shifted to its proximal reaches, Satur 1999; *chapter 2.2.2 / 2.5.1*) while sandy deposition was still taking place in central parts of the E-Fan area.

The gradual upward decrease in grain size from gravelly to coarse sand and progressively finer sand size may be related to reduction in grain size in the feeder system and/or denudation of the hinterland and/or subsiding tectonic activity which could have led to a decrease in sediment flux towards the continental shelf or an increase in distance from the input point, perhaps related to rising sea level. Conspicuous fining-upward trends are apparent at different hierarchies of scale indicating higher frequency changes of the above mechanisms (*chapter 2.4*; e.g. Campos Basin, Bruhn & Walker 1995). The grain size of the resultant lobe deposits depends on the size of the subaerial drainage basin acting as the sediment source, the gradient of the drainage basin and continental slope, shelf width and the distance between the source area and the depocentre of the lobe (Kenyon *et al.* 2002). Generally, the overall net sand content and grain size decrease in a downcurrent direction, however, coarse sand deposition took place in thick lobe deposits even in relatively distal reaches of the system (distal lobe zone: this study; well Gülbaşı 2: Naz *et al.* 1991) suggesting high flow volume and competence. The unique signatures of the Lobe B deposits (proximal lobe zone) demonstrate the strong influence of source control on lobe accumulation. That the source and textural composition can even control sand body geometries is demonstrated by Normark *et al.* (1998) for the Hueneme and St. Monica Fans.

2.5.4 Sea-level changes

Eustasy is regarded as one of the major controlling mechanisms for fan development. The central assumption of sequence stratigraphic* models is that sedimentation within deep-water systems increases during relative sea-level lowstand (fig. 2.47), while during transgression and sea-level highstand sedimentation diminishes or temporarily halts (e.g. Shanmugam *et al.* 1985; Posamentier & Vail 1988; Posamentier *et al.* 1991; Van Wagoner *et al.* 1990; Vail *et al.* 1991). However, an increasing number of submarine fans which developed during sea-level rise and highstand have been identified such as the Amazon Fan (Flood *et al.* 1991), Navy Fan (Piper & Normark 1983), Mississippi Fan (Kolla & Perlmutter 1993), Bengal Fan (Kuehl *et al.* 1989; Weber *et al.* 1997), Agadir turbidite system (Ericella *et al.* 1998) Campos Basin (Bruhn & Walker 1995), Makran (Prins *et al.* 2000), Porcupine Fans (Kolla & Macudra 1988), Congo and Magdelana fans (Heezen *et al.* 1964), Crati Fan (Ricci Lucchi *et al.* 1988, 1985). Balder Formation/Gryphon Field (Dixon & Pearce 1995; Purvis *et al.* 2002) Frigg Submarine Fan (Helland *et al.* 2002). Deposition during rising sea level appears to be favoured by narrow shelves, incised submarine canyons, shelf-parallel currents and tectonic activity of the basin margin and hinterland, the latter may provide high volumes of sediment (e.g. Reading & Richards 1994; Stow & Mayall 2000; Shanmugam 2000). When submarine canyons are connected with a shelf-edge delta (e.g. Amazon and Mississippi rivers) or directly connect with the river mouth (e.g. Indus and Zaire rivers), sediment may be transported straight into the basin (e.g. Burgess & Hovius 1998). These estuaries with deeply incised canyons may transfer as much as 6 - 8 times more sediment to the deep-sea than other types of river mouth (Wetzel 1993). Shelf-parallel currents may also feed sediment into incised canyons. These factors may result in continued or even increased sediment supply to the basin in spite of rising sea levels (e.g. Reading & Richards 1994; Burgess & Hovius 1998; Eschard 2001).

* „*Sequence stratigraphy* is the study of rock relationships within a chronostratigraphic framework of repetitive, genetically related strata bounded by surfaces of erosion or non-deposition, or their correlative conformities. The fundamental unit of sequence stratigraphy is the sequence, which is bounded by unconformities and their correlative conformities. A sequence can be subdivided into *system tracts*, which are defined by their position within the sequence and by the stacking pattern of parasequence sets and parasequences, bounded by marine-flooding surfaces. Boundaries of sequences, parasequence sets, and parasequences provide a chronostratigraphic framework for correlating and mapping sedimentary rocks." (Van Wagoner *et al.* 1987). It provides a useful framework for understanding the interplay between accommodation space, subsidence and/or uplift and rate of sea-level change in many sedimentary environments." (Kolla 1993)

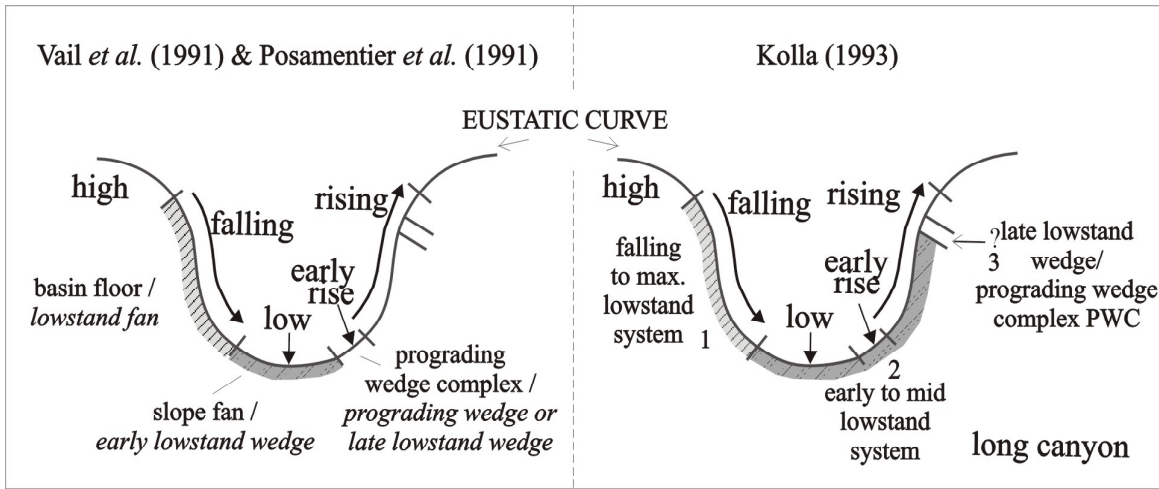


Figure 2.47: Terminologies of deep water system of Vail *et al.* (1991) and Posamentier *et al.* (1991) (*italics*) in comparison to Kolla's (1993) terminology for long canyons. (1 corresponds to basal- to lower, slope to basin system, 2: lowstand - early sea level rise - early Transgressive System Tract (TST), 3: early sea level rise - early TST.)

Previous studies proposed the initiation of the Cingöz fans to result from a fall in relative sea level, suggesting it to be an example of a typical lowstand fan system (Naz *et al.* 1991; Gürbüz 1993). However, more recently it has been proposed that the Cingöz fans present an example of fan systems developed during a transgressive phase (Yetiş *et al.* 1995; Kostrewa *et al.* 1997; Satur *et al.* 1997; Satur 1999). Their initiation is associated with rapid sediment supply into the basin as a consequence of tectonic activity within the source area (Satur 1999), probably related to a previous time of sea-level lowstand.

Sedimentary sequences suggesting rising sea level and/or sea-level fluctuations have been identified at various scales and in different environments within the E-Fan. Satur (1999) found distinct deepening resulting from sea-level rise recorded by initial shallow water sandstones and conglomerates to deeper-water turbidite sandstones within channels 3 / 4 respectively.

The analysis of the sandy basin-fill reveals higher frequency, 4th- and possibly 5th-order relative sea-level fluctuations* influencing sedimentary signatures:

- i. conspicuous fining upward at lobe scale (m to 10s of m) observed in many individual Lobe A, Lobe B and Lobe C deposits
- ii. overall fining upward at lobe-complex scale observed in the transition, proximal and distal lobe zone
- iii. gradual upward reduction in overall clast size within the channeling components of the CLTZ
- iv. the various channel-lobe transition deposits backfilling (or backstepping *sensu* Mutti & Normark 1987) their respective feeder channels
- v. progradation as recorded by the channeling and distributary channel component in the CLTZ and PLZ respectively and the episodic coarse onset of Lobe B deposition in the PLZ

Points i) to iv) record gradually rising sea level, while v) suggests that occasional phases of progradation are perhaps related to a temporary fall in local sea level. Source control, such as overall denudation, may additionally be governing the gradual reduction in grain size (*chapter 2.5.3*) and result in fining-upward sequences (e.g. Campos Basin/Offshore Brazil: Bruhn & Walker 1995). Relative sea-level changes may occur over short time frames (< 100 kyr) in response to both eustasy and tectonism (Normark *et al.* 1993; Posamentier *et al.* 1988) or even be related to the storage and release of continental water generating smaller

*

Eustatic cycles order *	1 st	2 nd	3 rd	4 th	5 th
Cycle (my) *	200 - 500	10 - 90	1 - 10	0.2 - 0.5	0.01 - 0.2

* Vail *et al.* (1977, 1991); Haq *et al.* (1987a,b)

changes (amplitudes: 1 – 10 m; Einsele & Ricken 1991). These higher-order fluctuations influence the distribution of sandstones, i.e. through progradation and retrogradation, and the internal architecture of components of the deep-water clastic system, i.e. fining-upward at various scales, confined geometries of Lobe A deposits resulting from backfilling of the older parts of the feeder system.

The overall retrogradational pattern of the E-Fan and its subsequent blanketing by thick basin plain deposits (e.g. Naz *et al.* 1991; Gürbüz 1993; Yetiş *et al.* 1995) indicates a landward shift of sedimentation in response to the gradually rising sea level. Coarse sediment is probably increasingly trapped on the shelf and coastal areas (e.g. Bouma 2000). The Cingöz fans were active for approximately 2.7 myr (Nazik & Gürbüz 1992), however, different authors give different timing of events (*see chapter 2.7.1*). Gürbüz (1993) suggests the E-Fan to fit a type I fan model *sensu* Mutti (1985a), while Satur (1999) believes that the E-Fan initially developed as a type I, then type II and finally a type III system (table 2.11). He relates this to the context of the sedimentary fill of the Adana Basin representing a full 2nd order eustatic sea-level cycle *sensu* Vail *et al.* (1977) and Haq *et al.* (1987a,b). However, there is no concrete field evidence proving the fan's Type I and Type III stages (*detailed discussion: chapter 2.7.3*).

Sequence Stratigraphic Model	System Tract	Sea level	E-Fan	Fan types# Examples in Literature
Lowstand fan (basin floor fan* / Type I#)	LST (= lowstand system tract; most basal stratigraphic unit of LST)	Relative sea-level fall and lowstand	Gravelly growth stage: canyon incision & sediment bypass; sediment transport farthest into the basin, Development of gravel lobes? Or extreme southern downcurrent deposition of thick, sandy lobe successions?	e.g. Chugach Turbidite System/Alaska (Nilsen 1985); Oligocene-early Messinian sand-rich turbidites/Italian Apennines (Cornamusini & Sandrelli 2002);
Early lowstand wedge (slope fan* / Type II#)	late LST to early TST (= transgressive system tract)	Rising sea level	Sandy growth stage: backfilling of feeder channels (inner valley fill), channel-attached lobes	e.g. Rocchetta Formation/ Italian Apennines (Cazzola <i>et al.</i> 1981); Macigno costiero (Cornamusini & Sandrelli 2002); Blanka Turbidite System/California (McLean & Howell 1985)
Late lowstand wedge (prograding wedge complex* / Type III#)	TST	Relative sea level approached maximum rate or rise	Muddy growth stage?: Channel-levee complex, small sandy lobe deposition ?	e.g. Delgada Fan (Wilde <i>et al.</i> 1985)

Table 2.11: Sequence stratigraphic model for different growth stages of E-Fan after Kolla (1993). Other terminology: * Vail *et al.* 1977, 1991, Posamentier & Erskine (1991) and # Mutti & Normark (1987).

2.5.5 Water depth, contourites and other controls

The study of mainly modern systems has shown that a variety of other controls may affect the sediment accumulation patterns in deep-water turbidite systems.

Water depth: Previous studies of the Cingöz Fan system suggest that fan accumulation in the western part took place under relatively shallow water conditions in the sublittoral zone between 0 - 200 m water depth (Satur 1999). The mixed and Nerities ichnofacies assemblage found in the E-Fan indicate an oligotrophic, less oxygenated and a probably more restricted, relatively deeper water environment (Demircan & Toker 1998). Nereites assemblages are characteristic of the abyssal zone, below 500 - >2000 m water depth (Seilacher 1967; Frey & Pemberton 1984), where they serve as a proxy for the redox boundary depth (Wetzel 2002). Satur (1999) and this study demonstrate that water conditions appear to deepen during the deposition of the E-Fan, however, absolute values cannot be determined. The confining shallow marine Karaisali carbonate platform formed before and just until after the initiation of the Cingöz Formation (Gürbüz 1993), however, it may probably have been drowned and/or buried by the subsequent landward

shift of the turbidite system due to rising sea level. Local upward shoaling indicated by the presence of Ophiomorpha (*pers. comm.* Kelling 1998) has been observed in the upper Cingöz in the extreme SE area of the W-Fan western section.

Contourite system: Various modern and subsurface examples exist where submarine fan deposits show reworking by contourite and bottom currents, e.g. Tertiary Sands Frigg Field/North Sea (Enjolras *et al.* 1986), Eocene sands Campos Basin/offshore Brazil (Mutti *et al.* 1980), Ewing Bank Block 826/Gulf of Mexico (Shanmugam *et al.* 1993), Gulf of Cadiz (Gonthier *et al.* 1984; Nelson *et al.* 1993) or primary bottom current deposition (Gulf of Cadiz: Habgood *et al.* 2002). Sandy contourites are generally fine grained, exhibiting typical bedload bedforms such as ripples, sediment waves, planar bedding and ribbons (Mutti & Normark 1987; Shanmugam *et al.* 1993). Resulting vertical sequences are not unlike the Bouma Sequence (Shanmugam 2000). However, intense bioturbation may destroy primary current structures (Mutti & Normark 1987; Nelson *et al.* 1993; Stow & Johansson 2000). These sandy contourites are restricted to particular morphologic and hydrodynamic settings which allow the enhancement of current velocity and for which an adequate sand supply is available (Stow & Johansson 2000). Most preserved ancient turbidite systems formed in collisional and post-collisional basins, which did not allow any significant development of contourite currents (Mutti & Normark 1987; Normark *et al.* 1993). In the E-Fan of the Cingöz Formation, reworking by contourite, bottom currents or even tidal currents was not observed.

Other controls: Submarine fan development in general may additionally be controlled by the overall annual river discharge, sediment concentration, river temperature, seawater salinity and temperature, organic supply, gas production or diapiric movements (e.g. Reading & Richards 1994; Kenyon *et al.* 2002). Seawater salinity and temperature play a crucial role in transforming suspension plumes into hyperpycnal flows by fostering particle flocculation (e.g. Normark & Piper, 1991)

2.6 Evolution of the E-Fan

A review of the E-Fan framework (this study) and detailed analysis of selected areas such as the gravelly feeder system (Satur 1999) and sandy basin-fill (this study), indicate a complex interaction of auto- and allocyclic mechanisms controlling the development history of the E-Fan system. Records of the earliest and latest evolutionary stages are poor, the sand-rich stage is only preserved in parts. The detailed lobe study areas represent unconnected time slices within the system.

Gravelly stage

Stage 1: (late? Burdigalian)

Nazik & Gürbüz (1992) suggest that the E-Fan became active during late Burdigalian. Gürbüz (1993) concluded that the initiation of the Cingöz system was driven by a drop in sea level, however, Satur (1999) believes fan initiation to be related to high sediment availability driven by tectonism in the source area and aided by the direct connection with the subaerial river system and the narrow shelf favouring sediment transport to the basin.

Satur's (1999) study of the feeder system indicates that during its earliest stage the E-Fan developed as a multiple-sourced, gravel-rich fan (fig. 2.48a). The corresponding lobe deposits are not exposed and their size, shape and grain-size therefore unknown. Gravelly channel-fill to sandy fan lobe deposits approximately 40 km to the south of the exposed feeder system suggest great downcurrent extend (Naz *et al.* 1991). Seismic evidence points to convex-upward shaped structures akin to lobe geometries in subcrop (Williams *et al.* 1995). Extensive faulting, however, prohibits any direct correlation with the exposed feeder system (Ünlügenç 1993). The exposed confluence in the NW of the E-Fan indicates that channels 1, 2 and 3 were active at the same time (Satur 1999), at least towards the top of this stage.

The marked gravelly appearance of this first stage may be related to the initial uplift of the Tauride Orogen, when coarse sediment was freed. Naz *et al.* (1991) described the Cingöz gravels in well Gülbaş 2 as "inner-fan valley-fill". Feeder channels 1 and 2 and possibly 3 may initially have formed one large, extensive feeder, which funnelled coarse sediment much farther into the basin. If sand was abundantly available at this stage is unknown, a gravelly fan system similar to Reading & Richards (1994) may have developed forming

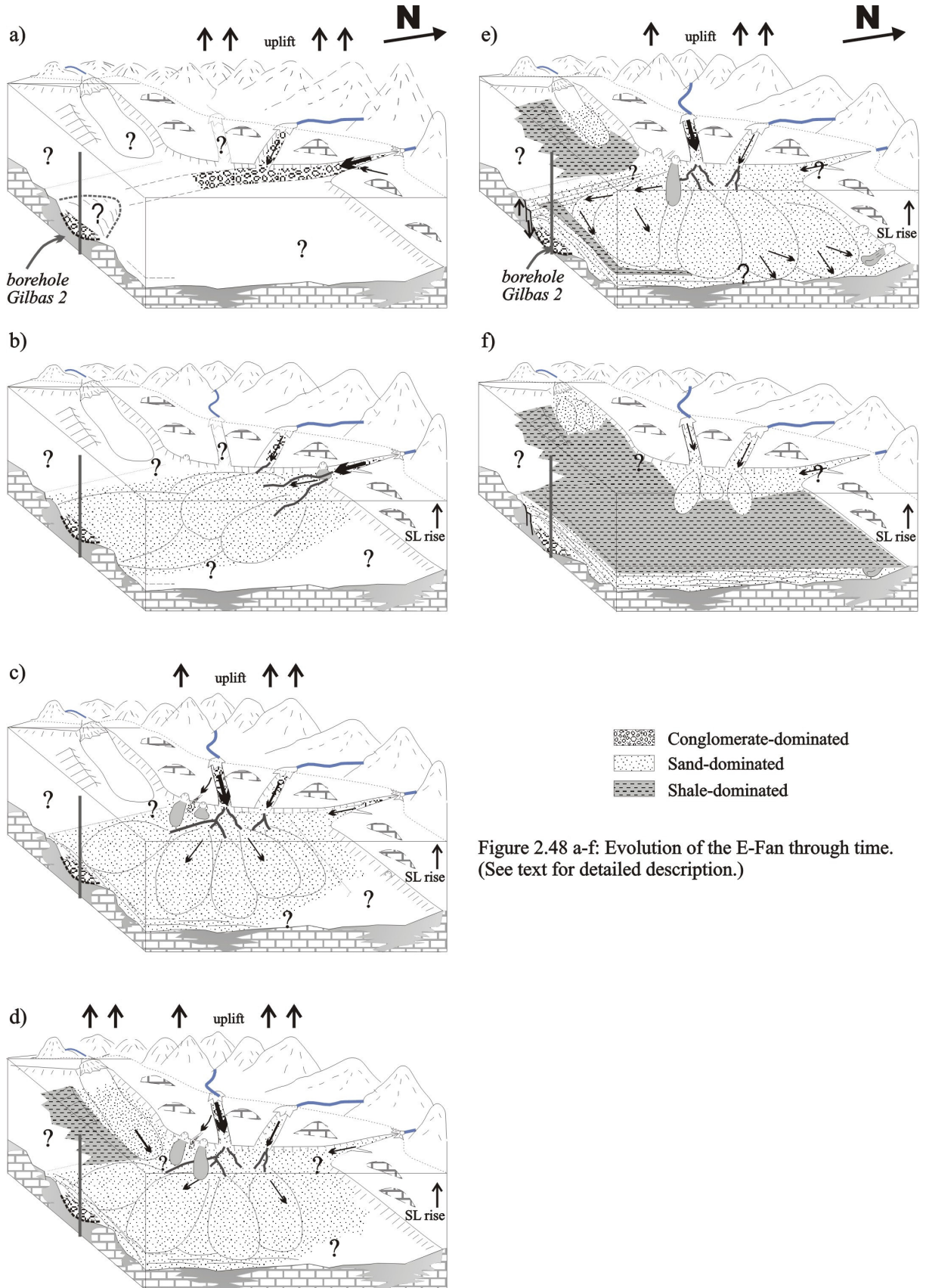


Figure 2.48 a-f: Evolution of the E-Fan through time. (See text for detailed description.)

gravelly lobe at the channel mouth akin to the Var fan lobe (Unterseh 1999) or the Porto lobe (Kenyon *et al.* 2002) at its mouth is possible (fig. 2.48a). The observed conglomeratic channel fill in the feeder system presents the latest stage of the gravelly system indicating backfilling of the conduit due to gradually rising sea level (Satur 1999).

Sandy stage

Stage 2: (late? Burdigalian)

The transition to the sand-rich phase is marked by the onset of coarse sandy deposition in thick channel-lobe transition (CLTZ) and lobe deposits with an extremely low shale content. They gradually backfill or backstep (*sensu* Mutti & Normark 1987) the conglomeratic feeder channel 1 deposits in the north and channel 3 / 4 deposits in the northwestern area respectively (fig. 2.48b). The palaeocurrent pattern indicates a switch from a mainly northern source (feeder channel 1 / CLTZ 1) to a mainly northwestern to western source (CLTZ 3 / 4). The younger proximal lobe zone was probably sourced from channels 3 and 4. The input from each channel is unknown. Flow mixing at their confluence is likely to have occurred and the subsequent depositional signature within the proximal lobe zone appears to be homogeneous (i.e. no differentiation between the potential sources). Prior to identification of feeder channels 3 and 4, this shift in transport direction was interpreted to result from flow deflection at a submarine high, deflecting sediments funnelled into the basin via feeder channel 1 (Gürbüz 1993; *pers. comm.* Kelling & Gürbüz 1996). No coeval sediments are exposed and/or preserved to the east of the proximal lobe zone and neither was sediment input from the north (channel 1) recorded. However, marginal fan sedimentation took place along the western flank of the E-Fan.

The latero-vertical growth pattern observed in the CLTZ 1 and younger proximal lobe zone (Lobes B) suggests sediment accumulation in a (semi-) confined space. The channel mouth and overlying channel-lobe transition zone associated with feeder channel 1 are partially deposited within the confines of the channel while the proximal lobes appear to have accumulated in an intrabasinal, probably fault-bounded depression. The latter strongly suggests synsedimentary tectonism to affect the accommodation space within the basin. Pre-depositional (fault-scarp) topography and differential subsidence in adjacent basin sectors control the sediment distribution pattern resulting in locally enhanced sediment accumulation (proximal lobe zone), restricted lateral dispersal and preferred (directional) funnelling of sediment further into the basin. Occasional progradation as suggested by the presence of distributary channels was also responsible for sediment transporting further into the basin.

Synsedimentary tectonism also affected the basin margin and source area resulting in frequent shelf/slope-sourced mass wasting events along the north (channel 1) and central E-Fan area as well as along the western margin. The observed west-ward shift in time and activity of the feeder channel system is believed to be controlled by tectonism in the source area. Satur (1999) puts the relative age of channel 4 as younger than channel 3, based on gravelly channel 4 deposits eroding into sandy transition deposits associated with channel 3. Later uplift of the feeder channel 4 source area probably resulted its later initiation and its prolonged funnelling of gravelly material into the basin at a time when feeders 1, 2 and 3 were already sourced by sandier material (fig. 2.48c). The respective source areas of the latter probably having experienced diminished tectonic activity, prolonged denudation and/or coarser sediment trapped in more proximal locations, thus providing overall smaller grain sizes. The apparently diminished sediment input of channel 1 at a later stage may further be explained by this process, resulting in the complete shut-down or a period of quiescence as it had experienced in its earlier development (Satur 1999). Whether uplift in the west may have resulted in a change of basin gradient (tilting towards the east) is unknown. This process might have deflected channel 1 flows to the east along the eastern margin, however, no data are available to support this hypothesis.

The distinct grain size change, sandy backfilling of the conglomeratic feeder systems and the westward shifting sediment source appear to be chiefly controlled by source area tectonism, i.e. differential uplift, and subsequent denudation of the respective sources combined with a gradually rising sea level initiating the apparent landward shift in sedimentation. Synsedimentary tectonism and higher frequency sea-level changes affect the sediment accumulation pattern within the basin. The observed westward shift in source area may be responsible for the later initiation of the W-Fan as suggested by Satur (1999).

This evolutionary stage of the E-Fan is akin to the low-efficiency fan type II of Mutti (1985a) or the sand-rich submarine fan model of Reading & Richards (1994) where the sand deposition took place in channels and in channel-attached lobes.

Stage 3: (incomplete ?) Praeorbulina glomerosa zone (PN8: late Burdigalian)

During this, probably incomplete, biozone (data from Nazik & Gürbüz 1992 and Gürbüz 1993), 450 m of mainly coarse lobe deposits were deposited in the central E-Fan area and approximately 700 m of granule sediment bodies interbedded with thick very fine-grained successions in the west. No upper Burdigalian fan sediments were recorded in the east. Their absence may either be due to non-deposition or, more likely, due to non-exposure, i.e. burial. The thickness differences between the central and western section may result from the incomplete sampling-range.

Regardless of the uncertain lower timing of this biozone, W-Fan sedimentation is prograding into an area previously occupied by E-Fan deposition (fig. 2.48d). Already 100 m below the presumed onset of this biozone, W-Fan sediments were recorded. These distinctive granule sandstone bodies, probably downcurrent equivalents of sandstone tongues *sensu* Satur (1999) and Satur *et al.* (2000), are rapidly fining upward into fan fringe sedimentation. Throughout, transport directions persistently point to the east (75 - 145°). Poor exposure prohibits tracing of the sandstone tongues in a downcurrent, eastern direction, therefore, the exact extent and influence of the western-derived flows are unknown. Flowmixing with channel 3 and 4 flows is likely, resulting deposits probably existing in subcrop (due to the direction and gradient of dip).

The W-Fan progradation is likely to be driven by increased, coarse sediment supply to the basin from the west underlining the proposed westward shift in differential uplift of the source area controlling sediment supply. The granule grain size suggest that the available coarse sediment was funnelled effectively towards the east favoured by the confined, elongate W-Fan subbasin (Satur 1999) at times acting as a channel-like fairway (Stow & Johansson 2000). However, the progradation of the coarse sediment bodies was relatively short-lived, rising sea level and/or diminished input from the west resulting in the retrogradation of the W-Fan giving way to fan fringe sedimentation.

Coarse sand deposition in thick lobe deposits and associated facies sourced from channels 3 and/or 4 is still rife in the central E-Fan area. If lobes were channel-attached and/or sandy channel-fill deposition took place can only be speculated, however, the development as a fan type II *sensu* Mutti (1985a) is likely. Gradual fining- and thinning of deposits and an increase in overall shale content equally suggest source area control (e.g. changing grain size, input and/or flow competence) under an overall rising sea level.

Stage 4 *Orbulina suturalis* zone (PN9-10: Langhian)

During Langhian times, the sediment dispersal pattern was governed by a complex, fault-scarp basinfloor topography which resulted in basin compartmentalisation leading to tectonic and/or bulk sediment weight, which induced differential subsidence of small, adjacent basin sectors. It favoured enhanced thickness accumulation in the central E-Fan area (~ 2000 m), inhibited lateral (western) sediment dispersal and encouraged flow deflection towards an overall SE to E direction (fig. 2.48e).

Sand-dominated deposition continued in the central and eastern E-Fan areas, accumulating 2000 m and 840 m of primarily sandy lobe and minor associated deposits respectively. (Recorded) deposition in the east sets in slightly above the Langhian/Burdigalian boundary, the encroaching fan sediments gradually aggrading against the slope. Channels 3 and/or 4 provided the bulk of the sediment supply to the basin. If lobes were channel-attached and/or sandy channel-fill deposition took place is unknown, however, source area denudation may have resulted in a mixed sedimentload possibly resulting in a type I fan of Mutti (1985a). In both the central and eastern areas, gradual thinning and fining upward towards the top marks the shift to fan fringe sedimentation probably driven by reduction in grain size due to denudation of the source area, diminished sediment input and/or flow competence and/or subsiding source area tectonism and a gradually rising sea level.

In the west, 250 m of W-Fan fringe sedimentation progressed (previously interpreted to represent deflected E-Fan fringe sedimentation (Gürbüz 1993). It marks the continued retrogradation of the W-Fan due to diminished sediment input and gradually rising sea level (Satur 1999; Satur *et al.* 2000) (fig. 2.48e).

Synsedimentary tectonism continues to trigger mass wasting events resulting in thick debrites interbedded with fan deposition (central E-Fan) and moulding the slope morphology (Cronin *et al.* 2000; this study).

Stage 5: *Globorotalia mayeri* zone (PN11: early Serravallian)

Rising sea level and diminished sediment input due to subsiding source area tectonisms and denudation of the hinterland lead to overall fan fringe sedimentation during the final depositional stage of the E-Fan system (central area: 80 m; western area: 110 m; eastern area: unknown) (fig. 2.48f). A channel-levee

complex (type III fan system) probably developed and sand deposition in smaller lobes may still have taken place in the most proximal fan position. Palaeocurrents (data: Gürbüz 1993) suggest that the western E-Fan area was still sourced from the west, implying much longer W-Fan activity than previously interpreted (e.g. Gürbüz 1993; Satur 1999). Shallowing in the extreme southeast of the W-Fan indicates a local high (*pers. comm.* Kelling 1998).

Stage 6 (late Serravallian)

A combination of subsiding tectonism and denudation of the source area and the gradually rising sea level result in decreased sediment input and/or sediment trapped in the proximal reaches of the shelf which effectively ended E-Fan clastic sedimentation. The Cingöz fans were covered by up to 1200 m thick basin plain deposits (Güvenç Formation; Naz *et al.* 1991).

2.7 Discussion

2.7.1 Biostratigraphic framework

The timing of fan initiation and the length of activity for the W- and E-Fan of the Cingöz system show stark discrepancies among workers. Yetiş (1988) suggests a late Burdigalian to Langhian age for the Cingöz Formation based on lithostratigraphic relationships with the other formations, while Naz *et al.* (1991) indicate an early Langhian to Serravallian age, the fan initiation related to the suggested early Langhian sea-level drop. Toker *et al.* (1998) put the depositional age of the Cingöz Formation from early-middle Miocene (Langhian: *Sphenolithus Leterorophus* Zone [NN5]) to middle Miocene (Serravallian: *Discoaster exilis* Zone [NN6]) based on calcareous nanoplankton, the age Satur (1999) appears to have used in his recent study. Nazik & Gürbüz (1992), Gürbüz (1993) and Cronin, Gürbüz, Hurst & Satur (2000) utilise the foraminiferal biozones which place the depositional age of the Cingöz Formation from late Burdigalian to Serravallian (*Praeorbulina glomerosa curva* [PN8], *Orbulina suturalis* [PN9-10] and lower? *Globorotalia mayeri* [PN 11?] zones).

Gürbüz (1993) suggests that the W-Fan was initiated and prograded towards the east already during the late Burdigalian, while Satur (1999) proposes an overall shorter-lived W-Fan sedimentation, its initiation only shortly after the onset of the Langhian. This study, utilising Gürbüz's (1993) biostratigraphic data, proposes that the W-Fan was active throughout the whole of the Cingöz depositional phase, right up to and including the *Globorotalia mayeri* zone, and that its occupation of the south-western, former "E-Fan" area persisted longer than previous studies suggested.

2.7.2 E-Fan vs W-Fan

Satur (1999) suggests the E- and the W-Fan to be defined as the eastern and western area of one single Cingöz fan system whose development was only separate during its initial (oldest Langhian: Satur 1999) and later development (Serravallian). He postulates that the western area supplied the bulk of the eastern area and that the marked differences in depositional style between the two "fan areas" are due to the underlying basinfloor topography, the "western area" subbasin being comparatively shallow and well confined.

This study questions the postulated bulk sediment supply from the west and suggests that a complex basinfloor topography resulted in enhanced thickness in the central E-Fan depositional area and the easterly deflection of the turbidite flows.

Satur (1999) postulates the following points:

- i. bulk sediment supply to the eastern fan area from the west
- ii. western source active slightly later (later early Langhian), separate development during its latest stage and earlier cessation (Serravallian) than eastern area deposition.

This study proposes that

- i. the W-Fan prograded into an area previously occupied by the E-Fan during late Burdigalian times. The magnitude of sediment transfer from west to east is unknown.

- Thus its influence, i.e. eastward depositional extent, can only be speculated upon in absence of any concrete depositional evidence. Potential sediments in the central E-Fan area recording W-Fan progradation and/or flow mixing with E-Fan feeders, may exist in subcrop. During Langhian, W-Fan sedimentation retrograded, leaving fringe sedimentation in place, while coarse sand deposition was still rife in the central and eastern E-Fan area. Satur's (1999) geochemical pilot study points to an E-Fan source for the Langhian Lobe C deposits.
- ii. the W-Fan was active for a much longer time than both Gürbüz (1993) and Satur (1999) suggested. W-Fan fringe sedimentation was still conspicuous during the Globorotalia mayeri zone (early Serravallian), deposits which were previously interpreted to represent deflected E-Fan sediments. One argument was the deeper-water fauna encountered, which is characteristic of the E-Fan depositional environment (Gürbüz 1993; *pers. comm.* Gürbüz & Kelling 1996). However, with rising sea level, conditions deepened and thus may account for the deeper water assemblage in this (W-Fan) area (Demircan & Toker 1998). Only towards the extreme top, shallowing was recorded.

Satur's (1999) suggested new nomenclature appears to be rather semantic. Regardless of it, he acknowledges that one Cingöz deepwater clastic system consists of two, more or less coeval depositional entities sourced from separate, distinct sources (W-feeder *versus* E-Fan feeder system). Their development was initially separate (Gürbüz 1993), then interfingered and was ultimately separate again (Gürbüz 1993; Satur 1999). The former and current Cingöz fan models are clearly biased towards over-emphasising the outcropping, relatively proximal conglomeratic and sandy deposits. The unknown dimension of the Cingöz systems' southern extent as indicated by borehole and seismic data (Naz *et al.* 1991; Williams *et al.* 1995) presents problems in understanding the greater picture of the Cingöz development. The considerable thickness of conglomeratic "inner-fan valley-fill" deposits (Naz *et al.* 1991) has not been adequately addressed in their existence in relation to the outcropping Cingöz deposits by any later study (e.g. Gürbüz 1993, Ünlügenç 1993; Williams *et al.* 1995; Yetiş *et al.* 1995; Satur 1999; this study). Clearly, problems exist with tying the borehole data into the fan models due to absence of (unpublished?) lithologic and biostratigraphic data, basin-wide marker beds and abundant faulting.

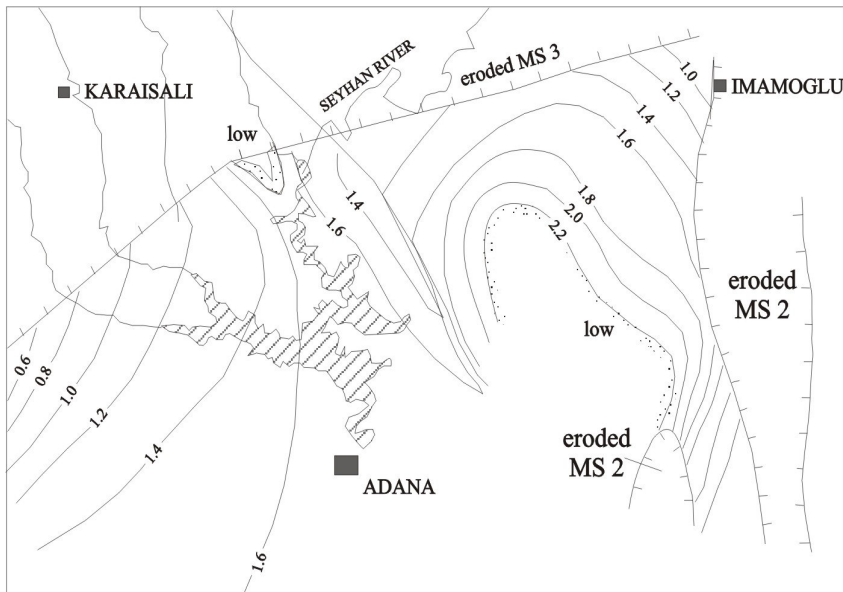


Figure 2.49: Isochron (thickness in seconds TWTT) for megasequence 2. The map show an area of thick megasequence 2 between Adana city and the İmamoğlu Fault Zone (eroded MS 2 on map; from Williams *et al.* 1995)

Naz *et al.* (1991) interpret the cored section to represent the downcurrent extend to the E-Fan (their Ayva Hill Fan). This study agrees, especially since the W-Fan appears to be strongly confined to a W-E trending subbasin. Williams *et al.* (1995) show a great, almost radial extent in a southern direction with a depositional thickening between Adana and the İmamoğlu Fault (fig. 2.49), lying in the direct southern extension of the exposed E-Fan. However, their described Megasequence 2 includes Kaplankaya, Cingöz and Güvenç deposits, all of unknown thicknesses and geometries.

2.7.3 Dynamic depositional model

The E-Fan represents a relatively small, coarse-grained and short-lived deep-water clastic system deposited in a Type C basin *sensu* Mutti & Normark (1987), with some elements of a Type D basin. Its initiation is

believed to result from high sediment availability within the source area (Satur 1999), perhaps during a time of lowered sea level (e.g. Naz *et al.* 1991; Görür 1992; Gürbüz 1993). Basin aggradation met with rapid sediment discharge from the uplifted Taurus Orogen and restricted sediment dispersal due to complex fault-scarp basin topography. It resulted in thick, locally extensive sediment accumulation, restricted (lateral) western dispersal and the eastern axial deflection of the E-Fan system during the sandy growth stage. The observed landward shift of the system resulted from a combination of subsiding source-area tectonism, denudation and a gradually rising sea level.

However, no single encompassing model can fully describe the spatial and temporal changes observed within the E-Fan, the changes from a gravel-rich to sand-rich and subsequently mud-rich? submarine fan system* (*sensu* Reading & Richards 1994) or the evolution through type I to III stages (*sensu* Mutti 1985a) as proposed by Satur (1999).

For the described gravelly-growth stage during late? Burdigalian times, which is solely known from the exposed conglomeratic northern feeders and the inner-fan valley-fill of Naz *et al.* (1991), the question of if and how much sand was available is crucial for its classification. If sand was abundantly available, it was probably deposited in sandy lobes downsystem of the recorded conglomeratic channel-fill deposits, thus being comparable to a type I system of Mutti (1985a) (fig. 2.50). However, if rapid tectonic uplift provided the sediment to the basin, it probably yielded very little sand-sized material at first. Then the E-Fan would initially have developed as a gravel-rich type of Reading & Richards (1994) where "smallish" gravel lobes form at the mouth of a channel similar to the modern gravelly systems such as the Porto canyon-mouth lobe (Kenyon *et al.* 2002) and the Var fan lobe (Unterseh 1999). Seismic data do not indicate channel-incision far to the south as suggested by Naz *et al.* (1991), but the apparent fault-scarp topography (Williams *et al.* 1995) probably controlled the channelized and/or non-channelized conglomeratic accumulation. Due to the overall lack of data neither model can be verified to correctly represent the gravelly-growth stage.

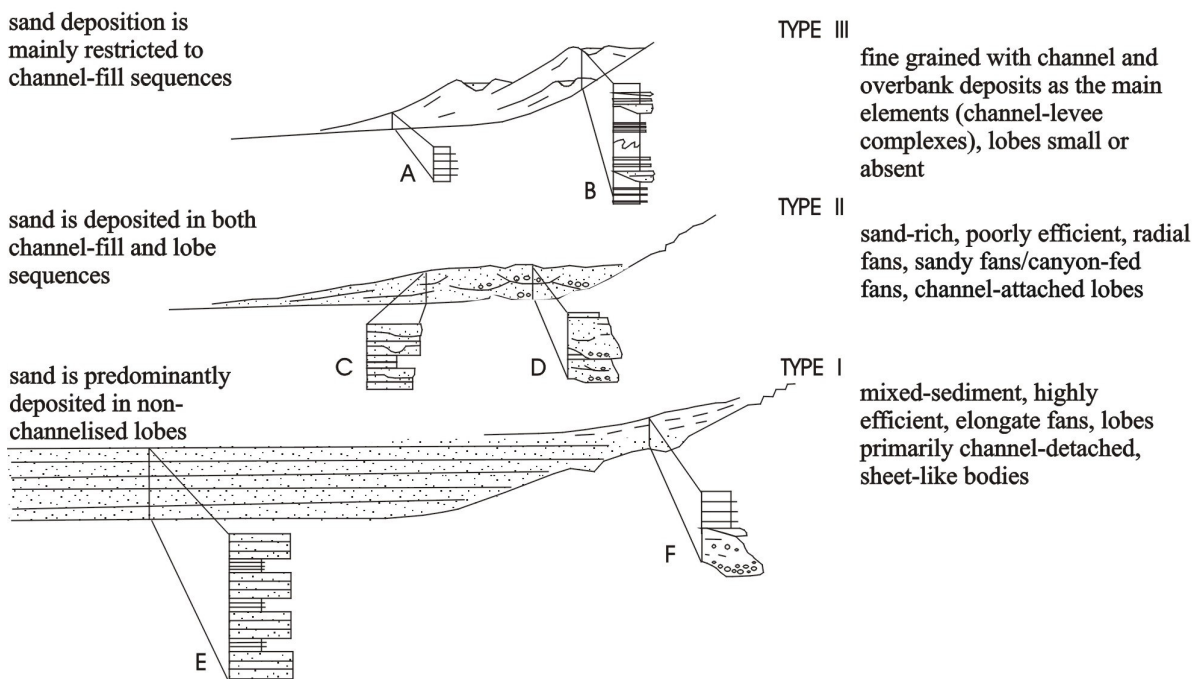


Figure 2.50: Schematic representation of three main types of turbidite deposits as characterised by relative amount of and position within the deposit of the sandy component (from Mutti 1985a).

The sand-rich phase of the E-Fan is marked by the onset of thick sandy sheet-like deposits backfilling the feeder system. Gürbüz (1993) rather too simplistically suggested that the whole of the E-Fan represents a type I system *sensu* Mutti (1985a), where sand is predominantly deposited in non-channelized lobes. Type I systems are synonymous with the highly efficient fans characteristic of elongate foreland basins (fig. 2.50).

* submarine fan systems *sensu* Reading & Richards (1994) are characterised by a single feeder, while multiple sourced systems should be classified as 'submarine ramp'. However, the E-Fan feeders are clearly defined and do appear to be active at slightly different stages thus the 'non-conforming classification' of multiple-sourced submarine fan is retained.

However, the sandy basin-fill of the E-Fan is more akin to sand-rich, poorly efficient systems, where coarser sand is deposited in smaller, channel-attached lobes and channel-fill sequences, such as the Lobes A and B backfilling the feeder channel during the late? Burdigalian. Conglomerates characterise the channeling component in the transition zones, but if during this stage sandy channel-fill deposition took place is unknown. The deposition of the thick, sand-rich Lobe C deposits during Langhian times took place in the eastern, more distal reaches of the system. It is not known if they are channel-attached lobes and if sand deposition took place in the feeders as the sequence stratigraphic approach would favour. If continued grain size reduction driven by source control resulted in a more sand/mud-rich system *sensu* Reading & Richards (1994) it might have favoured sand transport farther into the basin in spite of the rising sea level thus changing to a type I (?) system. Even very large, mud-rich systems such as Amazon Fan, for example, records 20 to > 100 m thick sand complexes of at times medium- to coarse-grained sand in the lower fan area (Flood *et al.* 1995).

Fan fringe sedimentation during the late Langhian and early Serravallian indicates a continued landward shift in the sand deposition probably driven by continued source-area denudation and rising sea level, resulting in a proposed channel-levee complex with probably no or few small sandy lobes developing in the proximal reaches (Satur 1999). No proximal fan sediments are preserved representing this stage.

Satur's (1999) model is driven by the sequence stratigraphic approach regarding sea-level rise as the most important factor controlling the evolution of the Cingöz system rather than integrating potential source control, i.e. changing sediment availability and grain size, which this study believes to be an important factor in governing the E-Fan evolution. That a switch in fan system *sensu* Mutti (1985a) may be independent of sea level, is documented by the sand-rich turbidites systems of the northern Apennines. They initially developed as type I system (late Oligocene to early Messinian) and changed to type II systems (Late Messinian to Pliocene) resulting from changes in the shape, geometry and dimension of the basins due to the emersion of a mountain chain that strongly altered the palaeodrainage pattern combined with tectonic fragmentation of the basin (Cornamusini & Sandrelli 2002).

2.7.4 Lobe accumulation

During the sandy-growth stage (late Burdigalian – Langhian), the sand deposition took place in thick, non-erosive, laterally extensive sheet-like deposits, some of which appear to be of lobate geometry. The transition zone (Lobe A) and proximal lobe (Lobe B) deposits do not fit the classical lobe definition *sensu* Mutti & Normark (1987), while Lobe C deposits of the distal lobe zone are more akin to it. The location and nature of the resultant lobes are primarily governed by the topographic restraints.

The use of the term "lobe" is ambiguous. A lobe *sensu strictu* refers to non-channelized depositional bodies of lobate geometry, however, different data sets, i.e. modern to ancient (outcrop/subsurface), yielded a greatly differing application of the term (*see reviews* in e.g. Shanmugam & Moiola 1991; Shanmugam 2000). Confusion and non-transferability of results are the consequence.

A detailed discussion on depositional lobes and related bodies, for example their definition, recognition, controls, reservoir characterisation and the potential problematic application of the term, are presented in chapter 5 with emphasis on the studied outcrop and subsurface examples (*chapter 3*).

2.7.5 Controls

A deep-water clastic system developing in a tectonic active setting is controlled by a complex interplay of the local and regional tectonism, relative sea-level variation, climate and the sediment supply pattern (e.g. Normark *et al.* 1993; Reading & Richards 1994; Stow & Johansson 2000). The retrogradational pattern of the E-Fan is striking and indicates the gradually rising sea level to be the fundamental control on its development as suggested by Satur's (1999) sequence stratigraphic-driven model. However, this study has shown that tectonism plays an important role in governing the E-Fan evolution and ultimately of the Cingöz Formation.

Source-area tectonism has been shown to influence the i) timing and spacing of sediment supply by activating different sources at different times probably through differential uplift, ii) resulting in the apparent westward shift in the supply transfer pattern through structurally controlled feeders and iii) in conjunction with probably a more humid climate, it controlled the available sediment grain size, flow

competence and capacity. Tectonism also controlled the geometry and topography of the host basin which strongly influenced the spatial and temporal development of the sediment accumulation. This in turn resulted in the observed locally enhanced deposition during late? Burdigalian and Langhian, the (western-) lateral restricted dispersal and the apparent easterly, axial flow deflection of the E-Fan during Langhian times. Through time, basinfloor topography was probably increasingly subdued through depositional smoothing of the relief.

The longitudinal, landward shift or retrogradation of the E-Fan system is expressed by the gradual reduction in grain size and the retrogradational pattern, i.e. the backstepping of more distal facies (e.g. channel-lobe transition zone) over more proximal facies (e.g. channel-fill sequences). This is likely to result from a combination of i) gradually rising sea level, ii) a tectonically driven decrease in the gradient of the continental margin, iii) gradual basin infilling and onlap and/or iv) a change in the energy, volume and load of sediment gravity flows building the turbidite system. The change in the energy, volume and load of the sediment gravity flows is probably related to the interplay of continental tectonics and climate overprinted by the gradually rising sea level. The rising sea level results in a greater transition area between the source and the basin, allowing sorting and deposition of coarser fractions there (e.g. Stow & Johansson 2000; Bouma 2000; Kenyon *et al.* 2002).

Tectonic control, i.e. source-area tectonism controlling sediment supply, rather than eustasy has been recognised in a number of transgressive systems to be the fundamental control resulting in the accumulation of thick deep-water massive sandstones (Stow & Johansson 2000), distinct fining-upward sequences (e.g. Campos Basin/offshore Brazil: Bruhn & Walker 1995), or landward shift of the system in combination with increasing hinterland aridity (e.g. Agadir turbidite system/offshore Morocco: Ericella *et al.* 1998). Even clastic progradation is not necessarily related to a fall in sea level but, in case of the deep-water clastic strata in the Carboniferous Culm Basin/Czech Republic, to changes in drainage basin size and/or climatic fluctuations within the source area (Hartley & Otava 2001). Sea-level changes are recognised to modify effects of longer-term changes in sedimentation driven by tectonic activity in the source area (e.g. Paola Basin/Tyrrhenian Sea: Trincardi *et al.* 1995) or may even be the reason for switching sediment supply patterns to a basin rather than tectonism (e.g. Monterey Fan: Normark & Piper 1991).

The temporal and spatial turbidite accumulation in the distinctively retrogradational E-Fan system appears to be controlled by source-area tectonism and the overall transgression taking place in the Adana Basin. Additionally, the direct connectivity with fan deltas made the eustatic signature less significant than sediment supply, which aided the direct and substantial supply of coarse-grained clastic material into the basin.

2.8 Conclusion

Through extensive field work focusing on the sand-rich, proximal basin fill of the eastern fan, investigation of the fan-slope contact and a detailed revision of the existing framework, reveals new insights into the sandy growth phase and factors controlling sediment accumulation through time.

- I) Time-stratigraphic changes indicate that the E-Fan system evolve from a gravel-dominated system during late? Burdigalian to a sand-dominated one in late Burdigalian – Langhian times. Initial source-area uplift resulted in the availability of very coarse sediment, probably feeding the gravelly growth stage, where small gravel lobes may have developed at the mouth of the feeder system. Progressive sea level rise and denudation of the hinterland led to the initiation of the sandy growth stage, where the bulk of the sand accumulated in thick, laterally extensive depositional lobes. During late Burdigalian, it initially developed as a type II fan *sensu* Mutti (1985a), however, continued source-area denudation probably resulted in a more mixed sediment supply, leading to a type I? system during Langhian times. During early Serravallian a channel-levee system (type III) developed with small or no lobe deposition.
- II) The changing spatial and temporal distribution and nature of the turbidite deposits suggests tectonism as a fundamental control, overprinted by the transgression in the Adana Basin. Source-area tectonism controlled the westward migration of the source area, the sediment supply pattern and in combination with climate resulted in a gradual grain size reduction. Tectonism also controlled the geometry and topography of the host

- basin, resulting in locally enhanced deposition, (western-) lateral restricted dispersal and the apparent eastern deflection of the E-Fan. The overall retrogradation is driven by the rising sea level and progressive denudation of the Taurus Orogen.
- III) During the sandy growth stage, the bulk of the sand accumulated in laterally extensive, thick, coarse-grained, sheet-like bodies of channel-lobe transition (Lobe A), proximal (Lobe B) and distal (Lobe C) depositional zones. Lobes A and B do not fit the classical lobe definition *sensu* Mutti & Normark (1987, 1991), while Lobes C are more akin to it. The size, geometry and vertical stacking of the lobes reflects to some degree their restricted spatial, aggradational development. Unique component associations characterise the various depositional environments: transition zone (Lobe A: 70 %, channeling 30 % with scours 5 %), proximal zone (Lobe B 90 %, distributary channels: 8 %, lobe fringe 2 %) and distal lobe zone (Lobe C: 65 %, lobe fringe 22 %, interlobe 4%, fan fringe 9 %). Conspicuous fining upward at lobe and zonal scale reflect the gradually rising sea level while sporadic phases of progradation and/or coarse clastic sediment supply suggest a combination of higher frequency sea-level fluctuations and tectonic control.
 - IV) The studied lobe depositional environments do not represent true downcurrent representatives of each other. However, conspicuous, general downcurrent changes can be observed. Throughout, the different lobe types are characterised by a high net sand content. This is decreasing in a downcurrent direction, accompanied by a gradual decrease in grain size, bed thickness and amalgamation. In a downcurrent direction, deposition from turbidity currents increases along with the overall shale content. The internal organisation at bed sub-packet- to lobe-scale becomes more ordered, while lobe stacking becomes increasingly less.
 - V) Thick debrites were identified in the western and central E-Fan area which previously had been interpreted to represent levee and/or mid-fan channel deposits. These debrites indicate major tectonic activity, e.g. uplift, in particularly the basin margin area triggering large shelf/slope failures. Their frequency and great size probably posed some major obstacles resulting in flow deflection and/or cannibalisation by the canyon-derived sandy flows. Major remobilisation (slumping) of Cingöz deposits was observed along the north-eastern margin.
 - VI) During a short timespan in late Burdigalian times, granule W-Fan sediments prograded towards the east. The magnitude of sediment transfer from west to east is unknown, ditto any depositional evidence. Rapidly, W-Fan fringe sedimentation pursued, its sedimentation only ceasing during the *Globorotalia mayeri* zone (NP11, early Serravallian). Thus, the W-Fan was active for much longer than previous studies had suggested.

2.9 Further work

A number of areas would require further work to permit an even better understanding of the development of the E-Fan and the Cingöz Formation as a whole, fostering a greater understanding on factors governing the evolution of relatively small, sand-rich deep-water clastic systems.

- I) A complete detailed biostratigraphic framework for the E-Fan / Cingöz Formation is needed to aid understanding the spatial and temporal development of the system. Incomplete and/or absent dating of especially the older evolutionary stages hinders complete reconstruction of the system's development. This is especially important in the light of the differing ages of fan initiation and cessation provided by different authors.
- II) The previous, field-based studies are clearly biased towards the channelized and non-channelized proximal fan deposits. Little seismic and borehole data are published, but their integration is needed in much more detail to fully understand the nature of the Cingöz Formation and factors controlling its evolution.

- III) The evolution of the Cingöz Formation has to be seen in the context of the evolution of the Neogene fill of the northern Adana Basin. Revision and/or more details of the biostratigraphic and lithostratigraphic framework are necessary to gain a fuller picture of the formations' relationships. Especially with regard to the subsurface data set, the suggested presence of, for example, Karaisali reefal and Kaplankaya slope, needs to be addressed.
- IV) Geochemical provenance studies as tested in a pilot study by Satur (1999) may further help to determine i) the distal extend of W-Fan progradation and ii) help tying borehole data into the existing data set. This geochemical stratigraphy might help differentiating the various and changing sources (channel 1 - 3 and/or 3 / 4) and counteract problems arising from faulting or missing biostratigraphy.
- V) No information on climatic conditions during the Middle Miocene is presently available. Climatic data would further enhance the knowledge of possible and/or changing controls of the Cingöz Formation.

2.10 Summary

The E-Fan of the Miocene Cingöz Formation, southern Turkey, represents a small, coarse-grained multiple sourced deep-water clastic system whose evolution was fundamentally governed by tectonism and the gradually rising sea level. Initially source area uplift resulted in the initiation of the fan system and the formation of a gravel-dominated system, depositing thick coarse clastics far into the basin.

Gradual denudation of the source area in combination with rising sea level led to a sand-dominated system. Sand was deposited in coarse-grained, aggradational channel-lobe transition zones and thick lobe deposits (akin to type II and later type I ? system *sensu* Mutti 1985a), backfilling the feeder system. Basinfloor topography played a crucial role in influencing the temporal and spatial sandstone distribution pattern resulting in locally enhanced deposition, (western-) lateral restricted development and the apparent eastern deflection of the E-Fan, while basin-margin and source-area tectonism controlled the timing and activity of the source-area supply. During its final stage (early Serravallian), the E-Fan probably developed as a channel-levee complex (type III system).

The marked retrogressional signature of the E-Fan is produced by a combination of gradually rising sea level, probably subsiding source-area tectonism and denudation of the hinterland. Episodic tectonic activity resulted in influx of coarse sediment into the basin, while higher frequency sea level fluctuations resulted in occasional progradation of the deep-water system. Clastic deposition is eventually shut off and thick basinal shales blanket the Cingöz Formation.

3 CHARACTERISATION OF SUBSURFACE LOBE DEPOSITS: S10 INTERVAL, SCAPA SANDSTONE MEMBER, SCAPA FIELD, BLOCK 14/19 NORTH SEA, UK

3.1 Geological background

3.1.1 Location

The Scapa Field is located in UK Block 14/19 in the Scapa-Highlander subbasin ("Scapa syncline") of the Witch Ground Graben (WGG), Outer Moray Firth, 112 miles (~ 175 km) north east of Aberdeen in a water depth of 385 feet (120 m). The field was discovered in 1975 by appraisal well 14/19-15 (McGann *et al.* 1991) and consists of the Main Scapa Field and the West Scapa Field, divided by the West Scapa Fault (fig. 3.1).

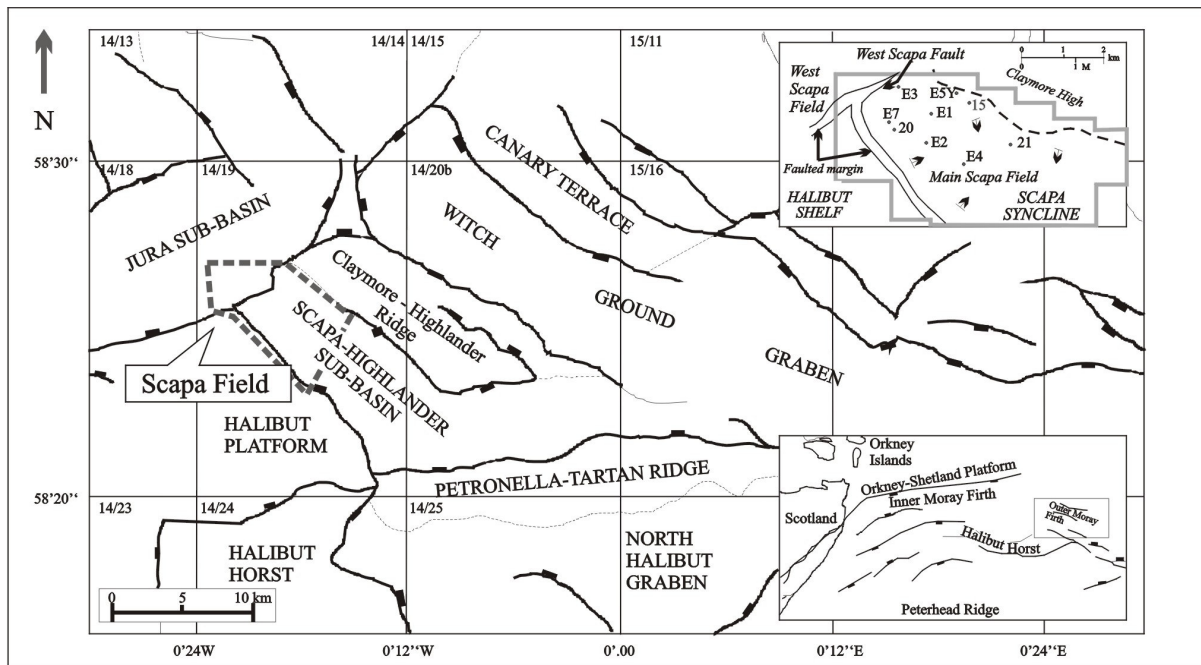


Fig 3.1: General map of the Outer Moray Firth showing the main structural elements and location of the Scapa Field. Lower inset: regional setting of the Outer Moray Firth (from McCants & Burley 1996), upper inset: elements of the Scapa Field and position of study wells.

Approximately 400 m of Early Cretaceous deep-marine sediments accumulated in the 8 x 4 km large, NW-SE trending Scapa syncline, which is located between the Halibut Shelf and Horst to the south and Claymore High to the north (fig. 3.1; Riley *et al.* 1992; Oakman & Partington 1998). The reservoir-forming sands and conglomerates of the Scapa Sandstone Member are a maximum of 586 feet (179 m) thick (Harker *et al.* 1987), forming the only other significant Early Cretaceous deep-marine play in the Central North Sea besides the Britannia field (Oakman & Partington 1998).

3.1.2 Tectono-sedimentary evolution and stratigraphy of the Scapa Syncline

In the Middle Jurassic the “Mid-Cimmerian Phase” introduced significant palaeogeographical changes in the North Sea area. The Central Graben and Viking Graben developed into major rift systems in the Late Jurassic following thermal collapse of the Jurassic Central North Sea volcanic province (Ziegler 1981). The NW-SE trending Witch Ground Graben (WGG) was initiated in the latest Jurassic forming a complex structure of submarine basins separated by intragaben highs (O’Driscoll *et al.* 1990). This process has often been related to tilt-block rotation during a long period of extension (Boote & Gustav 1987), or, more recently, to the regional transpression regime active from the Late Jurassic onwards, resulting in the syn-transpressional Scapa syncline (Oakman & Partington 1998).

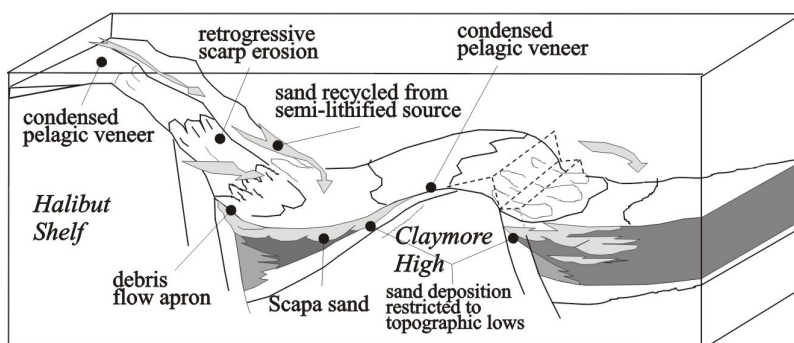


Fig 3.2: Reconstruction of the depositional environment in the Scapa-Subbasin during the Neocomian (Boote & Gustav 1987).

The rapid subsidence in late Kimmeridgian - early Volgian times produced a deep basin with graben collapse in late Volgian times (Late Cimmerian tectonism). During this period, the entire graben and surrounding platform were blanketed by Volgian - early Ryazanian black shales (**Kimmeridge Clay Formation**; Boote & Gustav 1987). A major phase of regional subsidence in

the Ryazanian introduced oxygenated conditions leading to the deposition of calcareous shales and coccolithic marls as lowest part of the transgressive **Valhall Formation** (Harker *et al.* 1987). Renewed Cimmerian tectonic activity resulted in emergence of the Halibut Horst, Claymore High and Tartan Ridge (O’Driscoll *et al.* 1990; Oakman & Partington 1998). During the late Ryazanian - late Valanginian large volumes of conglomeratic facies were deposited in the regions adjacent to the Halibut Shelf (fig. 3.2). Much of the material is interpreted to be Carboniferous, sourced directly from the fault scarp (Boote & Gustav 1987). Waning tectonism and gradual eustatic sea-level rise (Haq *et al.* 1987a,b) resulted in reduced conglomeratic input and the accumulation of sand-grade material on the Halibut Shelf. This material was subsequently redeposited as sand-rich turbidites across the Scapa syncline (O’Driscoll *et al.* 1990), forming the **Scapa Sandstone Member** of the Valhall Formation (early Valanginian – late Hauterivian) (figs. 3.2, 3.3; Harker *et al.* 1987). In the early Barremian, clastic sedimentation was cut off as sea level rose, ending sand deposition in the Scapa syncline (Harker *et al.* 1987; Riley *et al.* 1992). Marls and limestones of the Upper Valhall Formation blanketed the area, succeeded by Aptian-Albian shales and marls (**Sola and Rodby Formations**) and thick Late Cretaceous pelagic marls, limestones and biogenic carbonates (**Chalk Group**, fig. 3.3; Harker *et al.* 1987). Tertiary structural inversion was restricted to the Inner Moray Firth while a thick shallowing-up sequence of submarine fan to shallow marine/paralic sands was deposited over the Outer Moray Firth as gradual down-warping continued through the Tertiary and Quaternary. Little tectonic activity has occurred since (Hendry 1994).

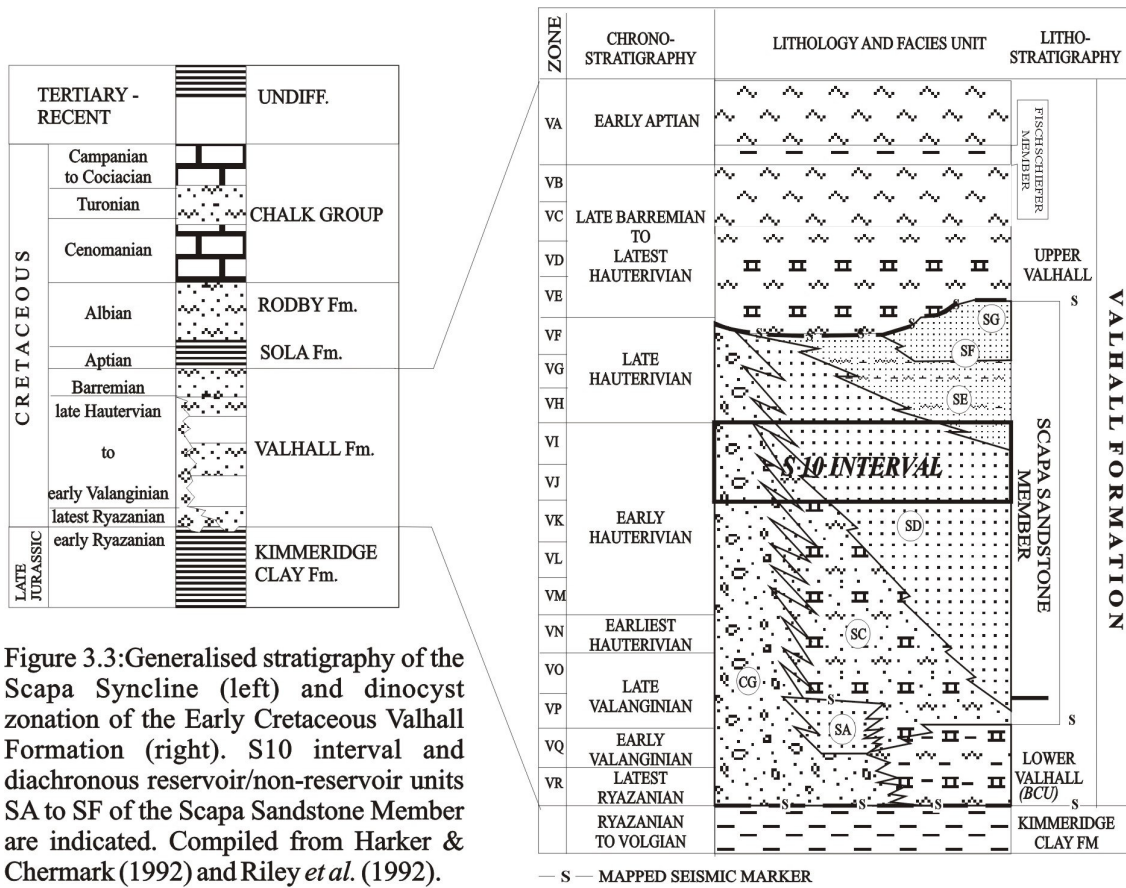


Figure 3.3: Generalised stratigraphy of the Scapa Syncline (left) and dinocyst zonation of the Early Cretaceous Valhall Formation (right). S10 interval and diachronous reservoir/non-reservoir units SA to SF of the Scapa Sandstone Member are indicated. Compiled from Harker & Chermak (1992) and Riley *et al.* (1992).

The current SE-plunging synclinal geometry of the Scapa Field is due to differential compaction resulting from increased loading during the Late Cretaceous and Tertiary when the Early Cretaceous conglomerates close to the Halibut Platform compacted to a lesser degree than the laterally equivalent marls and sands (McGann *et al.* 1991). Generally, very little faulting is present, except for the major faults that mark the southern limit of the field (fig. 3.4, McGann *et al.* 1991).

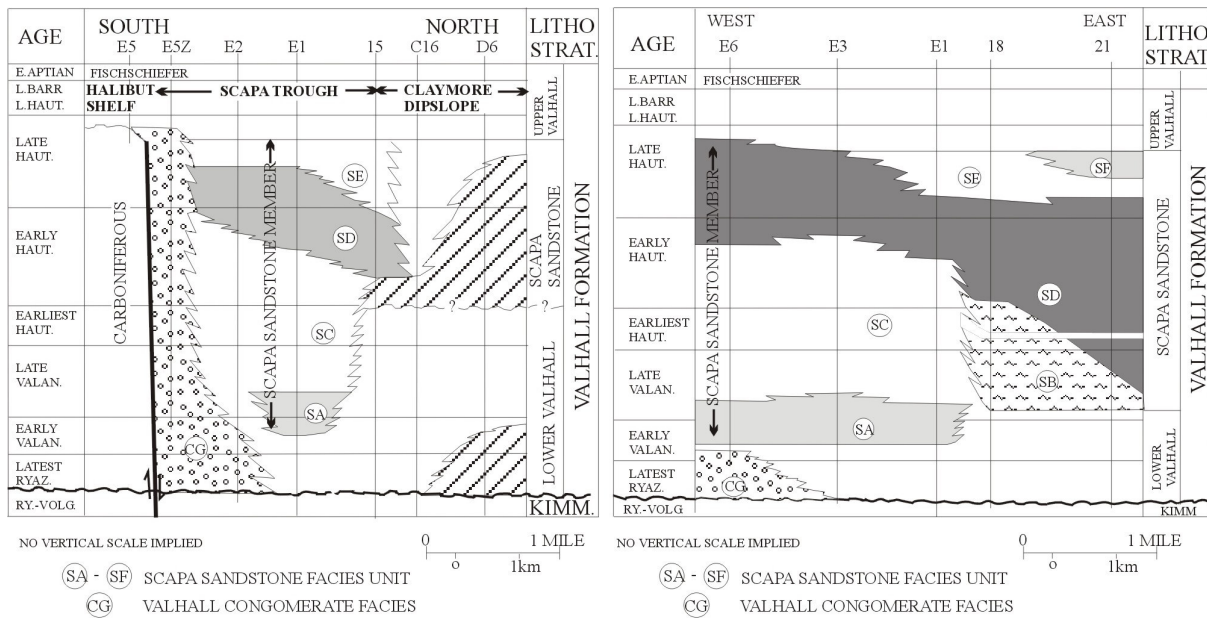


Figure 3.4: Schematic Scapa Field dip and strike stratigraphic sections showing complex relationships of reservoir and non-reservoir unit facies (from Riley *et al.* 1992).

3.1.3 The Scapa Sandstone Member

The Scapa Sandstone Member (SSM) forms part of the transgressive Valhall Formation (Harker *et al.* 1987). The Valhall Formation has a maximum stratigraphic extent from latest Ryazanian - Early Aptian which Riley *et al.* (1992) subdivided into 18 palynological zones principally based on dinocyst distribution, relative abundance and palynomorph associations (fig. 3.3). The SSM is dated Early Valangian (134 myr) to intra-late Hauterivian (126 myr; fig. 3.3; zones VG to VR in descending order). During this period, a maximum of 586 feet (179 m) of turbiditic sandstones, conglomerates and marls were deposited in a marine setting with water depth in the order of 500 ft (152 m) before rising sea level effectively ended clastic deposition (O’Driscoll *et al.* 1990; Riley *et al.* 1992).

Marked lateral and vertical lithological variations are present within the SSM. Laterally, a distinct bimodal distribution of facies can be observed with a conglomerate fringe (CG) close to the faulted margin of the Halibut Shelf while turbiditic sandstones, marls and limestone are deposited in the Scapa syncline (fig. 3.4). Vertically, the SSM is traditionally divided into several units: SA to SF. The thinly bedded, fine to medium-grained turbidite sands of units SA, SD, and SF form the reservoir units, while units SB, SC and SE are dominantly composed of tight sandstones, marls and muddy sandstones (fig. 3.4; McGann *et al.* 1991). These units are largely diachronous and their distribution is spatially and temporally restricted (Riley *et al.* 1992). Environmental and developmental reconstructions of the Scapa turbidite system are based on these diachronous units (e.g. Harker *et al.* 1991; McAfee 1993; Hendry 1994), however, Riley *et al.* (1992) present the dinocyst-based chronostratigraphic evolutionary model for the first time (fig. 3.5).

Initially, sand deposition (SA) only took place in the NW of the field (fig. 3.5a) while lower Valhall marls and limestones were deposited in the Scapa syncline (zone VP / late Valangian). Tightly cemented sandstones and limestones (unit SB) were deposited in the east (fig. 3.4) while unit SC marls, limestones and conglomerates cap unit SA in the northwest of Scapa (late Valangian - early Hauterivian). Unit SC is time-equivalent to units SA, SD and SE (fig. 3.4). In the Early Hauterivian (zone VM to VL) deposition of unit SD began in the southeast of the field (fig. 3.5b) and commenced during the early - late Hauterivian (zones VI/VJ) by which time the SD sand deposition covered most of the Scapa syncline (fig. 3.5c). Deposition during the SD took place as series of offset stacked, detached sand lobes and basinfloor fans (McAfee 1993). During the later Hauterivian, SD sand deposition continued in the northwest. Marls and tight sandstones of unit SE capped SD deposition in the central area (zone VG-VH) while a separate sandy fan system (SF) developed in the southeast (fig. 3.5d; zone VG). Throughout the deposition of the SSM, conglomerates were shed off and deposited along the faulted shelf margin. Clastic supply was cut off by

Late Hauterivian (dated as intra-zone VG) as the sea-level rose (Riley *et al.* 1992). Marls and limestones of the upper Valhall then blanketed the entire area (Harker *et al.* 1991).

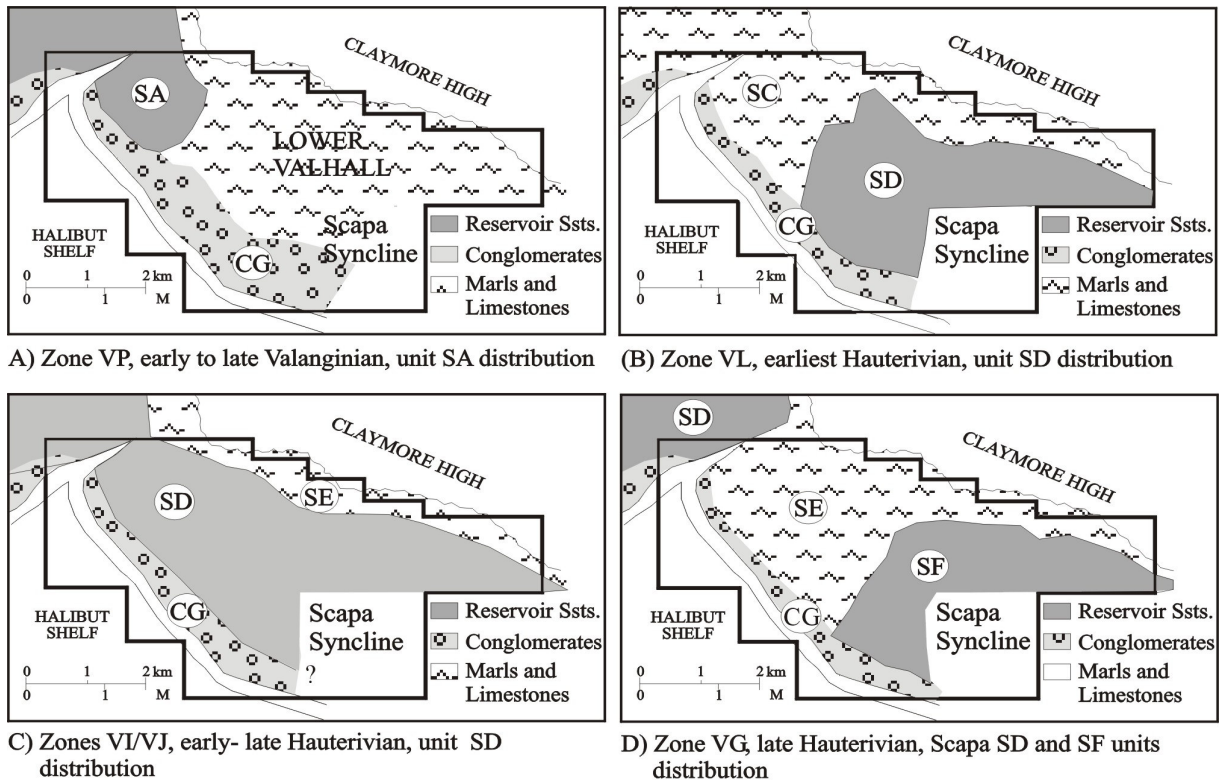


Fig 3.5: Distribution of reservoir / non-reservoir units of the Scapa Sandstone Member in the Main Scapa Field (from Riley *et al.* 1992).

The Scapa turbidite system is mineralogically relatively immature (Green 1990). The sandstone composition broadly ranges from fossiliferous quartz arenites to subarkoses and sublithoarkoses (Hendry 1994). Fossiliferous components include penecontemporaneous Valhall, Jurassic and older Late Palaeozoic taxa. Carboniferous reworking is particularly prominent in the conglomerate facies fringing the Halibut Shelf (e.g. Boote & Gustav 1987; Harker & Chermak 1992; Riley *et al.* 1992), while Late Jurassic and/or Neocomian reworking predominated in more distal locations (Riley *et al.* 1992). The abundance of stenohaline, bioclastic material throughout suggests that sands were reworked from a nearby shallow marine high-energy, high-productivity environment believed to be the Halibut Shelf (Hendry 1994). Occasional polymict shale-matrix conglomerate within unit SD are interpreted to reflect sporadic tectonism where material is derived directly from the fault scarp (Hendry 1994). Background sedimentation includes hemipelagic shales and marls and tuffs, the latter preserved as green shales (Harker & Chermak 1992; Hendry 1994).

Sediments entered the basin through persistent, preferred feeder zones along the Halibut Shelf, probably along structural lineaments (McAfee 1993). The focus of the sand deposition is known to have moved (fig. 3.5) (Riley *et al.* 1992), which is explained by antecedent lobe topography having influenced the path of successive flows. The SSM was deposited during a time of general eustatic sea level rise (Haq *et al.* 1987a,b; Harker *et al.* 1991) and the uplift history of the shelf may have influenced its facies distributions and thereby the nature of material reworked into the basin. Sand-poor non-reservoir intervals probably reflect temporary deepening of the clastic source area (shelf) and increased hemipelagite deposition (Hendry 1994). The narrow width of the Scapa syncline probably favoured axial deflection of the turbiditic flows by the steep ramp formed on the SE-flank of the Claymore High in the north (Oakman & Partington 1998).

The apparent lack of internal organisation suggests deposition analogue to a slope apron (McAfee 1993) or a submarine ramp environment (Hendry 1994) where the deposition of sediments is believed to take place in broad, shallow sandy channels and subordinate lobes (Boote & Gustav 1987; McAfee 1993).

3.2 The S10 Interval

Elf Occidental Caledonia Ltd reorganised the SSM into chronostratigraphic intervals ranging from S1 (lowerst) to S13 (uppermost) based on Riley's *et al.* (1992) dinocyst stratigraphy. The S10 interval comprises the late Early Hauterivian palynological zones VI and VJ (fig. 3.3, 3.6). It contains most of the oil-bearing unit SD as well as parts of the non-reservoir unit SE and the conglomeratic CG facies. Abundant lithological analysis, sedimentological and petrophysical data exist for unit SD (e.g. Harker & Chermak 1992; McAfee 1993; Hendry 1994), however, no detailed environmental and developmental analysis for the chronostratigraphic S10 interval and its (sub-) zones has been undertaken.

Chronostratigraphic interval	Dinocyst zone	Zone top datum	Dinocyst subzone	Subzone top datum
S 10	upper	VI		
	lower	VJ	VJ1	[not further described]
			VJ2	downsection increase <i>Athigmatocysta glabra</i>
			VJ3	localised downsection incr. <i>Oligosphaeridium sp.</i>

Figure 3.6: Dinocyst zones comprised in the S10 interval of the Scapa Sandstone Member (from Riley *et al.* 1992).

3.2.1 S10 framework

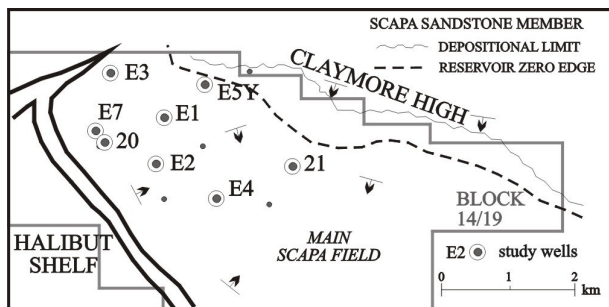


Figure 3.7: Location of study wells within the Scapa Main Field (after McGann *et al.* 1991).

The aim of this study is to characterise the non-channelized sandy turbidite facies (lobe deposits) and the controls governing their accumulation in the light of the spatial and temporal development of the S10 interval.

Previous studies focused on the diachronous SD unit and its subunits, thus a working S10 framework had to be established. Lithofacies analysis integrated with petrophysical data of 8 wells with proven S10 interval presence form the basic framework (fig. 3.7; table 3.1), supported by data compiled from published and unpublished reports. The study included:

- core logging of 785 feet TST (238 m) of S10 interval and undifferentiated SD/SC/SE which are presumed to be part of the S10 interval (enclosure 1)
- establishment of a refined lithofacies scheme to grasp subtle lithological variations (*chapter 3.2.1*)
- integration of petrophysical data for lithofacies reconstruction of uncored S10 interval (*chapter 3.2.1*)
- interwell correlation (*chapter 3.2.2*)
- definition of fan depositional environments *sensu* Mutti & Normark (1987, 1991) (*chapter 3.3*)
- analysis of spatial and temporal development of sandstone bodies and assemblages, establishing depositional model and controls of S10 interval and its (sub-) zones (*chapter 3.4*)

	14/19-20	14/19-21	14/19-E1	14/19-E2	14/19-E3	14/19-E4	14/19-E5Y	14/19-E7
S10 - total	176	47.5	193	nd (193-176?)	113	131	236	nd (176-113?)
VI	37	absent	32.5	nd (32.5-37?)	55	67	absent	nd (>37-<55?)
VJ - total	139	47.5	160.5	nd (160.5-139?)	58	64	236	nd (139-58 (100?))
VJ1	absent	4.5	49	nd (49 - > 0)	nd	nd	178	nd (absent?)
VJ2	48.4	25	40.4	nd (40.4-48.4?)	nd	nd	34	nd (<48.4)
VJ3	90.6	18	71	nd (71-92?)	nd	nd	24	nd(<92)

All thicknesses in feet TST.

Table 3.1: Thicknesses of S10 zones and subzones in study wells. Note that not always sharp boundaries exist between zones, presumably due to sampling range and quality. In these cases the maximal extend was often chosen as „true“ zone thickness and/or if bases/tops correspond to marked changes in wireline response. nd = non-differentiated, () = estimates based on neighbouring wells.

Lithofacies analysis

A lithofacies scheme to accommodate subtle facies variations was introduced. It is based on the grain size of the dominant components resulting in six lithofacies groups: **Gravel**, **Gravel-Sand**, **Sand**, **Sand-Mud**, **Shale** and **Biogenic** facies (fig. 3.8; plates 7 - 8). Further subdivisions are based on sedimentary structures and dominant clast lithologies leading to a total of 20 lithofacies types. Measured helium porosity and air permeability values are given for the different lithofacies types where available (data from McAfee 1993). The cored S10 interval is dominated by deposits of the S (58.7 %) and GS facies (25.5 %) (fig. 3.9). Less common are sediments of the G (8.6 %) and SM facies (5.6 %), while marls (BI facies: 1.2%) and SH deposits (0.2 %) are rare. Wells E1, E2, E5Y and E7 (west-central-north position) are characterised by gravel facies and an above average amount of sand facies (fig. 3.9; enclosure 1), while wells 20, 21, and E4 (proximal central-southern position) are dominated by S facies (20, 21; plate 8.2/3) and higher amounts of SM facies (E4, 21; plate 8.4-6). GS and G facies deposits (20, 21; plate 7) are rare.

Electrofacies analysis

a) Lithofacies reconstruction

The integration of petrophysical data became necessary to broadly interpret lithologies and changes in lithology of the uncored S10 interval. In a first step, the differentiated lithofacies group and types were calibrated against the wireline logs resulting in broadly recognisable petrophysical signatures for the various groups (table 3.2). Generally, shales appear to be the most easily recognisable lithology, characterised by high gamma-ray values and a clear negative separation of the density and neutron log. Shale-clast rich G

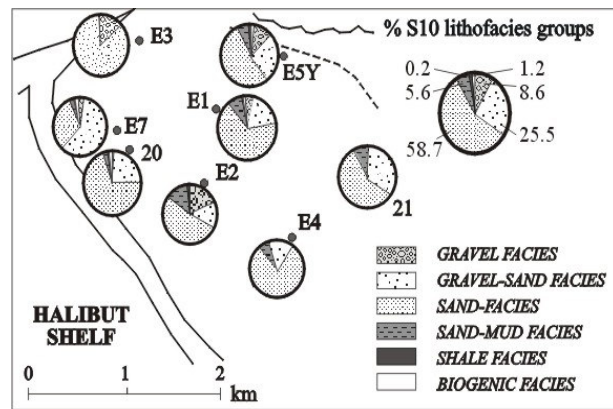


Figure 3.9: S10 Lithofacies group distribution in Main Scapa Area

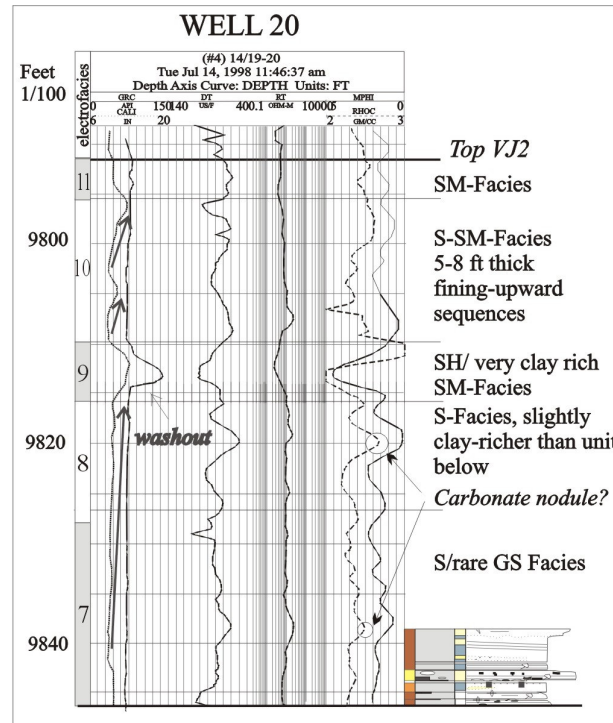


Figure 3.10: Example of lithofacies reconstruction by wireline analysis. See enclosure 1 for further lithofacies reconstruction and legend.

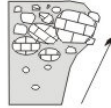
GRAVEL -Facies: gravel > 75%, sand < 25%

G1



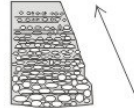
S10: 2.9%, debrite, disorganised, cs sand matrix, limestone, shale & sandstone clasts (max > 16 cm), some chaotic, slurred texture, ave. 124 cm, poro: 9.96 %, perm: 0.75 mD.

G2



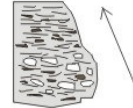
S10: 1.3%, debrite?, structureless, c-up to clast-supported conglomerate, clasts: limestone, rare shale (max. 13 cm), ave. 72 cm.

G3



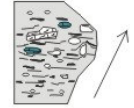
S10: 4.2%?, R1 - S1, graded stratified, well sorted, pebbly limestone clasts (max 4 cm) to cs sand, upward increase in sand matrix, little clay matrix, rare shale clasts, thickness: 33-226 cm, colour: green-grey; poro: 12.3 %, perm: 91.8mD.

G4



S10: 1.5%, R2-S1-2, graded-faintly stratified, high amount of brown-grey shale clasts (max. 15 cm), high vcs sand matrix, ave. 100 cm, colour: brown-black.

G5



S10: 1.5%, inverse grading, faintly stratified, floating clasts (max. 8 cm): marls (~BI), limestone, green shales, cs-ms sand matrix, some slurred texture, poorly-mod. Sorted, mod. Calcite cemented, ave. 48 cm, colour: grey-green.

G6



S10: 1.5%?, as G5, but dark grey argillaceous-sand matrix, some sandstone clasts, max clasts size (16 cm) soft sediment deformation (internal loading), poorly sorted, range: 45-250 cm, poro: 2.6 %, perm: 0.08 mD.

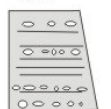
GRAVEL - SAND Facies: gravel < 25%, sand > 75%

GS1



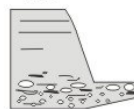
S10: 2.4%, similar to G3 but sand-rich (vcs/cs), S2-3, rare Tb-e divisions, distinct f-up, well sorted, max. clast size (4 cm), patchy cementation in dom. pebbly-rich areas, ave. 75 cm, poro: 13.43 %, perm: 61.98mD.

GS2



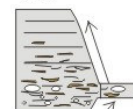
S10: 3.2%, Graded-stratified, bimodal: cs sand & limestone pebbles (max. 11 cm), traction structures, subtle f-up, brown, oil/water-logged sand, grey, calcite cemented pebble-rich areas, ave. 70 cm, poro: 11.04 %, perm: 30.93 mD.

GS3



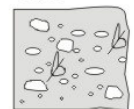
S10: 20.9%, S2-3/Tb-e, pebbly sandstone, cs-ms sand, distinct pebbly traction carpets with preferred calcite cementation, basal c-up, overall f-up, max. clast size: 6 cm, ave. 91 cm, poro: 19.65 %, perm: 185.7mD.

GS4



S10: 2.2%, as GS3 but much higher pebbly (max: 10.5 cm) shale-clast content, grey-grown, deformed clasts, poro: 10.85 %, perm: 90.62mD.

GS5



S10: 2.2%, as G1 but > 60% sand, injection features, deformed shale clasts, reworked nodules & shell fragments, vcs-ms sand matrix, slumps?, ave. 70 cm, poro: 5.9 %, perm: 25.43 mD.

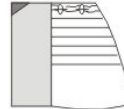
SAND-Facies: gravel < 2%, clay < 15%

S1



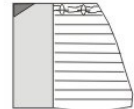
S10: 5.1%; S3/Ta, massive, dom. ms, little clay matrix, few float. shale clasts, water-escape struct. & bioturb., ave. 55 cm, max. 260 cm, PCA: brown/cream-oil/water-bearing, poro: 23.1 %, perm: 372.62 mD, WCA: grey/white-patchy calcite/nodule formation, poro: 5.1 %, perm: 2.24 mD.

S2



S10: 31.1% Ta-d; graded-stratified, dom. ms, some water escape, bioturbation (71%), slumping, ave. 72, amalgam. to 365 cm, pyrite, calcite cementation, poro: 42.8 %, perm: 183.85 mD.

S3



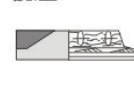
S10: 17.6% Tb-d; similar to S2 but without Ta, ave. 39 cm, poro: 19.18 %, perm: 175.97 mD.

SM1



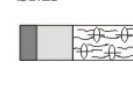
S10: 0.9% 'Muddy sandstone'; graded-stratified, vcs-ms sands; clay content (15-50%), shale clasts (65% of beds); poorly sorted; O 25 cm; com. bioturbated (56%); dom. grey, rarely green.

SM2



S10: 2.6% 'sand-mud couplet'; T(c)d,e; well sorted, ms-cs sands, calcite cementation weak, nodules rare; O 9cm; poro: 10.76 %, perm: 32.58 mD.

SM3



S10: 1.9% like SM3 but intensely bioturbated; 5 - 20 cm, poro: 2.81 mD.

SHALE Facies: clay and silt grade, sand < 5%

SH1



S10: 0.8% Td,e; black or green no bioturbation ave. 6.5 cm, poorly cemented.

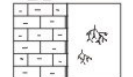
SH2



S10: 0.8%; Td,e; poorly sorted, sand lenses; intense bioturbation; 3-15 cm; dark grey, rarely green; poorly cemented.

Hemipelagic marls

BI



S10: 0.4% highly bioturbated (Chondrites/Anconichnus), subordinate silt/sand laminae (< 0.5%), rare bioclasts, 3-44 cm, greenish.

Legende

- vfs- very fine sand
- fs - fine sand
- ms - medium sand
- cs - coarse sand
- vcs - very coarse sand

shale content [diagram] sand content

WCA: well cemented area
PCA: poorly cemented area

- ⊕ ⊗ ⊛ bioturbation
- ⊂ shell fragments
- ↗ fining-upward
- ↘ coarsening-upward

Figure 3.8: Lithofacies classification scheme for the S10 interval. Poro-perm data from McAfee (1993).

and GS facies, for example, show slightly different wireline values than the remainder (table 3.2). The gamma-ray log is thus frequently used as shale content indicator (Rider 1996). Calcite in form of cement, nodules (both diagenetic) or as reworked limestone clasts and diagenetic pyrite* may strongly modify density readings (fig. 3.10; enclosure 1), the same applies to sedimentary structures, e.g. massive versus laminated sandstones (e.g. sonic log values: 60 vs 80, E2: 9130-45 ft), or oil/gas/water content (Rider 1996). The uncored intervals above and/or below the cored section appear to be dominated by shale-rich deposits of the SM and SH facies, interbedded with shale-rich S facies and sometimes clean S and rare GS facies deposits (enclosure 1). Marls (BI facies) are equally rare in the wireline record (e.g. E4, E5Y).

Lithofacies Group	Calliper CL in inch	Gamma-ray GR in API	Sonic log ΔL in $\nu s/ft$	Resistivity log RT in Ohm	Density log DL in g/cm^3	Neutron log NL in NPHI	Reference in ft log depth
G	norm	25 – 35 ave 30 shale clast-rich G5/G6: - 45	60 - 70	20 – 200 peaks 500 ave 120 shale clasts (G5) or matrix (G6) lower values	2.4 – 2.65 depending on degree of cementation / nodule form. / limestone clasts	0.05 – 0.15	e.g. E5Y: 9420 E5Y: 9450 E2: 9112-25
GS	norm	20 - 35, ave 30 shale clast-rich GS4: - 50	55 – 80	80 – 300 ave 100 peaks 500	2.5 – 2.6 pebbly limestones of GS3: 2.75	0.05 – 0.15 peaks 0.2	e.g. 21: 10604 E3: 10631 – 40 (pyrite) E5Y: 9428 – 44
S	norm	30 – 45 ave 35 high shale matrix: 45 - 60	65 – 90 ave varies for diff. Trend lines	70 – 200 peaks 400 ave 120	2.2 – 2.5 depending on degree of cementation / clasts / diagen. pyrite	0.15 – 0.25 erratic trends	e.g. E1: 9070 – 5 (pyrite) E2: 9087 (pyr.) E4: 9692 E4: 9658 - 80 E5Y: 9310 - 35
SM	norm / caving / wash-out	60 - 80	60 – 80	20 – 40 peaks: 100	2.3 – 2.55 depending on degree of cementation	0.1 – 0.2 occasional negative NL/DI separation: 0.45 peak	e.g. E1: 9208 - 13 E2 : 9070 - 80 E4: 9688
SH*	caving / Wash-out	up to 135	60 (low transit times)	60	2.5	0.1 occasional negative NL/DI separation: 0.4 peak	e.g. 20 : 9765 E2: 9148 E7: 9773
BI*	norm / little caving	30 - 65	70 - 80	20 – 40 peaks: 90 - 100	2.4-2.65	0.1 – 0.15	e.g. E5Y: 9496 E7: 9893

Table 3.2: Wireline readings of lithofacies groups (norm = normal, ave = average, max = maximum). Note that some values, i.e. sonic and neutron log values are usually higher for sands and coarser sediments and lower for shale-rich sediments, marls typically show a slight negative DL/NL separation (Rider 1996). The respective thicknesses of lithofacies groups BI, SH and often SM are mostly below resolution thickness (0.6 m) thus given values are approximations.

*density: pyrite = 4.8-5.17 g/cm^3 , carbonate = 2.66-2.74 g/cm^3 , organic matter = 1.2 g/cm^3 (Rider 1996)

b) Electrosequence analysis

Electrosequence analysis^{*} *sensu* Rider (1996) is used to identify recognisable and correlatable intervals within the cored and uncored successions of the S10 interval. Trend lines (> 1 m [bed scale], 10s m [sequences] or 100s [large structures of basin filling]) record a persistent change in log value of various tool measurements while baselines (10 - >100s m = electrosequence) reflect a constant value. The latter is typically used to characterise formations.

Lithologically, the S10 interval is similar to the under- and overlying intervals. The little overall thickness and small-scale internal lithology changes necessitate a detailed analysis of the wireline records, i.e. trend line analysis *sensu* Rider (1996; fig. 3.10; enclosure 1). Appendix 2 lists the differentiated trend lines with their characteristic average log values for the S10 interval and the undifferentiated SD unit of wells E2 and E7. Trend lines are of extremely variable thickness (3 - 27 ft, e.g. E5), their bases and tops characterised by distinct breaks in wireline response of one or more tool records (e.g. well E4). The trend lines often coincide with lithological sequences or groups of sequences (*chapter 3.3*), picking up distinct as well as subtle lithology variations (e.g. E5Y: S-SH [TL 12]; 20: S/GS-S/GS-S [TL 4/5/6]). Changing log values, e.g. gamma-ray recording shaling-upward (i.e. fining-upward: bell-shaped) or shaling-downward sequences (i.e. coarsening-upward: funnel-shaped), may comprise 1 or more trend lines (e.g. shale-up: E2: srS-SM [TL 11]; E3: srS-SM-SH [TL 2]/ shale-down: E3: SH-SM-srS [TL 1], E4: SH-SM-srS [6/7]; *chapter 3.3*), while blocky patterns record alternating sand-dominated/shale-dominated intervals (e.g. well 20: sand-dom. TL top 3-6; shale-dom. TL 1/2/base 3 and 7-9]. The number of trend lines identified for the different wells is largely a function of the overall thickness and lithological heterogeneity.

3.2.2 Interwell correlation

1. Biostratigraphy: the S10 interval comprises 2 dinocyst zones and subzones (VJ1-3/VI) and is present in all 8 study wells. However, subzone resolution and total extend are not known for all the study wells (table 3.1; enclosure 1).
2. Lithology-based correlations were only possible between wells E2 and E7 where the unique G6/G3 sequence occurs in both wells (plate 7; enclosure 1). A decrease in thickness (G6/G3) and grain size (G3) from wells E2 to E7 implies a more proximal position for E2 with respect to this facies association.

For well E2, the top of the S10 interval is located between 9040-9019 ft log depth, while no biostratigraphic subdivisions at all exist for well E7. Neighbouring wells E1 (0.7 km to N) and 20 (0.8 km to W; fig. 3.7) possess 193 and 176 ft TST respectively. Thus the S10 interval of well E2 may range between 176 - 193 ft TST (table 3.1). Depending on the actual thickness and top taken, the lowest S10 base may be at 9233 ft log depth and highest base at 9186 ft log depth [9040 ft log depth + 193 /176 ft = 9233 /9216 ft log depth and 9019 ft log depth + 193/176 ft = 9203/9186 ft log depth]. These estimates place the total cored section of well E2 within the S10 interval (enclosure 1) which corresponds to Riley *et al.* (1992) diagrammatic representation which approximately correlates the base of VJ with the base of unit SD, while the top is located within unit SE.

The unique lithofacies assemblage G6/G3 in well E2 is believed to be contained within zone VJ, based on i) stratigraphic considerations (proximity to the base of the sequence) and ii) great overall VJ thicknesses in the wells E1 and 20. Well E7 contains the same distinctive lithofacies assemblage and it is therefore suggested, that the top of the cored well E7 represents zone VJ (enclosure 1). The total S10 thickness in well E7 may range between 176 and 113 ft as recorded in the adjacent wells 20 (0.25 km to SSE) and well E3 (~ 0.85 km to NNE; fig. 3.7). The proximity to well 20 suggests that presence and thicknesses of subzones might be fairly similar (table 3.1). Base and top of the S10 interval in well E7 are difficult to define, however a good part (>50 ft ?) of the uncored SE non-reservoir unit are believed to belong to the S10 interval.

* "Electrosequence: an interval defined on wireline logs, through which there are consistent or consistently changing log responses and characteristics, sufficiently distinctive to separate it from other electrosequences." (Rider 1996).

3.3 Fan environments

3.3.1 Distributary channels

Bifurcation of a system's main feeder(s) result in a network of distributary channels funnelling sediment into the basin. They are known from modern and ancient deep-water clastic system (e.g. Navy Fan: Normark *et al.* 1979; Crati Fan (Ricci Lucchi *et al.* 1985; Mississippi Fan: Schwab *et al.* 1996; Agadir turbidite system: Ericella *et al.* 1998; Paola Basin systems (Trincardi *et al.* 1995); Cingöz Formation: *chapter 2*). The S10 distributary channel-fill deposits form discrete 1 – 6 m thick, gravel-rich successions with erosional bases, often sharp tops and display either abrupt (CH 1) or gradual (CH 2) fining-upward (fig. 3.11). These channels were probably between 80 – 500 m wide, based on average width/depth ratios for mid- and lower fan channels compiled from modern and ancient submarine fan systems (Clark & Pickering 1996), however, much smaller distributary channels (~20 m width) were recorded in the proximal lobe zone of the Cingöz Formation, E-Turkey (*chapter 2.4.2*).

a) Channel-fill 1 (braided*?)

1 to 3 m thick G/GS – SM/SH associations characterise CH 1 fills (e.g. E2: G6-G3-SH; plate 7.1) which form 4.3 % of the S10. The 0.4 - 2.0 m thick G/GS abruptly fine to 0.1 – 0.3 m thick SM/SH facies (blocky grain size curve), typically involving 2 - 4 beds (fig. 3.11). Internally, sharp contacts prevail, loading is occasionally present (e.g. E2: G3 onto G6 at 9116 ft). The upward increase in shale content is reflected by increasing GR and decreasing DL / RT values and partial borehole enlargement (E5Y: 9455 - 9448 ft).

The abrupt change in lithofacies from coarse gravel deposits resulting from highly energetic processes (gravely / gravel-sandy debris flows / sandy high-density turbidites) to very fine grained, mud-rich deposits indicating a tranquil depositional environment (low density turbidites; Tc-e) suggests a sudden deactivation of the channel as a conduit. The thick debrites and succeeding gravely-sandy high density flows probably plugged the channel forcing it to avulse (Pickering *et al.* 1995; Clark & Pickering 1996). The residual topography was then infilled by silts and muds. Anderton (1995) relates rapid changes in channel location to highly unstable areas within a fan system. The observed random facies arrangement (coarse facies) is characteristic of braided channel of broad sheet-like geometries (Wüllner & James 1989), this can, however, not be confirmed for the CH 1 deposits.

The unique G6/G3 association of wells E2 and E7 shows a marked decrease in grain size (E2: 16 to E7: 6) and dramatic thinning over ~ 1 km distance (E2: 2.50 m to E7: 0.45 m). The absence of this unique facies association in well 20 (~ 0.25 km SE of E7) underlines the linear, confined nature of these deposits most likely of channel geometry (fig. 3.11). A fault-scarp source is suggested for the polymict G6 facies, triggered by sporadic tectonism (Hendry 1994).

CH 1 elements are rare, forming shallow, isolated features in the central wells E5Y/E1 and proximal wells E2/E7 (fig. 3.12).

b) Channel-fill 2 (meandering?)

CH 2 infill sequences typically involve > 4 beds of 0.1 to > 2 m thick G/GS gradually fining-upward into finer-grained, 0.1 – 0.4 m thick S/SM facies (e.g. 21: (G)-GS-S-SM [10586 - 10569 ft]; fig. 3.11). The fining-upward is accompanied by a steady decrease of the sand/shale ratio, DL and RT values, while GR and NL gradual increase. However, occasionally a shaling-down accompanies the fining-upward trend (e.g. E1: 9210-9216 ft: GS4-S2) where a shale clast-rich basal GS facies fines upward into clean sandstones. The rip-up clasts and texture of GS4 may result from short transport distances following channel margin collapse (Clark & Pickering 1996; Johansson & Stow 1995).

Generally, the more gradual and orderly fining-upward of facies involving a greater number of beds indicates longer-lived conduits which are gradually migrating across the fan surface (e.g. Einsele *et al.* 1994; Pickering *et al.* 1995; Clark & Pickering 1996) which is typical of meandering channels (Anderton 1995). Their pod-like nature resulting in considerably varying sandbody thickness down the axis of the fairway

* Typically terminology derived from fluvial systems is applied to submarine fan channels such as braided, meandering, sinuous and straight (e.g. Hein & Walker 1982, Wüllner & James 1989), Clark & Pickering (1996), however, strongly doubt the unequivocal application of planform geometries to ancient outcrops.

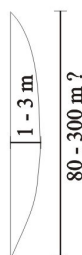
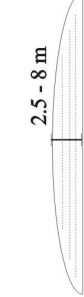
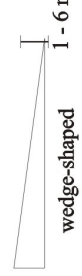


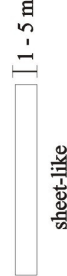


ENVIRONMENTS	SEDIMENTARY FACIES	WIRELINE RESPONSE	FACIES	ASSOCIATIONS/STACKING	GEOMETRY
CHANNEL-FILL CH I conglomerate-rich / abrupt fining-up 4.3 %	G/GS sharply topped by SM/SH facies erosive base, crude fining, 2 - 4 beds, med - thick bedded	upward + GR, occ. blocky, RT & NL decrease, DL variable	SH/SM G-Facies debris flows	lobes, CH II, OB isolated	 1 - 3 m 80 - 300 m ?
	CH II sand-rich / gradual fining-up 9 %	G/GS facies fining-upward to S/SM/SH-facies, upward increasing shale content, erosive bases, transitional and/or sharp top, Med. - thick-bedded, > 4 beds	upward increasing GR & NL, decreasing RT, DL variable	SM-S-Facies G-GS Facies	lobe, CH I, OB isolated, stacked with CH I
LOBE non-channelised sandy deposits 47 %	ms - cs S1-3, subordinate GS/SM, some GS dominated, sand/shale ratio: 9:1, med. - thick-bedded, small fining-ups forming crude large coarsening- and/or fining-ups little bioturbation	GR: 20-30, SL (60-70), low RT (20-100), variable DL & NL	S-rare GS-Facies S-rare SM-Facies	CH I/II (erosive contact), lobe fringe, rare interlobe (mostly transitional contacts) isolated, some stacking	 2.5 - 8 m sheet-like / lobate
LOBE FRINGE non-channelised deposits 28 %	fine S2-3 and SM, rare GS facies, sand/shale: 4:1, distally increasing shale content, med. - thin-bedded, dm-scale fining-up forming larger, crude coarsening- and/or fining-ups, highly bioturbated	mostly upward decreasing GR: 30-50 API, low RT, variable DL & NL	S-Facies S-SM-Facies	lobe, OB (proximal), fan fringe/basin plain (distal) isolated or stacked (distal)	 wedge-shaped 1 - 6 m
OVERBANK/ INTERLOBE non-channelised deposits 3.5 %	thin-bedded, shale-rich SH and SM facies, low sand/shale ratio (<1:1) differentiation based on environmental association	GR: -70 API, borehole enlargement, DL/NL negative separation	SH/SM Calliper Gamma-ray	A) lobe (transitional contacts), CH B) lobe, lobe fringe (both transitional contacts) A/B isolated	 A) 0.5 - 1.5 m wedge-shaped  B) 0.5 - 1.5 m shallow infill-geometry
FAN FRINGE / BASIN PLAIN shale-dominated deposits 9 %	thin-bedded SH and very shale-rich SM facies higher shale content than OB/interlobe deposits part of larger coarsening-up units hemipelagic intercalations = basin plain	GR: 70-135 API, borehole enlargement, DL/NL negative separation	SH/SM	shale-rich distal lobe fringe (transitional), some hemipelagites (sharp) isolated	 sheet-like 1 - 5 m
HEMPELAGITES 1.2 %	strongly bioturbated marls, rare 1-3 mm silt - fine sand laminae, sharp bases and tops. associations: a) SM3-Bi-SM3 (distal/prox.); b) S2-BI-S3 (prox.)	GR: -70 API, DL/NL slight negative separation	A) B)	a) basin plain deposits (distally) b) lobe, interlobe deposits (proximally)	 A) 0.05 - 0.45 m sheet-like  B) sheet-like ?

Figure 3.11: Sedimentological description and geometries of S10 fan environments, Main Scapa Field.

(Timbrell 1993). Meandering may also be forced by lobe topography, occasionally resulting in abrupt changes in direction (e.g. Navy Fan: Normark *et al.* 1979; Timbrell 1993). The CH 2 deposits (9% of S10) form mostly isolated features interbedded with lobe and rare OB deposits (fig. 3.12). Channel stacking is rare (e.g. E5Y: CH2/CH2; E1: CH2/CH1/CH2).

Boote & Gustav (1987) identified a variety of different channel types making up the bulk of the SSM. For the S10 interval two types were differentiated but if channel CH1 and CH2 sequences really represent different channels types, i.e. braided and meandering, is speculative. For one, well control is not tight enough to establish the true nature of the channels, but also the flow conditions leading to meandering or branching submarine turbidite channels are poorly known at present (Mutti & Normark 1987; Shanmugam 2000). A rapid vertical alternation in depositional style between the two “end-members” meandering and braided, however, is probably unlikely (e.g. E1 CH2/CH1/CH2). The observed sudden plugging of channels or channel segments by debris flow and other deposits, i.e. CH 1 infill, forcing channel avulsion may occur in both meandering or braided channel types (Clark & Pickering 1996). Rescoursing and/or reestablishment of channels in other locations by renewed turbidity current activity after channel plugging is likely (e.g. Frigg Field: Helland *et al.* 2002).

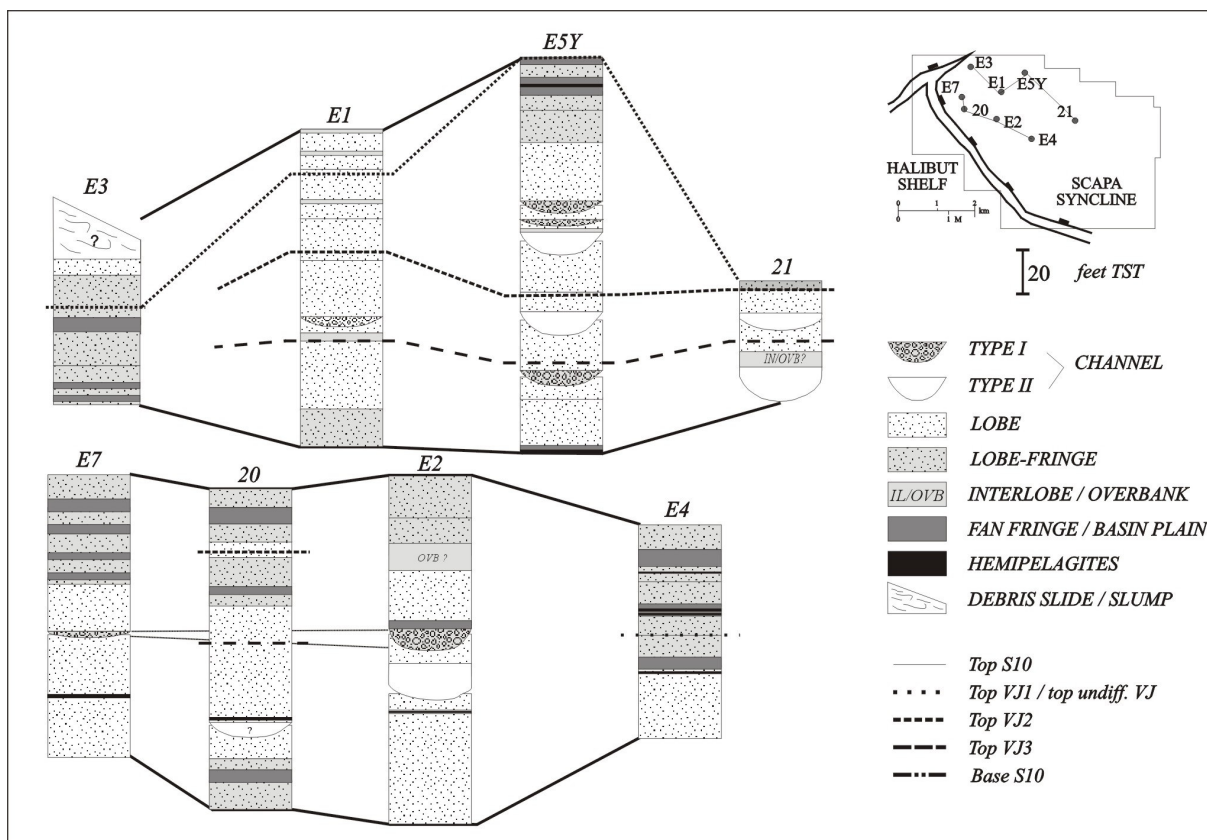


Figure 3.12: Spatial and temporal distribution of fan environments within the S10 interval, Main Scapa Field..

The distributary channels are associated with non-channelized sandy deposits and occasionally channel-related (overbank) deposits which would suggest a channel-lobe transition or proximal lobe environment (*sensu* Mutti & Normark 1987; 1991). However, channel-fill deposits are identified in proximal as well as distal positions (e.g. 21, E5Y; fig. 3.12) and at one stage near shelf-parallel fairways developed (E2-E7). Their distribution in time and space (fig. 3.12) paired with an apparent lack of a clear proximal-distal trend, suggests a complex network of pathways feeding the S10 system driven by upstream switching of feeder activity and fault-controlled sea-floor topography capturing flows thus allowing preferential pathways to bypass proximal depositional locations funneling sediment further into the basin (McAfee 1993; see *chapter 3.4*). Discrete channeling with occasional overbank formation may form but channeling also may well be less distinct developing along existing topographic lows.

The thick debrites encountered in well E3, containing shell fragments and reworked carbonate nodules and turbiditic sandstones probably represents reworked, semi-lithified Scapa deposits originating from along the West Scapa Fault (Hendry 1994). They probably represent localised buldges of debrite posing obstacles on which shelf-scoured S10 turbidites probably deflected and/or onlaped and/or ponded (Kneller 1995).

3.3.2 Non-channelized sand-dominated deposits

The bulk of the S10 interval is made up of sandy, non-channelized deposits (74 %). They are dominantly composed of S and minor GS and SM facies. Based on differing sand/shale ratio, bed thickness pattern, dominant grain size and dominant lithofacies type and association, the deposits can be classed as lobe and lobe fringe deposits (*sensu* Mutti & Normark 1987, 1991; fig. 3.11).

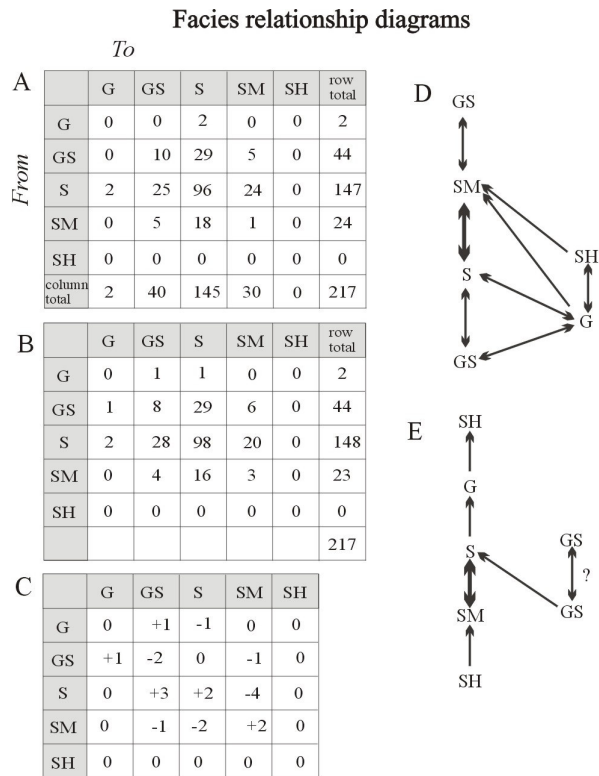


Figure 3.13: Facies relationship diagram for S10 lobe deposits: A) observed data array of bed transitions. Lithology recorded at the top of columns overlies those recorded in the rows. B) predicted data array assuming a random arrangement of lithologies. Calculated by cross-multiplying the rows and column totals of the data array and dividing by 217 (the total sample). C) differences between the observed number of transitions a) and the predicted number, assuming a random arrangement b). D) facies relationship diagram showing the most common upward and downward transitions for each lithology. E) facies relationship diagram showing the largest number of up- and downward transitions that occur for each lithology after subtracting those predicted if the beds were randomly arranged.

a) Lobe deposits

The lobe deposits (47 % of S10) are characterised by average sand/shale ratios of 9.5:1. Individual lobe packages are 2.5 - 21 m thick, composed of 0.40 - 0.80 m thick beds (fig. 3.11; enclosure 1), occasionally containing up to 4 m thick, commonly amalgamated megabeds akin to DWMS (deep water massive sands) of Stow & Johansson (2000) (e.g. E5Y: 9313-9326 ft). Erosion is rare (8 %, e.g. E1: 9171 ft) which is believed to result from solemarks and/or small localised scouring. The lobes are composed of dominantly S1-3 (> 60%) and varying amounts of GS1-4 facies, interbedded with rare thin-bedded SM2/SM3 turbidites. Occasionally, they are dominated by up to 75 % GS facies (e.g. E5Y: 9456 – 9423 ft [TL 2/3]; E7: 9931 - 9894 ft [TL 1/2]). The most common facies associations* are S – S (44 %), GS – S (13.4 %), S – GS (11.5 %), S – SM (11 %) (fig. 3.13). The mostly normally graded beds (78 %) usually contain little overall clay content (~ 5 vol.%), which is typically concentrated at the top of beds ($T_{d,e}$ of Bouma 1962). Here, bioturbation is particularly common (38 %, Zoophycus, Teichichnus, Planolites: enclosure 1). Syndimentary dewatering structures (11 %). And some soft-sediment deformation indicating loading or slumping are occasionally present.

Internally, the lobes are composed of 0.6 – 2.4 m thick, 2 - 4 bed thinning-/fining or thickening-/coarsening upward sequences, (fig. 3.11; 3.14) arranged to form crude 4 – 11 m thick asymmetric coarsening- and thickening-upward (42 %; e.g. E1: S – S/GS at 9255 – 9218 ft [TL 2]; E5Y: fs – ms S

* Facies associations are groups of facies that occur together and are considered to be genetically or environmentally related (Reading 1996). Common pitfalls in facies transition diagram analysis include stressing more common sequences, while the statistically insignificant, but geologically important ones are subordinated, i.e. misinterpretation of erosional or non-erosional contacts which provide important clues for the environmental interpretation (Reading 1986) and oversimplification by using lithofacies groups (n=6) rather than types (n=20) disregarding the true complexity of the system.

at 9336 – 9305 [TL 8/9]) or thinning- fining-upward sequences (28 %; e.g. well 21: 10537 - 10523 ft [TL 4]). The remainder are randomly arranged. The high amount of 2-bed sequences is believed to result from variations in flow volume, competence, thickness and/or topographic compensation (e.g. Mutti & Sonnino 1981; Kneller 1995; Chen & Hiscott 1999a) while the larger thickening- and coarsening upward sequences are believed to be generated by lobe progradation (e.g. Mutti & Ricci Lucchi 1972; Ricci Lucchi 1975b; Shanmugam & Muiola 1991; Mutti & Normark 1987, 1991). The observed random or thinning-fining upward patterns, however, may result from lobe aggradation (e.g. Ricci Lucchi & Valmori 1980; Hiscott 1981), retrogradation (*chapter 2.4.*) or interacting flows from different sources which may superimpose and overprint each other leaving no clear pattern (Heller & Dickinson 1985).

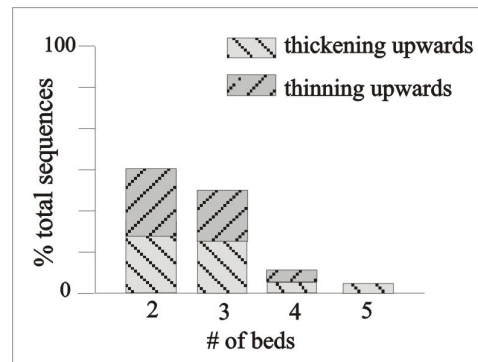


Figure 3.14: Asymmetric bed thickness pattern of S10 lobe deposits determined with 2-bed average smoothing method.

In wireline logs, the sandy lobe deposits are generally characterised by low GR values, often showing an upward decrease or increase in API values reflecting changing sand/shale ratio which are commonly interpreted to record coarsening-upward sequences or fining upward sequences respectively (Rider 1996), or they show no particular trend (e.g. top E1). Density readings are very much dependent on the state of cementation and pyrite formation. Clean, oil-logged sands show low readings (2.2 – 2.3 g/cm³), while pyrite formation, for example, increases to 2.75 g/cm³ (e.g. well E2: 9131 ft).

Like the lobe deposits described in the E-Fan of the Cingöz Formation (*chapter 2.4*), the Scapa lobes do not fit the classical depositional lobe model *sensu* Mutti & Normark (1987) where lobes form isolated bodies within mudstones or finer-grained, thinner-bedded turbidite deposits. The analysis of the Scapa lobes and the distribution of the fan components (fig. 3.12) indicates that classical proximal-distal trends as encountered in other fan systems, involving grain size and bed thickness decrease while internal organisation and shale content increase (e.g. Macigno Formation: Ghibaudo 1980; Kongsfjord Formation: Pickering 1981; Eocene Hecho Group: Mutti & Normark 1987; Rocchetta Formation: Cazzola *et al.* 1981; *chapter 2.4*) are absent in the S10 interval. On the contrary, a complex interdigitation of lithofacies and fan components exists resulting in a rather distinct central *versus* lateral depositional and varied vertical trends. The crudely defined S10 lobes form mostly isolated, occasionally stacked features (e.g. top E1) associated with channel, OB, lobe fringe or occasionally fan fringe deposits (fig. 3.12). While the shallow channels erosively cut into lobe deposits, other contacts are either gradational (lobe fringe) or sharp (OB; enclosure 1). Their association with shallow distributary channel-fill/OB deposits indicates a relatively proximal lobe depositional environment (e.g. *chapter 2.4.2*), the S10 component distribution, however, defies this simplified interpretation. Mutti & Normark (1987, 1991) believe these type of lobes to generally be of sheet-like geometry but of smaller areal extent. These “proximal” lobes are especially prominent in the central wells (E2, E1, E5Y) and to a lesser extent in the western proximal wells (20, E7; fig. 3.15). Well 21 to the distal east is an exception (fig. 3.12). Otherwise, lobes become increasingly associated with finer-grained lobe fringe / fan fringe deposits (E3, E4, top E5Y) suggesting more distal/marginal positions within the system (Pickering 1981; *chapter 2.4.3*). Analysis of grain size and bed thickness trends, indicates generally

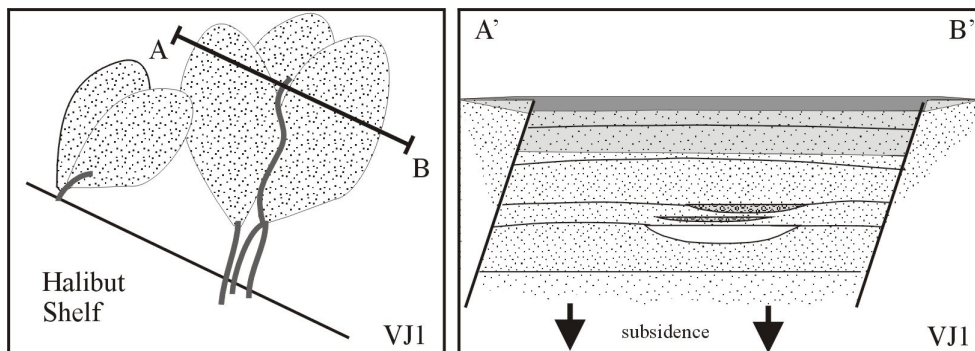


Figure 3.15: Schematic diagram showing depositional thickening in fault- and/or differential subsidence-induced intrabasinal depressions during VJ1.

coarser-grained and thicker-bedded in the E1, E5Y and E7 lobes. The contrast is especially striking in the closely spaced wells E7 (ms-vcs / mostly GS facies) and 20 (ms-cs / S facies), pointing

to potentially different source areas. Lobes in E5Y are generally coarser, but less coarse than in well E1 and may represent downcurrent equivalents of these. Correlation between wells is difficult, however, based on the fan environmental representation in space and time (fig. 3.12), none of the lobes appear to be basin-wide features but are rather of areally confined, probably elongate geometry (fig. 3.15; see *chapter 3.4.1*).

Vertically, all wells with exception of E1 and E3 display shaling-upward (fining-upward) from sandy lobe deposits to lobe fringe, interlobe and/or fan fringe/basin plain (fig. 3.12; enclosure). The basal E1, E3 and 20 are dominated by varying amounts of lobe fringe, interlobe and/or fan fringe/basin plain. Process sequence analysis (after Cronin 1994) which records flow at the time of deposition by using grain size and sedimentary structures as indicators of transport and depositional processes, confirm this trend for the cored S10 interval, almost always indicating the transition to less energetic, more tranquil depositional environments (appendix 3). This may be related to reduction in grain size in the feeder system or an increase in distance from the input point perhaps due to rising sea level (see *chapter 3.4*). Bed thickness trends as identified by RAM technique (Murray *et al.* 1996; *chapter 1.4*) partially reflect this trend. The lower part of E5Y (VJ3/VJ2) are dominated by thick units of thicker-bedded intervals, the top (VJ1) by thick units of thinner-bedded intervals, while well E1 shows a contrary trend. Wells E2 and E7, however, show less distinct organisation (appendix 4). Bed thickness is a function of flow volume rather than transport and depositional processes.

The internal organisation of the lobes is fairly crude (see *above*), it does not appear to improve towards more distal/marginal areas, although this is generally expected (e.g. Cingöz Formation: *chapter 2*; Eocene Hecho Group: Mutti & Normark 1987; Rocchetta Formation: Cazzola *et al.* 1981).

Lobe progradation, switching and overall aggradation may result in vertical stacking, representing stable depositional environments (Pickering 1981), probably in a confined space. Isolated lobes within areas of normally fan fringe sedimentation suggests episodic lobe migration into this particular area indicative of unstable depositional processes, possibly reflecting source control (Pickering 1981) or lobe switching (*chapter 2.4.3*). Seismic data indicates lobe thinning towards the shelfal area, thickening in a basinal direction, which McAfee (1993) as detached lobes *sensu* Mutti & Ricci Lucchi (1975). The development and geometries of the S10 lobe deposits appear to be governed by a combination of autocyclic control and allocyclic controls (see *chapter 3.4 for further discussion*).

b) Lobe fringe deposits

The lobe fringe deposits (28 %) form 1 - 6 m thick units of lower average sand:shale ratio (4:1; fig. 3.11). Their occurrence in core is rare, where they are characterised by fine-grained sandstones (S2/S3) and shale-rich SM (e.g. E1: S2-S3-SM2-SM3 at 9172-9177 ft; table 3.4) which are abundantly bioturbated (60 %). The thin-bedded (0.05 - 0.3 m) deposits, corresponding to intervals of below median thickness (appendix 4), are arranged in crude 2 - 6 ft fining-upward sequences composed of 2 - 4 beds.

Most of the lobe fringe deposits were identified from wireline record, where they are characterised by mostly higher API/GR readings than lobe deposits. They often form part of distinct shaling-upward or downward sequence in association with lobe and/or fan fringe deposits (shale-down/coarsening-up: lobe fringe to lobe: E1: 9278-9216 [TL 1/2]; interlobe-lobe fringe-lobe: 20: 9930-9905 [TL 3]; shaling-up/fining-up: lobe-lobe fringe-fan fringe: 20: 9790-9767 [TL 9]; E 7: 9853-9820 [TL 4-6]; enclosure 1). The contacts with lobe and fan fringe deposits are gradational in both proximal and distal locations (e.g. 20, E5Y). The lobe fringe deposits form isolated features in proximal (e.g. 20, E2, E4) and in distal / lateral position (e.g. zone VJ1: E3, E5Y) where they become increasingly more abundant (fig. 3.12).

Lobe fringes *sensu* Mutti (1977) represent the distal equivalents of coarse-grained and thick-bedded sandstone lobe deposits in both down-current and cross-current directions, representing a lateral / distal depositional environment (e.g. *chapter 2.4.3*). The deposits are of wedge-like, "fringing" geometry (fig. 3.11).

3.3.3 Shale-dominated deposits

Distinctly shale-dominated deposits (11.5 % of S10) occur in association with channel, lobe and lobe fringe deposits. They are typically composed of thin-bedded, fine-grained SM to SH facies (plate 8.5), with S facies occasionally interbedded (fig. 3.11). Preservation in core is rare (e.g. E2: SM-SM-S3-SM: 9082 ft) where they are characterised by high GR (70 API), low RT and distinct negative DL/NL separation. In the

uncored S10, shale-dominated deposits are fairly common, the higher GR values (80-135 API) suggest a higher shale content, i.e. mostly SH facies and/or very shale-rich SM facies, than observed in core.

The overall thickness ranges from 0.5 - 3 m in proximal (e.g. 20, E2, E4) to up to 5 m in distal locations (E3, E5Y). Their bases and tops are bound by sand-dominated units (fig. 3.12). They typically form the base of larger-scale 'shaling-down' (GR-) trend lines (ie. general coarsening-upward; e.g. E3: SH-SM - srS at 10745 - 10718 ft [TL 1], E4: SH-SM-srS at 9602 - 9587 ft [TL 6]; E5Y: SH/SM - srS at 9285-9272 ft [TL 11]) or the top of 'shaling-upward' (GR-) trend lines (ie. general fining-upward; e.g. 20: SM-SH at 9780 - 9763 ft [TL 9/10]; E2: srS-SM at 9077 - 9064 ft [TL 11]; E3: srS- SM-SH at 10718- 10690 ft [TL: 2]). Sharp bases and/or tops are rare (e.g. E5Y: S-SH at 9285 ft).

The association with channel, lobe and lobe fringe facies in relatively proximal fan locations (fig. 3.12) suggests their possible origin as overbank and/or interlobe deposits *sensu* Mutti (1977), with distal lobe fringe and hemipelagites a fan fringe and/or basin plain origin *sensu* Mutti (1977) and Mutti & Normark (1987) (fig. 3.11).

a) Overbank / Interlobe deposits

The fine-grained, thin-bedded, current-laminated sands and silts and graded mudstones of overbank (OB) deposits *sensu* Mutti (1977) and Mutti & Normark (1987, 1991) are found in association with channels where they form by lateral spreading of a mainly confined turbidity current (Mutti & Normark 1987, 1991). In the S10 interval, channel-lobe?-OB associations are present (e.g. well 21 at 10563 ft; E2 at 9130 ft). They form thin, irregularly bedded, maximal 0.5 - 2.1 m thick shale-dominated intercalations (fig. 3.11). The thick, distinctly bimodal SM1 facies (E2: 9070-9077 ft; 60% shale matrix, granule - pebble-sized grains, traction structures; plate 8.4) topped by SH is unique in its lithology, the high matrix content probably resulting from reworking and incorporation of shale-rich sediments into the flow. OB deposits generally possess a wedge-like geometry, thinning away from the channel (fig. 3.11; Mutti & Normark 1987; Clark & Pickering 1996).

The 0.6 - 3 m thick interlobe deposits separate thick-bedded, coarse-grained sandstone lobe and lobe fringe deposits (fig. 3.12). The contacts are transitional as part of shaling upward sequences (fining-upward?; e.g. well 20 at 9810 ft) indicating gradual lobe migration into or out of a particular area or abrupt, suggesting a sudden shift in depositional focus (e.g. E1 at 9125 ft; fig. 3.12). Interlobe deposits possess a lenticular geometry resulting from infilling of topography between lobe bulges (fig. 3.11; *chapter 2.4.3*).

The OB and interlobe deposits form approximately 3.5 % of the total S10 interval.

b) Fan fringe / basin plain deposits

In distal fan locations, up to 5 m thick, shale-dominated deposits are interbedded with distal lobe fringe sediments (fig. 3.12; e.g. E3, E4, E5Y). They are mostly identified by wireline response (fig. 3.11), where they appear to form part of shaling-upward and/or downward trends, from fan fringe to lobe fringe and *vice versa*, suggesting gradual migration of sand deposition to and/or out of these particular areas (e.g. E3: TL 1/2). Occasionally, sharp facies changes indicate a rapid shift in sand depositional locus (e.g. E5Y: 9285 ft). Fan fringe deposits are typically thin to very thin-bedded, very fine sandstone turbidites forming regularly bedded packets of sheet-like geometry (fig. 3.11; Mutti 1977; Pickering 1981), however, the fan fringe deposits of the S10 interval are very shale-rich. Occasionally, marls are interbedded with the fan fringe packages suggesting a basin plain origin (Mutti 1977; e.g. E5Y (TL1)).

The fan fringe / basin plain deposits form approximately 9 % of the S10 interval.

3.3.4 Hemipelagic marls

Hemipelagic marls (1.5 % of S10) form highly bioturbated beds of 5 - 45 cm TST with sharp bases and tops (fig. 3.11). Occasionally, they comprise mm-thick silt and very fine sand laminae. Marls are rare in the cored and uncored sections of the S10 interval (e.g. cored: wells 21, E2, E5Y; uncored: E4). They are commonly interbedded with SM / SH facies (e.g. E2: SM3-BI-SH at 9163 ft [plate 8.6]; E5Y: BI-SM3 at 9495 ft) or occasionally S facies (E7: S2-BI-S3 at 9893 ft).

The marl beds bear a striking resemblance to the marly clasts contained in the debrites and gravely high-density turbidite deposits (well 21 at 10585 ft), believed to derive from erosional unroofing at the fault scarp and/or shelfal environment (Hendry 1994; McAfee 1993). The marl beds in association SM/SH facies (e.g.

E2, E5Y) formed *in situ* while clastic sedimentation was temporarily suspended, pointing to an overall high carbonate background sedimentation (Harker & Chermak 1992). In distal locations, the marls are associated with basin plain / fan fringe deposits (e.g. E5Y, E4; fig. 3.12) while in relative proximal positions, the marls are associated with overbank / interlobe deposits and occasional lobe fringe deposits (e.g. E2, E7). In the latter locations, rapid shift in the depositional focus in the respective fan area probably resulted in a spatially confined temporary suspension in clastic sedimentation, resulting in a lensing depositional geometry. The distal marls mark the distal depositional limit of the S10 system at that particular point in time. They form laterally more extensive, sheet-like deposits (fig. 3.11).

3.4 Lobe Accumulation

The size and appearance of lobe deposits is a function of the size of the system, the basin size and its configuration and the volume of individual turbidity currents, grain size and many other factors. Lobe deposits can therefore have very different dimensions and shapes (Mutti & Normark 1987, 1991) which may change through time with changing controlling parameters. Scapa lobe accumulation needs to be viewed within the context of the overall development of the S10 system, which can be described in 4 separate stages: zones VJ (subzones VJ3-1) and VI (fig. 3.16).

3.4.1 Temporal and spatial development of the S10 Interval

VJ3 subzone

Deposition took place throughout the Main Scapa Field. The greatest depositional thickness was reached in central-western well 20 (92 ft TST), gradually declining towards the central-north (E5Y) and east (21) (fig. 3.16a). The depositional limit is delineated to the south by the conglomeratic wedge fringing the Halibut Shelf and the Claymore High to the north (Riley *et al.* 1992). To the west deposition takes place in the West Scapa Field occur, while the eastern depositional extend is unknown.

Channelized deposition in the east (21) started during the S9 interval (McAfee 1993) continues into VJ3. This eastern part of the field is probably fed by a source located further to the south (feeder area 1*). The central field area is underlain by shale-rich lobe fringe and/or fan fringe/basin plain deposits (S9 interval) which are now sharply overlain by sand and gravel-dominated lobe and channel-fill deposits (e.g. E1, proposed VJ3 zone of E2; E4; E5Y). Shifting depositional focus by lateral, westward? lobe migration (20, E1?) and/or fan progradation towards the basin (E5Y, E1?) in conjunction with (re-)activation of a southern source area feeding sediment into the central field (feeder area 2) are probably responsible for the high depositional thickness in the central axis (20-E2-E1-E5Y). Laterally, lobe deposits thin and fine (SE: E4) to lobe fringe and fan fringe/basin plain sedimentation (NW: E3). The proximal western area (E7) is dominated by coarse lobe deposition, probably sourced by a westerly lying source (feeder area 3?).

VJ2 subzone

Depositional trends established during VJ3 continues during subzone VJ2 (fig. 3.16b), however, sediment accumulation is much more uniform, ranging between 48.4 ft TST in the west (20) to 25 ft TST in the east (21). Lobe and channel-fill deposition dominate the central axis (20-E2?-E1-E5Y) and the east (21). Locally shifting depositional locus results in lobe migration (e.g. well 20: lobe/lobe fringe/interlobe). The SE (E4) is gradually dominated by shale-rich lobe fringe sedimentation which may be associated with either feeder area 1 or 2. In the NW (E3) fan fringe/basin plain deposition continues to dominate.

Deposition in the W (E7) is probably still dominated by lobe deposition. Shelf-parallel development of a distributary system suggests westward shifting sediment locus. Laterally coalescing deposition from different scoures (feeder area 2/3) is likely in the western syncline.

* the term “feeder area” instead of “feeder” is used to indicate that possibly a multitude of smaller feeders located in close proximity rather than a single, larger feeder conveyed material into the syncline.

VJ1 subzone

Marked areally restricted deposition in connection with extreme thickness variations characterise subzone VJ1 (fig. 3.15c). 178 ft TST of sediments accumulated in the central-north of the field (E5Y) rapidly declining towards the centre (E1: 49 ft) and east (21: 4.5 ft). VJ1 deposits are absent in proximal areas (20) and undifferentiated in the remaining wells.

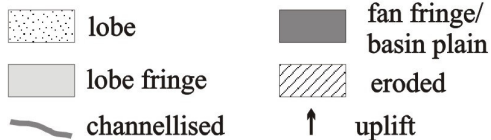
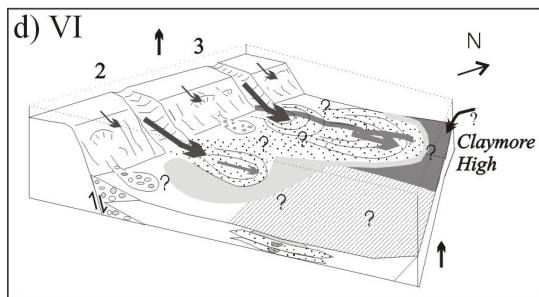
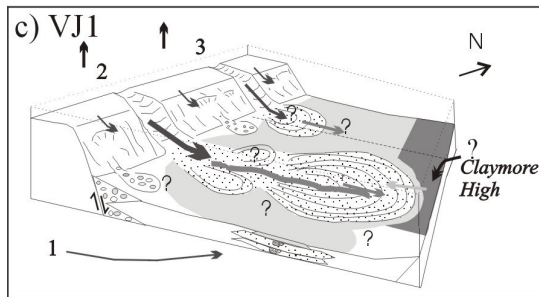
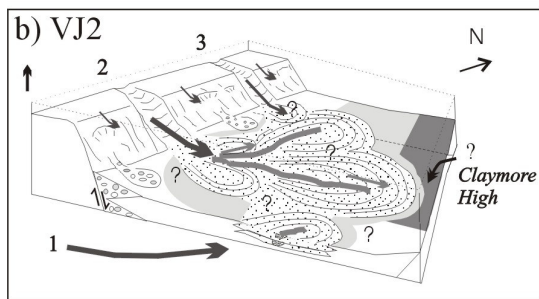
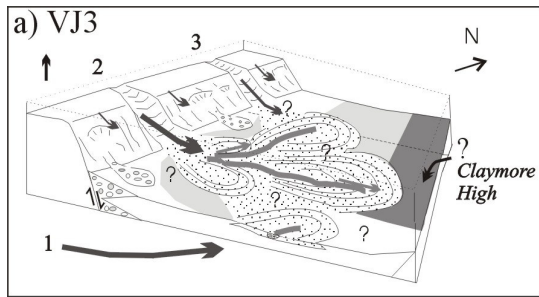


Figure 3.16: The spatial and temporal reconstruction of the S10 interval reveals changing feeder activity exerting a major influence on the locus of deposition.

In the east (21) thin lobe fringe deposition marks the decreased sediment influx from feeder area 1 resulting in retreating or migrating? lobe deposition. Shale-rich lobe fringe deposition probably continued in the NW and SE (undifferentiated zone VJ wells E3/E4). The central-north (E5Y) is dominated by coarse-grained lobe and channel-fill deposition, progressively fining and thinning to lobe fringe and fan fringe / basin plain deposition, while lobe deposition continues to be prominent in the centre (E1; fig. 16c). The extreme sediment accumulation in well E5Y may result from a combination of a fault-controlled? differential subsidence creating a local intrabasinal low compounded by sediment ponding and contribution from the Claymore High (see chapter 3.4.2: controls).

The absence of VJ1 deposits in proximal well 20 cannot merely be explained by temporary suspension of clastic deposition in this area resulting from a shift in the depositional locus. Due to the high carbonate background sedimentation (Harker & Chermak 1992) at least marls should have formed. It is thus likely that SM/SH or marl deposits were subsequently eroded.

VI zone

Deposition appears even more areally restricted, essentially resulting in two sandstone depositional areas (fig. 3.16d):

- i) in the central field area, lobe deposition dominates the southeast (E4: 67 ft), thinning and shaling to lobe (E1: 32.5 ft) and lobe fringe (20: 37 ft) sedimentation in central-proximal direction. The sediments are very likely sourced from feeder area 2. The SE shift in depositional locus probably is driven by antecedent depositional topography.
- ii) lobe deposition progrades north, suggesting feeder area 3 becoming increasingly active while intraformational breccias (E3) point to periods of intrabasinal tectonic instability in the north-western syncline.

Sedimentation from feeder area 1 appears to have ceased. No VI deposits are recorded in the E (21). Equally, VJ deposits are absent in the central-north (E5Y) is conspicuous. It is believed that initial hemipelagic and/or basin plain deposition took place, but differential uplift

in the NE and E led to their erosion (see chapter 3.4.2).

McAfee (1993) suggest renewed conglomeratic progradation into the basin whereas this study interpreted a lobe depositional environment for the uncored VI of well E4.

3.4.2 Controls

3.4.2.1 Basin physiography, geometry and seafloor topography

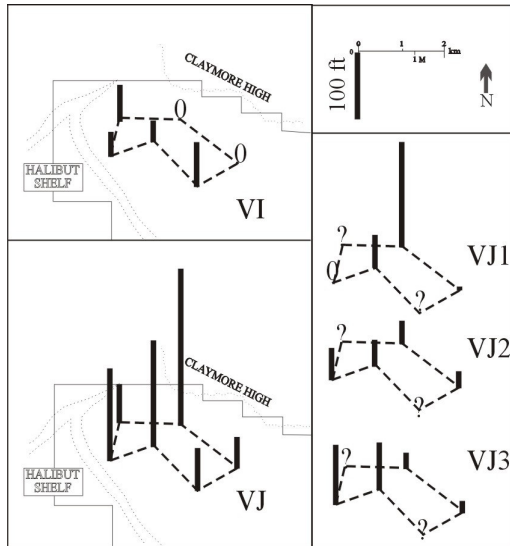


Figure 3.17: Thickness distribution of S10 zones and subzones projected into Main Scapa Field. Basin topography not considered.

al. 1991 believe differential compaction taking effect in the Hauterivian to be responsible for the synclinal geometry of the Scapa basin, where the conglomerates showed lesser compaction than the finer-grained basinal deposits. Within the basin, the underlying S9 shales were likely to form depressions probably enhanced through their syndimentary differential compaction (average compaction rates: shales 60 %, sands 20 % from Stow & Johansson 2000; e.g. Frigg Field: Heritier *et al.* 1978) while the sandy channelized / non-channelized S9 deposits formed topographic features. This “subcrop” lithology thus influences the accommodation space available for sand accumulation (e.g. Fladen Ground Spur: Freer *et al.* 1996; Rona Member/West Shetland Basin: Verstralen *et al.* 1995).

Throughout the S10, major variations in sedimentary thickness are conspicuous (fig. 3.17). Especially subzone VJ1 records extreme sediment accumulation in the central area (E2-E1-E5Y), dramatically thinning to the southeast and northwest respectively (fig. 3.17). A major NE-SW-running normal fault, the Mid Scapa Fault, is recognised to the west of the E2-E1-E5Y-line (fig. 3.18) and the existence of minor, parallel faults suggested throughout the syncline (McAfee 1993). McGann *et al.* (1991) observed fault movement along these reactivated Caledonian fault trends, however, less significant than concurrent faulting (i.e. Halibut Shelf fault), and very little throughout the Scapa Sandstone Member. However, even subtle fault-

Basin configuration, faulted and depositional topography exert a critical influence on original and preserved sandstone thickness and geometry of lobe deposits (e.g. Normark *et al.* 1993; Reading & Richards 1994; Schuppers 1995). The Scapa sediments were funnelled via multiple feeders from the southern Halibut Shelf into a small, maximal 4 x 8 km wide, fault-bounded basin (Oakman & Partington 1998). To the north and east the syncline was bound by the steep ramp of the Claymore High and the West Scapa Fault respectively while it extends further to the southeast as the Scapa-Highlander subbasin (McGann *et al.* 1991). A transfer zone to the Northern Claymore Area in the northwest allowed sediment transfer further into the basin during the Hauterivian (Harker & Chermak 1992).

The pre-S10 basin was marked by a heterogeneous system with thick sand and gravel deposits in the east (21), becoming sandier towards the central direction (E4). The north and west are underlain by thick units of shaly and marly hemipelagic deposits (E5Y, E3, 20). The debrites of the 200 – 700 m wide conglomeratic wedge shaped the physiography of slope/base-of-slope (fig. 3.7). McGann *et*

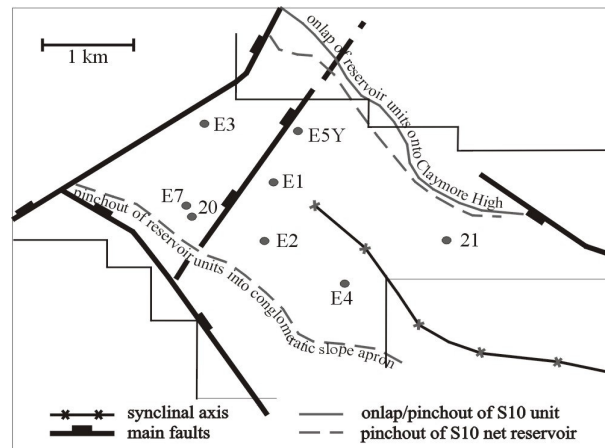


Figure 3.18: Main structural elements of the Main Scapa Field.

scarp topography and/or synsedimentary differential subsidence of fault-controlled basin sectors creating intrabasinal depressions may have forced preferred funnelling of sediments thus allowing for locally enhanced sediment accumulation, e.g. zone VJ1 of E5Y. The stacked, aggradational style of the primarily non-channelized, sheet-like sandy deposits together with the narrow, elongated depositional geometry further points to deposition in a confined setting. Similar controls on sediment accumulation are recorded in other deep-water clastic systems, for example, the Cingöz Formation/Turkey (*chapter 2*), Arktinos Sandstone/Greece (Schuppers 1995), Northern Area Claymore (Kane *et al.* 2002) and the Brae Field (Stow 1995b; *further examples: chapter 2.5.1*).

McAfee (1993) and Hendry (1994) believe sediment to have ponded against the Claymore High which acted as a barrier resulting in flow decrease leading to deposition of predominantly massive sand bodies (e.g. DWMS at top of cored E5Y; Kneller 1995; Gryphon Field: Purvis *et al.* 2002). This together with sediment input from the Claymore High (Hendry 1994) and axial deflection (McAfee 1993) may have further contributed to more localised deposition, especially close to the high.

Topography resulting from antecedent sediment deposition affected Scapa lobe accumulation at various scales:

- i) microsequences (up to 2.4 m; *chapter 3.3.2*) resulting from topographic irregularities are especially common in proximal lobe deposits (e.g. Normark *et al.* 1979; Mutti & Normark 1991; *chapter 2.4.2.1*).
- ii) macrosequences (2.5 - 21 m) at mostly asymmetric “intra” (i.e. individual lobes; E5Y, E7 enclosure 1) and “inter” lobe-scale (i.e. stacked lobes; E1, E2, E5Y) resulting from lobe migration, i.e. autocyclic lobe switching due to preceding topography and/or channel avulsion or allocyclic controls (e.g. Heritier *et al.* 1978; Pickering 1981; Normark *et al.* 1993; Bouma 2000; Garland *et al.* 1999) creating an offset-stacking pattern at lobe-scale.

Mass wasting events in shelfal areas or swamping of conduits can lead to the reconfiguration of the basin floor topography and shelfal physiography (Cronin *et al.* 1998). Intraformational debris flow deposits found in the north of the field (E3) and reported from other areas proximal to the faulted shelf margin (e.g. McAfee 1993; Hendry 1994) are very likely to have formed localised depositional buldges presenting further obstacles to flow forcing deflection (e.g. Kneller 1995) and/or plugging sediment pathways (e.g. CH I-fill; e.g. Reynolds & Gorskine 1987).

3.4.2.2 Tectonism

The Scapa-Highlander half-graben created under Late Jurassic transtensional conditions was exaggerated during the Late Cimmerian transpressional regime by inversion of older Jurassic structures above sea level (Oakman & Partington 1998) initiating clastic sedimentation in the Scapa syncline (Harker *et al.* 1987). Tectonism shaped the narrow, elongate basin geometry, basinfloor topography as well as dictating sediment pathways across the Halibut Shelf probably along tectonic lineaments (Boote & Gustav 1987; McGann *et al.* 1991; McAfee 1993; *chapter 3.4.2.1*) thus actively controlling the location of sediment accumulation within the basin (McAfee 1993). Deposition of the Scapa Sandstone Member (SSM) was affected by different stages of Late Cimmerian tectonism (K20/K30 of Jeremiah 2000; fig. 3.19) resulting in phases of high sediment input (units SA and SD) and shifting depocentres (Harker & Chermak 1992). Partial erosion of unit SA in the southeast of the field points to differential uplift within the syncline during the late Valanginian – early Hauterivian boundary (fig. 3.19), the so-called “Lower Valanginian Unconformity” (O’Driscoll *et al.* 1990) or “Late Valanginian event” (Riley *et al.* 1992).

Source-area tectonism lead to renewed and/or increased clastic deposition in the central Main Scapa Field (wells 20, E2, E2, E5Y). The observed northwestward migration of the depositional locus appears to be directly controlled by differential source area uplift driving the shift in feeder activity from the south east (feeder area 1) to northwest (feeder area 3) (fig. 3.16; *chapter 3.4.1*). Source area control expressed in shifting feeder activity is frequently encountered in deep-water clastic systems of active basins (e.g. Cingöz Formation: *chapter 2.5*; Paola Basin systems: Trincardi *et al.* 1995) which Stow (1985b: South Brae Field) illustratively termed “piano-key tectonics”. Hendry (1994) believes that source area uplift is additionally responsible for facies distribution within the SSM by controlling the nature of material reworked into the basin. This may lead to, for example, varying grain sizes in similar fan locations, such as the coarse sands of

well E7 and fine to medium-grained sands of well 20. Reoccurring seismic activity was most likely responsible for triggering frequent mass wasting events directly off the fault-scarp in the south (e.g. well E5; McAfee 1993), forming the conglomeratic slope apron and occasionally leading to intraformational debrites and slides in the northwest (well E3) and throughout the field (McAfee 1993; Hendry 1994).

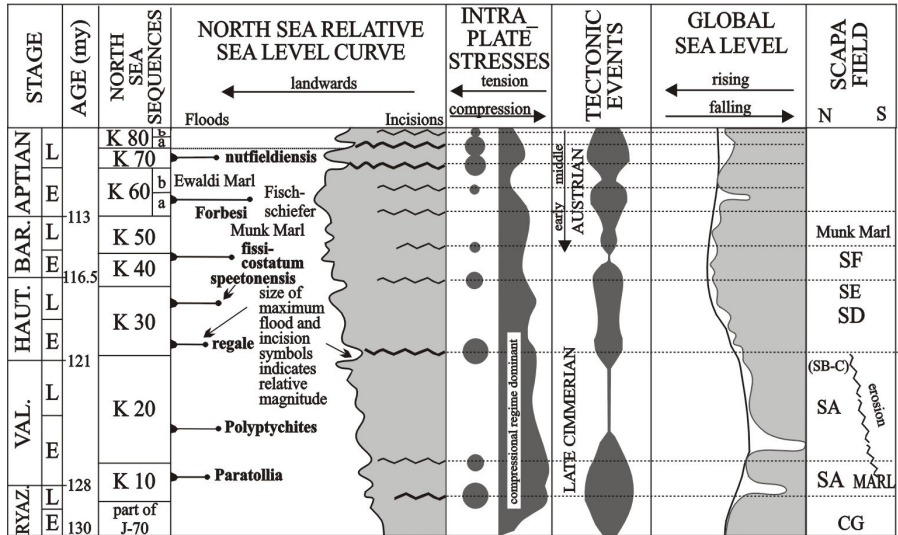


Figure 3.19: North Sea relative sea-level curve. Calibration of maximum flooding surfaces and eustatic sea-level oscillations with Late Cimmerian and Austrian tectonism that affected the North Sea Basin (modified from Jeremiah 2000). CG, SA-SF nomenclature after McGann *et al.* (1991). EE = erosional event corresponding to Lower Valangian unconformity of O’Driscoll *et al.* (1991) and Late Valangian event of Riley *et al.* (1992).

Tectonism also appears to have affected the S10 accommodation space. On the one hand, differential subsidence of closely spaced basin sectors resulted in localised enhanced thickness accumulation (*see* 3.4.2.3), on the other hand, in an environment with high carbonate background sedimentation (Harker *et al.* 1993) hemipelagic marl deposition should be expected if clastic sedimentation was temporarily suspended and thus the absence of zone VJ1 deposits in proximal well 20, zone VI deposits in wells E5Y and 21 indicate (renewed?) uplift and subsequent erosion in proximal (well 20) and particularly the northern-southern basin sector (wells E5Y, 21). If this distal uplift was in relation to movement of the Claymore High “pop-up” structure is speculative.

Although evidence suggests occasional uplift and local erosion within the Scapa syncline, basin subsidence is generally assumed for the time of deposition of the Valhall Formation. By the end of the Barremian, diminished tectonic activity combined with increased regional subsidence led to base level erosion and overstepping of the Halibut Horst ending clastic sedimentation (Boote & Gustav 1987).

3.4.2.3 Rate, type and source of sedimentary supply

The broadly slope parallel arrangement of marked bimodal facies points to different sediment sources and modes of deposition. The poorly sorted, 200 – 700 m wide apron of coarse debris fringing the Halibut Shelf results largely from mechanical slope destruction of the Halibut Shelf margin commencing in Late Ryazanian times (Boote & Gustav 1987; McAfee 1993) which in a basinward direction interfinger with SSM clastics (Riley *et al.* 1992).

The main source of the sandy SSM is believed to be the 10 – 20 km wide, shallow marine, high energy, high productivity Halibut Shelf, where predeposited Permian to Early Cretaceous sediments were eroded (Hancock 1990; Riley *et al.* 1992; Hendry 1994). Limited grain size ranges for both bioclastic and siliciclastic components imply some hydrodynamic sorting in the source area, prior to incorporation of the sands into gravity flows (Hendry 1994). Devonian Old Red Sandstone and older granitic intrusions were probably exposed on the Halibut Horst (Andrews *et al.* 1990) forming a significant, probably local terrestrial source. Additionally, dispersed vascular plant fragments, woody and coal debris are found throughout the SSM. It is uncertain, however, when the shelf was established, what the exact nature of the hinterland and sediment pathways were (Hendry 1994). Mass wasting on the fault-scarp provided additional locally-sourced sediments to the syncline (Boote & Gustav 1987) as well as minor sediment input from the Claymore High in the north (Hendry 1994). Occasionally tuffs, now preserved as green shales, were “shed” into the basin.

Off-shelf transport is typically controlled by a combination of river discharge, margin circulation and shelf sediment resuspension, the latter dominantly forced by tidal or storm wave activity and in times of river floods (e.g. Puig *et al.* 2003), while seismic activity is also known to trigger mass wasting events (e.g. Lebreiro *et al.* 1997). Hendry (1994) believes a combination of tectonism and storm wave activity to be responsible for the massive influx of poorly consolidated sands into the Scapa syncline.

The sediments were shed into an approximately 500 ft deep basin (O'Driscoll *et al.* 1990) of relatively warm waters (temperature ~14°C; Hendry 1994) while an overall seasonal climate prevailed (Hancock 1990). During the 8 myr of near continuous clastic SSM deposition (Oakman & Partington 1998), 179 m of sediments accumulated, averaging sedimentation rates of 0.02 m / 1000 years. However, the S10 interval is marked by strongly varying sediment accumulation between 15.5 - 77 m (fig. 3.17).

The analysis of the S10 deposits suggests that the bulk of the sediments was derived from gravely to sandy high-density turbiditic flows and subsequently diluted flows as indicated by the high number of fining-upwards at bed-scale. Some of the encountered massive deep-water sandstones (DWMS *sensu* Stow & Johansson 2000) may be the result of sandy debris flows. Gravely debris flow deposits are mostly confined to channel-fill sequences (CH I/CH II), while fault-scarp sourced debris flows, intraformational breccias (E3) and slumping indicate seismic activity and/or failure due to rapid sediment build-up (McAfee 1993; Hendry 1994). These may pose local obstacles to flow (Kneller 1995). The greater fossil diversity encountered in the conglomerates and pebbly sandstones points to a different and lower energy part of the source region than for the sands (Hendry 1994) indicating that grain size and composition are largely source-determined. Mud-rich sequences close to the steeply dipping faulted margin (e.g. well 20, E2) indicate sediment bypass with the bulk of the sands being deposited further into the basin (McAfee 1993). The origin of the frequently observed traction structures causes debate, McGann *et al.* (1991) believe them to result from bottom current reworking while Hendry (1994) and this study (fig. 3.8) advocate their primary depositional origin. Oxic bottom waters and localised low sediment input allowed for highly bioturbated deposits. Temporary suspension of clastic sedimentation resulted in the deposition of hemipelagic marls (e.g. well E2; E4, E5Y) and in more distal parts of the basin (McGann *et al.* 1991).

The incoming sediment was of sufficient volume to onlap and/or pond against and/or be deflected by the Claymore High. Sediment bypass in the north led to the deposition of Northern Claymore Area turbidites which are, however, sourced from a different source than SSM/S10 deposits (McAfee 1993; Hendry 1994). The full extent to the northwest has yet to be determined (McGann *et al.* 1991) while the southeastern Cretaceous turbidites of the Highlander Field may be correlatives of the SSM (Hendry 1994).

3.4.2.4 Sea level changes

The Scapa Sandstone Member was deposited under a gradually rising sea level intercepted by a mildly regressive phase in the mid-latest Hauterivian (Rawson & Riley 1982). Eventually rising sea level cut off clastic sediment supply during intra-zone VG (Late Hauterivian) drowning source areas and trapping sediment on the shelf while marls and limestones of the upper Valhall Formation blanketed the entire area (O'Driscoll *et al.* 1990; Riley *et al.* 1992). A number of North Sea deep-water clastic systems also developed during rising sea level e.g. Brae turbidite system: Stow 1985b, Balder Formation/Gryphon Field: Dixon & Pearce (1995); Purvis *et al.* (2002), Rona Member/West Shetland Basin: Verstralen *et al.* (1995); Frigg Submarine Fan: Helland *et al.* (2002). Previous workers (e.g. Harker & Chermak 1992; Hendry 1994) found the "Vailian" sequence stratigraphy not applicable to the Scapa depositional system as substantial clastic deposition within the overall carbonate system of the Valhall Formation classify "lowstand systems tract", while eustatic sea-level rise for the Neocomian is well-documented. Tectonism has been recognised as the fundamental control in driving clastic sedimentation throughout the North Sea (Harker & Chermak 1992) which led Jeremiah (2000) to establish a tectonic stratigraphy for the Outer Moray Firth (fig. 3.19). Relative sea-level changes may occur over short time frames (< 100 kyr) in response to both eustasy and tectonism (e.g. Posamentier *et al.* 1988; Normark *et al.* 1993; Bouma 2001). These higher-order fluctuations may influence the distribution of sandstones, i.e. through progradation and retrogradation, and the internal architecture of components of the deep-water clastic system, e.g. fining or coarsening-upward sequences.

Local tectonism along the Halibut Shelf was probably responsible for overriding eustatic control on deposition of the SSM. Differential source area uplift resulted in localised sea-level lowering exposing large volumes of shallow marine sediment to erosion by wave activity (McAfee 1993; Hendry 1994) leading to:

- i) the overall renewed sand progradation in central Scapa Field during the S10 interval
- ii) the observed northward shifting depositional locus
- iii) fining upward at lobe and well-scale (e.g. E5Y, E7, E2, 20, E4) indicating a deepening source area, while the distinct coarsening-upward encountered in wells E3 or continuous sandy deposition in well E1 suggest the localised overriding tectonic control on sedimentation.
- iv) repetition of fine-grained facies (fan fringe-fan fringe: top E5Y: VJ and E4, E7: VI) may simply related to autocyclic mechanisms (e.g. lobe switching) or suggest small-scale sea-level fluctuations during deposition.
- v) Localised reduced sections (missing latest early Hauterivian/zone VI: E5Y, 21) indicates intrabasinal uplift and thus localised sea level changes, exposing predeposited S10 sediments to erosion.

Thus the overall rising sea level during the SSM is punctuated by localised sea-level lowering as a direct result of source area and intrabasinal tectonics controlling sediment transfer into the syncline.

3.5 Discussion

3.5.1 Interwell correlation

Prior to Riley's *et al.* (1992) introduction of a biostratigraphic correlation scheme subdividing the SSM into a number of palynological zones (VG-VR), workers had utilised lithofacies in conjunction with wireline-based correlation between wells. This resulted in the establishment of diachronous reservoir / non-reservoir units SA-SF (O'Driscoll *et al.* 1990) leading to somewhat biased environmental reconstructions overemphasising the sandy reservoir intervals in comparison to their contemporaneous shale-rich and tight sandy non-reservoir deposits (e.g. McAfee 1993).

The correlatability of individual beds principally depends upon the volume of sediment supplied and the number of entry points to a system (Lebreiro *et al.* 1997), accordingly the S10 system (zones VJ/VI), which is characterised by marked temporally and spatially restricted sediment accumulation sourced by multiple feeders, no field-wide laterally continuous marker beds can be expected. Attempted correlation at lobe / bed packet scale between adjacent wells (e.g. E2/E1/E5Y) which appear to be sourced from the same feeder area, using, for example, presence and abundance of coal fragments and bioturbation, bed thickness patterns etc. (appendix 5) did not yield satisfactory results due to rather random patterns. Only, the biostratigraphic correlation appears to be reliable as far as its resolution, i.e. zone/subzone level and base/top boundaries, permits.

The presence of tuffs (green shales) is not extensive enough to permit tuff profiling and correlation across the S10 interval, a method which in conjunction with desanded profiles proved to support petrophysical correlation in other North Sea fields, e.g. Balder Formation (Hatton *et al.* 1992).

3.5.2 Depositional model and controls

Different depositional models have been suggested to fit the SSM such as sand-rich submarine fan (Boote & Gustav 1987), sand-rich slope apron (McAfee 1993), sand-rich submarine ramp system (Hendry 1994) and proximal basin-slope to basin-floor conglomeratic and sandy aprons (Oakman & Partington 1998). Although the S10 interval represents only a "time-slice" of the SSM, it appears to reflect controls and processes dominant throughout (e.g. Harker & Chermak 1992; Riley *et al.* 1992; McAfee 1993; Hendry 1994) and its detailed analysis may help addressing the Scapa system which proved problematic as indicated by the range of proposed models.

During the late Early Hauterivian (S10 interval), reworked terrestrial and shelfal sediments of multi-source origin were transported via persistent multiple feeders across the fault-bounded, conglomerate-lined Halibut Shelf into the shallow Scapa halfgraben ("syncline") during sea-level rise. Sediments were further funnelled into the basin by a broad, shallow distributary system leading to renewed, basin-wide sand progradation in the central graben area where the bulk of the sand-grade material was deposited in sheet-like lobe and fringe

deposits. Distinct fan geometry and morphology are poorly established and a rather complex superimposition and lateral coalescence of lithofacies and fan components exists. The sediment accumulation pattern varies considerably spatially and temporally with an overall northward shift in depositional locus mainly driven by source area tectonism. Intrabasinal depressions captured turbiditic flows resulting in a locally confined, aggradational depositional style. Further complicating the depositional pattern are minor sediment contributions off the fault-scarp and/or directly off the shelf and/or the Claymore High complexly interfingering with the main turbidite system while the Claymore High represents a barrier on which turbidites onlap, pond or are axially deflected. Localised basin uplift resulted in erosion particularly in the southeastern and distal northern basin sectors.

In absence of an overall fan-shaped geometry and morphology, Riley *et al.* (1992) suggest to regard the individual “fan lobes” developing at the mouth of the different feeders as small fans which laterally coalesce. Laterally coalescing deposits (e.g. Miller Field: Garland *et al.* 1999), lack of distinct fan morphology and geometry and a highly variable facies distribution pattern (e.g. Brae turbidite system: Stow 1985b) are commonly interpreted to be indicative of slope apron systems, in this case akin to the faulted slope apron of Stow (1985a). However, Reading & Richards (1994) argue that slope aprons are largely fed by a line-source such as a slope/shelf where extensive slumping provides the bulk of the sediment in addition to a subordinate channel systems. The narrow, 200 - 700 m wide conglomeratic fringe lining the Halibut Shelf is frequently referred to as a conglomeratic apron (e.g. McAfee 1993; Hendry 1994; Oakman & Partington 1998) resulting from mechanical destruction of the faulted slope (McAfee 1993) rather than a conglomeratic hinterland source. Although the nature of the feeder system, shelf and the hinterland are largely unknown (Hendry 1994) this and previous studies suggest that mostly reworked shelfal sediment was funnelled into the basin via multiple, persistent and probably structurally fixed feeders (e.g. McAfee 1993; Hendry 1994) with minor input directly off the shelf edge, fault-scarp and the Claymore High. These multiple sources give rise to a less coherent system with disorganised sequences (Reading 1991) which is interfingering with the conglomeratic apron. Seismic data shows thickening of SSM deposits towards a basinal direction (McAfee 1993). Reading & Richards (1994) and Richards *et al.* (1998) classify systems fed by multiple feeders and sources as submarine ramp systems, giving it a broader application than the original definition of Heller & Dickinson (1985). The S10 interval exhibits characteristics of a sand/mud-rich and a sand-rich submarine ramp *sensu* Reading & Richards (1994). Their difference is based on notably different seismic representation and characteristic architectural elements if the net sand content is > 70%, however, they do acknowledge that boundaries between systems are essentially transitional. Although, the turbiditic sandstones are very clean (Hendry 1994), considerable shale accumulations are recorded throughout the S10 interval expressed as shale-rich fan fringe and interlobe/OVB deposits (enclosure 1). Mud/sand-rich submarine ramp systems are characterised by significant channel and levee but subordinate lobe formation (fig. 1.3). This pars with the depositional model Boote & Gustav (1987) and McAfee (1993) proposed for the SSM/SD interval respectively. However, the S10 interval appears to be dominated by geographically restricted little to non-channelized, sheet-like sandy deposits, i.e lobe, lobe fringe and fan fringe deposits, with subordinate, shallow channeling (*further discussion chapter 3.5.3*). The S10 thus appears to be more akin to a sandier member of the mud/sand-rich submarine ramp *sensu* Reading & Richards (1994), such as the modern Crati Fan (Ricci Lucchi *et al.* 1985) and the Quaternary Paola Basin (Trincardi *et al.* 1995), or a sand-rich submarine ramp such as the Montrose, Claymore-Galley and Tye Fields (*in* Reading & Richards 1994) and the Western Annot Sandstones (Sinclair 2000). The few observed overbank deposits (fig. 3.12), a feature of mud/sand-rich ramp systems, may possibly reflect source-driven fluctuating sand/mud content which led to their occasional formation when more shale was available to the system. Hendry (1994) suggested a sand-rich SSM submarine ramp model analogue to the Greenlandic Hareelv Formation, a “non-organised, line-sourced ramp-like slope apron to basinal turbidite system” (Surlyk 1978, 1987), the latter displaying characteristics of both ramp and slope apron systems. A clear separation of sand-rich slope apron and submarine ramp systems is regarded as sometimes problematic as they represent end-members of transitional systems (fig. 3.20). However, a line-source supplying the bulk of S10 sediment by slumping characterising slope apron systems is not envisaged for the S10, even as there is no recorded evidence for cut and fill channels just the indication of distinct, structurally fixed feeders zones funneling sediment into the basin during general sea level rise. Through a distributary system, sand is transported further into the relatively small basin leading to basin-floor deposition.

For simplification Reading & Richards (1994) purposely do not consider basin geometry and topography in any of their models which may substantially influence the sediment accumulation pattern and thus the shape and dimension of the specific architectural element.

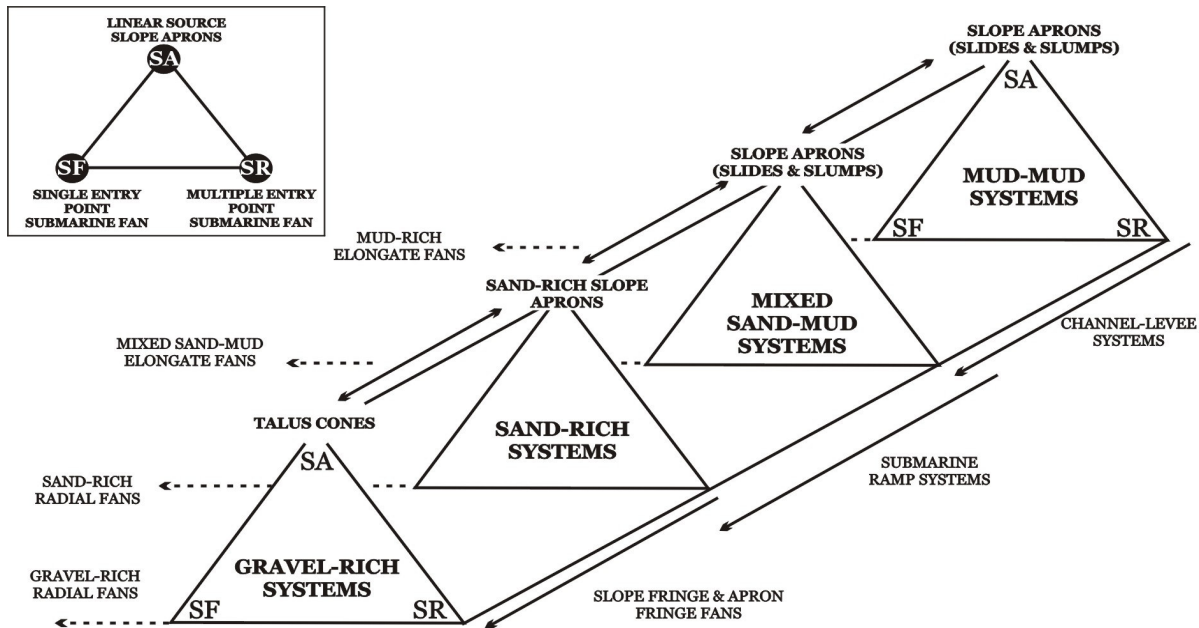


Figure 3.20: Classification of submarine-fans by (a) sediment supply mechanism, (b) dominant gain size and (c) number of entry points (from Richards *et al.* 1998).

Ultimately, the scale of observation plays an important role in the analysis of systems (Reading & Richards 1994). Riley *et al.* (1992) coalescing point-sourced “mini-fans” proves correct if only single feeders are considered, however, the (main) Scapa syncline appears to represent a multiple sourced mud/sand-rich to sand-rich submarine ramp-type system where the bulk of the sand is deposited in sandy little to non-channelized, laterally coalescing sediment bodies. A comprehensive analysis of the larger depositional system of the Scapa-Highlander Subbasin including the correlative, contemporaneous clastic deposits of the Highlander Field (Hendry 1994) and of the feeder system may yet yield a different perspective.

Many of the wells show overall fining-upward sequences indicating deepening conditions which is in accordance with the gradually rising sea level frequently described (Harker *et al.* 1987; Riley *et al.* 1992). However, some wells, notably well E1 in the central area remain distinctly coarse grained. This suggests other mechanisms than rising sea level to influence deposition. Harker *et al.* (1993) and Jeremiah (2000) consider tectonisms the most important control on sedimentation in the Outer Moray Firth, allowing, for example, the SSM system to develop an overall marl and shale depositional regime.

The depositional nature and the development of the S10 system appears to be fundamentally governed by tectonism. “Piano-key”-tectonism (*sensu* Stow 1985b) within the source area, uplifting different shelfal sectors at different times, effectively lowered sea level locally exposing poorly consolidated sediment to erosion/reworking through wave action and/or seismic events. Source area tectonism thus controlled the sediment supply to the basin and in combination with (older?) structural lineaments the pathways and thus the preferred geographic location of deposition within the basin (e.g. Miller Field: Garland *et al.* 1999). While the observed northward shift in time and activity of the feeders is a direct result of the shifting differential source area uplift, decreasing feeder activity probably follows denudation and subsiding source area tectonism.

Within the basin, the tectonic lineaments controlling the seafloor topography exerted the fundamental control on sediment accumulation resulting in the recorded aggradational, stacked pattern and elongate sandbody geometries. But flows captured by these intrabasinal depressions could due to the confinement become more erosional again akin to the accelerative flows of Kneller (1995) resulting in sediment transport further into the basin than under unconfined circumstances. Relocation of the fan axis resulted in repeated reconfiguration of the fan system as a consequence of either feeder channel switching, lobe offset, changing gradient and/or sediment flux.

Further complicating the sedimentary pattern are obstacle-forming debrites and slumps/slides off the different margins, resulting in deflection and/or ponding of turbidites (e.g. E3; well C15: Hendry 1994) The uplift and the intraformational erosion of VI deposits in the distal northern (E5Y) and eastern wells (21) will

most likely have contributed sediment to the active depositional areas. However, the nature of this probably unconsolidated, reworked sediment, the trigger of their remobilization and the transport and depositional process can only be speculated on.

Hydrodynamic sorting in the source area controlled the sedimentology and the nature of the largely turbiditic S10 system (Hendry 1994) which can lead to the accumulation of thick massive bodies particularly in restricted trough-basin fill complexes (Stow & Johansson 2000). Distinctly different overall grain sizes in closely adjacent wells 20/E7 suggest different sources of these.

Tectonism overriding rising sea level in controlling the nature of the S10 interval has frequently been observed in the North Sea (e.g. Brae turbidite system: Stow 1985b). Basin physiography and topography was been shown to fundamentally effect the shape of depositional elements as well as whole turbidite systems through progressive fault activity (e.g. Claymore Field: Kane *et al.* 2002), while topography can result in the preservation and/or erosion of sediments (e.g. VI subzone in wells E5Y/21).

Thus throughout the S10 interval tectonism enacted a fundamental control on sediment supply to the basin resulting in a phase of renewed sand progradation into the basin, as well as determining the location and shaping the overall geometry of the basinal deposits. The interplay of tectonism and sediment input thus fundamentally control the distribution of facies.

3.5.3 Lobe accumulation

Throughout the S10 interval, primarily non-channelized, sandy lobe deposits were accumulated. In proximal and distal positions lobe deposits appear to be channelized, i.e. associated with distributary channels, however, their association with lobe fringe / fan fringe deposits especially in the distal areas is more pronounced. The lobe deposits identified do not fit the classical lobe definition *sensu* Mutti & Normark (1987), their internal organisation, stacking pattern and geometry being strongly determined by shifting source area activity and confining seafloor topography.

The distinction of channelized and non-channelized sediments is not always easy. Also, complex relationships may exist between distributary channels and depositional lobes, when, for example, volumetrically large flows are not contained in the confines of a channel flow stripping leading to the development of “wing-like” sheet-sands outside of channel geometries, possibly developing into lobe-like bodies (e.g. CLTZ and proximal lobe zone of Cingöz Formation: *chapter 2.4.1*) which blurs the boundaries between these components. In outcrop these relationships may be relatively easy to establish - exposure permitting - however, when dealing with borehole data, this crucial lateral control is missing. In the subsurface, the identification of depositional environments relies heavily on the identification of facies associations and vertical sequences observed in a well. However, a comprehensive approach in subsurface analysis is essential, not only to determine the depositional environment and component associations, but also their temporal and spatial distribution, which requires the substantiation with seismic data.

The identification of lobes in the subsurface, its problems and limitations, are discussed in detail in chapter 5.

3.6 Conclusion

Previous studies have focused on analysing the diachronous SD reservoir unit, only the recently introduced more detailed biostratigraphic subdivision of the Scapa Sandstone Member enabled the reconstruction of zones VJ and VI, the so-called S10 interval.

- I) The S10 interval of the Scapa Sandstone Member appears to be akin to a multiple sourced mud/sand-rich to sand-rich submarine ramp system *sensu* Reading & Richards (1994) with some features of a slope apron system. Multiple feeder zones funnelling sediment off the Halibut Shelf and minor sources off the shelf, slope, Claymore High and intraformational sources give rise to a system with complex interdigitation of facies lacking clear proximal-distal trends. The S10 is dominated by sand lobe deposition and a subordinate distributary system, their location and geometry of sediment bodies are strongly determined by source-area and basinal tectonism.

- II) The S10 interval records renewed deep-water clastic progradation into the central Scapa Field area in an area which was previously dominated by shale-rich fan fringe (?) and basin-shale (?) S9 deposition. Internally, a distinct northward shift of sandy deposition occurs through zones VJ to VI.
- III) Although the S10 interval was deposited during gradually rising sea level, tectonism appears to be the fundamental control on the depositional nature and development of the S10 overriding sea level fluctuations. Lateral migration and local retrogradation of the system is in response to locally decreasing sediment supply and shifting sources caused by differential uplift of the source area. Source area tectonism controlled local sea level, the sediment volume and pathways into the Scapa syncline and thus the geographic location. Basinal tectonism resulted in probably fault-controlled intrabasinal depressions which captured flows resulting in thick aggradational patterns and localised, confined sediment accumulation.
- IV) Uplift in the eastern and distal northeastern area (21, E5Y) probably lead to intraformational erosion of zone VI.
- V) The bulk of the sand deposition took place in little to non-channelized, sheet-like lobe and lobe fringe deposits *sensu* Mutti & Normark (1987), however, their appearance is disparate to classical lobes. Sediment bypass close to the conglomeratic fringe resulted in detached lobes developing basinward from the base-of-slope. The shifting activity of the various feeder zones combined with a complex basinfloor topography resulted in localised, stacked, aggradational lobe accumulation of elongate geometry indicating that deposition was not altogether free to move. Individual lobes are mainly composed of sand high-density turbidites and diluted flows and possibly sandy debris flows *sensu* Shanmugam (1996).

3.7 Further work

In order to gain a more complete picture of the development of the S10 interval and the Scapa Sandstone Member (SSM) and thus the factors governing lobe accumulation in small, fault-controlled basins, further studies would benefit from:

- I) refined biostratigraphy of some of the already analysed wells to fully include and refine the existing as well as the inclusion of the other Main Scapa wells to verify and extend the S10 depositional model.
- II) extension of the present environmental and depositional model of the S10 interval for the whole SSM to examine larger spatial and temporal changes within the Scapa system including their controls.
- III) inclusion of profile desanding and tuff-stratigraphy for the S10 / SSM in aid of further, possibly more detailed interwell correlation.
- IV) inclusion of seismic data to gain more information about the nature of the feeder system (more stable due to incision?) as well as potential fault-scarp related topography within the actual syncline which may profoundly control the sediment accumulation pattern.

3.8 Summary

The S10 interval of the Scapa Sandstone Member forms part of the Lower Cretaceous infill of the Scapa Syncline in the north western Witch Ground Graben. During this time, a maximum of 236 ft (72 m) of sandstones, conglomerates and marls of early Valanginian to intra-late Hauterivian in age accumulated. The S10 interval records renewed clastic progradation into the central basin during a period of overall rising sea level. Localised source area uplift freed large volumes of sediments from the Halibut Shelf to the south

which were transported via turbiditic and sandy debris flows through fixed feeders across the fault-bounded, conglomerate-lined shelf into the narrow deep SE-NW trending syncline.

Sediments were further funnelled into the basin by a broad, shallow distributary system where the bulk of the sand-grade material was deposited in sheet-like lobe and fringe deposits. Distinct fan geometry and morphology are poorly established and a rather complex superimposition and lateral coalescence of lithofacies and fan components exists. The sediment accumulation pattern varies considerably spatially and temporally with an overall northward shift in depositional locus. Intrabasinal depressions captured turbiditic flows resulting in a locally confined, aggradational depositional style. Minor sediment contributions off the fault-scarp and/or directly off the shelf and/or the Claymore High complexly interfingering with the main turbidite system while the Claymore High represents a barrier on which turbidites onlap, pond or are axially deflected. Lateral migration and local retrogradation of the system is in response to locally decreasing sediment supply and shifting sources caused by differential uplift of the source area while intrabasinal tectonism resulted in localised erosion and sediment-remobilisation.

The S10 interval is best represented by the sand/mud-rich to sand-rich submarine ramp system *sensu* Reading & Richards (1994).

4 RESERVOIR CHARACTERISATION

As most sands in almost all submarine fan environments are originally porous and permeable, sandy depositional lobes *sensu* Mutti & Normark (1987) and related sheet-like sandy deposits provide excellent reservoirs if contiguous with adequate source beds (e.g. Normark *et al.* 1983; Richards & Bowman 1998). They are of great areal extent, tend to have a low percentage of total intergranular matrix and probably have some of the highest initial porosity (28 - 35 %) and permeability (200 - 4000 md) (McLean 1981; Risch *et al.* 1996).

Lobe and related sheet-like deposits do not form homogeneous reservoirs as different studies have shown (e.g. Schuppers 1995; Garland *et al.* 1999). Shales occurring at various scales within reservoirs constitute important barriers or baffles to fluid flow. Thus, for successful reservoir characterisation and hydrocarbon production, it is imperative to possess a detailed knowledge of the distribution of reservoir rocks and especially of their heterogeneities as well as their vertical and lateral geological variations. Much of the lobe character ultimately depends on the availability of sand and shale to a system. A combination of complex processes such as frequency of flow, composition, erosion, burial, compaction and diagenesis that occurred over millions of years fundamentally affect the reservoir, while, in particular, basin floor topography enacts one of the basic controls shaping lobe geometry and stacking pattern (e.g. Reading & Richards 1994).

The qualification of the geological variation of lobe deposits is typically undertaken at different scales, for example, the 3 scales of Mijnsen *et al.* (1993):

- i) *large-scale* variation between genetic units, for example lobes, is mainly concerned with geometries and internal configuration of sedimentary environments
- ii) *medium-scale* variation within genetic units is concerned with geometries and internal configuration of genetic units (e.g. width/depth ratios of genetic units, and sizes of baffles to flow).
- iii) *small-scale* variation due to compositional feature of the rocks is concerned with variation in rock properties caused by texture and composition of rocks, mainly porosity and permeability trends. Cementation and matrix content, for example, play an important role in reservoir reduction. The behaviour of density currents depositing turbidites can impart textural variations and sedimentary structures which contributed to permeability heterogeneity at probe permeameter, core plug and bed-scale.

Each reservoir scale is characterised by specific, intrinsic heterogeneities (Weber 1986). Hydrocarbon recovery greatly depends on good connectivity and interconnectedness, especially in thin reservoirs (Guerillot *et al.* (1992) and thus the classification and quantification of reservoir heterogeneities plays an important role in the quality of production forecast. The scale and orientation of shales as i) boundary shales (the surfaces between zones), ii) intrazone shales (heterogeneities within the zone) and iii) permeable/non-permeable lithotypes form the most important heterogeneities (e.g. Geehan & Underwood 1993).

Furthermore, the production potential may be influenced by faults which can compartmentalize reservoirs and modify depositional continuity (Bryant & Flint 1993), the timing of petroleum migration and burial depth (McLean 1981).

The quantification of geological variations within reservoirs depends on adequate sampling. Clearly, outcrops have the advantage of providing some lateral control allowing for a more thorough analysis of geological variations, but they are lacking the third dimension in horizontal direction. On the other hand, core data present only a billionth of the total reservoir volume, but in combination with seismic data a densely drilled field may provide some 3 D information on the distribution and geometry of the genetic units and heterogeneities (Matheron *et al.* 1987; Fox 1992; Mjinsse *et al.* 1993).

4.1 Lobe deposits of E-Fan, Cingöz Formation

The Cingöz Formation is characterised by a high net sand content, good 4-way stratigraphic and structural closures with the basinal Güvenç shales as proven hydrocarbon source (Satur 1999). The thick sandy lobe successions of the E-Fan provide good reservoir rocks, however, lenticular shale-rich debrites at different stratigraphic level form important barriers to vertical flow. Post depositional faulting further compartmentalizes this reservoir into kilometre-scale blocks. It thus possesses all the qualities of a potentially good hydrocarbon play.

The E-Fan lobe deposits (Lobes A, B, C) are analysed individually under the following aspects:

- small to large-scale reservoir potential excluding microscopic and poro/permeability analysis
- small to large-scale heterogeneities
- production aspects

4.1.1 Lobe A

Reservoir and heterogeneities (fig. 4.1):

<i>SCALE</i>	<i>RESERVOIR</i>	<i>HETEROGENEITIES</i>
<i>SMALL</i>	<ul style="list-style-type: none"> • vcs to cs sandstone and pebbly sandstone • poorly to moderately sorted • S₁₋₃, rare R₁₋₃ (Lowe 1982), DWMS, sandy debris flows (<i>sensu</i> Shanmugam 1996) • ~ 95 % net sand • 0.6 to 3.0 m thick x > 0.3 km • amalgamated, no shale partings 	<ul style="list-style-type: none"> • localised accumulations of pebble to small cobble-sized clasts, associated with erosive beds
<i>MEDIUM</i>	<ul style="list-style-type: none"> • 5 – 33 m thick, 600 – 1200 m wide • 96 % net sand • elongate, sheet-like bodies • crude fining-upward 	<ul style="list-style-type: none"> • 1% shale content • rare, inextensive shale beds (0.15 thick x >10 m wide), erosionally cut off • lobes may pass into channeling
<i>LARGE</i>	<ul style="list-style-type: none"> • mixed shingled-compensational stacking • highly amalgamated • 150 m thick / max width 1200 m, widening downflow • 84 % net sand, 15% conglomerates • crude fining upward 	<ul style="list-style-type: none"> • lateral thinning & increasing shale content • occasional shale-rich debrites along margins • channeling with shale-clast-rich conglomerate

Production aspect:

The sandy, highly amalgamated Lobe A deposits may essentially be regarded as one large flow unit* with excellent vertical and horizontal connectivity. No CLTZ-wide barriers to flow developed and only few local

* flow unit are assumed to be laterally and vertically continuous sharing i) similar porosity; ii) similar permeability; iii) similar bedding characteristics (Hearn *et al.* 1984), basically combining sedimentological and petrophysical reservoir characteristics

barriers exist. The distribution of reservoir rocks and flow barriers indicates (fig. 4.1) that the best production area would be the central depositional area where only rare linear shale-matrix rich or shale clast-rich conglomerates within the channeling component may form baffles to flow. Towards the lateral margins, reservoir quality becomes relatively poorer due to the development of localised wedge-shaped shale-rich debrites, and thin shale beds. However, their erosional cut-off by succeeding flows and the subsequent amalgamation of sandstone beds ensures good vertical connectivity. The essentially unorganised vertical development throughout especially the lower 80 m suggests good reservoir quality while the gradual fining- and shaling upward into more classical lobe deposits overlying the CLTZ (*see* chapter 2.2) points to overall reservoir reduction. Equally reduced reservoir quality is anticipated in a downcurrent direction where grain size decrease and shale increase probably lead to a higher frequency of laterally persistent shale-rich intervals.

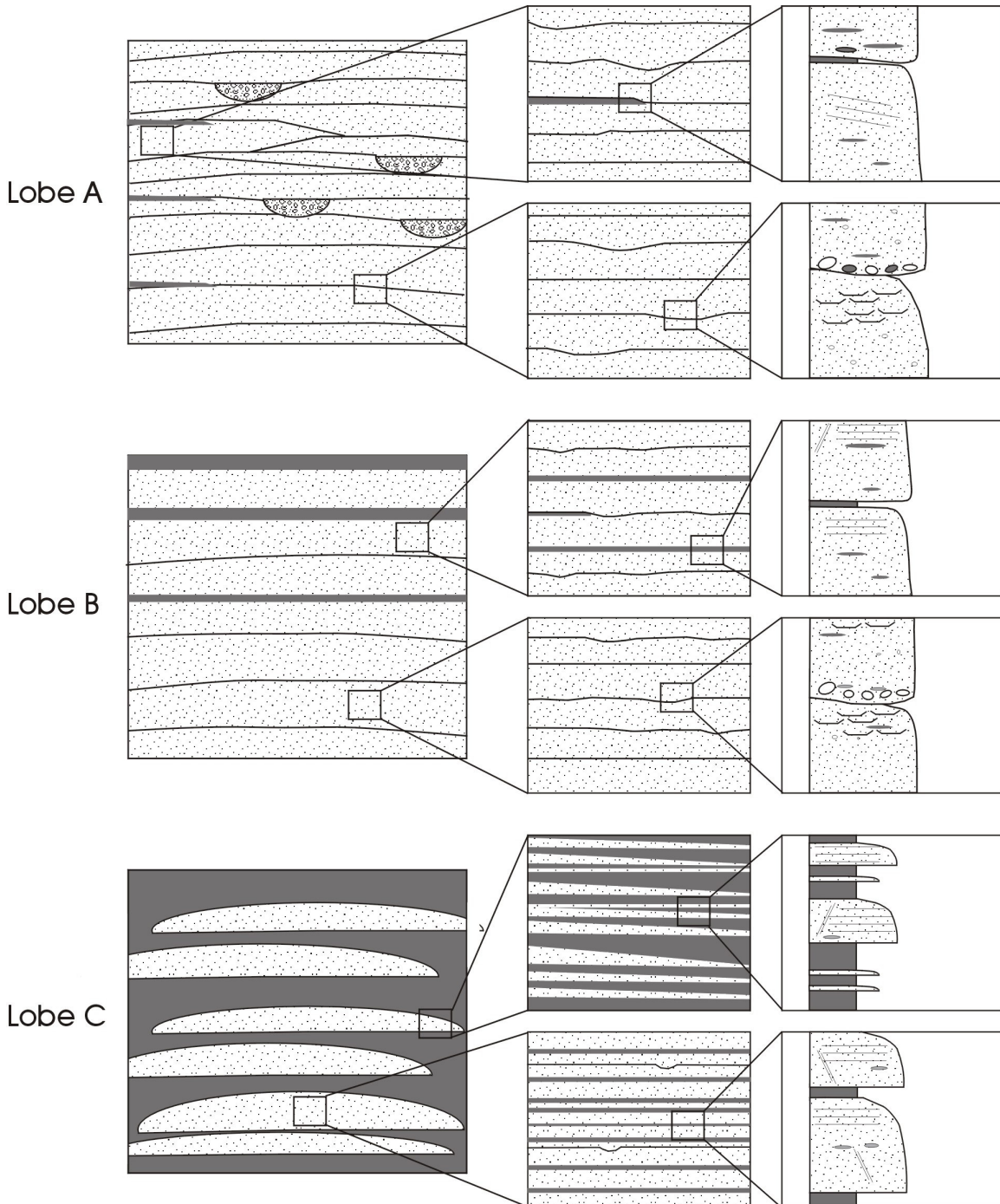


Figure 4.1: Reservoir characterisation of Cingöz lobe deposits at lobe complex-, lobe- and bed-scale.

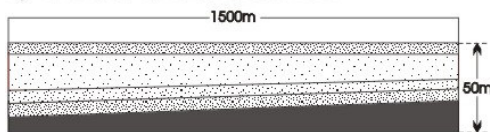
Strong reservoir layering akin to the layer-cake model (fig. 4.2; 70 % Lobe A deposits) with interspersed elements akin to channel-fill or jigsaw model (30 % channeling components) characterises the CLTZ. Potential reservoir compartmentalisation through faulting is probably negligible in this sand-rich environment.

4.1.2 Lobes B

Reservoir and heterogeneities (fig. 4.1):

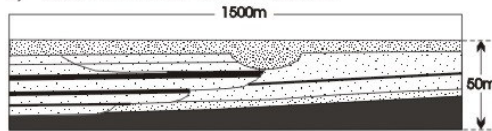
<i>SCALE</i>	<i>RESERVOIR</i>	<i>HETEROGENEITIES</i>
<i>SMALL</i>	<ul style="list-style-type: none"> • cs sandstone & pebbly sandstone • moderately sorted • R₃, S₁₋₃ (Lowe 1982), DWMS, sandy debris flows (<i>sensu</i> Shanmugam 1996) • ~ 95 % net sand • 0.4 - 1.2 m thick / > 1.2 km width • 3-4 m thick composite beds • vertical burrowing 	<ul style="list-style-type: none"> • randomly located clustered shale rip-up clasts • rare, inextensive (0.5 – 2/7 m) mud-lined amalgamation surfaces • discrete shale-clast horizons (> 1 – 10s m) at various levels within beds
<i>MEDIUM</i>	<ul style="list-style-type: none"> • 8 – 50 m thick, > 1200 m width, > 2.4 – > 4.8 km downcurrent extent • > 95 % net sand • highly amalgamated • elongate, sheet-like bodies • crude fining/thinning-upward 	<ul style="list-style-type: none"> • rare thin (0.5 – 4 cm) shale partings, laterally extensive [absent in lower lobes, towards top increasingly abundant] • overall lateral thinning/fining, shale increase, mostly passing into lobe fringe
<i>LARGE</i>	<ul style="list-style-type: none"> • 300 m thick, > 3 km width • 100 % net sand [lower part] upward decrease to 95 % • mixed shingled-compensational stacking • lower part, highly amalgamated • crude fining/thinning upward 	<ul style="list-style-type: none"> • upward increase in shale content • upward increase in thickness (2 - 6 m) and abundance of laterally extensive lobe fringe deposits (75 % net sand) • cut by rare, linear distributary channels (80 % net sand, distinct shale partings)

A) LAYER-CAKE RESERVOIR TYPE



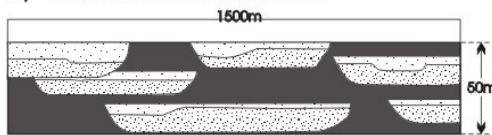
Distinct layering with marked continuity and gradual thickness variation.

B) LAYER-CAKE RESERVOIR TYPE



Different sand bodies fitting together without major gaps. Occasional low permeable zones can occur locally between adjacent or superimposed sand bodies.

C) LABYRINTH RESERVOIR TYPE



Complex arrangements of sand pods and lenses often appearing discontinuous in sections.

Production aspect:

The best quality reservoir rock of the sand-rich, stacked proximal Lobe B are formed by the lower, highly amalgamated lobe deposits. The high degree of amalgamation is responsible for creating thick flow units of excellent reservoir properties due to i) the thick, sand-rich homogeneous beds, ii) the general lack of interbedded shales and iii) the great lateral extent of individual beds, composite sandstone units and the individual lobes themselves. The sharp contrast in bed thickness between the sandstone units and the thin-bedded, shale-rich intervals allows for a straightforward zonation. The whole of the lower Lobe B deposits can essentially be regarded as one thick flow unit, while in the middle and upper part, increasingly frequent and laterally extensive lobe fringe and individual shale beds compartmentalise at inter- (between) and intra- (within) lobe level (fig. 4.1). The lower net sand lobe fringe deposits due to their finer grain size will result in a lower “plug” permeability while the interbedded shale layers reduce the overall effective vertical permeability (K_{VE}). Bioturbation is not abundant, it may however locally increase the permeability of shale partings and beds. The resultant large-scale layering will effectively confine fluid flow to layer-parallel reservoir zones of sheet-like high net-to-gross units.

Figure 4.2: Basic reservoir types from Weber & Van Geuns (1990).

The proximal Lobe B complex is akin to a layer-cake reservoir (fig. 4.1), with some isolated, linear distributary channels forming localised baffles to flow with their partially shale-rich deposits. Individual Lobe B bodies and the larger complex are marked by moderately-defined vertical organisation allowing a reasonable prediction of the distribution of high-quality reservoir rocks. The overall thinning-upward trend combined with an upward decrease in amalgamation results in a vertical increase in reservoir compartmentalisation and a pronounced thinning of flow units. In an upstream direction, the Lobe B are probably connected to coarser-grained CLTZ deposits while in a downstream direction, increasing shale breaks between the massive sandstone units and decreasing amalgamation and grain size are expected resulting in an overall thinning of flow units.

Faulting is common in the proximal lobe zone. If non-sealing, they may in fact enhance the reservoir quality by offsetting thin impermeable shales against thick sands thus allowing for greater connectivity within the reservoir (fig. 4.3). Large (> 2 km) well-spacing within the excellent Lobe B reservoir may still ensure good recovery. Localised, wedge-shaped debris flows as observed further to the west of the study area, may potentially form localised barriers to flow.

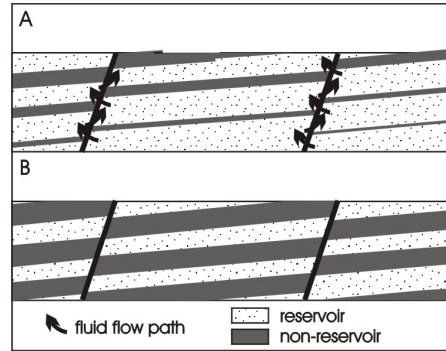


Figure 4.3: Schematic representation of reservoir changes as a result of non-sealing faulting. A: reservoir enhancement due to improved connectivity, e.g. Lobe B deposits. B: reservoir reduction due to reduced connectivity or isolation of reservoir bodies, e.g. Lobe C deposits.

4.1.3 Lobe C

Reservoir and heterogeneities (fig. 4.1):

SCALE

RESERVOIR

HETEROGENEITIES

SMALL

- ms - cs sandstone
- moderately - well sorted
- S₁₋₃ (Lowe 1982), T_{a-c(d)} (Bouma 1962), rare sandy debris flows (*sensu* Shanmugam 1996)
- 90 - 100 % net sand
- 0.6 - 1.2 m thick / > 0.3 km width
- up to 2.5 m thick composite beds
- sheet-like

- shale-clast lined amalgamation surfaces or discrete horizons [2-8 cm x >10s m]
- inextensive (0.5 - 15 m), shale-lined amalgamation surfaces
- localised, clustered shale rip-up clasts [few m²]
- rare mud-lined internal scours

MEDIUM

- 4 - 35 m thick, > 0.3 km width
- > 60 to 70 % net sand, max 95 % sand
- rare lobe amalgamation
- sheet-like, some lobate geometry
- well developed asymmetric sequences
- lateral thinning/fining

- laterally extensive, thin (2 - 15 cm) shale / fine sand alternations separating sandstones bodies
- rare slumped units (max. 1.2 m thick)
- lateral shale increase, passing into lobe fringe
- vertical separation by lobe fringe and/or interlobe deposits

LARGE

- 800 m thick, > 0.3 km width (outcrop limit)
- isolated lobes (marginal/basinward)
- some mixed shingled-compensational stacking (central depot area)
- net sand < 80 - 95 % (margin - centre)
- fining/thinning & shale increase towards margin and basin

- lobes/stacked lobes separated by laterally extensive lobe fringe (60 % net sand) or lenticular interlobe (<50 % net sand) deposits
- upward/basinward increase in shale content
- localised shale-rich debrites (?)
- marginal areas with either onlap, debrites or slumps up to 10s of m thick.
- overall fining upward to basin plain deposits

Production aspect:

Individual sandstone beds or amalgamated beds can be regarded as flow units separated by near impermeable fine sand / shale alterations. Internally, little variation in thickness, net sand content and/or sedimentary structures was recorded, which, however, may locally affect vertical fluid flow (fig. 4.4):

- i) Thickness variations are largely a function of the size and depth of occasional, shallow scouring.
- ii) Scours are shallow and do not erode through shales into underlying sandstone body (e.g. fig. 4.4c)
- iii) Grain size profiling shows that most trends are persistent throughout beds, being either normally graded or more often marked by abrupt grain size breaks and rapid fining at top. However, grain sizes may vary laterally with small patches of different grain sizes developing locally (figs. 4.4a: bed 8; 4.4c: bed 2). Subtle amalgamation surfaces indicate that succeeding flows possessed the capacity to erode into predeposited sandstones. Thus individual sandstone beds may be the result of one or more flows.
- iv) Dish structures, typically confined to 0.25 to 4 m², vary laterally in type, amount and presence, although the reason for this is not fully understood (Stow & Johansson 2000; e.g. figs. 4.4a: beds, 1,8,9; 4.4b: bed 2). They result from pore fluid movement (Nichols *et al.* 1994) and their absence may be due to the final depositional mechanism in high-density turbidites or sandy debris flows or by the rate of sediment supply to and through the basal layer or a combination of these factors. These horizons may be zones of low vertical permeability because clay mineral coatings can effectively plug pore throats while the porosity remains almost unaffected (Hurst & Buller 1984).
- v) Highly bioturbated tops and frequent, but irregular spaced burrowing persists. The type and infill of the burrows varies considerably throughout individual beds, however, clay-lined walls and relatively coarser sediment infill are the most common type of infill.
- vi) Amalgamation surfaces are subtle. Clay-draped amalgamation surfaces appear to be inextensive (0.5 to 15 m; e.g. fig. 4.4b).
- vii) Clustered or discrete, laterally extensive shale clast horizons appear at various, though never basal, levels throughout turbidite beds (figs. 4.4a: beds 2,6; 4.4b: beds 1,3). They mark distinct rheological interfacies within the flow (Postma *et al.* 1988) resulting from freezing or thickening of the inertia flow layer which forces the gliding clast to a progressively higher level within the flow leaving the clasts trapped “suspended” above the base of the resulting turbidite. These fine-grained rip-up clasts and/or low density outsized clasts can complicate the patterns of fluid flow through reservoir rocks (Hughes *et al.* 1995).
- viii) Lateral and vertical net-to-gross are largely a function of presence and abundance of shale clasts or shale partings (fig. 4.5)

The laterally extensive shale/fine sand alternations separating individual beds (flow units) result in a strongly layered, laterally extensive, sheet-like reservoir with good horizontal permeabilities but poor to no vertical permeability. Lobe C deposits and the related environments are strongly bioturbated. This may locally lead to enhanced vertical permeability by breaking down shale barriers, however, this has not been observed at outcrop scale. Neither were sand dykes nor scouring of sufficient downward extent to connect with underlying sandstone beds. The central Lobes C possess good overall reservoir quality (larger grain size, higher sand content, high connectivity due to intense burrowing, little interbedded shales). Their well predictable stacking pattern and vertical and lateral trends in grain size and thickness development, point to the thickest, coarsest sandstone beds with fewest shales interbedded in the central depositional area. In a basinward and marginal direction the reservoir quality decreases. These marginal lobes and/or lobe margins possess reasonably good but variable reservoir quality due to smaller grain sizes, lower sand content, thicker interbedded shales. Reservoir quality of the various slope contact relationships are qualified by the change in net sand content. Thus, pinch-out where grain size does not change infers good reservoir quality almost right to the pinch-out limit of sand units (Hurst *et al.* 1999), while onlap (gradual grain size and thickness reduction) and slumping (deformed and chaotic structures) result in declining reservoir potential.

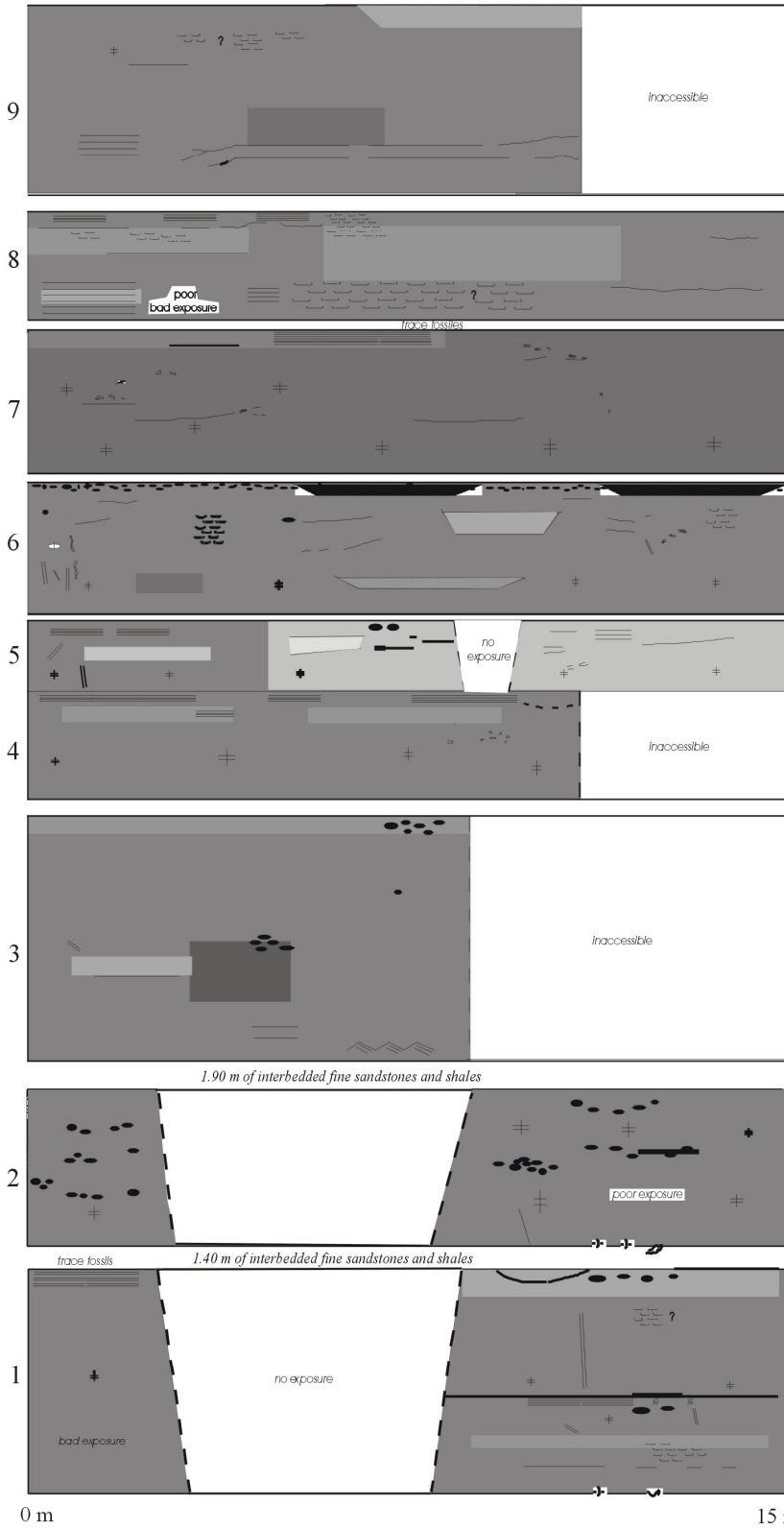
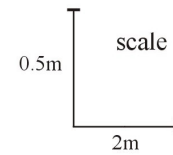


Figure 4.4a: lateral log within central lobe C deposits (m 0.4-13 of fig 2.33/(1) of fig. 2.32). Photograph showing lateral log meters 5-13 of corresponding beds. Interbedded fines are not represented in lateral log. For legend see fig. 4.4b,c.



The well sorted, laterally extensive Lobe C deposits are essentially of layer-cake type reservoir, however, with much greater reservoir compartmentalisation than Lobe B deposits due to the greater abundance and thickness of shale-rich deposits (fig. 4.1). Individual lobes are composed of a multitude of relatively thin horizontal flow units which are separated by lower net sand fringe and shale-rich interlobe deposits. If faulting, as occasionally observed in the field, is sufficiently important, it may result in the offset of reservoir lobes against poorer quality lobe fringe or non-reservoir interlobe deposits, strongly compartmentalising the reservoir (fig. 4.3). Interwell correlation will prove to be difficult and for effective hydrocarbon recovery, narrower (<1 – 2 km) well-spacing than in Lobe B deposits is necessary. Considering the growth pattern of the lobes, thin beds will increase in a downdip direction resulting in further reservoir reduction.

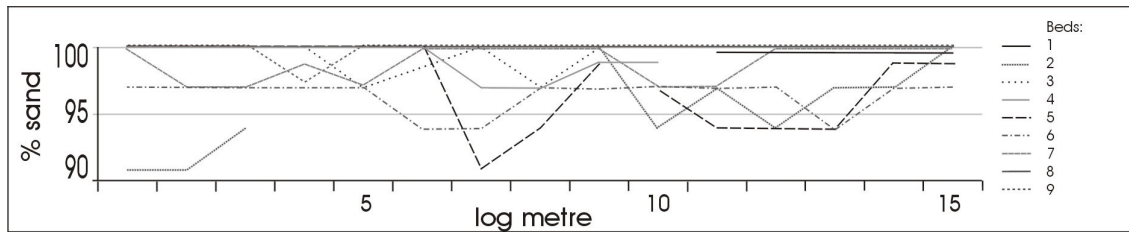


Figure 4.5: diagrammatic representation of net sand content in lateral log (fig. 4.4a). Changes are primarily due to shale clasts nets and thin, inextensive clay-draped amalgamation planes.

4.2 Lobe deposits of the S10 interval, Scapa Sandstone Member

The Scapa field is a structural-stratigraphic trap. The up-dip limit of the reservoir to the NE is by onlap termination onto the Claymore High. To the SW fault closure and/or sand pinch-out into cemented conglomerates associated with the Halibut Shelf boundary fault are present. Limestones and marls of the Valhall Formation form reservoir caprock integrity. The underlying Kimmeridge Clay Formation constitutes the source rock with emplacement thought to have taken place during the Early Tertiary (McGann *et al.* 1991). The Scapa Field reservoir is a good example of diagenesis overriding lithology- and/or component-based reservoir characterisation. The Scapa Sandstone Member has been subdivided into reservoir (SA/SD/SF) and non-reservoir (SB/SC/SE) units which are largely diachronous. The non-reservoir units comprise a higher proportion of heterolithics and shales but also tightly cemented sandstones (Hendry 1994).

SCALE	RESERVOIR	HETEROGENEITIES	<i>theoretical</i> PRODUCTION ASPECT
SMALL	<ul style="list-style-type: none"> • cs - fs sandstone • clean sandstones • thickness: 0.4 – 0.8 m • DWMS up to 4 m • highly bioturbated tops • GS / S facies 	<ul style="list-style-type: none"> • shale-rich tops • variable calcite cementation and nodule formation 	<ul style="list-style-type: none"> • thin shale breaks bar vertical flow, however, abundant bioturbation may break down structures and reduce those barriers
MEDIUM	<ul style="list-style-type: none"> • lobe thickness: few 100s m width 	<ul style="list-style-type: none"> • thin shale partings • interbedded SM and SH facies • lateral / distal passing into shale-rich lobe fringe and ultimately fan fringe deposits 	<ul style="list-style-type: none"> • declining reservoir quality towards lobe margins • SM/SH form important barriers to flow
LARGE	<ul style="list-style-type: none"> • up to 21 m thick • complex lateral and vertical interdigitation of lithofacies / fan components resulting from the largely superimposed localised deposition 	<ul style="list-style-type: none"> • localised debris flows • lobes/stacked lobes separated by laterally inextensive shales • linear distributary channels • shale-rich OVB/interlobe, lobe and fan fringe deposits 	<ul style="list-style-type: none"> • no basin-wide barriers of baffles to fluid flow exist • declining reservoir quality towards lobe and field margins

The S10 interval constitutes a sand-rich phase of the SSM, covering nearly the whole of the Scapa syncline. It comprises mostly rocks of the SD reservoir and SE non-reservoir unit. The theoretically good reservoir potential of lobe sandstones (*see below*) is considerably reduced by calcite cementation. A large range of permeabilities were recorded in the major lithofacies resulting from varying degrees of laterally extensive calcite cementation to small, localised calcitic nodule formation (enclosure 1; fig. 3.8).

4.3 Postdepositional changes and reservoir delineation

The elongate and lenticular lobes of the Cingöz Formation and Scapa S10 interval potentially form good stratigraphic traps, however, the delineation of the respective reservoirs is/will be difficult due to the commonly gradual transitions between lobe and interlobe packages. Therefore the recognition and understanding of the growth pattern of lobes is critical to sand prediction and hence hydrocarbon recovery. The orientation of the reservoir bodies and barriers or baffles to flow are an essential part in understanding the reservoir, however, in case of the Cingöz Formation, the lack of 3-D exposures and the essentially time-stratigraphically unconnected study sections, cannot properly resolve sandbody orientation.

Postdepositional changes to a reservoir stem mainly from compaction and diagenesis and are not considered in this study. Differential compaction during burial may affect, for example, the seismic expression of lobe deposits, by preserving or enhancing the overall concave-up lenticular sandbody geometry or result in oversteepened margins. Generally, during burial original porosity may be substantially reduced mechanically at shallow depth or by pressure solution at deeper levels. With burial depth, permeability decreases substantially. The high sand/shale ratio of the Lobe A/B and some of the Lobe C are more likely to retain higher porosities and permeabilities at greater depth than the marginal Lobe C deposits with are interbedded with thicker shale sequences, as shale dewatering during burial can result in early diagenetic cementation. This might only be inhibited by early hydrocarbon migration (McLean 1981). Diagenesis can have an overriding effect on lithologic reservoir characterisation as seen in the Scapa Field. The level of reservoir characterisation carried out on the E-Fan lobe deposits thus provides an indication of the general reservoir geometry and potential for these types of lobe depositional environments.

5 DISCUSSION OF LOBE DEPOSITS

Depositional lobes are recognised as one of the elemental building blocks of deep-water clastic systems (Mutti & Normark 1987, 1991). They have been identified in a variety of different systems (fig. 5.1) where their development, size and character appear to be fundamentally controlled by the availability of sand to the system (Reading & Richards 1994). Depositional lobes in ancient fans were first defined by Mutti & Ghibaudo (1972) and are located in the outer fan environment (*sensu* Mutti & Ricci Lucchi 1972) as either channel-attached lobes (characterising poorly efficient systems, i.e. high sand : mud ratio) or detached lobes (highly efficient systems: low sand:mud ratio; Mutti & Ricci Lucchi 1975). Diagnostic criteria for their identification in ancient systems were formulated by Mutti & Normark (1987, 1991; *see chapter 1.3.1 for list of criteria*). However, these “classical” lobes (e.g. Marnosa Arenacea: Ricci Lucchi & Valmori 1980; Hecho Group: Mutti & Ricci Lucchi 1975; Mutti 1985b; Macigno Formation: Ghibaudo 1980; Kongsfjord Formation: Pickering 1981) are not common, more often sandbodies with one or more “atypical” depositional lobe characteristics are described, illustrating the dilemma with the rigid *sensu stricto* application. The large-scale lobate geometry, for example, is not readily identified in outcrop and has often been inferred by other field criteria which are primarily based on vertical bed stacking patterns and facies association. However, the analysis of vertical cycles as an instrument to identify depositional environments is among the most controversial ones as are the transport and depositional mechanisms of the deep-water clastics.

The following discussion focuses on these controversial issues as well as the recognition of lobes in the subsurface, limitations of outcrop-subsurface knowledge transfer, the state of deep-water clastic models with respect to lobe deposits and summarises proposed new lobe definitions.

PRINCIPAL ARCHITECTURAL ELEMENTS

SYSTEM TYPE	WEDGES	CHANNELS	LOBES	SHEETS	CHAOTIC MOUNDS
GRAVEL-RICH SYSTEMS		CHUTES 			
SAND-RICH SYSTEMS		BRAIDED 	CHANNELIZED LOBES 		
MUD/SAND-RICH SYSTEMS		CHANNEL-LEVEE 	DEPOSITIONAL LOBES 		SLUMPS & SLIDES
MUD-RICH SYSTEMS		CHANNEL-LEVEE 	DEPOSITIONAL LOBES 		SLUMPS & SLIDES

Figure 5.1: Principal architectural elements of deep-marine systems based on outcrop, wireline log and seismic data. Submarine fan, ramp and slope apron systems display a predictable arrangement of architectural elements, which vary between turbidite system class (Richards & Bowman 1998).

5.1 Depositional lobes in ancient systems

5.1.1 Turbidites versus sandy debris flow deposits

Depositional lobes *sensu stricto* are composed of sandstones exhibiting complete classical Bouma sequences (Facies C1, C2 of Mutti & Ricci Lucchi 1972, 1975), which are the product of low density turbidity currents (LDT). In case of turbidity currents containing less fines, coarse grained, graded and internally unstratified divisions of the Bouma sequences dominate and water-escape structures are common (Facies B1; Mutti & Normark 1987). However, normal grading, the fundamental criterion of the turbidite paradigm (Kuenen & Migliorini 1950), was found to be not too common in deep-water clastic systems (e.g. Kneller 1995; Miall 1999). This apparent lack of normally graded Bouma-turbidites and the abundance of inversely graded, massive or normally graded sandstones with floating clasts and quartz granules, has been explained to be the result of high density turbidity currents (HTC; Lowe 1982; Postma 1986; Postma *et al.* 1988), an intermediate between LDT* and SDF* of non-turbulent flow rheology. Kneller's (1995) time-space matrix (fig 1.2) and Kneller & Branney (1995) explore the idea of extremely varied flow behaviour of turbidity currents being responsible for these non-typical attributes. But it is notably Shanmugam *et al.* (1995) and Shanmugam (1996, 2000) who argue against the HDT and related concepts (*see* Shanmugam 1996, 2000 *for detailed discussion on turbidites and sandy debris flows*) suggesting the typical HDT features are in fact the product of SDF (although Pickering *et al.* 1989 suggest that very large SDF may even be turbulent in part). The basic question is if HDT are turbidites or, indeed, sandy debris flows as suggested by Shanmugam (1996; 2000). To date, two schools exist, one advocating the bulk of the deep-sea sediment originating from turbidite (LDT/HDT) deposition (e.g. Hiscott *et al.* 1997; Bouma *et al.* 1997, Lowe 1997; Stow & Mayall 2000), the other stressing the hitherto neglected importance of sandy debris flows forming a significant amount of deep-water clastics (e.g. Shanmugam *et al.* 1995; Shanmugam & Moiola 1997; Shanmugam 2000). With the strong HDT paradigm and gradual acceptance of some aspects of the SDF-concept, many workers now believe that a combination of the two processes and other resedimentation processes are responsible for the deposition of deep-water clastics and transformation between the processes is the norm (Stow & Johansson 2000). The latter thus suggest that both HDT and SDF are responsible for forming deep-water massive sands (DWMS) which may develop as lobe and sheet sands forming stacked lobes and distal fan deposits respectively (e.g. North Sea Frigg and Heimdal Fields). Purvis *et al.* (2002) believe at least partial deposition by SDF to be responsible for the massive nature of sands, mounded geometry and lack of classic Bouma sequences of the North Sea Gryphon Field. The lobes of the Miocene Cingöz Formation (*chapter 2*) and the Early Cretaceous Scapa Formation (*chapter 3*) are suggested to result from a combination of LDT/HDT and SDF processes. However, translating the SDF concept *sensu stricto* to the

* turbidites: Newtonian rheology and turbulent state from which deposition occurs through suspension settling
debris flows: plastic rheology and laminar state from which deposition occurs through freezing (Middelton 1993)

Cingöz lobe deposits (table 5.1), i.e. normally graded deposits with floating clasts and granules represent SDF instead of HDT, very few true turbidites remain, most of the deposit would in fact classify as SDF.

Transport mechanism	Lobe A	Lobe B	Lobe C
turbidites* (LDT/HDT) (NG)	45	59	75
SDF (NG, floating clasts/granules; massive, inversely graded)	45	46	58
“true” turbidites (LDT; NG, Bouma sequence)	21	27	44

Table 5.1:
% normally graded turbidites (LDT/HDT), % SDF of (LDT/HDT) and resulting true turbidites. NG = normally graded
* note that the remaining beds are either massive or inversely graded.

The genetic implication of HDT and SDF transporting mechanisms is of great importance to the petroleum industry as the predicted facies associations, heterogeneities and geometries will be different, affecting reservoir geometry. (Slatt *et al.* 1997; Stow & Johansson 2000):

- Newtonian fluids are more likely to spread laterally than plastic debris flows although SDFs are also capable of producing laterally extensive deposits (e.g. Slatt *et al.* 1997; Shanmugam 2000)
- deposition by settling (LDT) and freezing (SDF) results in different sandbody geometry, the latter may develop debris levees (Shanmugam 2000; Stow & Johansson 2000)
- SDF and HDT may emplace thick units of massive sands in deep-water (Stow & Johansson 2000)
- high frequency LDT and SDF may both develop amalgamated deposits with lateral connectivity and sheet-like geometry (Shanmugam 2000)
- SDF may be more sensitive to basinfloor topography due to their higher density (McCaffrey in Purvis *et al.* 2002)
- SDF can travel long distances (>100 km) on gentle slopes (< 1°) while mud-free sandy turbidity currents are rather short-lived (Schwab *et al.* 1996; Shanmugam 2000, Stow & Johansson 2000)
- SDF may be characterised by a sharp, blocks frontal snout; tension may lead to discontinuous, disconnected frontal sandbodies (Shanmugam *et al.* 1995; Shanmugam 2000).

Presently, the distinction between HDT and SDT is difficult at best and no consensus has yet been reached as far as the dominance of one process over the other is concerned, and the concept of facies-related processes requires further work (Stow & Johansson 2000). Further complicating the turbidite *versus* sandy debris flow debate is the fact that bottom current activity may modify deep-water clastic deposits (e.g. Tertiary Sands Frigg Field/North Sea: Enjolras *et al.* 1986; *for further examples see chapter 2.5.5*), and even produce vertical sequences akin to the Bouma sequence (Shanmugam 2000). However, Mutti & Normark (1987) and Normark *et al.* (1993) suggest that in small basins like the Northern Adana Basin or Scapa Subbasin any significant bottom currents are unlikely to develop.

5.1.2 Vertical sequences – fact or fiction

Mutti & Normark (1987) suggest that depositional lobes are characterised by superposed, small-scale thickening-upward microsequences or compensation cycles. However, the concept of asymmetric vertical bed thickness cycles (or megasequences) as proposed by Mutti & Ricci Lucchi (1972) and Ricci Lucchi (1975b) as an easy, diagnostic tool for the discrimination of depositional environments is obsolete (e.g. Miall 1999; Chen & Hiscott 1999a). Amongst mostly random vertical trends dominating fan successions (Anderton 1995), occasional discrete asymmetric vertical bed thickness (and grain size) sequences appear to exist at lobe-scale, but their identification and interpretation in ancient turbidite successions is controversial. Critique is essentially twofold:

- the methodologies employed to discriminate vertical bed thickness trends
- the different types and scales of vertical trends and the responsible mechanisms

Methodologies

In the discrimination of vertical trends subjective, visual appraisal, limited databases (e.g. single section: Lowey 1992; Murray *et al.* 1996), inappropriate test methods (e.g. Fourier analysis testing fixed cyclic periodicities; RUD very sensitive to noise: Murray *et al.* 1996) and incorrectly plotted diagrams (e.g. Hiscotts 1981 critique on Ghibaudo's 1980 plotting) produce unreliable results. The general lack of uniformity between workers regarding analysis and interpretation of type of sequences make comparisons between studies difficult and questionable. Lowey (1992), for example, suggests a visual-statistical approach in the identification of megasequences, which Murry *et al.* (1996) and Chen & Hiscott (1999a) reject on the basis of not obtaining objective, reproducible data. They latter propose to 1) split a vertical section (one-dimensional data) into segments using a combination of the split-moving window and maximum-likelihood estimation techniques, 2) check potential segment boundaries against field data to exclude potential errors, 3) test for asymmetry (with Kendall's rank, Spearman's rank and Pearson's correlation tests) and 4) test for randomness in order to identify potential symmetric or irregular trends (*see* Chen & Hiscott 1999a *for detailed discussion*). Crucial to their proposed procedure and the application of other statistical methods is their consistent application to large datasets. In the case of the Cingöz and Scapa data, this basic requirement is not fulfilled as sections are very short or contain numerous short breaks. The results have thus to be viewed with caution as already indicated (*chapters 2.4.4 and 3.3.2*). Applying their testing to previously interpreted sections, Chen & Hiscott (1999a) did not find a statistical significance of the discriminated vertical asymmetric trends in identifying the depositional environment.

Mechanisms

Initially, the concept of fan progradation creating thickening/coarsening-upward sequences was paramount (e.g. Mutti & Ricci Lucchi 1972) and Normark *et al.* (1993) still suggest that lobes are commonly characterised by thickening-/coarsening-upward sequences. However, vertical aggradation was soon recognised as dominant mechanism, especially in confined settings (e.g. Ricci Lucchi & Valmori 1980; Ricci Lucchi 1985; Shanmugam & Muiola 1988; Chen & Hiscott 1999a), generating random or thinning/fining-upward cycles (table 5.2: *also see chapter 2.4*). However, to large portions of ancient deep-water clastic systems, any form of regular cyclicality, symmetric or asymmetric, appears to be absent (e.g. Nilsen 1980; Piper & Stow 1991) and Anderton (1995), in fact, advocates the predominance of random

SCALE	PATTERN	MECHANISM	REFERENCE
Microscale [< 10 beds]	asymmetric thick-up/ coarsen-up	topographic compensation	Mutti & Sonnino (1980) Mutti & Normark (1987)
	symmetric	compensation	Stow & Johansson (2000)
	random	irregular variations in flow volume, concentrations, sorting, grain size, sea floor topography, flow path, nature of obstacle to flow	compilation in Chen & Hiscott (1999a)
Mesoscale [lobe-scale: 10s of m] (megasequences <i>sensu</i> Ricci Lucchi 1975b)	asymmetric	thick-up/ coarsen-up	topographic compensation lat. shift of channels & lobes MacDonald (1986) Link & Welton (1982)
		thin-up/ fine-up	topographic compensation aggradation retrogradation/lateral shifting this study
	random	lobe swithing, upstream channel avulsion, topographic lobe-to- lobe compensation aggradation	Chen & Hiscott (1999a) Ricci Lucchi (1985)

Table 5. 2: Vertical bed thickness trends at intra- and lobe-scale and their interpretation from selected references.

processes, generating a great number of vertical successions[♦]. These are more likely to relate to stable and unstable areas within a fan system. Vertical successions in lobe deposits result from a complex combination of allocyclic and autocyclic mechanism which control deposition in the distal fan (Normark & Piper 1991). Irregular time, space and magnitude of flow trigger (Eisele & Ricken 1991), flow behaviour of differently composed flows, i.e. downcurrent flow expansion on lobes of mixed or sandy flows while large sand flows may initially erode rather than deposit (Savoie & Piper 1990), topographic compensation (e.g. Mutti & Sonnino 1981; Mutti *et al.* 1994), aggradation etc. result in a variety of micro-scale (m-scale) bed thickness patterns. At lobe-scale, asymmetric sequences are commonly related either to progressive lobe progradation, retrogradation in response to changing sediment input and/or sea-level changes and/or lateral migration or as fining upward and/or random organisation implying aggradation (table 5.2).

5.1.3 Geometries – to be or not to be

All standard models suggest a diagnostic lobate geometry for depositional lobes (e.g. Mutti & Ricci Lucchi 1972, 1975; Stow 1985a; Reading & Richards 1994; Bouma 2000). However, the architecture of deep-water clastic systems in restricted basin settings differs considerably from open deep-water basins and none of these models take into account the modifying effects of basin configuration and underlying seafloor topography which can fundamentally affect the shape, dimension and stacking pattern of lobe deposits (e.g. Normark *et al.* 1993; Reading 1991; Reading & Richards 1994). Thus very few field studies exist where lobate geometries are in fact recorded by either mounded cross-section (e.g. Lauge Koch Land system: Surlyk 1995; limited evidence Cingöz Lobe C) or detailed correlation patterns across 10s of km (fig. 5.2; Mutti *et al.* 1994, Ricci Lucchi 1995). Advocating a strict generic application of the term “lobe” itself (plan view lobate geometry/externally mounded), Normark *et al.* (1993) suggest that the majority of lobe deposits can be described with the sufficiently broad terms: sheet-like, mounded, unconfined and confined. Thus deposits that comprise the lobe element can include:

- sheet-like bodies that in some cases have virtual basinwide extent (e.g. Macigno Formation: Ghibaudo 1980; Hecho Group: Mutti 1985b)
- slightly mounded bodies that can occur at the terminus of basin margin channels (e.g. Lauge Koch Land system: Surlyk 1995; Marnoso-Arenacea Formation/inner Basin, pre-Contessa [lenticular/strongly elongate/wedging] Ricci Lucchi & Valmori 1980; Cingöz Lobe C, Scapa S10 lobes; Kongsfjord Formation: Pickering 1981; Cingöz W-Fan [fig. 5.3] Satur 1999, Satur *et al.* 2000)
- confined bodies that formed as the fill of a variety of both structural and erosional depressions (e.g. Arakynthos sandstone: Schuppers 1995; Lobe A/B: Cingöz E-Fan, Scapa S10 lobes; ‘depositional tongues’ Cingöz W-Fan [fig. 5.3] Satur 1999, Satur *et al.* 2000; backfilling channel geometries: Mutti & Normark 1991; Normark *et al.* (1993), e.g. lower Lobe A deposits: Cingöz E-Fan).

Many of the documented lobe deposits developed in confined basins. Basin margin or intrabasinal confinement can lead to i) maintaining flow competence over long distances (e.g. Scapa S10 lobes; Normark

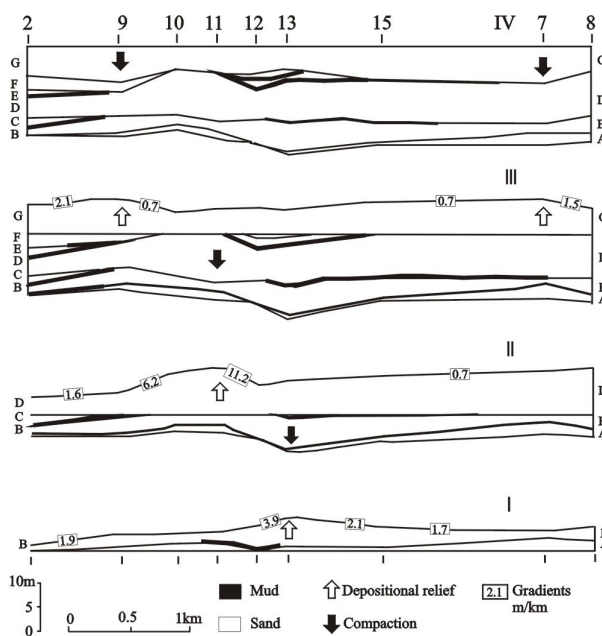


Figure 5.2: Internal stacking pattern of a sandstone body (lobe) deposited in a distal depositional zone of a large Type I system (Miocene Laga Formation, northern Apennines). Note effects of both compensation and compaction on the geometry of individual sandstone beds (from Mutti *et al.* 1994).

[♦] i.e. **uniform**: repetition of same process, **sequence**: progressive change / asymmetric cycles, **cycles**: patterns changing one way or another: e.g. symmetric cycles, **chaotic**: random organisation / no patterns can be recognised

& Piper 1991) and/or ii) flow deflection (e.g. E-Fan; Marnoso-Arenacea/Italy: Ricci Lucchi 1981, 1985; Miocene Turbidite Systems/San Joaquin Basin: Nilsen *et al.* 2002; Annot Sandstone/France: Kneller & McCaffrey 1999; Sinclair 2000; Northern Area Claymore: Kane *et al.* 2002) and iii) in localised depositional thickening (e.g. Cingöz Lobe C; Marnoso-Arenacea/Italy: Ricci Lucchi 1981; Gryphon Field/North Sea: Purvis *et al.* 2002; Monterey & Delgada Fans/offshore California: Wilde *et al.* 1985). Confinement also has a fundamental impact on the stacking and aggradational pattern (fig. 5.2). The highly amalgamated Cingöz Lobe A and B deposits, for example, form thick successions of amalgamated,

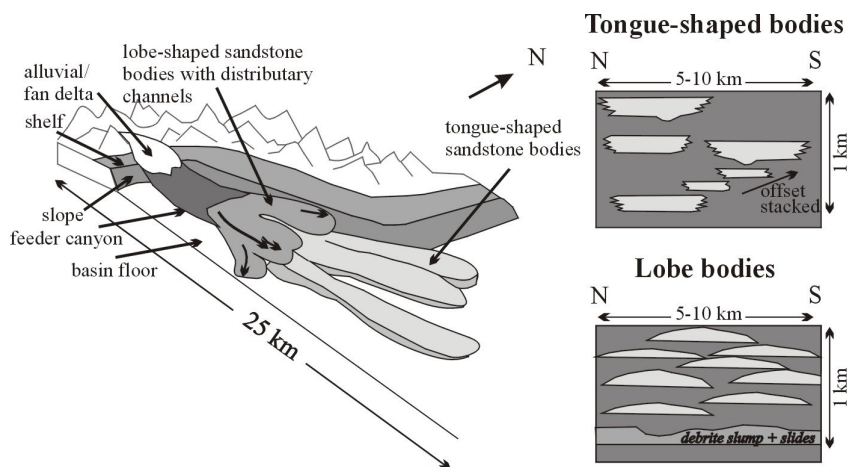


Fig. 5.3: Evolution of the western sector of the deep-water clastic system as sea-level rose in the Lower to Middle Miocene western area of the Cingöz Fan (W-Fan). An alluvial fan/fan delta feeds into the canyon during the early stages of development. The canyon bypasses the contemporaneous shallow marine carbonate shelf. During maximum progradation, the canyon restricts lateral deposition and low sinuosity tongues extend downdip on the basin floor. Later sand lobes with distributary channels develop during retrogradation of the fan. Characteristic sandstone geometry of tongue and lobe-shaped depositional bodies. Compensation cycles and stacking occur within the sheet-like beds of the tongue-shaped bodies. The lobes are composed of laterally thinning and thickening beds that form 30-50 m thick, siltstone and sandstone dominated packages. (From Satur *et al.* 2000)

5.2 Lobes in the subsurface

Mitchum (1985) first related mounded seismic expression with internal bidirectionally downlapping reflections within the lower fan sub-environment to sheetlike lobe sandstones in accordance with the sequence stratigraphic model. And although modern 3-D seismic is able to resolve sandbody geometries within reservoirs revealing stacking patterns and planform geometry (Mitchum *et al.* 1993), it is the combined use of seismic and borehole data which allows a comprehensive analysis of the depositional environments and architectural attributes. Hewlett & Jordan (1993), for example, present one of the first published studies that integrate core data with well logs and multifold seismic, thereby clearly distinguishing individual channel and lobe facies (non-channelized, sheetlike deposits), while Garland *et al.* (1999) were able to recognise depositional lobes in the Miller Field / North Sea. However, lobe deposits do not always appear to be of lobate geometries when interpreted on seismic (fig. 5.4; Pink Reservoir/Gulf of Mexico: Chapin *et al.* 1996), reflecting the strong influence of predepositional topography, depositional mounding, differential compaction and lateral coalescing of deposition on geometries (Garland *et al.* 1999).

Without the aid of seismic, subsurface interpretation relies heavily on the interpretation of single vertical sequences (e.g. individual wells). The recognition of genetic facies associations is important for environmental interpretation (Byant & Flint (1993) and bed thickness measurements and especially the determination of the hierarchically significant bed boundaries are an essential criteria for determining sandbody geometry (Reading 1996; Hurst *et al.* 1999).

aggradationally and/or offset stacked lobes with a near negligible amount of fines interbedded. In case of the Cingöz lobes, the fundamental controls appear to be the availability of sand and shale to the system and deposition in a confined space.

Mobilisation by syn- to postdepositional processes can further modify lobe geometry such as sand remobilisation and injection (e.g. Shanmugam *et al.* 1995; Shanmugam 2000; Purvis *et al.* 2002) or extreme differential compaction creating oversteepened, mould-like geometries (Heritier *et al.* 1979; Stow & Johansson 2000).

5.3 Outcrop versus subsurface data: opportunities and limitations

Outcrop data serve as analogues for subsurface systems with the aim to grasp their potential complexity in order to enhance reservoir characterisation and ultimately hydrocarbon recovery. Purvis *et al.* (2002) demonstrate that simple 1:1 translation of outcrop data may not adequately represent a complex subsurface system and that sometimes novel approaches are needed. Modelling the Balder reservoir sands of the Gryphon Field / North Sea, they utilised a combination of the Tabernas / Spain and Jackfork Group / USA representing different stages of the field. As with this example and all other knowledge transfer from outcrop to subsurface or modern to ancient systems, one has to be aware of the strengths and limitations of each data set.

a) data sets

Outcrop analysis

It is evident that the lateral extent of outcrops, though limited through tilting formations and outcrop size, allows for a thorough analysis of the depositional environment thus providing valuable information on deep-water clastic systems (Mutti & Normark 1987). With the description of bedding surface hierarchies (Allen 1980), the move from a series of laterally correlated to 1-D vertical sections to 2-D descriptions was taken, however, crucial 3rd dimension in a horizontal direction is lacking mostly due to inadequate exposure (Hurst *et al.* 1999). Detailed mapping and stratigraphic analysis of well-exposed sections, however, may provide some information on the extent and shape of deposits (Mutti & Normark 1987).

Subsurface analysis

In the ideal case, subsurface analysis can draw on both borehole (core and wireline) and seismic data. Although boreholes provide only a billionth of the total reservoir volume, they permit a very detailed description of the reservoir through interpretation of the depositional environment and providing rock property data (Fox 1992). It is imperative to calibrate wireline data with cores. Interwell correlation based on borehole data is difficult at best, mostly operating under severe simplifications (*see below*). Seismic, in contrast, does provide information at interwell scale and modern 3-D seismic and/or a densely drilled fields may provide some 3 D information on the distribution, stacking pattern and geometry of the genetic units and heterogeneities (Matheron *et al.* 1987; Mijnsen *et al.* 1993; Mitchum *et al.* 1993).

b) knowledge transfer and limitations

Scale of observation

Outcrop and subsurface data provide different types of data gathered at different scales. Lobe deposits described from outcrop have lithologic significance, whereas lobes described on multichannel seismic reflection or side-looking sonar data are strictly a geometric description unless further data indicates their depositional lobe character (e.g. Hewlett & Jordan 1993; Garland *et al.* 1999). In order to produce useful comparisons between geological features in deep-water systems it is imperative that these are made at similar spatial and temporal scales and their interpretations should be constrained within an accurate stratigraphic framework (Mutti & Normark 1987). Although the actual lobe deposits of the Cingöz

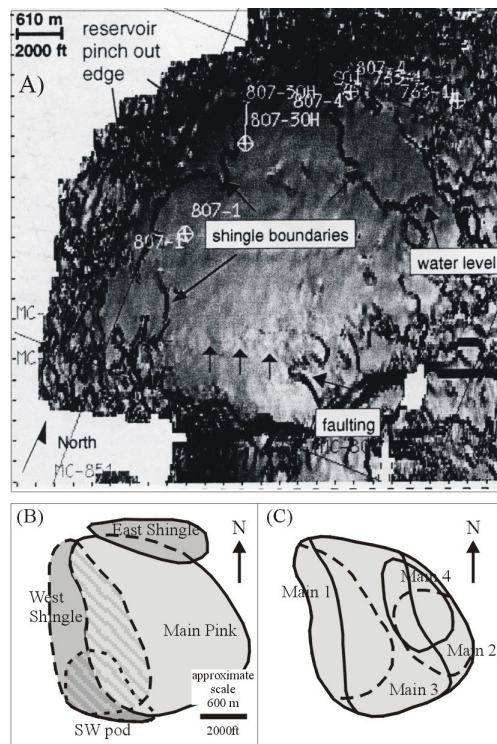


Figure 5.4: A) Seismic dip map, showing some stratigraphic and structural features of Main Pink Reservoir, Gulf of Mexico. Dark gray = high local gradient, light gray = low local gradient. B) Schematic, plan view drawing of four principal sand bodies of the Simple Model. C) Smaller-scale shingles within the Main Pink in the Complex Model. (From Chapin *et al.* 1996)

Formation and Scapa Sandstone Member are nearly of similar scales (i.e. thickness), the temporal and spatial evolution of the two systems differ fundamentally.

Scaling

In the subsurface upscaling, from, selected small-scale sedimentary key features that in turn are diagnostic of larger-scale geometric features limits their value in reservoir characterisation. Particularly data such as permeabilities and porosities which represent the properties of the immediate surrounding of the wells (micro-scale) are, with severe simplifications, upscaled to meso- and mega-scale and used for interwell correlation (Mijssen *et al.* 1993). Hurst *et al.* (1999) propose the reverse, to downscale mapped or seismically detectable features to interwell-scale packages ever mindful of the underlying paleotopography. They believe that once these features are constrained, modelling will result in a better reflection of the reservoir including its smaller-scale characteristics.

Translating the detailed outcrop study (Lobe A/B/C) in terms of heterogeneities to an imaginary core, fundamentally different results would be expected for upscaling. The discontinuous shale-draped amalgamation planes of the Lobe C may be overemphasised to represent continuous shale-barriers because of the overall “shale-rich” nature of the deposits while the paucity of shales in Lobe B might lead to underestimating the proven lateral extend, i.e. erosional cut-off as observed in Lobe A.

Bounding surfaces

Introduced by Allen (1983) for fluvial deposits, the concept of bounding surfaces has been translated to channelized deep-water clastic deposits (e.g. Pickering *et al.* 1995). The importance of the scheme is that it reflects changes in depositional pattern. It assumes that similar architectural elements (or building blocks) of ancient and modern systems are comparable based on facies, geometry and bounding surface hierarchy through plan and/or sectional analysis. Hurst *et al.* (1999) suggest that this approach already allows for enhanced comparison between outcrop and subsurface data.

Correlations

In outcrop as well as in subsurface correlations rely on biostratigraphical data, correlatable marker horizons, pressure data, the application of submarine fan models and seismic data. However, high sedimentation rates in sand-rich systems may prevent detailed biostratigraphic correlation patterns (e.g. E-Fan, Cingöz Formation), while in the case of the Scapa S10 interval, biostratigraphy provides the only viable source of interwell correlation. Also, marker beds prove to be only of local significance (S10 interval) or are absent (E-Fan). The application of wireline data for subsurface systems is equally limited (*see above*).

Bed thickness is generally an unreliable characteristic for interwell correlation. Hurst *et al.* (1999) found that individual beds and bed packages display thickness variations driven by offset-stacking over distances > 100 m and would thus be inadequate for interwell correlation with typical well spacing of 0.7 to 1 km. They propose the use of thicker composite units for correlation which can be traced and identified over kms. Mutti *et al.* (1994) suggest that high-resolution correlation patterns are possible in deep-water clastic systems based on high-frequency cyclic stacking patterns, e.g. cyclic stacking pattern of Oligocene Ranzano Sandstone/Northern Apennines.

5.4 Lobes - a fundamental element in models

Results from COMFAN I (Bouma 1983) revealed that modern and ancient fan systems are highly dynamic and complex features. The initial vision of an all-encompassing model with fixed fan segments such as inner, middle and outer fan (e.g. Mutti & Ricci Lucchi 1972; Walker 1978; Shanmugam & Muiola, 1988) proved to be too simplistic and was subsequently abandoned (Normark 1991; Walker 1992; Miall 1999). However, the lobe element, including sheetlike, mounded and confined non-channelized deposits, continues to be recognised as a fundamental deep-water clastic element (fig. 5.1; e.g. Stow 1985a; Mutti & Normark 1987, 1991; Reading & Richards 1994; Richards *et al.* 1998; Bouma 2001), where the formation of lobes is requiring relatively stable channels to focus multiple flows onto specific sites in the basin (Galloway 1998). However, Shanmugam (2000) criticizes that fan models comprising channels and lobes are all too simplistic and continue to dominate deep-water sedimentology and sequence stratigraphy. Shanmugam’s (2000) critique may be somewhat justified as lobe elements are well documented in ancient systems on which many models are based but in modern systems they are still largely unknown (Mutti & Normark 1991), which

partly stems from the difficulty of properly sampling modern sandy deposits. And while modern systems basically represent a static snap-shot of the present, ancient systems cover a significant time and evolutionary span and may consequently be more complex. Nevertheless, small, sand-rich fans are very common and form the majority of outcrop studies and in subsurface hydrocarbon exploration. One may suspect that “this results from greater economic interest or better preservation potential for these fans, but it probably does reflect their importance as a depositional environment” (Kenyon *et al.* 2002).

Deep-water clastic systems and the lobe element are controlled in their development by many factors including the basin size and configuration, amount and type of sediment available for resedimentation processes, rates of deposition, (frequency and volume of gravity flows), local tectonic control, bottom current activity, and relative sea level variations (e.g. *chapter 2.5*; Normark *et al.* 1993). Each system is governed by a combination of these and other factors resulting in unique facies characteristics, internal stacking patterns and types of geometry of, e.g. the lobe element, which may vary greatly between systems. Embracing this variety with broader definitions to include hitherto non-typical lobe deposits is suggested (*see below*; Normark *et al.* 1993).

In modern and subsurface systems, lobes are a decidedly geometric feature. Recognition of lobes in the subsurfaces is aided by the sequence stratigraphic concept as it provides the base for linking mounded seismic facies with bidirectionally downlapping reflectors with sheet-like turbidite deposits (Mitchum 1985; Shanmugam 2000). The sequence stratigraphic fan model is particularly relevant to seismic stratigraphy as seismic tends to reflect chronostratigraphic boundaries rather than lithostratigraphic units (Bryant & Flint 1993). The sequence stratigraphic model feeds on the central assumption that sedimentation increases during relative sea-level lowstand and many researchers associate the maximum depositional activity with the late phase of the sea level lowering and the beginning of a transgressive systems tract (e.g. Kolla & Perlmutter 1993). However, many recent studies have shown that in tectonically active basin, with narrow shelves and direct connection with the hinterland via incised canyons, sea level variations may be of lesser significance (e.g. Cingöz Formation, Scapa Sandstone Member; *chapter 2.5.2*). Typically, the base of channel incision is considered to be a major timeline in sequence stratigraphy, however, Cronin *et al.* (1998) demonstrate that in the Campodarbe Group, the major phase of basin reorganisation is related to slump and debris flow deposition and suggest that, contrary to popular believe, sandy channeling presents a period of relative quiescence. This demonstrates that no simple relationships exist between sea level and deposition in deep-water clastic systems, limiting the application of the sequence stratigraphic concept.

5.5 Lobes or what?

Like other studies before, this study has shown that the term depositional lobe *sensu stricto* is too restricted to reflect the variety of laterally extensive, non-channelized sand deposits observed in deep-water clastic systems. While the majority of criteria appear to fit, fundamental differences were recorded where geometry and vertical sequences are concerned. In the last decade it has become clear that a more embracing *sensu lato* definition is needed to adequately reflect the variety of documented, non-typical lobes. In a first step, Normark *et al.* (1993) formulated a broader definition which enables to include the majority of the documented non-channelized, sandy deep-water clastic deposits in the lobe elements such as sheetlike, mounded, unconfined, confined deposits (*see chapter 5.2.3*).

In their models, Reading & Richards (1994) and Richards *et al.* (1994) differentiate between channelized

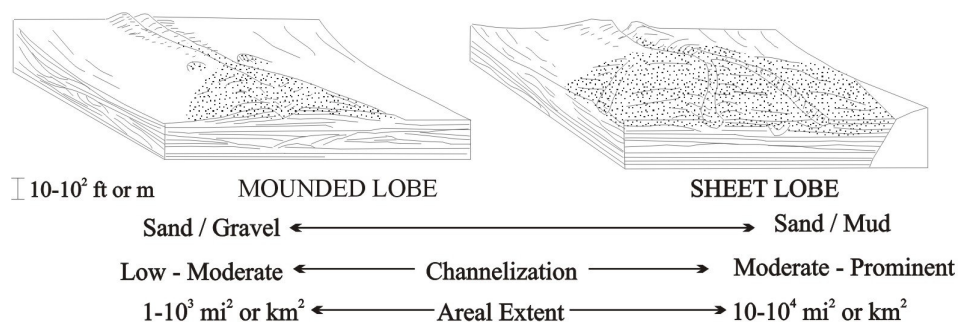


Figure 5.5: Block diagrams illustrating the morphology and stratigraphic geometry of coarse-grained mounded turbidite lobes and finer sand to muddy turbidite sheet lobes. No horizontal scale. (From Galloway & Hobday 1996).

and depositional lobe and sheet deposits. Channelized lobes have been described in modern and ancient systems, for example the depositional lobes of the Mississippi, which are essentially made up of channelized, laterally less extensive sand deposits (Schwab *et al.* 1996) or the channelized lobe of the upper Ebro fan of Nelson *et al.* (1985), which Shanmugam & Muiola (1991) interpret to represent a channel-levee complex. The Lobe A and B of the E-Fan Cingöz Formation display some degree of channeling which differs greatly from the above examples, while the Scapa S10 lobes may represent a “hybrid” model where structural confinement leads to prolonged flow competence and relatively distal channeling in connection with overall lobe deposition. Galloway & Hobday (1996) suggest that grain size is a fundamental control in the appearance of the lobe, coarser lobes are mounded and contain less channeling while finer-grained lobes are of sheetlike geometry and with some channeling (fig. 5.5); while Reading & Richards (1994) and Richards *et al.* (1998) propose the opposite (fig. 5.1). Their sheets and lobes are differentiated based on sand content (sheets: < 30 %; lobes: 30 – 70 %) and geometry.

The recognition of depositional lobes *sensu lato* can be carried out by various means. In outcrop they may simply be defined as set of unchannelized sandstone bodies located in the proximal to distal fan environment which are fed by channelized flows from adjacent basin margin areas and/or by sheet flows directly derived from large shelf edge failures (Ghibaudo 1980, Normark *et al.* 1993). Careful facies analysis provides further information on the nature of the lobe deposits and Shanmugam (2000) cautions to keep depositional processes in mind when carrying out environmental interpretations. Larger-scale (> 100s of m) mapping can help reveal the sandbody geometry. The documentation of the latter in conjunction with the stacking pattern are recognised as critical in characterisation of any architectural element (Stow & Mayall 2000). Chen & Hiscott (1999b) advocate the use of statistically determined degree of sandbed clustering as an additional tool for discrimination. They found lobe deposits to be characterised by a moderate clustering of bed thickness, grain size and sandstone percentage, inferred by a medium Hurst K and a moderate departure from the mean value of K for random sequences. Hurst K is an estimator of the degree of clustering of high and low values or thin and thick beds.

Following this discussion, depositional lobes *sensu lato* or the lobe element can be described as:

- laterally extensive, non-channelized, sandy deep-water clastics
- in proximal locations or confined settings, some degree of channeling may be present
- geometries range from sheetlike, mounded, confined to unconfined (Normark *et al.* 1993)
- transport and depositional mechanisms range from low density (LDT) to high density (HDT) turbidity currents and sandy debris flows (SDF) resulting in a suite of graded, non-graded, inversely graded and massive primarily sandy deposits (e.g. Stow & Johansson 2000; Shanmugam 2000)
- individual or compound beds may range in bed thicknesses from thin- to thick-bedded and in sand-rich systems to megabeds or DWMS (*sensu* Stow & Johansson 2000)
- bed amalgamation, shallow scouring and floating clasts appear to be common
- vertical sequences are not diagnostic of the depositional environment. At micro- to mega-scale they may range from distinctly asymmetric to random generated by a variety of auto- or allocyclic mechanisms
- characterised by moderate sand bed clustering (Chen & Hiscott 1999b)
- much of the lobe character is a direct result of the controlling mechanisms and of the availability of sand to the basin.

6 CONCLUSION AND FURTHER WORK

The study of the non-channelized sand lobe element has shown that lobe deposits are characterised by a range of features which do not conform with the *sensu stricto* definition of Mutti & Normark (1987, 1991). Studying lobe deposits in outcrop enhanced the understanding of potential controlling factors on the lobe development of the S10 lobes, and although the Miocene Cingöz Formation and the E-Cretaceous Scapa Sandstone Member share some broad characteristics, i.e. tectonically controlled deposition during overall

transgression, the scale and temporal differences make the Cingöz Formation (E-Fan) an unsuitable analogue for the Scapa Formation (S10 interval).

- I. Depositional lobes *sensu lato* can be defined as laterally extensive, non-channelized sandy deep-water clastic deposits resulting from LDT/HDT and SDF processes. In proximal or confined settings, some degree of channeling may be present. They are of sheet-like, mounded, unconfined and/or confined geometry. Diagnostic vertical sequences do not exist, however, occasional symmetric or asymmetric sequences may result from a variety of auto- and/or allocyclic mechanisms. Moderate sandbed clustering may be a statistically diagnostic criteria. The unique character of a depositional lobe depends largely on the controlling mechanisms (e.g. sand:mud ratio, tectonic setting, sea level changes, rate and type of sediment supply) governing the respective system and on the availability of sand to the system.

E-Fan, Cingöz Formation:

- II. The E-Fan of the Mid-Miocene Cingöz Formation (southern Turkey) represents a regressive, extremely sand-rich, multi-sourced deep-water clastic system deposited in a triple junction escape basin sourced from the emerging Tauride Orogen.
- III. Time-stratigraphic changes saw the E-Fan system evolve from a gravel-dominated system during late Burdigalian to a sand-dominated system in late Burdigalian – Langhian times and from a type II to type I ? system *sensu* Mutti (1985a), probably resulting from progressive sea-level rise and denudation of the hinterland. The changing spatial and temporal distribution and the character of the resedimented deposits points to tectonism as the fundamental mechanism controlling the sediment supply pattern and the depositional geometry of the fan and its building blocks. Locally enhanced deposition, (western-) lateral restricted dispersal and the apparent eastern deflection of the E-Fan are the most apparent results. The overall retrogradation of the E-Fan is driven by the rising sea level and progressive denudation of the Taurus orogen.
- IV. During the sandy growth stage, the bulk of the sand accumulated in laterally extensive, thick, coarse-grained, sheet-like bodies of channel-lobe transition (Lobe A), proximal (Lobe B) and distal (Lobe C) depositional zones. Lobes A and B do not fit the classical lobe definition *sensu* Mutti & Normark (1987, 1991), while Lobes C are more akin to it. The size, geometry and vertical stacking of the lobes reflect to some degree their restricted spatial, aggradational development. Unique component associations characterise the various depositional environments, with some degree of channeling characterising the proximally located lobes. Conspicuous downcurrent changes involve a decrease in the net sand content, an apparent increase in internal organisation. Conspicuous fining upward at lobe and system scale reflect the gradually rising sea level, while sporadic phases of progradation and/or coarse clastic sediment supply, suggest that a combination of higher frequency sea-level fluctuations and tectonism control lobe development. Lobe stacking becomes increasingly less common.
- V. The macro- and megascopic reservoir characterisation of the Cingöz lobe deposits clearly shows their interest as exploration target due their great areal extend, the overall high net sand content and the extremely good vertical and lateral connectivity. Flow barriers, such as shale layers, are absent in the most proximal areas (Lobe A/B) and only appear in a down-current direction, compartmentalising the distal reservoir (Lobe C).
- VI. Contrary to previous development models, thick, dominantly muddy debris flow deposits form a major feature in the E-Fan and indicate repeated tectonic activity throughout the sandy growth stage. The W-Fan prograded into the formerly E-Fan depositional area during late Burdigalian times was active much longer than previously suggested. The net sand transfer from west to east is unknown.

Further work:

The study of the E-Fan, the Cingöz Formation and subsequently the Neogene fill of the Northern Adana Basin would benefit from the integration of yet unpublished seismic and core data located further to the south which could help construct a more comprehensive model of the gravelly and sandy growth stage of the E-Fan and other formations. Together with a more detailed biostratigraphic and geochemical framework, hitherto non- or poorly integrated sections may be tied into the overall framework. Especially the geochemical data could counteract problems arising from faulting or missing biostratigraphy.

S10 interval, Scapa Sandstone Member:

- VII. The S10 interval of the Lower Cretaceous Scapa Sandstone Member (Scapa Field, UK block 14/19, North Sea) is akin to a multiple sourced mud/sand-rich to sand-rich submarine ramp system *sensu* Reading & Richards (1994) with some features of a slope apron system. The multiple feeder zones funnel sediment off the Halibut Shelf and together with minor sources off the shelf, slope, Claymore High and intraformational sources give rise to a system with complex interdigitation of facies lacking clear proximal-distal trends. The S10 interval records renewed deep-water clastic progradation into the central Scapa Field area.
- VIII. Although the S10 interval was deposited during gradually rising sea level, tectonism appears to be the fundamental control overriding sea level fluctuations. Lateral, northward migration during subzones VJ-VI and local retrogradation of the system is in response to locally decreasing sediment supply and shifting sources caused by differential uplift of the source area. Source area tectonism controlled local sea level, the sediment volume and pathways into the Scapa syncline and thus the geographic location. Basinal tectonism resulted in probably fault-controlled intrabasinal depressions which captured flows resulting in thick aggradational patterns and localised, confined sediment accumulation. Localised basinal uplift resulted in areally confined erosion.
- IX. The S10 interval is dominated by sandy lobe deposition and a subordinate distributary system. The little to non-channelized depositional lobe and lobe fringe deposits are unlike classical lobes *sensu* Mutti & Normark (1987). Sediment bypass close to the conglomeratic fringe resulted in detached lobes developing basinward from the base-of-slope. The shifting activity of the various feeder zones combined with a complex basinfloor topography resulted in localised, stacked, aggradational lobe accumulation of elongate geometry indicating that deposition was not altogether free to move. Individual lobes are mainly composed of high- and low-density sandy turbidites and possibly sandy debris flows *sensu* Shanmugam (1996).
- X. The chronostratigraphic S10 interval comprises the diachronous SD reservoir unit and parts of the SC/SE non-reservoir units. The sandstones of the S10 lobe deposits display a wide range of permeability values indicating that flow units and reservoir compartmentalisation are fundamentally controlled by the degree of carbonate cementation.

Further work:

To gain a more complete picture of the development of the S10 interval and the Scapa Sandstone Member and thus the factors governing lobe accumulation in small, fault-controlled basin, further work would benefit from a refined biostratigraphic framework to fully include some of the study wells and refine S10 depositional model. The inclusion of seismic data may further help to unravel sandbody geometry. Additionally, extending the present environmental and depositional model of the S10 interval for the whole SSM would enable to examine larger spatial and temporal changes within the Scapa system including their controls.

REFERENCES

- Aksu, A.E., Calon, T., Piper, D.W.J., Turgut, S. & Izdar, E. (1992) Architecture of later orogenic Quaternary basins in northeastern Mediterranean Sea. *Tectonophysics* 210, 191 - 213.
- Allen, J.R.L. (1971) Mixing at turbidity current heads and its geological implications. *Journal of Sedimentary Petrology* 41, 97 - 113.
- Allen, J.R.L. (1983) Studies in fluvial sedimentation: bars, bar-complexes and sandstone sheets (low sinuosity braided streams) in the Brownstones (L. Devonian), Welsch Borders. *Sedimentary Geology* 33, 237 – 293.
- Aktaş, G. & Robertson, A.H.F. (1984) The Maden Complex, SE Turkey: evolution of a Neotethyan continental margin. In: Dixon, J.E. & Robertson, A.H.F. (eds) *The geological evolution of the eastern Mediterranean*. Geol. Soc. London Special Publication 17, 375 – 402.
- Anderton, R. (1995) Sequences, cycles and other nonsense: are submarine fan models any use in reservoir geology? In: Hartley, A.J. & Prosser, D.J. (eds) *Characterization of deep marine clastic systems*. Geol. Soc. London Special Publication 94, 5 - 11.
- Andrews, I.J., Long, D., Richards, P.C., Thomson, A.R., Brown, S., Chesher, J.A., & McCormac (1990) *The geology of the Moray Firth*. UK Offshore Regional Report, BGS, HMSO, London, 96p.
- Boote, D.R.D. & Gustav, S.H. (1987) Evolving depositional systems within an active rift, Witch Ground Graben, North Sea. In: Brooks, J. & Glennie, K.W. (eds) *Petroleum geology of north west Europe*. Graham & Trotman, London, 819 - 833.
- Bouma, A. (1962) *Sedimentology of some flysch deposits: A graphical approach to facies interpretation*. Elsevier, Amsterdam, 168 p.
- Bouma, A. (1983) COMFAN. *Geo-Marine Letters* 3: 2-4, 53 - 224.
- Bouma, A. (2000) Coarse-grained and fine-grained turbidite systems as end member models: applicability and dangers. *Marine Petroleum Geology* 17, 137 - 143.
- Bouma, A. (2001) Fine-grained submarine fans as possible recorders of long- and short-term climatic changes. *Global and Planetary Change* 28, 85 - 91.
- Bouma, A.H., Coleman, J.M. & DSDP Leg 96 Shipboard Scientists (1985) Mississippi Fan Leg 96 program and principal results. In: Bouma, A.H., Barnes, A.H. & Normark, W.R. (eds) *Submarine fans and related turbidite systems*. New York, Springer-Verlag, 247 - 252.
- Bouma, A.H., DeVries, M.B., & Stone, C.G. (1997) Reinterpretation of depositional processes in a classic flysch sequence (Pennsylvanian Jackfork Group), Ouachita Mountains, Arkansas and Oklahoma: Discussion. *AAPG Bulletin*, Vol 81:3, 470 - 472.
- Bruhn, C.H.L. & Walker, R.G. (1995) High-resolution stratigraphy and sedimentary evolution of coarse-grained canyon-filling turbidites from the Upper Cretaceous transgressive megasequence, Campos Basin, offshore Brazil. *Journal of Sedimentary Research* B65: 4, 426 - 442.
- Burgess, P.M. & Hovius, N. (1998) Rates of delta progradation during highstands: consequences for timing of deposition in deep-marine systems. *Journal of the Geol. Soc. London*, 155, 217 - 222.
- Burgess, P.M., Flint, S.S. & Johnson, S. (2000) Sequence stratigraphic interpretation of turbiditic strata: an example from Jurassic strata of the Neuquen basin, Argentina. *GSA Bulletin* 112: 11, 1650 – 1666.
- Bryant, I.D. & Flint, S.S. (1993) Quantitative clastic reservoir geological modelling: problems and perspectives. In: Flint, S.S. and Bryant, I.D. (eds) *The geological modelling of hydrocarbon reservoirs and outcrop analogues*. Oxford, Blackwell Scientific Publishers, 3 - 20.
- Cazzola, C., Fonesu, F., Mutti, E., Rampone, G., Sonnino, M. & Vigna, B. (1981) Geometry and facies of small, fault controlled deep-sea fan system in a transgressive depositional setting (Tertiary Piedmont Basin, northwest Italy). In: Ricci Lucchi, F. (ed) *Excursion guidebook; 2nd European Regional IAS Meeting*. Bologna, 5 - 56.
- Cazzola, C., Mutti, E. & Vigna, B. (1985) Cengio turbidite system, Italy. In: Bouma, A.H., Normark, W.R. & Barnes, N.E. (eds) *Submarine fans and related turbidite systems*. New York, Springer Verlag, 179 - 183.
- Chapin, M.A., Tiller, G.M. & Mahaffie, M.J. (1996) 3-D architecture modeling using high resolution seismic data and sparse well control: example from the Mars “Pink” reservoir, Mississippi Canyon area, Gulf of Mexico. In: Weimer, P. & Davis, T.L. (eds) *AAPG Studies in Geology 42 and SEG Geophysical Development Series 5*, AAPG/SEG, Tulsa, 124 - 132.
- Chen, C. & Hiscott, R.N. (1999a) Statistical analysis of turbidite cycles in submarine-fan successions: tests for short-term persistence. *Journal of Sedimentary Research* 69:2, 486 - 504.

- Chen, C. & Hiscott, R.N. (1999b) Statistical analysis of facies clustering in submarine-fan successions. *Journal of Sedimentary Research* 69: 2, 505 - 517.
- Clark, J.D. & Pickering, K.T. (1996) *Submarine channels: processes and architecture*. London, Vallis Press, 231 p.
- Clift, P.D., Shimizu, N., Layne, G.D., Blusztajn, J.S., Gaedicke, C., Schlüter, H.U., Clarke, M.K. & Amjad, A. (2001) Development of the Indus Fan and its significance for the erosional history of the Western Himalaya and Karakoram. *GSA Bulletin* 113: 8, 1039 - 1051.
- Cornamusini, G. & Sandrelli, F. (2002) Architecture and depositional evolution of a foredeep's sand-rich turbidite system of the northern Apennines. 16th International Sedimentological Congress, Johannesburg, 60 - 61. [abstract]
- Cronin, B.T. (1994) Channel-fill architecture in deepwater sequences: variability, quantification and applications. Ph.D. Thesis, University of Wales, Cardiff, 332 p. [unpublished]
- Cronin, B.T., Owen, D., Hartley, H. & Kneller, B. (1998). Slumps, debris flows and sandy deepwater channel systems: implications for the application of sequence stratigraphy to deepwater clastic systems. *Journal of the Geol. Soc., London*, 155, 429 - 432.
- Cronin, B.T., Gürbüz, K., Hurst, A., & Satur, N. (2000) Vertical and lateral organisation of a carbonate deep-water slope marginal to a submarine fan system, Miocene, southern Turkey. *Sedimentology* 47, 801 - 824.
- Damuth, J.E. & Flood, R.D. (1985) Amazon Fan, Atlantic Ocean. In: Bouma, A.H., Barnes, N.E. & Normark, W.R. (eds) *Submarine fans and related turbidites systems*. New York, Springer Verlag, 97 - 106.
- Damuth, J.E., Flood, R.D., Kowsmann, R.O., Belderson, R.H. & Gorini, M.A. (1988) Anatomy and growth patterns of Amazon deep-sea fan revealed by long-range side-scan sonar (GLORIA) and high-resolution seismic studies. *AAPG Bulletin* 72, 885 - 911.
- Davis, J.C. (1986) *Statistics and data analysis in geology*. Second edition. John Wiley & Sons, New York, 646 p.
- Dermican, H. & Toker, V. (1998) The role of trace fossils in basin analysis: Cingöz Formation and associated facies, southern Turkey, as a case study. In: Third International Turkish Geology Symposium. Middle Eastern Technical University, Ankara, Turkey, 218. [abstract]
- Dewey, J.F., Hempton, M.R., Kidd, W.S.F., Saröglü, F. & Sengör, A.M.C. (1986) Shortening of continental lithosphere: the neotectonics of eastern Anatolia: a young collision zone. *Special Publication of the Geol. Soc. London*, 3 - 36.
- Dixon, R.J. & Pearce, J. (1995) Tertiary sequence stratigraphy and play fairway definition, Bruce-Beryl Embayment, Quadrant 9, UKCS. In: Steel *et al.* (eds) *Sequence stratigraphy of the Northwest European margin*. NPF Special Publication 5, 443 - 469.
- Einsele, G. (1991) Submarine mass flow deposits and turbidites. In: Einsele, G., Ricken, W. & Seilacher, A. (eds) *Cycles and events in stratigraphy*. Springer Verlag Berlin, 313 - 339.
- Einsele, G. & Ricken, W. (1991) Introductory remarks – larger cycles and sequences. In: Einsele, G., Ricken, W. & Seilacher, A. (eds) *Cycles and events in stratigraphy*. Springer Verlag Berlin, 611 - 616.
- Einsele, G., Liu, B., Dürr, S., Frisch, W., Liu, G., Luterbacher, H.P., Ratschbacher, L., Ricken, W., Wendt, J., Wetzel, A., Yu, G. & Zheng, H. (1994) The Xigaze forearc basin: evolution and facies architecture (Cretaceous, Tibet). *Sedimentary Geology* 90, 1 – 32.
- Ercilla, G., Alonso, B., Perey-Belzuz, F., Estrada, F., Baraza, J. Farran, M. Canals, M. & Masson, D. (1998) Origin, sedimentary processes and depositional evolution of the Agadir turbidite system, central eastern Atlantic. *Journal of the Geol. Soc. London*, 155, 929 - 939.
- Ericella, G., Alonso, B., Estrada, F., Chiocci, F.L., Baraza, J. & Farran, M. (2002) The Magdalena Turbidite System (Caribbean Sea): present-day morphology and architecture model. *Marine Geology* 185, 302 – 318.
- Enjolras, J.M., Gouadain, J., Mutti, E. & Pizon, J. (1986) New turbiditic model for the lower Tertiary sands in the South Viking Graben. In: Spencer, A.M., Holter, E., Campbell, C.J., Hanslein, S.H., Nysther, E. & Ormaasen, E.G. (eds) *Habitat of hydrocarbons on the Norwegian continental shelf*. Graham & Trotman, London, 171 - 178.
- Eschard, R. (2001) Geological factors controlling sediment transport from platform to deep basin: a review. *Marine and Petroleum Geology* 18, 487 – 490.
- Friedman, G.M. & Sanders, J.E. (1997) Dispelling the myth of seafloor tranquility. *Geotimes* 42, 24 - 27.
- Flood, R.C., Manley, P.L., Kowsmann, R.O., Appi, C.J. & Pirmez, C. (1991) Seismic facies and later Quaternary growth of the Amazon submarine fan. In: Weimer, P. & Link, M.H. (eds) *Seismic facies and sedimentary processes of modern and ancient submarine fans and turbidite systems*. New York, Springer Verlag, 247 - 272.
- Flood, R.D., Piper, D.J.W. & Shipboard Scientific Party (1995) Proceedings of the Ocean Drilling Program, initial Reports. In: Flood, R.D., Piper, D.J.W. & Klaus, A. (eds) *Ocean Drilling Program*. College Station, A & M University Texas 155, 5 - 16.

- Floyd, P.A., Kelling, G., Gökçen, S.L. & Gökçen, N. (1992) Arc-related origin of volcanoclastic sequences in the Misis Complex, Southern Turkey. *Journal of Geology* 100, 221 - 230.
- Foster C. (1995) Vertical sequences in turbidite successions: fact or fiction. Ph.D thesis, University of Southampton, 275 p. [unpublished]
- Freer, G., Hurst, A. & Middleton, P. (1996) Upper Jurassic sandstone reservoir quality and distribution on the Fladen Ground Spur. In: Hurst *et al.* (eds) *Geology of the Humber Group: Central Graben and Moray Firth*, UKCS. Geological Special Publication No. 114, 235 - 249.
- Frey, R.W. & Pemberton, S.G. (1984) Trace fossil facies models. In: Walker, R.G. (ed.) *Facies models*. Geoscience Canada Reprint Series, 189 - 207.
- Fox, C. (article editor; 1992) Reservoir characterisation using expert knowledge, data and statistics. *Oilfield Review* 4: 1, 25 - 39.
- Galloway, W.E (1998) Siliciclastic slope and base-of slope depositional systems: component facies, stratigraphic architecture, and classification. *AAPG Bulletin* 82: 4, 569 – 595.
- Galloway, W.E. & Hobday, D.K. (1996) *Terrigenous clastic depositional systems* (2nd edition). Springer Verlag Heidelberg, 489 p.
- Garland, C.R., Haughton, P., King, R.F. & Moulds T.P. (1999) Capturing reservoir heterogeneity in a sand-rich submarine fan, Miller Field. In: Fleet, A.J. & Boldy, S.A.R. (eds) *Petroleum Geology of northwestern Europe: Proceedings of the 5th Conference*. Geol. Soc. London, 1199 - 1208.
- Garrison, L.E., Kenyon, N.H. & Bouma, A.H. (1982) Channel systems and lobe construction in the Mississippi Fan. *Geo-Marine Letters* 2, 31 - 39.
- Geehan, G.W. & Underwood, J. (1993) The use of length distribution in geological modelling. *IAS Special Publication* 15, 205 - 212.
- Ghibaudo, G. (1980) Deep-sea fan deposits in the Macigno Formation (Middle-Upper Oligocene) of the Gordana Valley, Northern Apennines, Italy. *Journal of Sedimentary Petrology* 50: 3, 0723 - 0742.
- Ghibaudo, G. (1981) Deep-sea fan deposits in the Macigno Formation (Middle-Upper Oligocene) of the Gordana Valley, Northern Apennines, Italy – Reply. *Journal of Sedimentary Petrology*, 51-3. 1021 - 1033.
- Ghibaudo, G. (1992). Subaqueous sediment gravity flow deposits: practical criteria for their field description and classification. *Sedimentology* 39, 423 - 424.
- Gökçen, S.L., Kelling, G., Gökçen, N. & Floyd, P.A. (1988) Sedimentology of a Late Cenozoic collisional sequences: the Misis Complex, Adana, Southern Turkey. *Newsletter Stratigraphy* 24, 111 - 135.
- Gonthier, E.G., Faugeres, J.C. & Stow, D.A.V (1984) Contourite facies of the Faro Drift, Gulf of Cadiz. In: Stow, D.A.V. & Piper, D.J.W. (eds) *Fine-grained sediments: deep-water processes and facies*. Geol. Soc. London Special Publication, 275 - 292.
- Görür, N. (1977) Sedimentology of the Karaisali limestone and associated clastics (Miocene) of the northwest flank of the Adana Basin, Turkey. Ph.D thesis, University of London, 244 p. [unpublished]
- Görür, N. (1979) Karaisali kirectasinin (Miyosen) sedimentolojisi. *Türkiye Jeoloji Kurumu Bulteni* 22, 227 - 235.
- Görür, N. (1992) A tectonically controlled alluvial fan which developed into a marine fan-delta at a complex triple junction: Miocene Gildirli Formation of the Adana Basin, Turkey. *Sedimentary Geology* 81, 243 - 252.
- Green, S. (1990) Scapa Field re-correlation study and petrographic summary. *Occidental Petroleum (Caledonia) Internal Report*, 24 p. [unpublished]
- Guerillot, D.R, Lemouzy, P.M. & Ravenne, C. (1992) How reservoir characterization can help to improve production forecasts. *Revue de l'Institut Français du Pétrole* 47: 1, 58 - 67.
- Gürbüz, K. (1993) Identification and evolution of Miocene submarine fans in the Adana Basin, Turkey. Ph.D. thesis, University of Keele, UK, 327 p. [unpublished]
- Gürbüz, K. & Kelling G. (1992) Internal/external controls on submarine fan development: two examples from the Neogene of southern Turkey. 29th Int. Geol. Congress, Kyoto 2, 292. [abstract]
- Gürbüz, K. & Kelling G. (1993) Provenance of Miocene submarine fans in the northern Adana Basin, southern Turkey: a test of discriminate function analysis. *Geological Journal* 28, 277 - 293.
- Habgood, E., Kenyon, N., Akhmetyanov, A., Gardner, J. & Mulder, T. (2002) Bottom current and gravity flow process interaction: unusual examples from the Gulf of Cadiz. 16th International Sedimentological congress, 138. [abstract]
- Hampton, M.A. (1975) Competence of fine-grained debris flows. *Journal of Sedimentary Petrology* 45:4, 834 - 844.
- Haq, B.U., Hardenbol, J. & Vail, P.R. (1987a) Chronology of fluctuating sea levels since the Triassic. *Science* 235, 1156 - 1167.

- Haq, B.U., Hardenbol, J. & Vail, P.R. (1987b) Mesozoic and Cenozoic chronostratigraphy and cycles of sea-level change. In: Wilgus, C.K., Hastings, B.S., Kendall, C.G., Posamentier, H.W., Ross, C.A. & Van Wagoner, J.C. (eds) Sea-level changes: an integrated approach. SEPM Special Publication, 72 - 108.
- Hancock, J.M. (1990) Cretaceous. In: Glennie, K.W. (ed) Introduction to the petroleum geology of the North Sea. Blackwell Scientific Publications, Oxford, 255 - 272.
- Harker, S.D., Gustav, S.H. & Riley, L.A. (1987) Triassic to Cenomanian stratigraphy of the Witch Ground Graben. In: Brooks, J. & Glennie, K. (eds) Petroleum geology of north west Europe. Graham & Trotman, 809 – 818.
- Harker, S.D. & Chermak, A. (1992) Detection and prediction of Lower Cretaceous sandstone distribution in the Scapa Field, North Sea. In: Hardman, R.F.P. (ed) Exploration Britain: geological insights for the next decade. Geol. Soc. London Special Publication 67, 221 - 246.
- Harker, S.D., Grean, S.C.H. & Romani, R.S. (1991) The Claymore Field, Block 14/19, UK North Sea. In: Abbotts, I. L. (ed) United Kingdom Oil and Gas Fields, 25 Years commemorative volume. Geol. Soc. London Memoir 14, 269 - 278.
- Harker, S.D., Mantel, K.A., Morton, D.J. & Riley, L.A. (1993) The stratigraphy of Oxfordian - Kimmeridgian (Late Jurassic) reservoir sandstones in the Witch Ground Graben, United Kingdom North Sea. AAPG Bulletin 77: 10, 1693 - 1709.
- Harland, W.B., Armstrong, R.L., Cox, V.A. & Smith, A.G. (1990) A geologic time scale 1989. Cambridge University Press, New York, 263 p.
- Harms, J.C. & Fahnestock, R.K. (1965) Stratification, bed forms, and flow phenomena (with an example from the Rio Grande). In: Middleton, G.V. (ed) Primary sedimentary structures and their hydrodynamic interpretation. Tulsa, SEPM Special Publication, 84 - 115.
- Hartley, H.J. & Otava, J. (2001) Sediment provenance and dispersal in a deep marine foreland basin: the Lower Carboniferous Culm Basin, Czech Republic. Journal of the Geol. Soc. London 158, 137 - 150.
- Hatton, I.R., Reeder, M., Newman, M.S.T.J. & Roberts, D. (1992) Techniques and applications of petrophysical correlation in submarine fan environments, early Tertiary sequences. North Sea. In: Hurst, A., Griffiths, C.M. & Worthington, P.F. (eds) Geological applications of wireline logs II. Geol. Soc. London Special Publication 65, 21 - 30.
- Hearn, C.J., Ebanks, W.J.Jr., Tye, R.S. & Ranganathan, V (1984) Geological factors influencing reservoir performance of the Hartzog Draw Field, Wyoming. Journal of Petroleum Technology 35, 1335 - 1344.
- Heezen, B.C. & Hollister, C.D. (1971) The face of the deep. Oxford University Press, New York, 659 p.
- Heezen, B.C., Menzies, R.J., Schneider, E.D., Ewing, W.M. & Granelli, N.C. (1964) Congo submarine canyon. AAPG Bulletin 48, 1126 – 1149.
- Hein, F.J. & Walker, R.G. (1982) The Cambro-Ordovician Cap Enrage Formation, Quebec, Canada: conglomeratic deposits of a braided submarine channel with terraces. Sedimentology 29, 309 - 329.
- Helland, O., Wathne, E.I. & Nemeč, W. (2002) Sedimentology of the Early Eocene Frigg Submarine Fan, North Sea. In: 16th International Sedimentological Congress, 153 - 154. [abstract]
- Heller, P. & Dickinson, W.R. (1985) Submarine ramp facies model for delta-fed, sand-rich turbidite systems. AAPG Bulletin 69, 960 – 976.
- Hempton, M.R. (1982) Structure and deformation history of the Bitlis Suture near Lake Hazar, southeastern Turkey, GSA Bulletin 96, 233 – 243.
- Hempton, A. (1982) The North Anatolian fault and complexities of continental escape. Journal of Structural Geology 4, 502 - 504.
- Hendry, J.P. (1994) Diagenetic evolution of the Scapa Member Sandstones (SD Unit), Block 14/19, Outer Moray Firth. Aberdeen University, UK, 130 p. [unpublished]
- Heritier, F.E., Lossel, P. & Wathne, E. (1979) Frigg Field – large submarine –fan trap in Lower Eocene rocks of North Sea Viking Graben. AAPG Bulletin 63: 11, 1999 - 2020.
- Hewlett, J.S. & Jordan, D.W. (1993) Stratigraphic and combination traps within a seismic sequence framework, Miocene Stevens Turbidites, Bakersfield, Arch, California. In: Weimer, P. & Posamentir, H.W. (eds) Siliciclastic sequence stratigraphy: recent developments and applications. AAPG Memoir 58, 135 – 162.
- Hiscott, R.N. (1981) Deep-sea fan deposits in the Macigno Formation (Middle-Upper Oligocene) of Gordana Valley, Northern Apennines, Italy - Discussion. Journal of Sedimentary Petrology 51, 1015 - 1033.
- Hiscott, R., Pickering, K., Bouma, A., Kneller, B., Postma, G. & Soh, J. (1997) Basin-floor fans in the North Sea: sequence stratigraphic models vs. sedimentary facies: Discussion. AAPG Bulletin 81, 662 - 665.
- Hughes, S.R., Alexander, J. & Druitt, T.H. (1995) Anisotropic grain fabric: volcanic and laboratory analogues for turbidites. In: Hartley, A.J. & Prosser, D.J. (eds) Characterization of deep marine clastic systems. Geol. Soc. London Special Publication 94, 51 - 62.

- Hughes Clarke, J.E., Shor, A.N., Piper, D.J.W. & Mayer, L.A. (1990) Large-scale current-induced erosion and deposition in the path of the 1929 Grand Banks turbidity current. *Sedimentology* 37, 613 - 629.
- Hurst, A. & Buller, A.T. (1984) Dish structures in some Paleocene deep-sea sandstones (Norwegian Sector, North Sea): origin of the dish-forming clays and their effect on reservoir quality. *Journal of Sedimentary Petrology* 54: 4, 1206 - 1211.
- Hurst, A., Verstralen, I., Cronin, B. & Hartley, A. J. (1999) Sand-rich fairways in deepwater clastic reservoirs: genetic units, capturing uncertainty and a new approach to reservoir modelling. *AAPB Bulletin* 83: 7, 1096 - 1118.
- Hodgson, D.M., Hodgetts, D., Howell, J., Keogh, K., Flint, S., Drinkwater, N. & Van der Werff, W. (2002) Impact on subtle basin-floor topography on lateral and frontal submarine fan pinchout. 16th International Sedimentological Congress, 156. [abstract]
- Jackson, J. & McKenzie, D.P. (1984) Active tectonics of the Alpine-Himalayan belt between western Turkey and Pakistan. *Geophysical Journal of the Royal Astronomical Society of London* 77, 184 - 264.
- Jeremiah, J.M. (2000) Lower Cretaceous turbidites of the Moray Firth: sequence stratigraphical framework and reservoir distribution. *Petroleum Geoscience* 6: 4, 309 - 328.
- Johansson, M. & Stow, D.A.V. (1995) A classification scheme for shale clasts in deep-water sandstones. *Geol. Soc London Special Publication* 94, 221 - 241.
- Johansson, M., Braakenburg, N.E., Stow, D.A.V. & Faugères, J.C. (1998) Deep-water massive sands, facies, processes and channel geometry in the Numidian Flysch, Sicily. *Sedimentary Geology* 115, 233 - 265.
- Kane, K., Gupta, S., Johanson, H. & Trudgill, B. (2002) The response of turbidite dispersal growth pathways to normal fault propagation and basin confinement: an example from the North Halibut Graben, Outer Moray Firth, North Sea. 16th International Sedimentological Congress, 185 - 186. [abstract]
- Kano, Y. & Takeuchi, K. (1989) Origin of mudstone clasts in turbidites of the Miocene Ushikiri Formation, Shima Peninsula, Southwest Japan. *Sedimentary Geology* 62, 79 - 87.
- Karig, D.E. & Kozlu, H. (1990) Late Palaeogene-Neogene evolution of the triple junction near Karamanmaraş, south-central Turkey. *Journal of the Geol. Soc. London* 147, 1023 - 1034.
- Kelling, G., Gökçen, S., Floyd, P., & Gökçen, N. (1987) Neogene tectonics and plate convergence in the eastern Mediterranean: new data from southern Turkey. *Geology* 15, 425 - 429.
- Kenyon, N.H., Klauke, I., Millington, J. & Ivanov, M.K. (2002) Sandy submarine canyon-mouth lobes on the western margin of Corsica and Sardinia, Mediterranean Sea. *Marine Geology* 184, 69 - 84.
- Kneller, B. (1995) Beyond the turbidite paradigm: physical models for deposition of turbidites and their implication for reservoir prediction. In: Hartley, A & Prosser, J. (eds) *Characterisation of deep marine clastic systems*. *Geol. Soc. London Special Publication*, 31 - 50.
- Kneller, B. & Branney, M.J. (1995) Sustained high-density turbidity currents and the deposition of thick massive sands. *Sedimentology* 42, 607 - 616.
- Kneller, B., Edwards, D., McCaffrey, W. & Moore, R. (1991) Oblique reflection of turbidity currents. *Geology* 14, 250 - 252.
- Kneller, B. & McCaffrey, W.D. (1999) Depositional effects of flow non-uniformity and stratification within turbidity currents approaching a bounding slope: deflection, reflection and facies variation. *Journal of Sedimentary Research*. 69/5, Section A, 980 - 991.
- Kolla, V. (1993) Lowstand deep-water siliciclastic depositional systems: characteristics and terminologies in sequence stratigraphy and sedimentology. *Bulletin Centre Recherche Exploration-Production Elf Aquitaine* 17, 67 - 78.
- Kolla, V. & Macudra, D.B.Jr. (1988) Sea-level changes and timing of turbidity-current events in deep-sea fan systems. In: Wilgus, C.K., Hastins, B.S., Kendall, C.G., Posamentier, H.W., Ross, C.A. & Van Wagoner, J.C. (eds) *Sea level change - an integrated approach*. *SEPM Special Publication* 42, 381 - 392.
- Kolla, V. & Perlmutter, M.A. (1993) Timing of turbidite sedimentation on the Mississippi Fan. *AAPG Bulletin* 77, 1129 - 1141.
- Kostrewa, R., Hurst, A., Cronin, B. & Kelling, G. (1997) Sedimentology and geometry of turbidite lobe deposits: Eastern fan, Miocene Cingöz Formation, southern Turkey. In: Burgess, P.M. & Keighley, D. (eds) *BSRG Liverpool 1997*, 63. [abstract]
- Kuehl, S.A., Hariu, T.M. & Moore, W.S. (1989) Shelf sedimentation off the Ganges-Brahmaputra river system: evidence for sediment bypassing to the Bengal Fan. *Geology* 17: 12, 1132 - 1135.
- Kuenen, Ph.H. & Migliorini, C.I. (1950) Turbidity currents as a cause of graded bedding. *Journal of Geology* 58, 91-127.

- Lebreiro, S.M., McCave, N., Weaver, P.P.E. (1997) Late Quaternary turbidite emplacement on the Horseshoe Abyssal Plain (Iberian Margin). *Journal of Sedimentary Research* 67: 5, 856 - 870.
- Link, M.H. & Welton, J.E. (1982) Sedimentology and reservoir potential of Matilija Sandstone: an Eocene sand-rich deep-sea fan and shallow marine complex, California. *AAPG Bulletin* 66: 10, 1514 - 1534.
- Lowe, D. (1982) Sediment gravity flows: II. Depositional models with special reference to the deposits of high-density turbidity currents. *Journal of Sedimentary Petrology* 52, 279 - 297.
- Lowe, D. (1997): Reinterpretation of depositional processes in a classic flysch sequence (Pennsylvanian Jackfork Group), Ouachita Mountains, Arkansas and Oklahoma: Discussion. *AAPG Bulletin* 81:3, 460 - 465.
- Lowey, G.W. (1992) Variation in bed thickness in a turbidite succession, Dezadeash Formation (Jurassic-Cretaceous), Yukon, Canada: evidence of thinning-upward and thickening-upward cycles. *Sedimentary Geology* 78, 217 - 232.
- Matheron, G. Beucher, H., de Fourquet, C., Galli, A, Guerillot, D. & Ravenne, C. (1987) Conditional simulation of the geometry of fluvio-deltaic reservoirs. Presentation at the 62nd annual technical conference and Exhibition of the SPE, SPE 16753
- McAfee, A. (1993) Early Cretaceous reservoir integration study Scapa and Northern Area Claymore fields, Block 14/19, UKCS. Core Laboratories report for Elf Enterprise Caledonia Ltd., Aberdeen, 198p. [unpublished]
- McCants, C.Y. & Burley, S.D. (1996) Reservoir architecture and diagenesis in downthrown fault block plays: the lowlander prospect of Block 14/206, Witch Ground Graben, Outer Moray Firth, UK North Sea. In: Hurst, A., Johnson, H.D., Burley, S.D. Canham, A.C. & Mackertich, D.S. (eds) *Geology of the Humber Group; Central Graben and Moray Firth, UKCS. Geol. Soc. London Special Publication* 114, 251 - 285.
- McGann, G.J., Green, S.C.H., Harker, S.D. & Romani, R.S. (1991) The Scapa Field, Block 14/19, UK North Sea. In: Abbotts, I.L. (ed) *United Kingdom Oil and Gas Fields, 25 Years Commemorative Volume. Geol. Soc. Memoir* 14, 369 - 376.
- McLean, H. (1981) Reservoir properties of submarine-fan facies: Great Valley Sequence, California. *Journal of Sedimentary Petrology* 51: 3, 0865 - 0872.
- McLean, H. & Howell, D.G. (1985) Blanca Turbidite System, California. In: Bouma, A.H., Normark, W.R. & Barnes, N.E. (eds) *Submarine fans and related systems. Springer-Verlag, New York*, 167 - 172.
- Miall, A.D. (1985): Architectural-elements analysis: A new method of facies analysis applied to fluvial deposits. *Earth-Science Reviews* 22, 261 - 308.
- Miall, A.D. (1999) Perspectives: in defence of facies classifications and models. *Journal of Sedimentary Research* 69: 1, 2 - 5.
- Middleton, G.V. & Hampton, M.A. (1976) Subaqueous sediment transport by sediment gravity flows. In: Stanley, D.J. & Swift, D.J.P. (eds) *Marine sediment transport and environmental management. New York, Wiley*, 197 - 218.
- Middleton, G.V. (1993) Sediment deposition from turbidity currents. *Annual review Earth Planetary Sciences* 21, 89 - 114.
- Millington, J.J. (1995) Morphology and architecture of confined and unconfined flow transition in modern and ancient deep water fan systems. Ph.D. thesis, University of Leicester, UK, 297 p. [unpublished]
- Millington, J. & Clark, J. D. (1995) Submarine canyon and associated base-of-slope sheet system: the Eocene Charo-Arro system, south-central Pyrenees, Spain. In: Pickering, K., Hiscott, R., Kenyon, N., Ricci Lucchi, F. & Smith, R. (eds) *Atlas of deepwater environments: architectural styles in turbidite systems. Chapman & Hall, London*, 150 - 156.
- Mitchum Jr, R.M. (1985) Seismic stratigraphic expression of submarine fans. In: Berg, O.R. & Woolverton, D.G. (eds) *Seismic stratigraphy II: An integrated approach to hydrocarbon exploration. AAPG Memoir* 39, 117 - 136.
- Mitchum Jr, R.M., Sangree, J.B., Vail, P.R. & Wornardt, W.W (1993) Recognizing sequences and systems tracts from well logs, seismic data and biostratigraphy: examples from late Cenezoic of the Gulf of Mexico. In: Weimer, P. & Posamentir (eds) *Siliciclastic sequence stratigraphy: recent developments and applications. AAPG Memoir* 58, 163 - 197.
- Mijnssen, F.C.H., Tyler, N. & Weber, K.J. (1993) Knowledge base development for the estimation of reservoir rock properties in the interwell area: examples from the Texan Gulf Coast. *IAS Special Publication* 15, 169 - 180.
- Muck, M.T. & Underwood, M.B. (1990) Upslope flow of turbidity currents: a comparison among field observations, theory and laboratory models. *Geology* 18, 54 - 57.
- Mulder, T. & Cochonat, P. (1996) Classification of offshore mass movements. *Journal of Sedimentary Research* 66, 43 - 57.
- Murray, C.J., Lowe, D.R., Graham, S.A., Martinez, R.A., Zeng, J., Carroll, A.R., Cox, R., Hendirx, M., Heubeck, X., Miller, D., Moxon, I.W., Sobel, E., Wendebourg, J. & Williams, T. (1996) Statistical analysis of bed-thickness patterns

- in a turbidite section from the Great Valley Sequence, Cache Creek, Northern California. *Journal of Sedimentary Research* 66: 5, 900 – 908.
- Mutti, E. (1977) Distinctive thin-bedded turbidite facies and related depositional environments in the Eocene Hecho Group (South-central Pyrenees, Spain). *Sedimentology* 24, 107 - 131.
- Mutti, E. (1979) Sedimentation detritique (fluviale, littorale et marine). Cours 3e cycle rouend. Université de Fribourg. Switzerland, 353 - 419.
- Mutti, E. (1985a). Turbidite systems and their relations to depositional sequences. In: Zuffa, G. G. (ed) *Provenance of Arenites*. Reidel Publishing Company, 65 - 93.
- Mutti, E. (1985b) Hecho Turbidite System, Spain. In: Bouma, A.H., Normark, W.R. & Barnes, N.E. (eds) *Submarine fans and related turbidite systems*. Springer Verlag New York, 205 - 208.
- Mutti, E. (1992) Turbidite sandstone, Agip Milan, 272 p.
- Mutti, E. (1996) Flood-generated sandstone facies in ancient fluvio-deltaic systems. IAS Special Lecture Tour. [abstract]
- Mutti, E. & Ghibaudo, G. (1972) Un esempio di torbiditi di conoide sottomarina esterna-Le Arenarie di Salvatore (Formazione di Bobbio, Miocene) nell' Appennino di Piacenza. *Memorie dell' Accademia della Scienze di Torino, Classe di Scienze Fisiche, Matematiche e Naturalis, Serie 4*, 40 p.
- Mutti, E. & Johns, D.R. (1978) The role of sedimentary by-passing in the genesis of fan fringe and basin plain turbidites in the Hecho Group system (South-central Pyrenees). *Mem. Soc. Geol. Italia* 18, 15 - 22.
- Mutti, E. & Normark, W. R. (1987) Comparing examples of modern and ancient turbidite systems: problems and concepts. In: Leggett, F. K. & Zuffa, G. G. (eds) *Marine clastic sedimentology*. Graham & Trotman, London, 1 - 38.
- Mutti, E. & Normark, W. R. (1991) An integrated approach to the study of turbidite systems. In: Weimer, P. & Link, M. H. (eds) *Seismic facies and sedimentary processes of submarine fans and turbidite systems*. Springer Verlag, New York, 75 - 106.
- Mutti, E. & Ricci Lucchi, F. (1972) Turbidites of the northern Apennines: introduction to facies analysis. (English translation by T. H. Nilson 1978). *International Geological Review* 20, 125 - 166.
- Mutti, E. & Ricci Lucchi, F. (1975) Turbidite facies and facies associations. In: Mutti, E., Parea, G.C., Ricci Lucchi, F., Sagri, M., Zanzucchi, G., Ghibaudo, G. & Jaccarine, S (eds) *Examples of turbidite facies and facies associations from selected formations of the Northern Apennines*. 9th International Sedimentology Congress, Nice-75. Field trip guidebook A-11, 21 - 36.
- Mutti, E. & Sonnino, M. (1981) Compensation cycles: a diagnostic feature of turbidite sandstone lobes. IAS 2nd European Meeting, Bologna, 120 – 123 [abstract].
- Mutti, E., Nilsen, T. H. & Ricci Lucchi, F. (1978) Outer fan depositional lobes of the Laga Formation (Upper Miocene and Lower Pliocene), east-central Italy. In: Stanley, D. J. & Kelling, G. (eds) *Sedimentation in submarine fans, canyons and trenches*. Dowden, Hutchinson & Ross, Stroudsburg, Pennsylvania, 210 - 223.
- Mutti, E., Barros, K., Possato, S. & Rumenos, L. (1980) Deep-sea fan turbidites sediments winnowed by bottom currents in the Eocene of the Campos Basin, Brazilian offshore. IAS 1st European Meeting, 114. [abstract]
- Mutti, E., Remacha, E., Sgavetti, M., Rosell, J., Valloni, R. & Zamorano, M. (1985) Stratigraphy and facies characteristics of the Eocene Hecho Group turbidite system, South-central Pyrenees. In: Mila, M. D. & Rosell, J. (eds) *IAS 6th European Regional Meeting, Excursion Guidebook, Lerida*, 521 - 576.
- Mutti, E., Davoli, G., Mora, S. & Papani, L. (1994) Internal stacking patterns of ancient turbidite systems from collisional basins. In: Weimer, P., Bouma, A.H. & Perkins, B.F. (eds) *Submarine fans and turbidite systems. Sequence Stratigraphy, Reservoir Architecture and Production Characteristics*. Gulf of Mexico and International. GCSSEPM Foundation 15th Research Conference, Houston, 257 - 267.
- Naz, H., Cuhadar, O. & Yehiyay, G. (1991) Middle Miocene Cingöz deep-sea fan deposits of the Adana Basin, Southern Turkey. In: Sungurlu, O. (ed) *Tectonics and hydrocarbon potential of Anatolia and surrounding regions*. Ankara, 190 - 121.
- Nazik, A. & Gürbüz, K. (1992) Karaisalı-Çatalan-Egner yöresinin (KB-Adana) alt-orta Miyosen istifinin planktonik foraminifer gyostratigrafisi. *Turkiye Jeoloji Bulteni* 35, 67 - 80.
- Nelson, C.H., Maldonado, A., Coumes, H.G. & Monaco, A. (1985) Ebro fan, Mediterranean. In: Bouma, A.H., Normark, W.R. & Barnes, N.E. (eds) *Submarine fans and related systems*: Springer Verlag, New York, 121 – 127.
- Nelson, C.H., Baraz, J. & Maldonado, A. (1993) Mediterranean undercurrent sandy contourites, Gulf of Cadiz, Spain. *Sedimentary Geology* 82, 103 - 131.
- Nichols, R.J., Sparks, R.S.J. & Wilson, C.J.N. (1994) Experimental studies of the fluidization of layered sediments and formation of fluid escape structures. *Sedimentology* 41, 233 - 253.

- Nilsen, T.H. (1980) Modern and ancient submarine fans: discussion. *AAPG Bulletin* 64, 1094 – 1112.
- Nilsen, T.H. (1985) Chugach Turbidites system, Alaska. In: Bouma, A.H., Normark, W.R. & Barnes, N.E. (eds) *Submarine fans and related systems*: Springer Verlag, New York, 185 – 192.
- Nilsen, T.H., Boote, D.R.D. & Reid, S.A. (2002a) Lower and Middle Tertiary sequence stratigraphy, depositional systems, tectonic framework, and paleogeography of the southern San Joaquin Basin, California. 16th International Sedimentological Congress, Johannesburg, 281. [abstract]
- Nilsen, T.H., Gregory, G.J. & Wylie Jr., A.S. (2002b) Confined Miocene sand-rich turbidite sedimentation in the southern Temblor Range and adjacent Midway-Sunset Oil Field, San Joaquin Basin, California. 16th International Sedimentological Congress, 282. [abstract]
- Normark, W.R. (1970) Growth patterns of deep-sea fans. *AAPG Bulletin* 54, 2170 - 2195.
- Normark, W. R. (1978) Fan valleys, channels and depositional lobes on modern submarine fans: characters for recognition of sandy turbidite environments. *AAPG Bulletin* 62, 912 - 931.
- Normark, W.R. (1991) Turbidite elements and the obsolescence of the suprafan concept. *Giornale di Geologia*, ser 3^a, 53/2, 1 - 10.
- Normark, W.R. & Piper, D.J.W. (1985) Navy Fan, Pacific Ocean. In: Bouma, A.H., Barnes, A.H. & Normark, W.R., (eds) *Submarine fans and related turbidite systems*. Springer Verlag, New York, 87 - 94.
- Normark, W.R. & Piper, D.J.W. (1991) Initiation processes and flow evolution of turbidity currents: implications for the depositional record. In: *From Shoreline to Abyss*. SEPM Special Publication 46, 207 - 230.
- Normark, W.R., Piper, D.J.W. & Hesse, G.R. (1979) Distributary channels, sand lobes and mesotopography of Navy submarine fan, California Borderland, with application to ancient fan sediments. *Sedimentology* 26, 749 - 744.
- Normark, W.R., Piper, D.J.W., Stow, D.A.V. (1983) Quaternary development of channels, levees, and lobes on Middle Laurentian Fan. *AAPG Bulletin*, 67: 9, 1400 - 1409.
- Normark, W.R., Posamentier, H. & Mutti, E. (1993) Turbidite Systems: state of the art and future directions. *Reviews of Geophysics* 3-2, 91 - 116.
- Normark, W.R., Piper, D.J.W. & Hiscott, R.N. (1998) Sea level controls on the textural characteristics and depositional architecture of the Hueneme and associated submarine fan systems, Santa Monica Basin, California. *Sedimentology* 45, 53 – 70.
- Oakman, C.D. & Partington, M.S. (1998) Cretaceous. In: Glennie, K.W. (ed) *Petroleum Geology of the North Sea*. Basic concepts and recent advances. 4th edition. Blackwell Science, London, 294 – 349.
- O'Driscoll, W., Hindle, A.D. & Long, D.C. (1990) The structural controls on Upper Jurassic and Lower Cretaceous reservoir sandstones in the Witch Ground Graben, UK North Sea. In: Hardman, R.F.P. & Brooks, J. (eds) *Tectonic events responsible for Britain's oil and gas reserves*. Geol. Soc. Special Publication 55, 299 – 323.
- Özçelik, N. (1993) Facies and environmental aspects of the Güvenç Formation in the Adana Basin. Ph.D thesis, Cukurova University, Turkey, 215 p. [unpublished]
- Pettingill, H.S. (1998) Turbidite plays' immaturity mean big potential remains. *Oil and Gas Journal*, Oct. 5, 106 - 112.
- Pickering, K. (1981) Two types of outer fan lobe sequence, from the Late Precambrian Kongsfjord Formation submarine fan, Finnmark, North Norway. *Journal of Sedimentary Petrology* 51: 4, 1277 - 1286.
- Pickering, K. & Hiscott, R.N. (1985) Contained (reflected) turbidity currents from the Middle Ordovician Cloridorme Formation, Quebec, Canada: an alternative to the antidune hypothesis. *Sedimentology*, 32, 373 - 394.
- Pickering, K. T., Stow, D. A. V., Watson, M. and Hiscott, R. N. (1986). Deepwater facies, processes and models: a review and classification scheme for modern and ancient sediments. *Earth Science Review* 22, 75 - 175.
- Pickering, K., Hiscott, R.N., & Hein, F.J. (1989) Deep marine environments: clastic sedimentation and tectonics. Unwin Hyman, London. 416 p.
- Pickering, K., Clark, J., Smith, R., Hiscott, R., Ricci Lucchi, F. & Kenyon, N. (1995). Architectural element analysis of turbidite systems, and selected topical problems for sand-prone deepwater systems. In: Pickering, K., Hiscott, R., Kenyon, N., Ricci Lucchi, F. & Smith, R. (eds) *Atlas of deepwater environments: architectural styles in turbidite systems*. Chapman & Hall, London, 1 - 11.
- Piper, D.J.W. & Normark, W.R. (1983) Turbidite depositional patterns and flow characteristics, Navy submarine fan, California Borderland. *Sedimentology* 30, 681 - 694.
- Piper, D.J.W. & Stow, D.A.V. (1991) Fine grained turbidites. In: Einsele, G., Ricken, W. & Seilacher, A. (eds) *Cycles and events in stratigraphy*. Springer Verlag, Berlin Heidelberg, 360 - 376.
- Pinet, P. & Souriau, M. (1988) Continental erosion and large-scale relief. *Tectonophysics* 7, 563 - 582.
- Pirmez C., Hiscott, R.N. & Kronen, D.J. (1997) 2. Sandy turbidite successions at the base of channel-levee systems of the Amazon Fan revealed by FMS logs and cores: unraveling the facies architecture of large submarine fans. In: Flood,

- R.D., Piper, D.J.W., Klaus, A., Peterson, L.C. (Eds.) Proceedings of the Ocean Drilling Program, Scientific Results, Vol. 115, p. 7 - 33.
- Posamentier, H.W. & Erskine, R. (1991) Seismic expression and recognition criteria of ancient submarine fans. In: Weimer, P. & Link, M.H. (eds) Seismic facies and sedimentary processes of submarine fans and turbidite systems. Springer Verlag, New York, 197 - 222.
- Posamentier, H.W. & Vail, P.R. (1988) Eustatic controls on clastic deposition II – sequence and system tract models. In: Wilgus, C.K., Hastings, B.S., Kendall, C.G., Posamentier, H.W., Ross, C.A. & Van Wagoner, J.C. (eds) Sea level change – an integrated approach. SEPM Special Publication 42, 125 - 154.
- Posamentier, H.W., Jervey, M.T. & Vail, P.R. (1988) Eustatic controls on clastic deposition I – conceptual framework. In: Wilgus, C.H. Hastings, B.S., Kendall, C.G., Posamentier, H.W., Ross, C.A. & Van Wagoner, J.C. (eds) Sea level change – an integrated approach. SEPM Special Publication 42, 109 - 124.
- Posamentier, H.W., Erskine, R. & Mitchum Jr, R. (1991) Models of submarine-fan deposits within a sequence stratigraphic framework. In: Weimer, P. & Link, M. (eds) Seismic facies and sedimentary processes of submarine fans and turbidite systems. Springer Verlag, New York, 127 - 137.
- Postma, G. (1986) Classification for sedimentary gravity-flow deposits based on flow conditions during sedimentation. *Geology*, 291 - 296.
- Postma, G., Nemec, W. & Kleinspenn, K.L (1988) Large floating clasts in turbidites: a mechanism for their emplacement. *Sedimentary Geology* 58, 47 - 61.
- Prins, M.A. & Postma, G. (2000) Effects of climate, sea level, and tectonics unravelled for last deglaciation turbidite records of the Arabian Sea. *Geology* 28: 4, 375 - 378.
- Prins, M.A., Postma, G. & Weltje, G.J. (2000) Controls on terrigenous sediment supply to the Arabian Sea during the late Quaternary: the Makran continental slope. *Marine Geology* 169, 351 - 371.
- Purvis, K., Kao, J., Flanagan, K., Henderson, J. & Duranti, D. (2002) Complex reservoir geometries in a deep water clastic sequence, Gryphon Field, UKCS: injection structures, geological modelling and reservoir simulation. *Marine and Petroleum Geology* 19, 161 - 179.
- Puig, P., Ogston, A.S., Mullenbach, B.L., Nittrouer, C.A. & Sternberg, R.W. (2003) Shelf-to-canyon sediment-transport processes on the Eel continental margin (northern California). *Marine Geology* 193, 129 - 149.
- Rawson, P.E. & Riley, L.A. (1982) Latest Jurassic-Early Cretaceous events and the “Late Cimmerian Unconformity” in the North Sea Area. *AAPG Bulletin* 66: 12, 2628 - 2648.
- Ravenne, C. (1992) Annot Sandstone. Field Trip Guide, TREDMAR 1992. In: Ravenne, C. & Vially, R. (eds) Observation of outcrops at a seismic scale in view of seismic stratigraphic interpretation. AAPG Mediterranean Basins Conference Nice 1988, France, Field Trip 2, 68 p.
- Reading, H.G. (1991) The classification of deep-sea depositional systems by sediment caliber and feeder system. *Journal of Geol. Soc. London*, 148, 427 - 430.
- Reading, H.G. (1996) Sedimentary environments: processes, facies and stratigraphy. Blackwell Science (3rd Edition), Oxford, 688 p.
- Reading, H.G. & Richards, M. (1994) Turbidite systems in deepwater basin margins classified by grain-size and feeder system. *AAPG Bulletin* 78, 792 - 822.
- Reynolds, S. & Gorsline, D.S. (1987) Nicolas and Eel submarine fans, California continental borderland. *AAPG Bulletin* 7: 4, 452 - 463.
- Ricci Lucchi, F. (1975a) Miocene palaeogeography and basin analysis in the Periadriatic Apennines. In: Squyre C. (ed) Reprinted from *Geology of Italy*. Petroleum Exploration Society of Libya, 111 p.
- Ricci Lucchi, F. (1975b) Depositional cycles in two turbidite formations of Northern Apennines (Italy). *Journal of Sedimentary Petrology* 45, 3 - 43.
- Ricci Lucchi, F. (1981) The Marnoso-Arenacea: A migrating turbidite basin "over-supplied" by a highly efficient dispersal system. In: Ricci Lucchi, F. (ed) IAS Excursion Guidebook, with contributions on sedimentology on some Italian basins. 2nd European Regional Meeting, Bologna, Italy, 231 - 303.
- Ricci Lucchi, F. (1985) Marnosa-Arenacea turbidite system, Italy. In: Bouma, A.H., Normark, W.R. & Barnes, N.E. (eds) Submarine fans and related turbidite systems. New York, Springer Verlag, 209 - 216.
- Ricci Lucchi, F. (1995) Contessa and associated megaturbidites: long distance (120 x 25 km) correlation of individual beds in a Miocene Foredeep. In: Pickering, K.T., Hiscott, R.N., Kenyon, N.H., Ricci Lucchi, F. & Smith, R.D.A. (eds) Atlas of deep-water environments: Architectural style in turbidite systems, London, Chapman & Hall, 300 - 302.
- Ricci Lucchi, F. & Valmori, E. (1980) Basinwide turbidites in the Miocene, oversupplied deep-sea plain: a geometrical analysis. *Sedimentology* 27, 241 - 270.

- Ricci Lucchi, F., Colella, A., Gabbianelli, G., Rossi, S. & Normark, W. R. (1984) The Crati submarine fan, Ionian Sea. *Geo-Marine Letters* 3, 71 - 77.
- Ricci Lucchi, F., Colella, A., Gabbianelli, G., Rossi, S. & Normark, W. R. (1985) Crati Fan, Mediterranean. In: Bouma, A. H., Normark, W. R. & Barnes, A. H. (eds) *Submarine fans and related turbidite systems*. Springer-Verlag, New York, 51 - 57.
- Richards, M. & Bowman, M. (1998) Submarine fans and related depositional systems II: variability in reservoir architecture and wireline log character. *Marine and Petroleum Geology* 15, 821 - 839.
- Richards, M., Bowman, M. & Reading, H. (1998) Submarine-fan systems I: characterisation and stratigraphic prediction. *Marine and Petroleum Geology* 15, 689 - 717.
- Rider, M.H. (1996) *The Geological Interpretation of Well Logs*. Blackie Halsted Press, Glasgow, 175 p.
- Riley, L.A., Harker, S.D. & Green, S.C.H. (1992) Lower Cretaceous palynology and sandstones distribution in the Scapa Field, UK North Sea. *Journal of Petroleum Geology* 15: 1, 97 - 110.
- Risch, D.L., Donaldson, B.E., Taylor, C.K. (1996) Deep-water facies analysis using 3-D seismic sequence stratigraphy and workstation techniques: an example from Plio-Pleistocene strata, Northern Gulf of Mexico. In: Weimer, P. & Davies, T.L. (eds) *Application of 3-D seismic data to Exploration and Production*. AAPG Studies in Geology 42 and SEG Geophysical Development Series 5. AAPG/SEG, Tulsa, 143 - 148.
- Robertson, A.H.F. (1998) Mesozoic - Tertiary tectonic evolution of the easternmost Mediterranean area: integration of marine and land evidence. In: Robertson, A.H.F., Emis, K-C., Richter, C. & Camerlenghi, A. (eds.) *Proceedings of the Ocean Drilling Program, Scientific Results*. Springer Verlag, New York, 723 - 782.
- Robertson, A.H.F., Eaton, S., Follows, E.J. & McCallum, J.E. (1991) The role of local tectonics versus global sea-level change in the Neogene evolution of the Cyprus active margin. *IAS Special Publications* 12, 331 - 369.
- Satur, N. (1999) Internal architecture, facies distribution and reservoir modelling of the Cingöz deepwater clastic system in southern Turkey. PhD thesis, Aberdeen University, 203 p. [unpublished]
- Satur, N., Hurst, A., Cronin, B. & Kelling, G. (1997) Downsystem variations within the proximal parts of a multisourced, bypass turbidite fan, southern Turkey. In: Burgess, P.M. & Keighley, D. (eds) *BSRG Liverpool 1997*, 93. [abstract]
- Satur, N., Hurst, A., Cronin, B. & Kelling, G., Gürbüz, K. (2000) Sand body geometry in a sand-rich, deep-water clastic system, Miocene Cingöz Formation of southern Turkey. *Marine and Petroleum Geology* 17, 239 - 252.
- Savary, B., Quaegebeur, G., Merran, Y., Ferry, S. & Machhour, L. (2002) Geometry of a calcarenitic turbidite lobe, Barremian, Subalpine Basin, S-E France. 16th International Sedimentological Congress, Johannesburg, 323. [abstract]
- Savoie, B. & Piper, D.J.W. (1990) What controls depositional architecture of the Var Canyon-Fan system? Evidence from side-scan sonar images and high resolution and very high resolution seismic profiles. 13th Int. Sedimentological Congress, Nottingham, 478. [abstract].
- Schmidt, G. (1961) Stratigraphic nomenclature for the Adana region petroleum district VII. *Petroleum Administration Bulletin* 6, 47 - 63.
- Schuppers, J.D. (1995) Characterisation of deep-marine clastic sediments from foreland basins. Ph.D. Thesis, University of Technology at Delft, The Netherlands, 272 p. [unpublished]
- Schwab, W.C., Lee, H.J., Twichell, D.C., Locat, J., Nelson, C.H., McArthur, W.G. & Kenyon, N.H. (1996) Sediment mass-flow processes on a depositional lobe, outer Mississippi Fan. *Journal of Sedimentary Research* 66: 5, 916 - 927.
- Seilacher, A. (1967) Bathymetry of trace fossils. *Marine Geology* 5, 413 - 428.
- Selley, R.C. (1969) Studies of sequences in sediments using a simple mathematical device. *Journal of the Geol. Soc.* 125, 557 - 581.
- Sengör, A.M.C. (1979) Mid-Mesozoic closure of Permo-Triassic Tethys and its implications. *Nature* 279, 590 - 593.
- Sengör, A.M.C. & Yilmaz, Y. (1981) Tethyan plate tectonic evolution of Turkey: a plate tectonic approach. *Tectonophysics* 75, 181 - 241.
- Sengör, A.M.C., Görür, N. & Saroglu, F. (1985) Strike-slip faulting and related basin formation in zones of tectonic escape: Turkey as a case study. In: Biddle, K.T. & Christie-Blick, N. (eds) *Strike-slip deformation, basin formation and sedimentation*. SEPM Special Publication 37, 227 - 264.
- Shanmugam, G. (1996) High density turbidity currents: are they sandy debris flows? *Journal of Sedimentary Research* 66: 2 - 10.
- Shanmugam, G. (1997) The Bouma sequence and the turbidite mind set. *Earth Science Reviews* 42, 37 - 41.
- Shanmugam, G. (2000) 50 years of the turbidite paradigm (1950s-1990s): deep-water processes and facies models – a critical perspective. *Marine and Petroleum Geology* 17, 285 - 342.

- Shanmugam, G. & Moiola, R.J. (1988) Submarine fans; characteristics, models, classification and reservoir potential. *Earth Science Reviews* 24, 383 - 428.
- Shanmugam, G. & Moiola, R.J. (1991) Types of submarine fan lobes: models and implications. *AAPG Bulletin* 75, 156 - 179.
- Shanmugam, G. & Moiola, R.J. (1997) Reinterpretation of depositional processes in a classic flysch sequence (Pennsylvanian Jackfork Group), Ouachita Mountains, Arkansas and Oklahoma: Reply. *AAPG Bulletin* 81, 476 - 491.
- Shanmugam, G. Moiola, R.J & Damuth, J.E. (1985) Eustatic control of submarine fan development. In: Bouma, A.H., Normark, W.R. & Barnes, N.E (eds) *Submarine fans and related turbidite systems*. Springer Verlag, New York, 23 – 28.
- Shanmugam, G., Spalding, T.D. & Rofheart, D.H. (1993) Process sedimentology and reservoir quality of deep-marine bottom-current reworked sands (sandy contourites): an example from the Gulf of Mexico. *AAPG Bulletin* 77: 7, 1241 – 1259.
- Shanmugam, G., Bloch, R.B., Mitchell, S.M, Beamish, G.W.J., Hodgkinson, R.J., Damuth, J.E., Straume, T., Syvertsen, S.E. & Shields, K.E. (1995) Basin-floor fans in the North Sea: sequence stratigraphic models vs. sedimentary facies. *AAPG Bulletin* 79, 477 - 512.
- Shanmugam, G., Bloch, R.B., Darmuth J.E. & Hodgkinson, R. (1997) Basin-floor fans in the North Sea: sequence stratigraphic models vs sedimentary facies: Reply. *AAPG Bulletin* 81, 666 - 672.
- Shor, A.N., Piper, D.J.W., Hugh Clarke, J.E. & Mayer, L.A. (1990) Giant flute-like scours and other erosional features formed by the 1929 Grand Banks turbidity current. *Sedimentology* 37, 631 - 645.
- Sinclair, H.D. (1994) The influence of lateral basinal slopes on turbidite sedimentation in the Annot sandstones of SE France. *Journal of Sedimentary Research* A64, 42 - 54.
- Sinclair, H.D. (2000) Delta-fed turbidites infilling topographically complex basins: a new depositional model for the Annot Sandstone, SE France. *Journal of Sedimentary Research* 70: 3, 504 – 519.
- Sixsmith, P., Grecula, M., Flint, S., Johnson, S. & Wickens, H. deV. (2002) Using sequence stratigraphy as a predictive tool in deepwater sandstones: lessons from the Karoo Basin of South Africa. 16th International Sedimentological Congress, Johannesburg, 333 - 334. [abstract]
- Slatt, R.M., Weimer, P. & Stone, C.G. (1997) Reinterpretation of depositional processes in a classic flysch sequence (Pennsylvanian Jackfork Group) Ouachita Mountains, Arkansas and Oklahoma: Discussion. *AAPG Bulletin* 81: 3, 449 - 459.
- Stow, D.A.V. (1985a) Deep-sea clastics: where are we and where are we going? In: Brenchley, P. J. & Williams, B.P.J. (eds) *Sedimentology: Recent developments and applied aspects*. Geol. Soc. London Special Publication 18, 67 - 93.
- Stow, D.A.V. (1985b) Brae oilfield turbidite system, North Sea. In: Bouma, A.H., Normark, W.R. & Barnes, N.E. (eds) *Submarine fans and related systems*. Springer Verlag, New York, 231 - 236.
- Stow, D.A.V. & Johansson, M. (2000) Deep-water massive sands: nature, origin and hydrocarbon implications. *Marine Petroleum Geology* 17, 145 - 174.
- Stow, D. A. V. & Shanmugam, G. (1980) Sequence of structures in fine-grained turbidites; comparison of recent deep-sea and ancient flysch sediment. *Sedimentary Geology* 25, 23 - 42.
- Stow, D.A.V. & Mayall, M. (2000) Deep-water sedimentary systems: new models for the 21st century. *Marine Petroleum Geology* 17, 125 - 135.
- Stow, D.A.V., Reading, H.G. & Collinson, J.D. (1996) Deep seas. In: Reading, H.G. (ed) *Sedimentary Environments: Processes, facies and stratigraphy*. Blackwell Science, Oxford, 395 - 454.
- Surlyk, F. (1978) Submarine fan sedimentation along fault scarps on filled fault blocks (Jurassic – Cretaceous boundary, East Greenland). *Bulletin of Greenland Geology* 128, 108 p.
- Surlyk, F. (1987) Slope and deep shelf gully sandstones, Upper Jurassic, East Greenland. *AAPG Bulletin* 71: 4, 464 - 475.
- Surlyk, F. (1995) Deep-sea fan valleys, channels, lobes and fringes of the Silurian Peary Land Group, North Greenland. In: Pickering, K.T., Hiscott, R.N. Kenyon, N.H., Ricci Lucchi, F. & Smith, R.D.A. (eds) *Atlas of deep water environments: architectural styles in turbidite systems*, Chapman & Hall, London, 124 - 138.
- Timbrell, G. (1993) Sandstone architecture of the Balder Formation depositional system, UK Quadrant 9 and adjacent areas. In: Parker, J. P. (ed) *Petroleum Geology of North West Europe*. Geol. Soc. London, 59 - 71.
- Toker, V., Dermişan, H., Yildiz, A. & Sevim, S. (1998). Biostratigraphy and palaeoecology of deep-marine sediments of the lower-middle Miocene Cingöz Formation (Adana- Turkey). In: *Third International Turkish Geology Symposium*, Middle Eastern technical University, Ankara, Turkey, 225. [abstract]
- Trincardi, F., Correggiari, A., Field, M.E. & Normark, W.R. (1995) Turbidite deposition from multiple sources: Quaternary Paola Basin (Eastern Tyrrhenian Sea). *Journal of Sedimentary Research* B65: 4, 469 - 483.

- Tucker, A. (1996) *Sedimentary rocks in the field*. Chichester, Wiley. 2nd edition, 153 p.
- Tyler, N., Galloway, W.E., Garrett, C.M. Jr. & Ewing, T.E. (1984) Oil accumulation, production characteristics and targets for additional recovery in major oil reservoirs in Texas. Texas University Bureau of Economic Geology, Geologic Circular 84: 2, 33 p.
- Ünlügenç, U.C. (1993) Controls on Cenozoic sedimentation in the Adana Basin, southern Turkey. Volume I. Ph.D. thesis, University of Keele, UK, 229 p. [unpublished]
- Ünlügenç, U.C., Kelling, G. & Demirkol, C. (1992) Aspects of basin evolution in the Neogene Adana Basin, SE Turkey. In: Savascin, M.Y. & Eronat, A.H. (eds) *Proceedings of the International Earth Science Congress on Aegean Regions, Izmir 1990*, 353 - 370.
- Ünlügenç, U.C., Demirkol, C. & Safak, U. (1993) Stratigraphical and sedimentological characteristics of the Karsanti Basin fill to the N-E of the Adana Basin. Proc. A. Suat Erk Geology Symposium, Ankara 1991, 215 - 227.
- Unterseh, S. (1999) *Cartographie et caractérisation du fond marin par sondeur multifaisceaux*. Thèse de Doctorat. Inst. National Polytech. Lorraine, Nancy, 234 p. [unpublished]
- Van Wagoner, J. C., Mitchum, R. M., Posamentier, H. W. and Vail, P. R. (1987) Seismic stratigraphy interpretations using sequence stratigraphy, part II: Key definitions of sequence stratigraphy. In: Bally, A.W. (ed) *Atlas of seismic stratigraphy*. American Association of Petroleum Geologist, Studies in Geology 27, 1 - 10.
- Van Wagoner, J.C., Mitchum, R.M, Campion, K.M. & Rahmanian, V.D. (1990) Siliciclastic sequence stratigraphy in well logs, cores and outcrops: AAPG Methods in Exploration 7, 55 p.
- Vail, P.R., Mitchum, R.M., Todd, R.G., Widmier, J.M., Thompson, S., Sangree, J.B., Bubb, J.N. & Hatlelid, W.G. (1977) Seismic stratigraphy and global changes of sea level, parts 1-6. In: Payton, C. E. (ed) *Seismic stratigraphy - Applications to Hydrocarbon Research*. AAPG Memoirs, 49 - 133.
- Vail, P.R., Audemard, F., Bowman, S.A., Eisner, P.N. & Perez-Cruz, C. (1991) The stratigraphic signatures of tectonics, eustasy and sedimentology – an overview. In: Einsele, G., Ricken, W. & Seilacher, A. (eds) *Cycles and events in stratigraphy*. Springer Verlag Berlin Heidelberg, 617 - 659.
- Verstralen, I., Hartley, A. & Hurst, A. (1995) The sedimentological record of a late Jurassic transgression: Rona Member (Kimmeridge Clay Formation equivalent), West Shetland Basin, UKCS. In: Hartley, A.H. & Prosser, D.J. (eds) *Characterization of deep marine clastic systems*. Geol. Soc. Special Publication 94, 155 - 176.
- Walker, R. G. (1978) Deepwater sandstone facies and ancient submarine fans: models for exploration for stratigraphic traps. AAPG Bulletin 62, 932 - 966.
- Walker, R. G. (1980) Modern and ancient submarine fans: reply. AAPG Bulletin 64, 1101 - 1108.
- Walker, R.G. (1992) Turbidites and submarine fans. In: Walker, R.G. & James, N.P. (eds) *Facies models – response to sea-level change*. Geological Association of Canada, 239 – 263.
- Weber, K.J (1986) How heterogeneity affects oil recovery. In: Lake, L.W. & Carrol Jr. H.B. (eds) *Reservoir Characterisation*. Academic Press Inc. Orlando, 487 - 544.
- Weber, K.J. & Van Geuns, L.C. (1990) Framework for constructing clastic reservoir simulation models. *Journal of Petroleum Technology* 42, 1248 - 1297.
- Weber, M.E., Wiedicke, M.H., Kudrass, H.R., Hübscher, D. & Erlenkeuser, H. (1997) Active growth of the Bengal Fan during sea-level rise and highstand. *Geology* 25: 4, 315 - 318.
- Weimer, P. (1989) Sequence stratigraphy of the Mississippi Fan (Plio - Pleistocene), Gulf of Mexico. *Geo-Marine Letters* 9, 185 - 272.
- Weimer, P. & Link, M. H. (1991) *Seismic facies and sedimentary processes of submarine fans and turbidite systems*. Springer-Verlag New York. 447 p.
- Wetzel, A. (1993) The transfer of river load to deep-sea fans: a quantitative approach. AAPG Bulletin 77: 10, 1679 - 1692.
- Wetzel, A. (2002) Nereites as proxy for the paleo-redox boundary in deep-sea sediments. 16th International Sedimentological Congress, Johannesburg, 403. [abstract]
- Wilde, P., Normark, W.R., Chase, T.E. & Gutmacher, C.E. (1985) Potential petroleum reservoirs on deep-sea fans off Central California. In: Bouma, a.H., Normark, W.R. & Barnes, N.E. (eds) *Submarine fans and related turbidite systems*. 35 - 42.
- Williams, G., Ünlügenç, U., Kelling, G., & Demirkol, Ç. (1995) Tectonic controls on stratigraphic evolution on the Adana Basin, Turkey. *Journal of the Geol. Soc. London* 152, 873 - 882.
- Wüllner, D.E & James, W.C. (1989) Braided and meandering submarine fan channel deposits, Tesnus Formation, Marathon Basin, West Texas. *Sedimentary Geology* 62, 27 – 45.

- Wynn, R.B., Masson, D.G., Stow, D.A.V. & Weaver, P.P.E. (2000) The Northwest African slope apron: a modern analogue for deep-water systems with complex seafloor topography. *Marine and Petroleum Geology* 17, 253 - 265.
- Wynn, R.B., Kenyon, N.H., Masson, D.G., Stow, D.A.V. & Weaver, P.P.E. (2002) –Characterization and recognition of deep-water channel-lobe transition zones. *AAPG Bulletin* 86: 8, 1441 – 1462.
- Yetiş, C. (1988) Reorganization of the Tertiary stratigraphy in the Adana Basin, southern Turkey. *Newsletters Stratigraphy* 20, 42 - 58.
- Yetiş, C. & Demirkol, C. (1986) A detailed geologic investigation of the western side of the Adana Basin. *Miner Res Explor Inst. Rep no 8037 – 8037a*.
- Yetiş, C., Kelling, G., Gökçen, S. & Baroz, F. (1995) A revised stratigraphic framework for Late Cenozoic sequences in the northeastern Mediterranean region. *Geologische Rundschau* 84, 794 - 812.
- Yilmaz, Y. (1993) New evidence and model on the evolution of the southeast Anatolian orogeny. *AAPG Bulletin* 105, 251 - 271.
- Ziegler, P.A. (1981) Evolution of Sedimentary Basins in North-West Europe. In: *Petroleum Geology of the Continental Shelf of north-west Europ*. Institute of Petroleum, London, 3 - 39.

PHOTOPLATES

PLATE 1

1. Photograph showing the well forested northern and north-eastern flank of the E-Fan, Cingöz Formation. The apex is located to the right (north). In the foreground shelfal carbonates (Karaisali Formation) are exposed, followed by silty slope deposits (Kaplankaya Formation) which are largely eroded. The sandy E-Fan deposits are cliff-building (background). The cliffs reach approximately 200 m in height in the north.
2. The main feeder channel (1) represents a mixed erosional-depositional system of mainly conglomeratic infill. The picture shows channel-fill facies from near the base of feeder channel (1) where R1-3 conglomerates (Lowe 1982) eroded into underlying R1-2 conglomerates (scale: 1m). Photograph courtesy of N. Satur).
3. Overlying feeder channel (1) deposits to the north (left) are thin-bedded, predominantly medium sand sized channel-mouth and levee deposits (a) gradually coarsening- and thickening-upward into thick-bedded, very coarse-grained sandstones to pebbly conglomerates of the lower channel-lobe transition zone (b).
4. View of the northern proximal lobe zone where thick-bedded, laterally extensive coarse-grained sandstones and pebbly sandstones are exposed along the east-facing side of the Karadönme Valley. This area was sourced from the NW-W (feeder channels 3 and 4) and downcurrent transport directions point to the SE-E (north to the right; scale: 140 m from track at base to top of hill).
5. The lobe package in the central section are composed of medium to thick-bedded, coarse to medium-grained sandstone beds (S_{1-3} of Lowe 1982). They are characterised by a high sand : shale ratio (7:1). Small-scale post-depositional deformation is rife through the sandy basin-fill of the E-Fan (hammer for scale).
6. The associated interlobe deposits of the central section are typically composed of 1 - 15 cm thick, fine- to medium-grained sandstone beds ($T_{b-d,e}$ of Bouma 19962). The sand : shale ratio is low (2:1). These interlobe deposits are seen to be onlapping a shale-rich debrite containing large floating clasts and deformed sandstone beds (arrow; hammer for scale).
7. Thick debris flow deposits are occasionally interbedded with the turbiditic fan sedimentation suggesting sporadic tectonic activity. Previously interpreted as mid-fan channel and levee deposits at Kuscusofolu Village (Gürbüz 1993) are reinterpreted to represent an 80 m thick debrite. A squeezed-out, chaotic shale-rich layer (a) containing deformed sandstone beds is overlain by an unroofing sequence of chaotic Cingöz channel-fill material (b), deformed, discontinuous package of sandstone beds (c) topped by a 35 m thick shale-dominated layer containing well-rounded floating clasts and shallow water fossils (d) typical of the Kaplankaya slope Formation. The debris flow is onlapped by lobe fringe deposits (e) which gradually thicken-upward into distinct lobe packages.

PLATE 1

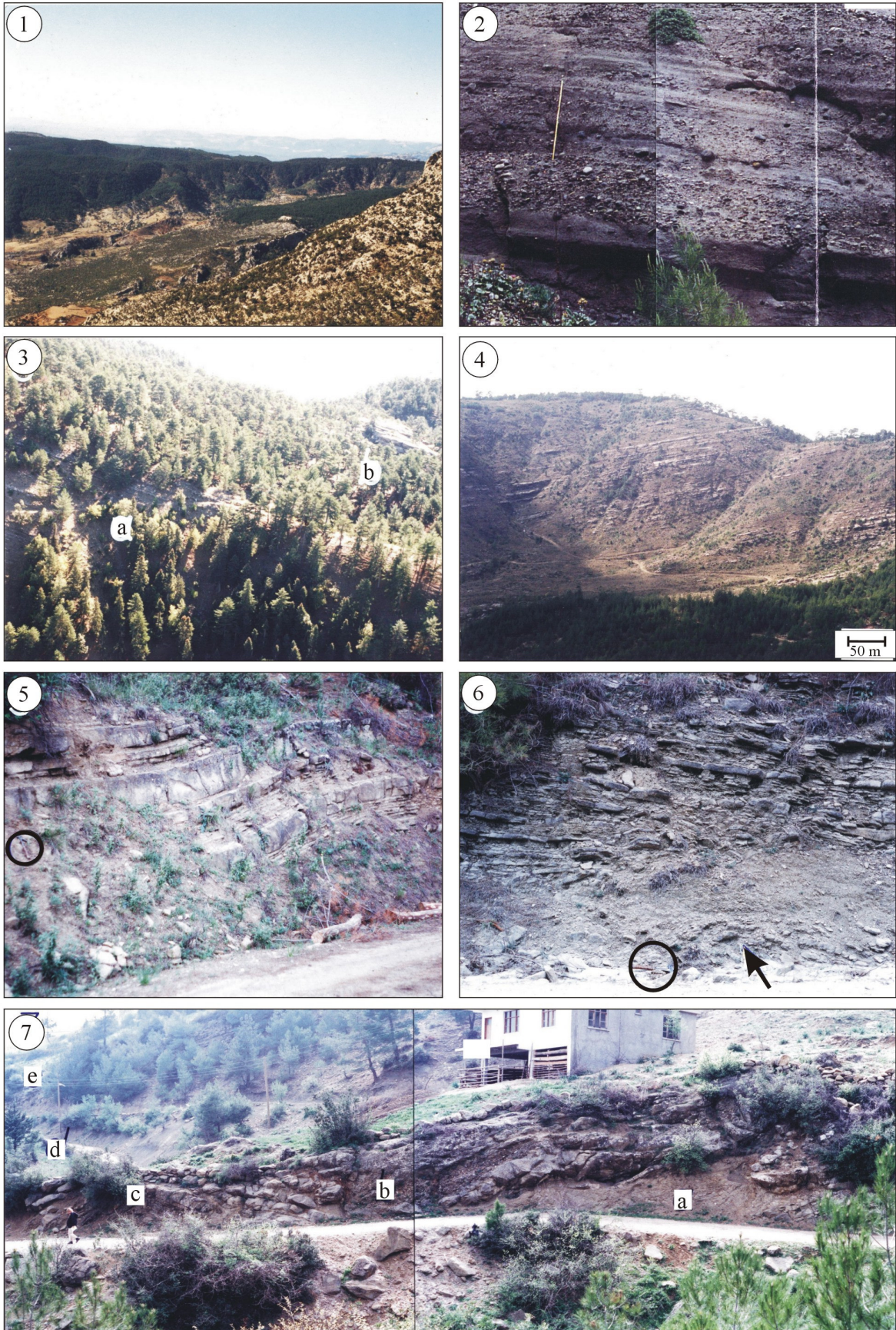


PLATE 2

1. Detail of debris flow deposit at Kuscusofolu Village (plate 1.7) showing well-rounded clasts and shallow-water fossils embedded in chaotic silt matrix reminiscent of Kaplankaya slope deposits (hammer for scale).
2. The northwestern marginal E-Fan (W1) is dominated by coarse-grained turbiditic fan sediments (S_{1-3} of Lowe 1982) sporadically interbedded with shelf/slope-derived debrites. These debrites mainly contain (shelfal-) limestones, deformed clasts of Kaplankaya slope material and a few well-rounded, mostly ophiolitic cobbles in a chaotic, shale-dominated matrix with a high shallow-water fossil content. Finer-grained lobe fringe deposits (T_{b-d} of Bouma 1962) onlap debrite (hammer for scale).
3. Thick successions of thin-bedded, medium to fine-grained turbidite sandstones ($T_{(a)-d,e}$ of Bouma 1962) representing fan fringe sedimentation of the E-Fan dominate the western section (hammer for scale).
4. An approximately 10 m thick prominent, shale-rich debris flow marked by a chaotic matrix, few well-rounded floating clasts (arrow), fragments of deformed sandstone beds (arrow) and a high shallow-water fossil content indicating sporadic slope collapse following overloading and/or seismic activity is interbedded with fan fringe sedimentation (W2). A previous interpretation suggested these deposits to represent overbank/levee sedimentation (Gürbüz 1993).
5. Up to 4 m thick, massive very coarse to granule sandstones and small pebbly gravelstones (R_{2-3}, S_{1-3} of Lowe 1982) dominate the highly amalgamated sandstone package representing prograding western fan sand tongues *sensu* Satur (1999) into an area otherwise receiving fan fringe sedimentation at Cingöz Village (person for scale). These W-Fan deposits are characterised by a very high sand:shale ratio (30:1) and the coarseness of its deposits.
6. Groove casts and other solemarks are commonly observed at the bases of the individual beds of the sand tongues, eroding into the thin shales separating sandstone beds (compass for scale).
7. Associated with the coarse-grained W-Fan sand tongues are up to 15 m thick successions of very finely laminated shales ($T_{d,e}$ of Bouma 1962; T_3 of Stow & Shanmugam 1980). These shales are distinctly finer-grained and contain a much lower net sand content than the recorded W-Fan fringe sedimentation (W3). Person for scale.
8. Along the Seyhan River in the east of the E-Fan, distal lobe deposits (a), lobe fringe (b) and interlobe deposits (c) are well exposed, forming laterally extensive sediment bodies at outcrop scale (person for scale). A gradual thinning- and fining upward from the lower lobe deposits towards the interlobe deposits is present, the latter are sharply overlain by the abrupt onset of renewed lobe sedimentation.

PLATE 2

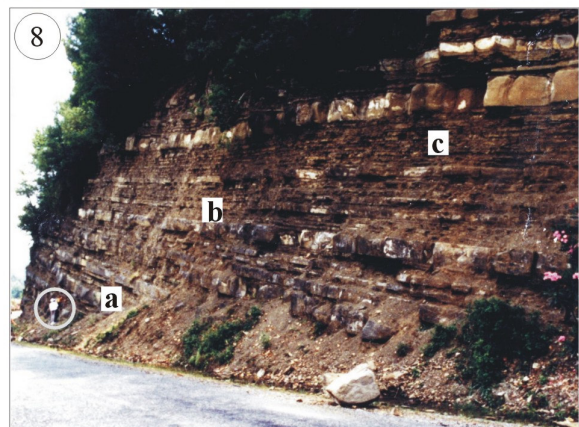
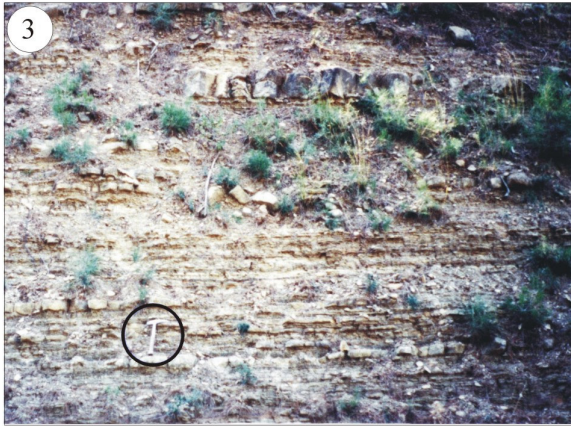


PLATE 3

1. Fan turbidites (a) along the northwestern margin of the E-Fan onlap (arrow) the irregular topography of the laterally confining, approximately 8° angled slope (b) [Location Log C of fig. 2.13].
2. Abrupt pinch-out of fan sediments against the irregular slope topography is commonly observed along the northwestern margin. Shallow “slope pockets” are infilled by fan sediments resulting in a stepped contact. The underlying slope morphology appears to be a direct result of synsedimentary sliding and slumping of slope deposits triggered bei oversteepening and/or seismic activity leaving an irregular topography behind. Debrites are occasional intercalated (arrow pointing at floating pebble) [Location Log B of fig. 2.13].
3. Syn- to postsedimentary movement along the fan-slope contact aggravates the infill-termination against the steep slope (hammer for scale).
4. a) Along the northeastern margin, close to Capikare Village, up to 12 m thick slumped fan sediments overlie the slope. The presence of slumps indicates a certain amount of upslope transport and deposition above the active fan surfaces allowing for semi-lithified deposits to subsequently slump down onto the fan. The outcrops is located in a fault-displaced slab of Cingöz fan deposits north of the main fan [Location 2b of fig. 2.10).

b) Line drawing emphasising the irregular slope topography (dashed line) and the bedding disorder within the Kaplankaya slope formation (b). Fan deposits overlying the slumped package (a) display irregular thickness distribution suggesting compensation of the underlying relief. Telephone posts for scale: hight approximately 4 m.
5. The photograph shows a thick montone Kaplankaya slope succession (1) at the bottom, succeeded by a lenticular debrites (2) and mixed calci-clastic turbidites (3) infilling a shallow slope gully geometry, just before the onset of clastic fan turbidite sedimentation (4). The basal fan turbidites display dramatic thickness decrease towards their pinch-out, possibly as a result of the underlying topography [Location Log A of fig. 2.13].
6. Detail of the slope gully infill showing at least 2 debrites separated by lensing mixed calci-clastic turbidites of shelf/slope origin. The basal debris flow showing large floating clasts (arrow) in a chaotic shaley matrix (hammer for scale).

PLATE 3

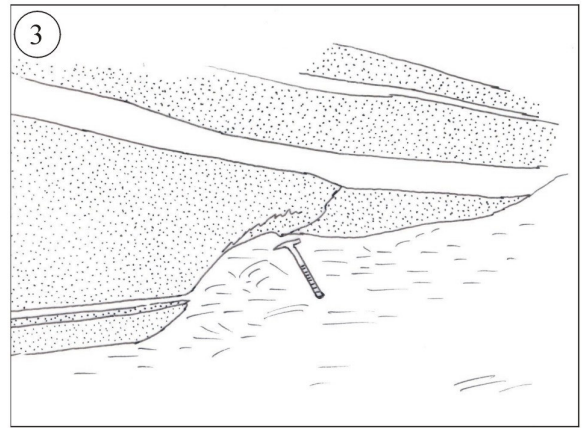
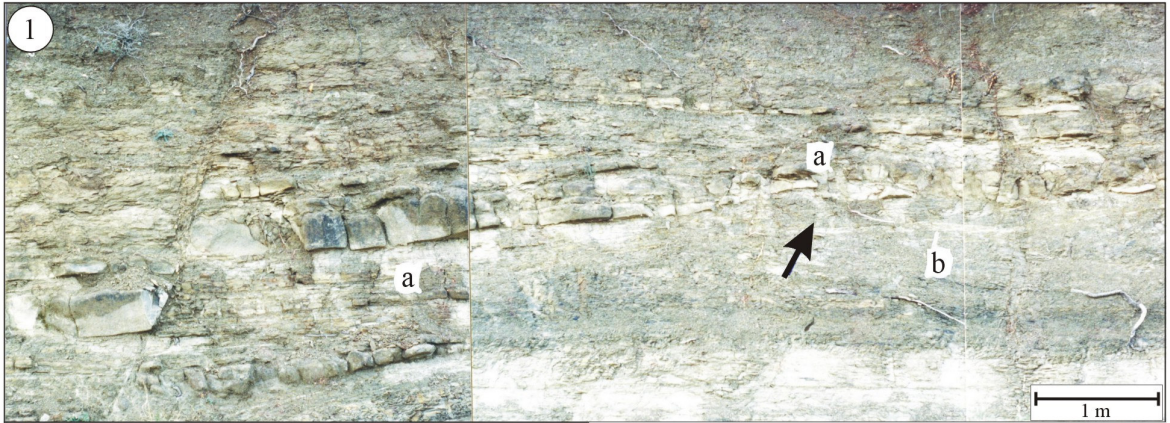


PLATE 4

1. Picture showing the lower, well exposed part of the channel-lobe transition zone. Extensive, highly amalgamated sandstones and pebbly sandstones of lobe A deposits dominate the lower part of the section while the conglomeratic channeling component with its abundant cut- and fill structures and pinching out geometries are cliff-building. A laterally extensive, low angle unconformity lies at the base of the cliff. Throughout, the net sand content is very high, shales are only preserved as clasts within conglomerates. Lines 1 to 4 indicate position of logs of fig. 2.18.
2. Multiple infill of a small, shallow cut- and fill structure within the channeling component (scale: 1 m showing at least 3 erosional-depositional stages (arrows) represented by 1) pebbly conglomerate (R_1 of Lowe 1982), 2) coarse-grained sandstone and a fining-upward of a pebbly - cobbly conglomerate (R_1) into a coarse-grained sandstone ($R_1S_{1,2}$).
3. a) A basal cut- and fill structure showing a near symmetrical 3-stage gravelly-sandstone couplets (a,b) and gravelly sandstone infill (c) *sensu* Ghibaudo (1992) which is cut by a laterally extensive low angle unconformity (d) located in the lower channel-lobe transition zone. The unconformity can be traced over 40 m and is believed to result from mega-scale scouring typical of channel-lobe transition zones (Mutti & Normark 1987). The unconformity is overlain by R_{1-3} conglomeratic channeling deposits, exhibiting massive bases and crudely stratified tops can be classed as deposits (Lowe 1982), exhibiting massive bases and crudely stratified tops.

b) Line drawing depicting the erosional surfaces (a-d).
4. The bulk of the channel-lobe transition zone is made up of laterally extensive, thick, parallel-bedded sandstones (S_{1-3} of Lowe 1982) which form up to 30 m thick lobe A deposits (scale: 1 m). The sediments are highly amalgamated, shale partings and or/shale beds are rarely observed. Bedding irregularities result from basal scouring. The irregular bed thickness results from basal scouring (arrows).
5. Amalgamation and traction carpets are abundant within the lobe A deposits (hammer for scale). The amalgamation planes almost never contain shale partings. Inclined traction structures as seen in the picture may be delineated by small pebbles (arrows).
6. Within the lobe A deposits, sandstones beds very rarely fine upward to fine-sand size (pencil for scale). Small clay chips are present and coalified material and plant debris delineate fine lamination at the very top of the bed (S_{1-3} , T_d of Lowe 1982 and Bouma 1962).
7. The oblique plan view of a scour reveals shallow scouring and a pebbly to cobbly, matrix-supported conglomeratic infill (R_1 of Lowe 1982; hammer for scale). The maximum clast size present is 12 cm. Scours in plan view are commonly observed on the bed surfaces within the channeling component, however, pervasive coating by lichens and weathering (foreground) are frequent.

PLATE 4

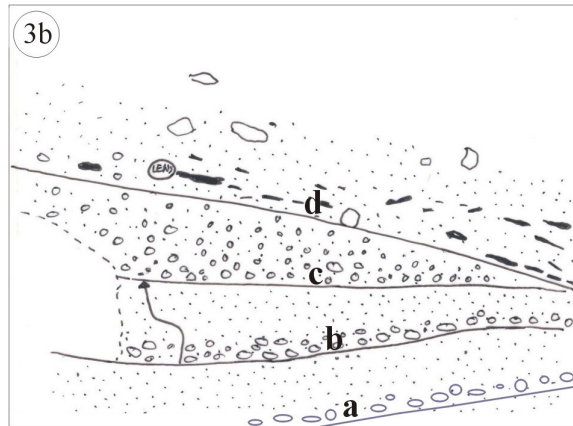
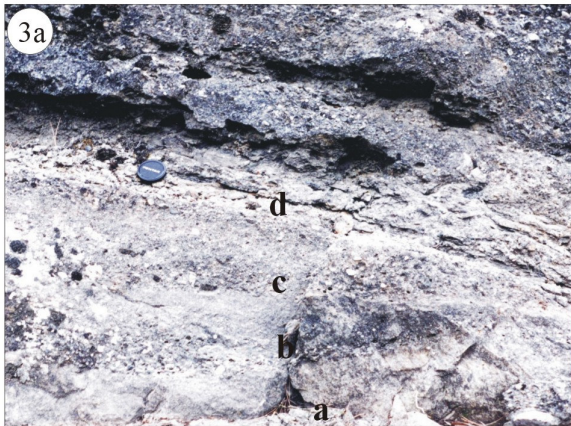


PLATE 5

1. The Lobe B deposits of the proximal lobe zone are composed of thick-bedded, laterally extensive sandstones (person for scale). The deposits are highly amalgamated and characterised by a high net sand content. Note the pervasive covering by lichens.
2. Water-escape features, such as these burst-through features (sand volcanoes) which heavily deform the original traction carpet lamination, are common in Lobe B deposits of the proximal lobe zone (lens cap for scale at bottom left).
3. A coarse-grained sandstone ($S_{1,2}$ of Lowe 1982) with traction structures is erosionally cut into by a granule sandstone (hammer for scale). The presence of an escape burrow (arrow) burrowing through both beds suggests at times rapid sedimentation rates within lobe B depositional environment.
4. Massive composite sandstone are common within the lobe B deposits (hammer for scale). With their often poorly distinguished amalgamation surfaces, the lack of grading and an abundance of floating shale clasts they resemble deep-water massive sandstones (DWMS) of Stow & Johansson (2000).
5. Within the highly amalgamated lobe B deposits wedging beds (arrow) feature rarely (hammer for scale). They are believed to compensate topographic expression of previously deposited deposits. More often small-scale wedging geometries are associated with the depositional wings of distributary channels.
6. Detail of the offset-stacked distributary channels near the top of the proximal lobe zone (hammer for scale). Distributary channel (2) cuts down into the stacked channel-fill deposit of distributary channel (1). The channels were too shallow to contain volumetrically larger flows which resulted in “wing-like” deposition outwith the channel margins (3). Selective erosion may account for the stepped channel margin (arrow).
7. Thin-bedded, medium to fine sand-sized sandstones ($T_{(b)c-d,e}$ of Bouma 1962) and interbedded shales represent the finest fraction of the lobe fringe deposits of the proximal lobe zone (pen for scale). Their occurrence is rare, occasionally separating lobe B packages. They are characterised by a low sand:shale ratio (2:1).

PLATE 5

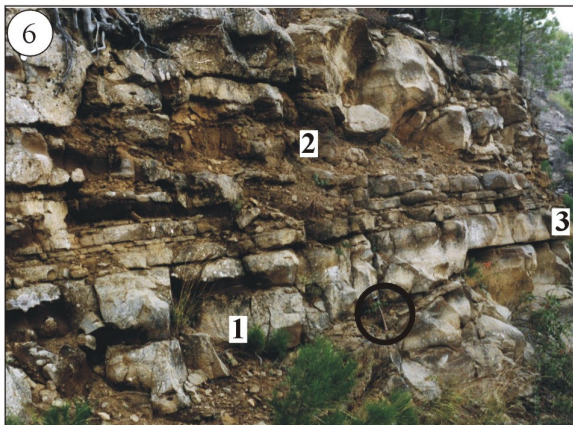
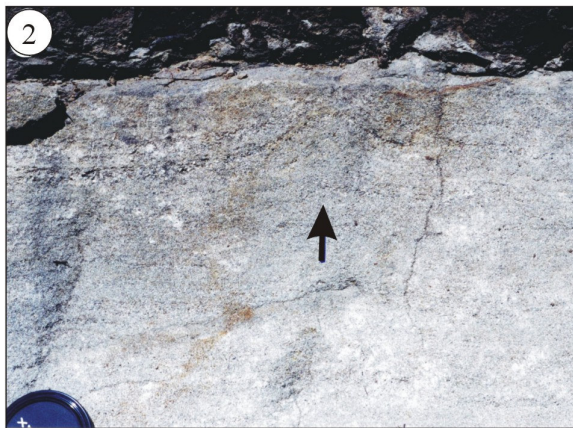


PLATE 6

1. The Lobe C deposits of the distal lobe zone are characterised by laterally extensive, parallel bedded sandstones (scale: 1 m). The sandstones are typically composed of coarse- to medium-grained sandstones, separated by a few cm of thick fine sandstone and shale intercalations. The net sand content is in average greater than 80 %.
2. Sharp-based sandstone with massive bases, uniformity in grain size nearly throughout the whole bed and only rapid fining at the top are commonly observed (pen for scale). They can be classified as S_{2-3} (Lowe 1982) or T_{a-d} (Bouma 1962). Note the faintly aligned, weathered shale chips at the top right and burrow at the bottom right (arrow). Both features are commonly found within the Lobe C sediments.
3. Excellent preservation of bioturbation on bedding surfaces can be observed in the lobe C deposits. *Zoophycus* is a commonly found trace fossils (lenscap for scale).
4. Slumping, especially involving sandstone beds, is rarely observed within the distal lobe environment (scale: 1 m). The shown slump package (arrow; slump axis pointing to left) is composed of medium sand-sized beds intercalated with shales and fine sand typical of lobe fringe deposits. As semi-lithified sediments they may have collapsed into an intervening depression (interlobe environment?) The sharp onset of thick, relatively coarse lobe deposits suggests a sudden shift of lobe sedimentation into this particular area.
5. The groove casts at the sole of this bed show a 30° divergence in transport direction, pointing to a general NE (25 - 55°) direction (hammer for scale).
6. This lobe fringe package is marked by a distinct coarsening- and thickening-upward sequence believed to result from lobe migration into this particular area. The net sand content increases from approximately 50 to 75 %.
7. The fine-grained interlobe deposits are characterised by a low net sand content (~ 60 %). They are composed of thin-bedded, fine-grained sandstones ($T_{c-d,e}$ of Bouma 1962; hammer for scale). The presence of the thick, isolated sandstone bed suggests that occasionally larger turbiditic flows reached into this otherwise relatively quiet depositional environment.
8. The top of the Seyhan River section is characterised by thick, monotone successions of fan fringe deposits (person for scale). Turbiditic flows capable of depositing thicker and coarser sandstone beds (arrow) only occasionally reach this area.

PLATE 6

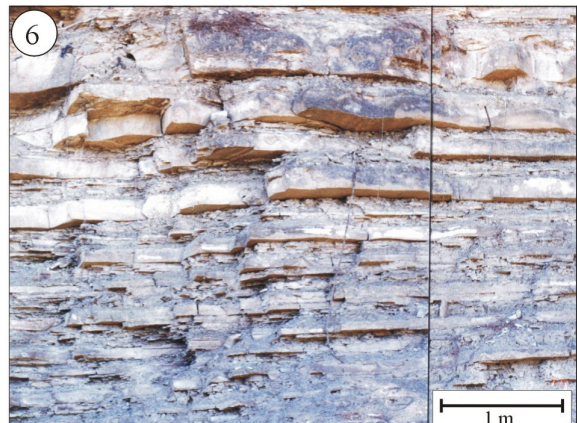
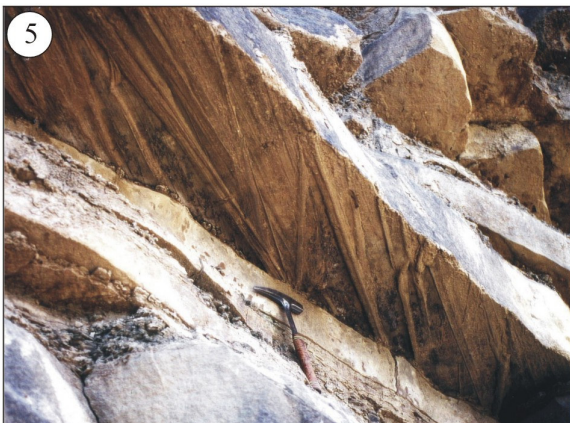


PLATE 7

1. Top of matrix-supported G5 deposit with large marl (1) and smaller limestone clasts. Small, deformed shale clasts are roughly aligned, some synsedimentary deformation (loading? arrow) is present (14/19-21: 10573 ft).
2. Sand-shale, matrix-rich debris flow deposits (G6, bottom) overlain by clean gravelly, limestone clast-rich conglomerate (G3, top). G3 loading into G6 (arrow). Maximum clast size G6 is 10 cm and G3 is 2.5 cm. G6 facies contains shell fragments (arrow; 14/19-E7: 9856 – 9855 ft).
3. Well cemented GS2 deposit with distinct pebble-delineated traction carpets (1). Reverse grading, i.e. upward increase in pebble size. Winnowing of sand along traction surface (?). Succeeding flow eroded into GS facies (arrow; 14/19-21: 10592.5 ft).
4. GS3 facies with abundant aligned, subangular shale rip-up clasts and smaller limestone pebbles in coarse sand matrix. Some shale clasts are thoroughly bioturbated (1). Overlying sandstone erodes into GS3 deposit (arrow; 14/19-E7: 9891 ft).
5. Poorly sorted, pebble-rich area shows preferential carbonate cementation (nodule; 14/19-20: 9869 ft).

PLATE 7

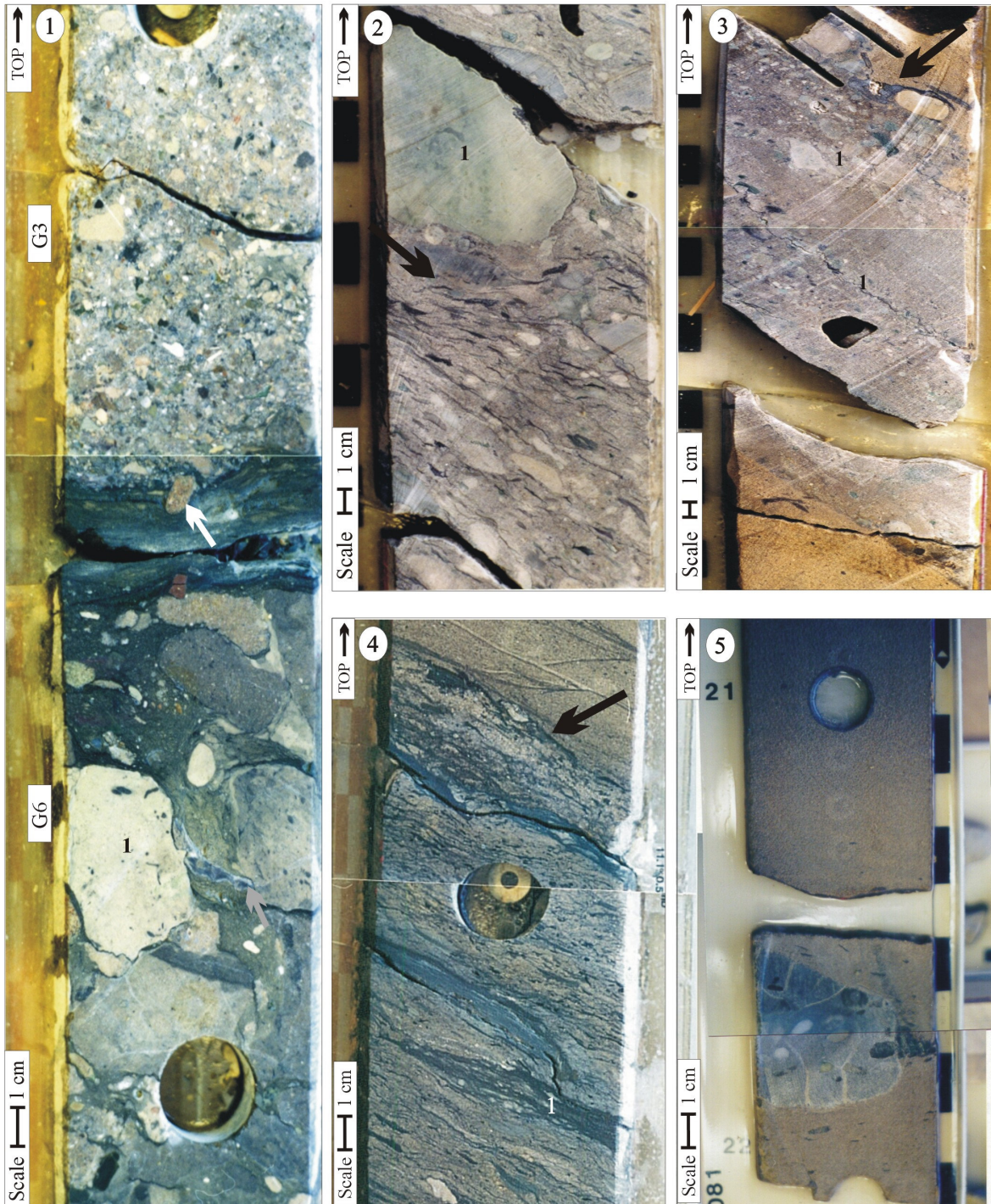
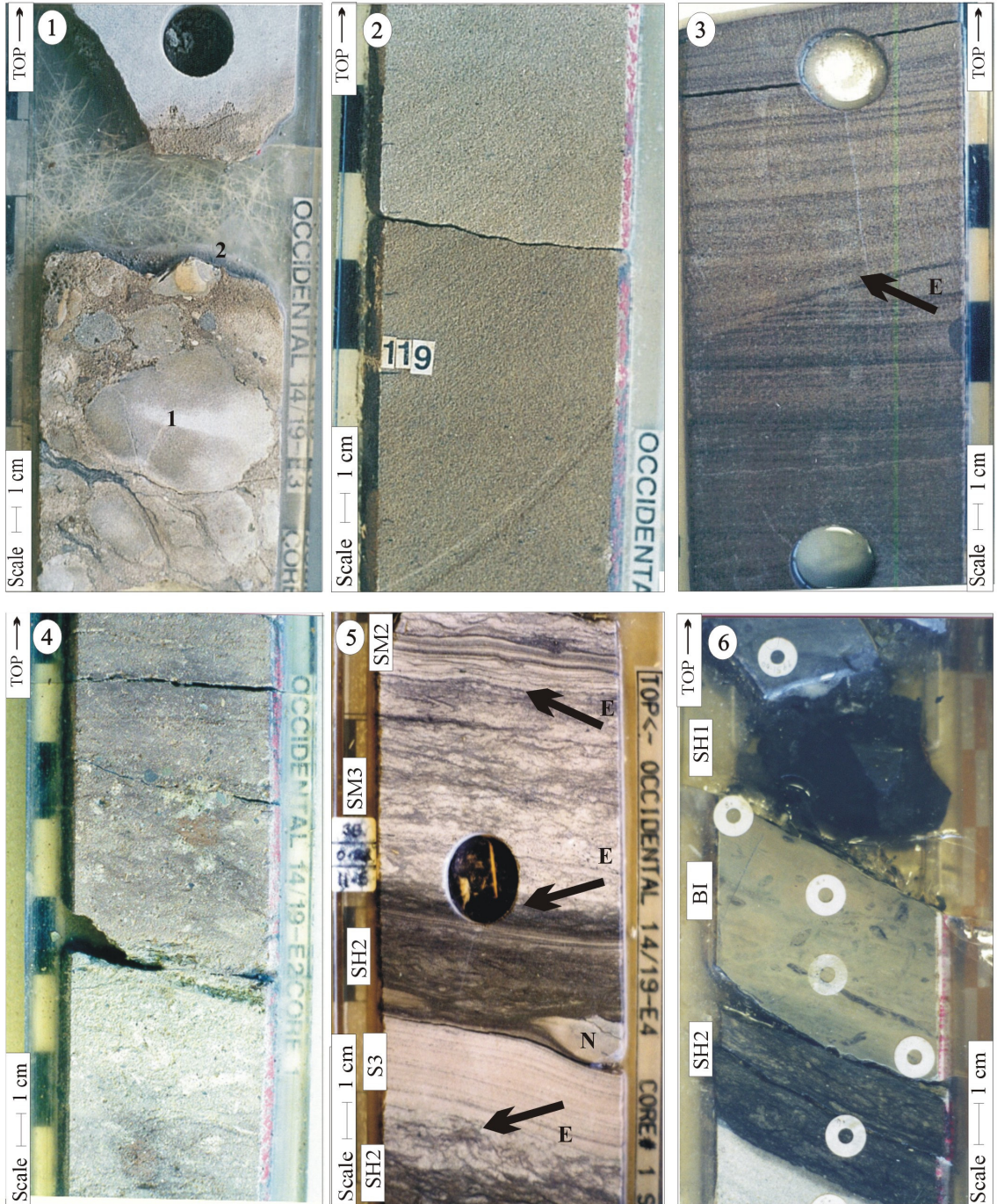


PLATE 8

1. Disorganised GS5 deposit with reworked carbonate nodules (1) and shell fragments (2: gastropod; 14-19-E3: 10668 ft)
2. Medium-grained, massive S1 sandstone (14/19-E2: 9134.5 ft).
3. Medium-grained, well laminated S3 sandstone cut into (arrow) underlying fine-grained, well laminated top of S2 sandstone (14/19-E2: 9099 ft).
4. Bimodal SM1 facies with reddish shale matrix and granule to small pebble-sized grains. The shale content is greater than 15% (14/19-E2: 9075 ft).
5. Succession of thin-bedded SH2-S3-SH2-SM3-SM2 deposits(14/19-E4: 9685 ft). Erosive contacts are common (arrows), nodule formation (N) rare.
6. Highly bioturbated marls (hemipelagic Bi facies) interbedded with SH1 facies (top) and highly bioturbated thin-bedded turbidites of SM3 lithofacies type.(14/19- E2: 9163 ft).

PLATE 8



APPENDIX

APPENDIX 1

LIST OF STUDY WELLS

Grey boxes: maximum S10 interval (VJ/VI dinocyst subzones).

Bold letters: SD subdivisions; SD5 horizon has been reassigned to SE horizon (McAfee 1993)

Bold italics: cored intervals

All thickness given in feet TST (True Stratigraphic Thickness).

	14/19-20	14/19-21	14/19-E1	14/19-E2	14/19-E3	14/19-E4	14/19-E5Y	14/19-E7
	TST (feet)	TST (feet)	TST (feet)	TST (feet)	TST (feet)	TST (feet)	TST (feet)	TST (feet)
SF2	-	143,26	-	-	-	59,35	-	-
SF1	-	30,70	-	-	-	57,37	-	-
SE	96	63,80	19,44	81,39	8,61	31,21	24,54	72,21
SD5	28	-	15,47	35,51	21,17	30,22	33,52	14,52
SD4	78	<i>105,80</i>	<i>104,76</i>	<i>107,32</i>	<i>35,53</i>	<i>112,21</i>	<i>77,41</i>	<i>71,28</i>
SD3	35	-	<i>49,21</i>	<i>52,47</i>	<i>51,68</i>	-	<i>62,44</i>	<i>49,87</i>
SD2	16	-	<i>47,22</i>	<i>48,47</i>	-	-	<i>47,01</i>	<i>20,1</i>
SD1	-	<i>56,45</i>	-	-	-	<i>100,36</i>	-	-
S10	176	47.5	175-193	no record	113	131	246	no record
SC4	72	-	-	-	-	-	-	79,21
SC3	54	-	53,08	41,49	110,9	-	47,01	30,52
SC2	44	-	58,71	55,46	62,45	30,23	76,65	61,42
SC1	100	-	45,9	-	42,71	82,58	-	91,38
SA2	144	-	84,87	-	320,74	-	-	185,35
SA1	-	-	-	-	112,54	-	-	-
LV/CG	not calc.	not calc.	not calc.	not calc.	not calc.	not calc.	not calc.	not calc.

APPENDIX 2

ELECTROSEQUENCE ANALYSIS and LITHOFACIES

Table of differentiated trend lines for S10 interval of study wells. Sequences are listed from base to top, thicknesses given in feet log depth.

Well 14/19-20

- 1 - 12 ft: **GR: 70-40 (2x); CL: little WO; SL: 80-60; RL:- ; DL: 2.45; NL: 0.15-0.25:** 2 smaller 6-9 ft thick shaling-down (c-up?; SH/SM-srS; SH/SM-srS)
- 2 - 18 ft: **GR: 45-100-40; CL: WO; SL: 80; RL:-; DL: 2.35; NL: 0.3, some negative separation: srS-SM-SH-SM-srS**
- 3 - 15 ft: **GR: 30; CL:- ; SL: 70-60; RT: 60; DL: 2.2 - 2.55; NL: 0.1:** SM-S/GS? (c-up).
- 4 - 23 ft: **GR: 35; CL: -; SL: 80-60; RT: 90; DL: 2.35; NL: 0.13:** crude 5-8 feet c-ups (GS-SM, vcs S-BI)
- 5 - 36 ft: **GR: 35; CL: -; SL: erratic 80; RT: 100; DL: 2.4; NL: 0.15:** mostly smaller subtle c-ups (vcs/gr S-GS, cs-ms S- rare GS)
- 6 - 30 ft: **GR: 20-30; CL: -; SL: 70-90; RT: 100; DL: 2.35; NL: 0.15:** slight shale-up (S-SM facies)
- 7 - 6 ft: **GR: 60; CL: WO; SL: 100; RT: 30; DL: 2.0-3.0; NL: 0.5-0.05: negative separation:** very shale-rich SM/Sh facies
- 8 - 14 ft: **GR: 20-40; CL: -; SL: 60-80; RT: 200-50; DL: 2.2-25; NL: 0.15:** shale-up (SrS/SM-SM)
- 9 - 28 ft: **GR: 20-80; CL: WO; SL: 80-100; RL: 80-10; DL: 2.4; NL: 0.15-0.45; occ. negative separation:** initial shale-down, then shale-up to very shale-rich SM/sH facies.
- 10 - 17 ft: **GR: 80-50; CL: WO!; SL: 100; RL: -; DL: 2.4; NL: erratic up to 0.45, occ. negative separation:** shale-down: SH/SM-S?, top little shale-up

Well 14/19-21

- 1 - 13 ft: **GR: 50-30; CL: -; SL: 75; RT: 60; DL: 2.45; NL: 0.75:** GS-vcs-ms S, f-up
- 2 - 4 ft: **GR: 75; CL: little WO; SL: 90; RT: 20; DL: 2.3; NL: 3:** SM1-SM2/3-facies, f-up
- 3 - 15 ft: **GR: 37-20; CL: -; SL: 70. RT: 50; DL: 2.4; NL: 0.125:** GS-S, 2 8 ft thick f-ups, erosive base
- 4 - 17 ft: **GR: 20-40; CL: -; SL: 65; RT: 40; DL: 2.45; NL: 0.1:** (GS)-S-(SM), 3-5 ft f-ups; ms-fs S2/S3 facies, increase in SM
- 5 - 7 ft: **GR: 45; CL: -; SL: 65; RT: 20; DL: 2.425; NL: 0.15:** S/SM - gradual shale-up

Well 14/19-E1

- 1 - 10 ft: **GR: 55; CL: WO; SL: 70; CL: 2.75; NL: -0.025:** shale-rich,SM/S(?) facies, gradational base, sharp top
- 2 - 53 ft: **GR: 50-20; CL: occ. WO; SL: 75-65; RL: 20, DL: 2.6; NL: wiggly/0.1/0.2:** shaling-down trend S-SM/shale-rich S to clean S
- 3 - 9 ft: **GR: 20-60; CL: WO; SL: 75; RT: 30; DL: 2.55; NL: 2.45-2.95:** shale-up/f-up (S-SM/SH), top shale-down (SM-fs S); ~ 20% shale content; green shales
- 4 - 20 ft: **GR: 40-30; CL: -; SL: 60-70; RT: 100-40; DL: 2.5; NL: 0.15:** smaller f-ups (G-S; GS-S), little shale content, rare bioturbation.
- 5 - 22 ft: **GR: 30; CL -;SL: 70; RT: 40; DL: 2.45; NL: 0.15:** dominantly S facies, smaller f-ups, little shale overall shale content.
- 6 - 33 ft: **GR: 20-40-30; CL: -; SL: 50-80; RT: 70; DL: 2.35; NL: 0.15:** basal shale-up, then shale-down: 3 8 – 14 ft. fining-ups (S-SM; GS-S-SM; S-SM) mod. to strong bioturbation (63% of beds); abundant shale clasts (45% of beds).
- 7 - 44 ft: **GR: 50-20; CL: -; SL: 60-80;RT: 50; DL: variable 2.35-2.6: NL: erratic 0.05-0.30:** slight overall shale-down, smaller fining-upward sequences (GS/S-SM)

Well 14-19-E3

- 1 - 28 ft - **GR: 55-35; CL: some WO; SL: 75-60; RT: -; DL: variable; NL: 0.2-0.05, occ. negative separation:** overall shale-down: 3 smaller 6-12 ft shale-downs (SH/SM; SM-srS)
- 2 - 31 ft: **GR: 40-60, CL: -; SL: 60-90; RL: -; DL: 2.6; NL: 0.05, occ. negative separation:** overall shale-up srS-SM/srSM-SH
- 3 - 31 ft: **GR: 60-20; CL: -; SL: 70; RT: 25; DL: 2.5; NL: 0.1:** overall shale-down (s-up) SM-S/GS
- 4 - 30 ft: **GR: 20; CL: -; SL: 60; RT: 100; DL: 2.6; NL: 0.05:** c-up S?/GS-G (G1/GS5)
- 5 - 10 ft: **GR: 20; CL: -; SL: 70-80-60; RL: 80; DL: 2.4; NL: 0.15:** GS/G or clean S

Well 14/19-E4

- 1 - 34 ft: GR: 35-50; CL: - top WO; SL: 70-65; RT: 20; DL: 2.45-2.55; NL: 0.125-0.1: GS-csS, csS-ms/fsS, f-ups, vcs S-fs (SM)-facies, 2 f-ups, abundant bioturb. (60% of beds), 3-5 ft thick f-ups of clean msS/rare GS-SM/SH-facies, small-scale f-rare GS and little SM1 and SH/SM facies, overall f-up, marl? (9645 ft)
- 2 - 9 ft: GR: 75; CL: WO; SL: 80; RT: 10-29; DL: 2.48; NL: 0.35: SH-Facies
- 3 - 16 ft: GR: 80-25; CL: little WO; SL: 70-80; DL/NL: basal neg. sep.: SH- clean GS/S-SM-Facies (4-6 ft, f-ups/c-up)
- 4 - 10 ft: GR: 60-25; CL: -; SL: 75; DL 2.5 (2.875); DL/NL: some neg. sep.: 5-8 ft thick c-ups SM-S -Marls? (9610 / 9604 ft)
- 5 - 13 ft: GR: 75; CL: little WO; SL: 75; DL/NL: neg. separation: SH/SM-S-Facies
- 6 - 13 ft: GR: 50-30; CL: -; SL: 75; DL/NL: some neg. separation: large c-up: SH/SM-S-Facies

Well 14/19-E5Y

- 1 - 33 ft: GR: 40-20; CL: -; SL: 70; RT: 20-80; DL: variable 2.4; NL: 0.15: subtle shale-down BI-SM-S-GS (c-up)
- 2 - 20 ft: GR: 20-30; CL: -; SL: 70-60; RT: 80; DL: 2.45-2.55; NL: 0.15-0.1: subtle shale-up, erosive base (G), f-ups G-ms S, GS-G-S
- 3 - 23 ft: GR: 30-25; CL: -; SL: 70-60; RT: 100; DL: 2.4; NL: 0.125: subtle shale-down but f-up (GS-ms S)
- 4 - 29 ft: GR: 20-30; CL: -; SL: 60-70; RT: 300-80; DL: variable 2.425; NL: 0.125: shale-up then shale down, but overall f-up, smaller f-ups (G- vcsS/ ms/fs S2/S3-SM2/SM3), erosion common (25% of beds) marking bases of smaller f-ups. Bioturbation (35%) and shale content (<10% increasing to 20%)
- 5 - 21 ft: GR: 20-35; CL: -; SL: 80-70; RT: 80-150-50; DL: 2.35; NL: 0.125: shale-up/f-up (GS-vcs/ms S facies)
- 6 - 26 ft: GR: 20-30-20; CL: -; SL: 60-80; RT: 400-70-100; DL: 2.42; NL: 0.15: shale-up/down (2 f-ups: GS-fsS; ms S-fs S/SM; GS-S-SM; c-up: csS-G; csS-vcsS)
- 7 - 8 ft: GR: 20-45; CL: little WO; SL: 60; RT: 100-30; DL: 2.6; NL: 0.1: shale-up/f-up (G-SH-SM)
- 8 - 16 ft: GR: 25; CL: -; SL: 60-90-60; RT: 90; DL: 2.4; NL: 0.1: f-up (Gs-S-SM)
- 9 - 19 ft: GR: 25-35; CL: -; SL: 90-60; RT: 150; DL: 2.2-2.5; NL: 0.2: shale-up/f-up: DWMS ms S to SM
- 10 - 20 ft: GR: 45-20; CL: -; SL: 75; RT: -; DL: 2.325; NL: 0.1-0.2: shale-down/Cup (SM-S; marl? (9300 ft)
- 11 - 15 ft: GR: 90-30; CL: little WO; SL: 80; RT: -; DL: 2.35; NL: 0.2: some negative separation: shale-down/c-up (SH/ very shale-rich SM-S)
- 12 - 22 ft: GR: 70-40; CL: WO; SL: 80-100; RL: -; DL: 2.6; NL: 0.25: negative separation: shale-down/c-up (SH/SM/Marl?-S), top shale-up/f-up (S-SM/SH)

Well 14/19-E2

- 1 - 30 ft: GR: 20/30-10; CL: -; SL: 7-80; RT: -; DL: 2.35, variable; NL: 0.15: clean GS/S, slight overall shale-down, smaller 4-8 ft shale-downs, occ. pyritisation?/ strong cementation.
- 2 - 21 ft: GR: 45-30(2x); CL: -; SL: 100-50; RT: 50-200; DL: 2.35; NL: 0.1: 2 shale-downs/c-up (S-SM)
- 3 - 10 ft: GR: 30; CL: -; SL: irr. 90-60; RT: 100; DL: 2.4; NL: 0.1: shale-up/f-up S-SM-BI-SM
- 4 - 23 ft: GR: 30-45-30; CL: -; SL: 80-60-90; RT: 90-40-90; DL: 2.5; NL: 0.05-0.2: shale-up-down (S/G-S/G-SM-S)
- 5 - 14 ft: GR: 30-60; CL: -; SL: 60-110-70; RL: 50; DL: 2.4; NL: 0.15: overall shale-up/f-up G/GS-vcS/SM
- 6 - 15 ft: GR: 45-30; CL: -; SL: 60; RL: 30-80; DL: 2.6; NL: 0.1: shale-down/C-up (S-G)
- 7 - 17 ft: GR: 45-60; CL: -; SL: 70-110; RL: 60; DL: 2.4; NL: 0.15-0.2: subtle shale-up ((G)-S-SM/S-SM)
- 8 - 35 ft: GR: 40-100; CL: WO, SL: wiggly 80-100; RL: ~ 30; DL/NL neg. separation: overall shale-up in smaller shale-ups (S-SM; S-SM-SH).
- 9 - 15 ft: GR: 100-10; CL: some WO, SL: 80; RL: -; DL: 2.65/NL: 0.45-0.1: neg. separation: shale-down (2) SM/SH-srS, srS;-S
- 10 - 28 ft: GR: 10-40-10; CL: occ. WO; SL: 80-90; RL: -; DL: 2.6 / NL: 0.25-0.3: neg. separation: basal shale-up (f-up), (S-SM), gradual shale-down (srSM-S 2x)

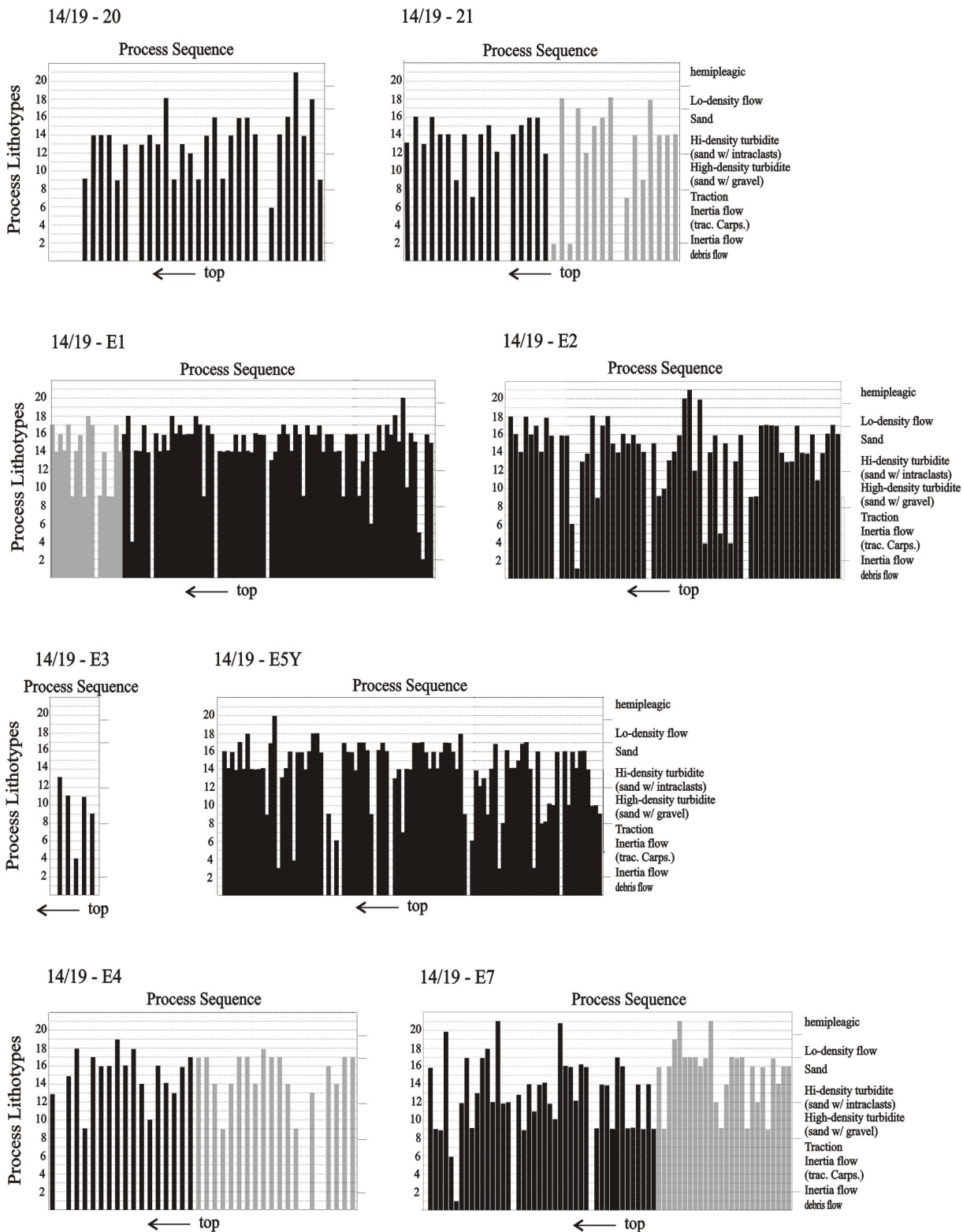
Well 14/19-E7

- 1 - 43 ft: GR: 25; CL: -; SL: 75; RT: 120; DL: 2.35; NL: 0.15: crude, smaller f-up/C-ups (GS dominated, rare S/SM)
- 2 - 30 ft: GR: 35; CL: -; SL: 75; RL: 120; DL: 2.35; NL: 0.15: small f-up (S-BI), c-up fs S-vcsGS, GS4-Gs3; vcs S - GS3
- 3 - 25 ft: GR: 40-20; CL: -; SL: 75; RT: 100; DL: 2.45; NL: 0.175: shale-down but f-up GS-vcs S, GS-SM
- 4 - 8 ft: GR: 30-20; CL: -; SL: 55; RT: 30-500; DL: 2.65; NL: 0.025: f-up/c-up: G6(6.4 cm)/G3(1.8 cm) -SH-Facies; top GS (max. clast size: 3.5 cm)
- 5 - 18 ft: GR: 20; CL: -; SL: 85; RT: 100; DL: 2.35; NL: 0.2: subtle 3-5 ft f-ups: vcs S-facies
- 6 - 42 ft: GR: 40-60; CL: distinct WO; SL: 60; DL: 2.7; NL: 0.15. distinct negative separation: 8-15 ft. shale-ups (srS-SM-SH).

APPENDIX 3 Process Sequences

Process sequences: lithofacies types (n = 20) are transformed into qualified measures of flow power, using grain size and sedimentary structures as indicators of transport and depositional processes, arranged into descending order of energy (after Cronin 1994).

S10 deposits
 S9/S11 deposits



APPENDIX 4

Bed thickness analysis by RUNS analysis (Davis 1986; Murray *et al.* 1996) for determination of asymmetry within successions:

RAM : runs about median

RUD: runs up and runs down

(Simple and two-bed moving average)

14/19-E1

RAM analysis: median 31.5 cm

001000101010100100000011100100010001-gap-0000111011-gap-1110100001001-gap-0110101111101111001 r: 40

RUD analysis:

1100010101010110011101010010101010-gap-0110101001-gap-0101011001010-gap-010110101101011 runs: 59

RUD analysis (2-bed moving average):

11001101010101100110110101101110101-gap-111001100-gap-1101011011010-gap-01010010111101 runs: 48

14/19-E5Y

RAM analysis: median 46.9 cm

0011110110111000001000100110111111001000100000101000000000000111100000010100111110101110 r: 34

RUD analysis:

0101001010101010011001101110101011011101011101001011100101010000101010101010101010 runs: 67

RUD analysis (2-bed moving average):

1101010001100011011100110111011101110111000111010010110001011100001110111101101001110101 runs: 48

Undifferentiated SD bed thickness analysis

14/19-E2

RAM analysis: median 23.9 cm

1011110111000011-gap-10100011000011110-gap-1000110000101111-gap-101010100 # of runs: 30

RUD analysis:

0110010111010010 - gap - 0101111010011010 - gap - 001100010101000 - gap - 01010100 # of runs: 44

RUD analysis (2-bed moving average):

011011011011011 - gap - 010111001011100 - gap - 00110011011100 - gap - 11011101 # of runs: 34

14/19-E7

RAM analysis: median 42.5 cm

0010101010000110010000011011101100111100-gap-110101111011-gap-1101001001000111 # of runs: 37

RUD analysis:

0010101010101110010010111010001101100100 - gap - 00101101010 - gap - 001011001010101 # of runs: 48

RUD analysis (2-bed moving average):

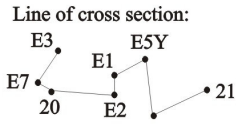
01101110100111001101111101000110110110 - gap - 0011100001 - gap - 00101101100110 # of runs: 34

Summary statistics

	E1	E5Y	E2	E7
number of runs about median	40	34	30	37
number of runs up and down	48(59)	48(67)	34(44)	34(48)
number of long runs up (>3)	2	8	6	4
number of long runs down (>3)	0	4	0	2
longest run up	3	5	4	6
longest run down	2	4	2	4

() simple RUD, other 2-bedmoving average

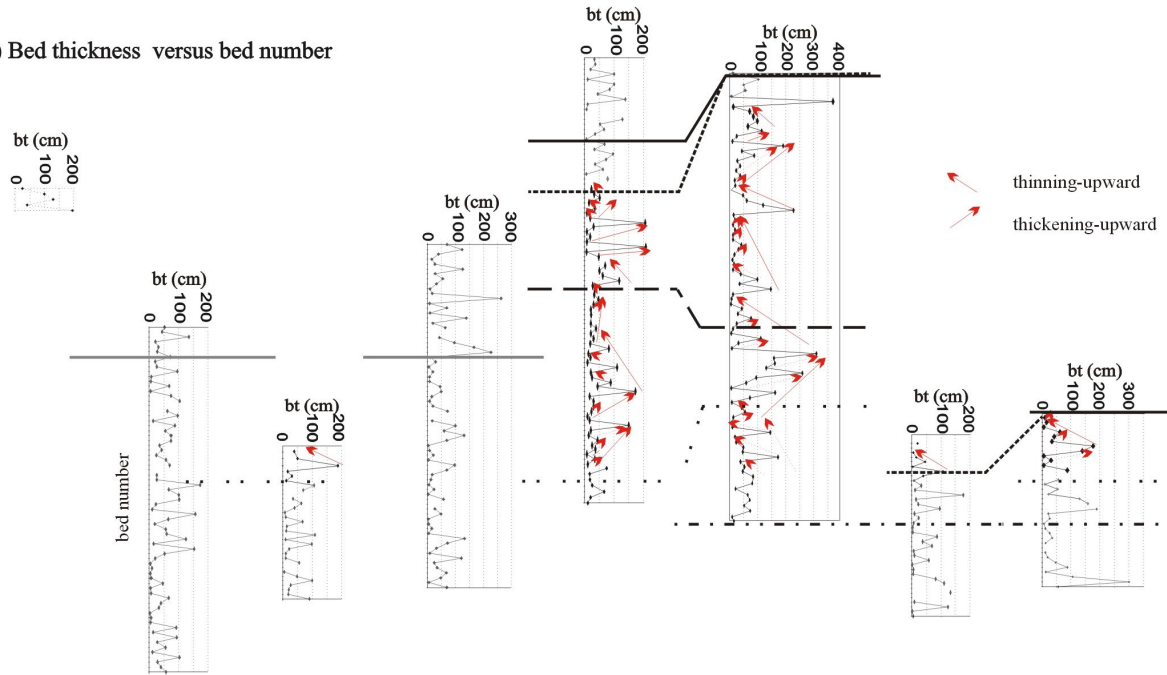
APPENDIX 5



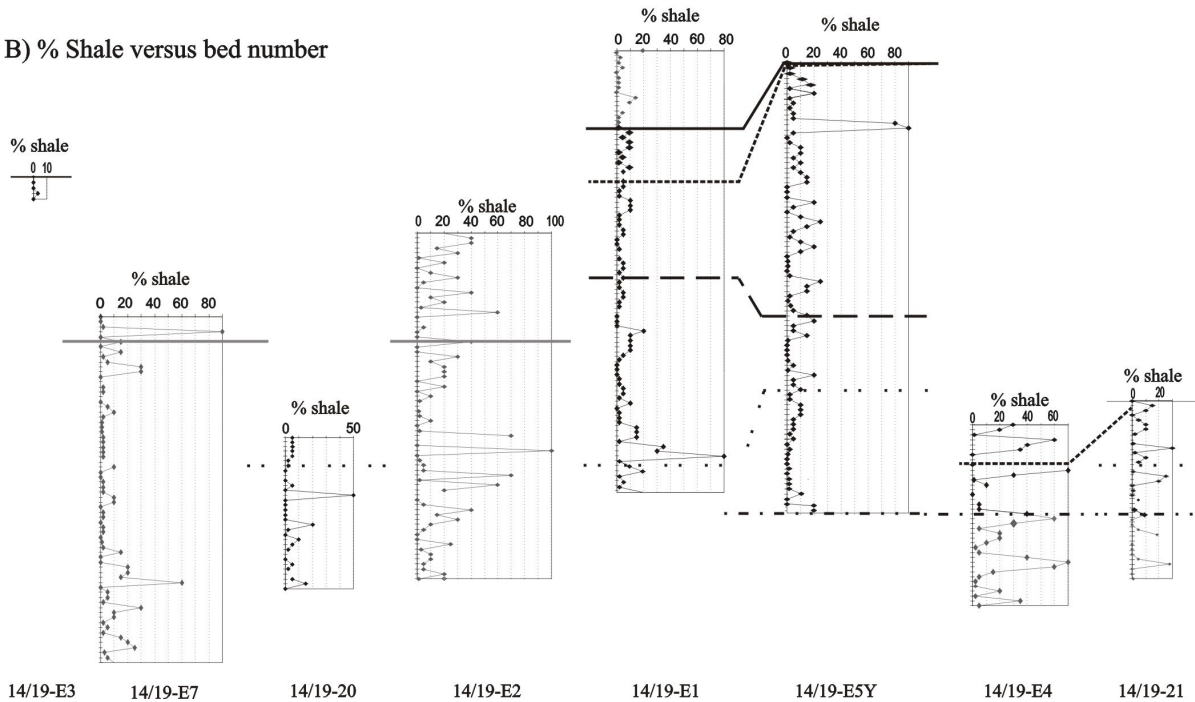
Sedimentary-based correlation between S10 study wells:
 all graphs display bed number along the y-axis versus various measurable sedimentary features.
 Graphs display bed numbers from base (bottom) to top of cored S10 interval (black data points) and the undifferentiated SD/SE (grey data points). The biostratigraphic correlation (*sensu* Riley *et al.* 1992 and CoreLab 1993) scheme is superimposed.

- ◆ individual bed
- (blank) Gap
- E2-E7 correlation
- Top S10
- - - Top VJ1
- - - Top VJ2
- · · Top VJ3
- · · Base S10

A) Bed thickness versus bed number



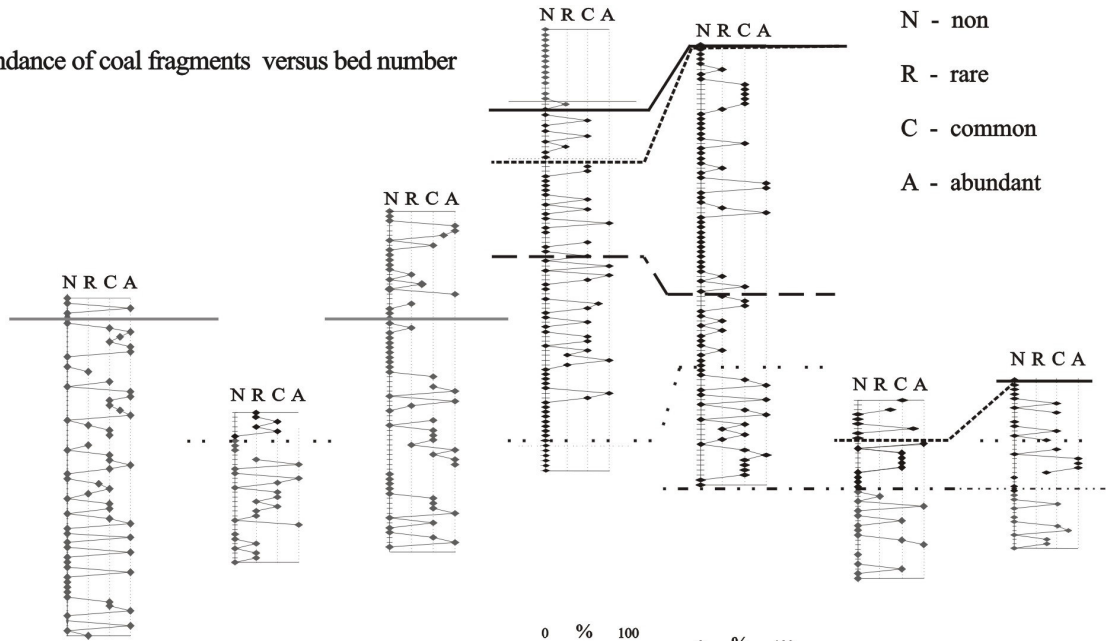
B) % Shale versus bed number



C) Abundance of coal fragments versus bed number

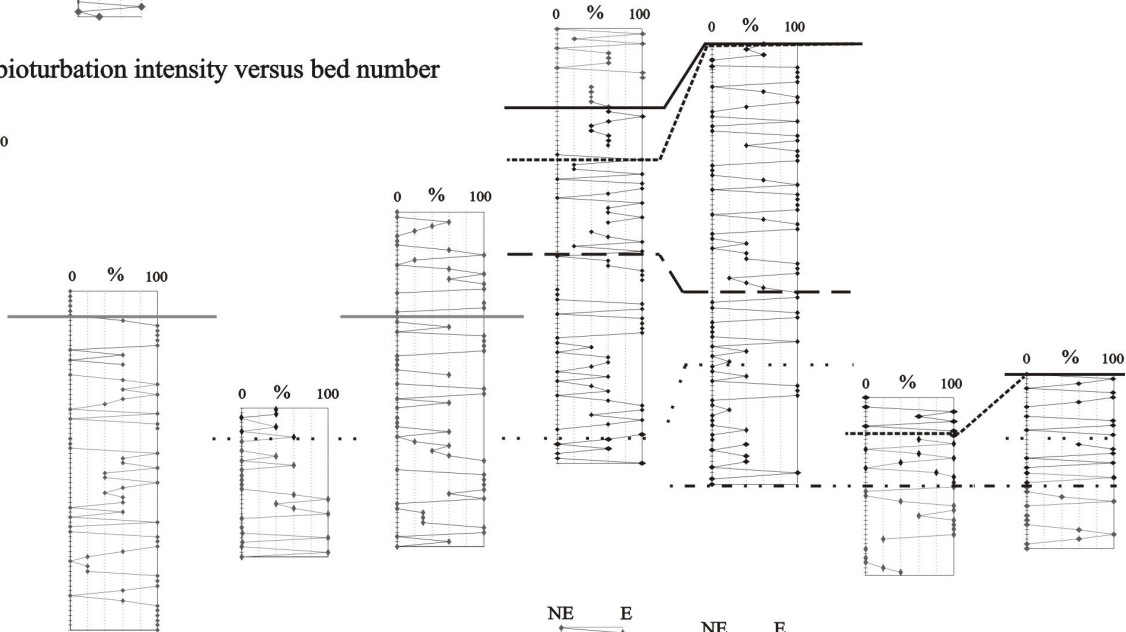
NRCA

N - non
R - rare
C - common
A - abundant



D) % bioturbation intensity versus bed number

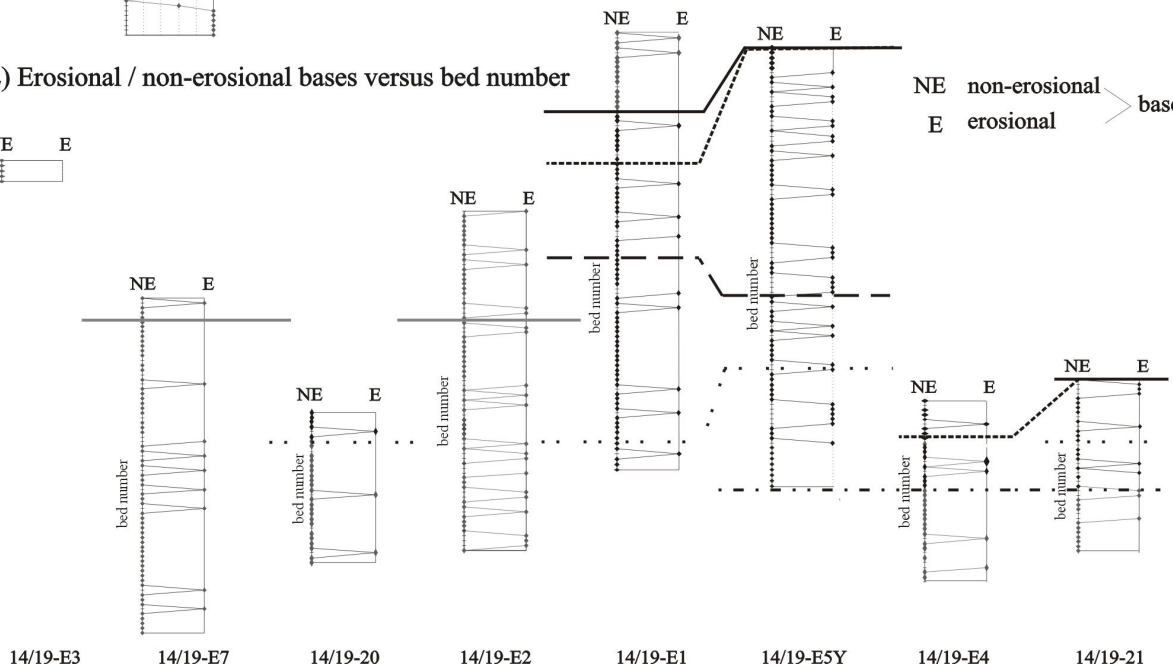
0 % 80



E) Erosional / non-erosional bases versus bed number

NE E

NE non-erosional bases
E erosional bases



14/19-E3

14/19-E7

14/19-20

14/19-E2

14/19-E1

14/19-E5Y

14/19-E4

14/19-21

ENCLOSURE

BILDUNGSGANG

Renate Kostrewa
c/o SNV, PO Box 3941
Dar es Salaam, Tanzania

Datum und Geburtsort: 23.09.67 in Bülach / Schweiz
Nationalität: deutsch
Familienstand: verheiratet, zwei Kinder

Bildung:

- 09/84-6/85 Austauschschülerin, Foothills Composite High School, Okotoks, Alta. (CAN)
- 1988 Abitur, Heilig Geist Gymnasium Menden
- 1988 – 1995 Geologiestudium, Eberhard-Karls Universität Tübingen
- 08/91 – 05/92 Austauschstudent, Northern Arizona University in Flagstaff (USA)
- 5. 04 1995 Diplom in Geologie an der Eberhard-Karls Universität Tübingen (Note: 1.3)
Diplomarbeit: „Sedimentology of the Stubensandstein Rivers, Mainhardter Wald, Northern Württemberg.“ (Prof. T. Aigner)
Diplomkartierung: „Fazieskartierung von Givetian Mud Mounds des Ahnet-Beckens, Zentral Sahara, Algerien.“ (Prof. Dr. J. Wendt)
- 02/1996 Beginn Promotion an den Universitäten Aberdeen/ Keele (UK) und
seit 01/01/2000 an der Universität Tübingen (D)
- 09/97-03/98 TESOL Certificate, Teilzeitausbildung, Aberdeen College (UK)

Arbeitsverhältnisse (post diplom):

- 05-06/95 Geotechnische Assistentin, Umwelt Wirtschaft GmbH, Stuttgart, Abteilung Hydrogeologie und Geotechnik
- 07-09/95 Wissenschaftliche Angestellte (Kurzprojekt), Katholische Universität Leuven in Zusammenarbeit mit dem Belgian Geological Survey (B)
- WS 97 & 98 Dozentin für Environmental Geology, Centre for Continuing Education, Aberdeen University (UK)
- 09 – 12/ 99 Englischlehrerin, Glasgow International English and Business School (UK)
- 01/01-12/02 Jugendprojektkoordinatorin, Mohale's Hoek Development Forum, Lesotho

Akademische Lehrer:

Prof. T. Aigner, Prof H-P. Luterbacher, Prof. J. Wendt (alle Tübingen), Dr. L. Middelton, Dr. R. Blakey (beide Flagstaff), Prof. A. Hurst (Aberdeen), Prof. G. Kelling (Keele), Prof. R. Swennen (Leuven)

